



# ***PSAN Inflator Test Program and Predictive Aging Model Final Report***

***October 2019***

*Submitted by:  
Northrop Grumman for the  
Independent Testing Coalition*

*Submitted to:  
National Highway Traffic  
Safety Administration*

***NORTHROP GRUMMAN***

northropgrumman.com

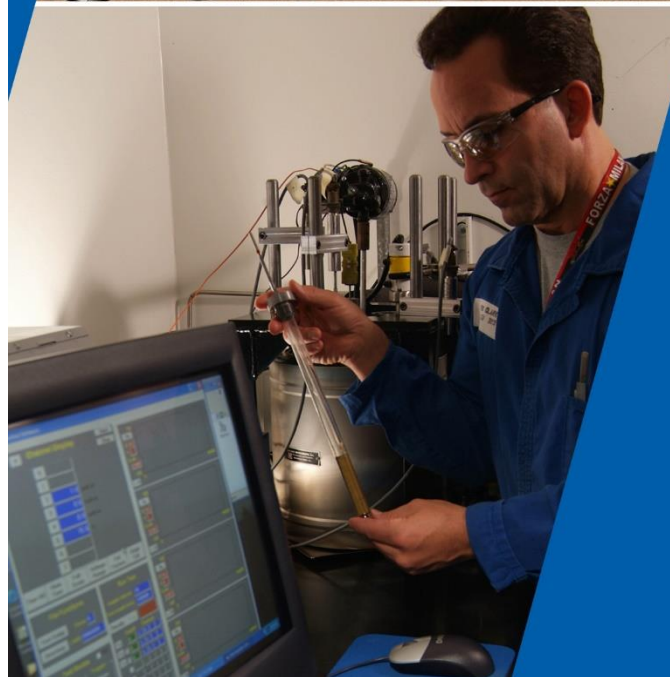
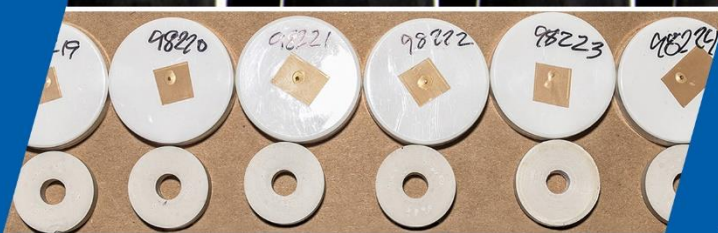
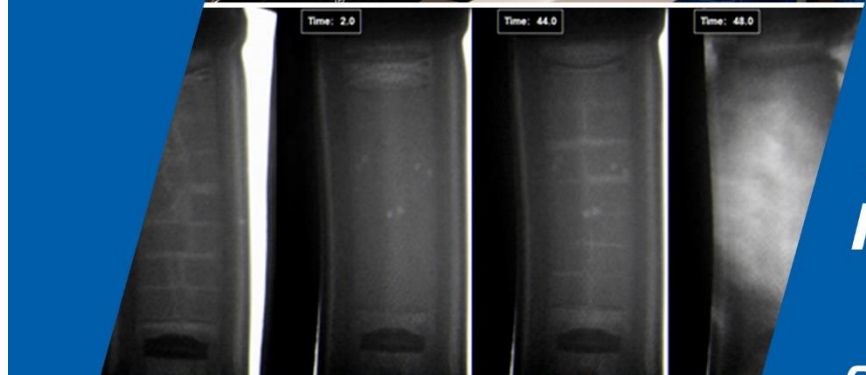


**TABLE OF CONTENTS**

	<u>Page</u>
EXECUTIVE SUMMARY .....	1
INVESTIGATION SCOPE .....	4
TECHNICAL APPROACH.....	5
SUMMARY MODEL RESULTS AND CONCLUSIONS.....	9
PREDICTIVE AGING MODEL .....	16
Introduction .....	16
Environment Module.....	17
Inflator Module .....	21
Performance Module .....	23
Key Inputs, Key Outputs, and Anchoring / Parameterization Data .....	26
INFLATOR DESIGN .....	28
Passenger Inflator .....	28
Main Propellant .....	30
Ignition System.....	31
Gas Cooling System .....	32
Pressure Vessel .....	33
Moisture Protection System.....	33
Auto-ignition System.....	34
Suspension System .....	35
Driver Inflators.....	35
Main Propellant .....	36
Ignition System.....	37
Propellant Gas Cooling System.....	39
Pressure Vessel .....	39
Moisture Protection System.....	40
Auto-ignition System.....	41
Suspension System .....	42
SCIENTIFIC AGING TEST PROGRAM.....	43
Moisture Levels.....	46
Temperature Levels.....	49
Temperature Cycle .....	50
Laboratory Testing Overview .....	51
Moisture Testing.....	52

---

Propellant Density .....	56
Propellant Burn Rate .....	62
Tank Testing.....	67
Observations .....	67
SENSITIVITY STUDIES AND KEY ASSUMPTIONS .....	71
Sensitivity Studies .....	71
Key Assumptions .....	73
SUMMARY AND CONCLUSIONS .....	75
PATHS TO INCREASED MODEL FIDELITY .....	77
ADDENDA.....	78
A. Sources of Information and Acknowledgements .....	78
B. ITC Membership and Purpose .....	78
C. Northrop Grumman Relevant Qualifications and Background .....	78
APPENDIX A. PROBABILITY OF FAILURE CURVES AND FULL TABLES FOR THE SEVEN INFLATORS.....	A-1
APPENDIX B. DETAILED TRADE STUDY TABLE OF RESULTS .....	B-1
APPENDIX C. INTERIM REPORT BY NGIS .....	C-1
APPENDIX D. CORRELATION OF VARIOUS CLIMATE ZONES AND CITES .....	D-1

## LIST OF FIGURES

	<u>Page</u>
Figure 1. Root Cause Fault Tree .....	2
Figure 2. Forward Looking Aging Showing Advantage of Future Testing or Surveillance Efforts in Determining the Future Aging of the 2004L Propellant-based Inflators.....	4
Figure 3. Three-part Approach to Aging and Surveillance Used in the Rocket Motor Industry...	6
Figure 4. Inflators Investigated .....	7
Figure 5. Design Highlights .....	7
Figure 6. Predictive Aging Program Flow .....	9
Figure 7. Field Failure Rates for PSPI-L Inflators in T3 Highest Temperature Vehicles .....	12
Figure 8. Field Failure Rates for PSDI-5 Inflators in T2 Middle Temperature Vehicles .....	13
Figure 9. Architecture of the Takata Inflator Predictive Aging Model .....	17
Figure 10. Definition of Vehicle Temperature Bands Taken from Empirical Data. ....	19
Figure 11. Moisture Movement in a Vehicle Cabin .....	19
Figure 12. Inflator Moisture Movement Diagram .....	21
Figure 13. Pressure vs Time Traces for a Virgin Inflator Showing Inherent Variation .....	25
Figure 14. Apparent Burn Rate vs Pressure for Different Propellant Density with the Augmented Burning Variation Highlighted; Lower Density Results in Higher Pressure.....	25
Figure 15. Typical Passenger Inflator Cross Section.....	29
Figure 16. Typical Passenger Inflator Exploded View .....	30
Figure 17. Main Propellant Geometries and Types .....	30
Figure 18. Wafer Breakup on Ignition .....	31
Figure 19. Typical Passenger Ignition System .....	32
Figure 20. Typical Passenger Cooling Screen .....	33
Figure 21. Typical Passenger Pressure Vessel.....	33
Figure 22. Typical Passenger Moisture Protection System .....	34
Figure 23. Typical Passenger AI Cup.....	34
Figure 24. Typical Passenger Wafer Suppression System.....	35
Figure 25. Driver Inflators Section View .....	36
Figure 26. Driver Inflator Exploded View.....	36
Figure 27. Driver Inflator Main Propellant Forms.....	37
Figure 28. PSDI-5 Ignition System.....	38
Figure 29. PSDI-X Ignition System.....	38
Figure 30. Propellant Gas Cooling System.....	39
Figure 31. PSDI-5 Pressure Vessel.....	39
Figure 32. PSDI-X Pressure Vessel.....	40
Figure 33. PSDI-5 External Leak Paths .....	40
Figure 34. PSDI-X External Leak Paths .....	41
Figure 35. PSDI-5 Auto Ignition System.....	41
Figure 36. Driver Tablet Suspension System .....	42
Figure 37. Hardware Flow .....	46
Figure 38. MEAF PSPI-L Primary Chamber Moisture Levels in Zone 1 .....	47
Figure 39. MEAF PSPI-L Secondary Chamber Moisture Levels in Zone 1 .....	47
Figure 40. Vehicle Peak Temperatures from ATLAS Testing .....	49
Figure 41. PAB Inflator Temperature – Chamber Soak ATLAS Zone 1 .....	50
Figure 42. Humidity Equilibrium Study .....	51

Figure 43. Total Moisture in 3110, AIB and 13X as a Function of Temperature Cycles for PSPI-LD DU Inflators ..... 53

Figure 44. Total Moisture in 3110 and 2004 as a Function of Temperature Cycles for PSDI-5 ZA Inflators..... 54

Figure 45. Total Moisture in AIB, 2004L and 13X as a Function of Temperature Cycles for PSPI-X TX Inflators ..... 55

Figure 46. Total Moisture in AIB, 2004L and 13X as a Function of Temperature Cycles for PSDI-X SV Inflators ..... 56

Figure 47. Driver Inflator 2004/2004L Primary Tablet Caliper Density Measurements ..... 58

Figure 48. Driver Inflator 2004/2004L Secondary Tablet Caliper Density Measurements ..... 59

Figure 49. Passenger Inflator 2004/2004L Primary Caliper Density Measurements ..... 61

Figure 50. Passenger Inflator 2004/2004L Secondary Caliper Density Measurements ..... 62

Figure 51. Propellant Density Decrease Can Yield Augmented Burning. Data courtesy of Takata ..... 63

Figure 52. Burn Rate vs Pressure Plots for 2004 Wafers from PSPI-L FD/LT Inflators Cycled 1,920 4-Hour Cycles. .... 64

Figure 53. Burn Rate vs Pressure Plots for 2004 Wafers from PSPI-LD DU Inflators Cycled 1,920 4-Hour Cycles ..... 65

Figure 54. Burn Rate vs Pressure Plots for 2004 Wafers from PSPI-LD DU Inflators Cycled 1,920 4-Hour Cycles. .... 65

Figure 55. Burn Rate vs Pressure Plots for 2004 Tablets from PSDI-5/5D Inflators Cycled 1,920 4-Hour Cycles ..... 66

Figure 56. Burn Rate vs Pressure Plots for 2004L Tablets from PSDI-X SV Inflators Cycled 1,920 4-Hour Cycles ..... 67

Figure 57. PSPI-L LT Density vs. Peak Combustion Pressure..... 68

Figure 58. PSPI-LD DU Density vs. Peak Combustion Pressure..... 68

Figure 59. PSPI-X TX Density vs. Peak Combustion Pressure..... 69

Figure 60. PSDI-5 ZA Density vs. Peak Combustion Pressure..... 69

Figure 61. PSDI-5D GE Density vs. Peak Combustion Pressure ..... 70

Figure 62. PSDI-5D GE Density vs. Peak Combustion Pressure ..... 70

Figure 63. PSPI-X SV Density vs. Peak Combustion Pressure ..... 71

Figure 64. Tablets Removed From the Primary Chamber of a High Moisture PSDI-5D GE Inflator Cycled 1920 Times from 20 to 70 C..... 71

Figure 65. PSPI and PSDI Pressure vs Time Ballistic Testing Exhibits a characteristic Ballistic Response to Lower Density due to Field Aging ..... 74

Figure 66. PSPI Inflators from the Scientific Aging Study Exhibit the same characteristic Ballistic Response to aging as the Field-aged Inflators. .... 75

**LIST OF TABLES**

	<u>Page</u>
Table 1. Propellant Systems Studied During Phase II .....	5
Table 2. Model Output as Years Until a Predicted Probability of 1 in 10,000 Chance of a Failure for an Inflator when Deployed .....	11
Table 3. Probability of Failure for PSPI-X Inflators Showing the Impact on the Predicted Age Based on Adjustments in Model Parameters including an Extreme Level Not Predicted in the Field .....	15
Table 4. Probability of Failure for PSPI-X Inflators Showing the Impact on the Predicted Age Based on Adjustments in Model Parameters in T3 Vehicles in Miami to 0.01 POF with 1% Usage. The values from 40% RH to 44% RH are considered most viable.....	15
Table 5. Example Ballistics DOE .....	24
Table 6. Key Inputs, Model Parameters, Subroutines, Outputs and Parameterization / Anchoring Data for the Environment, Inflator and Performance Modules .....	26
Table 7. Accelerated Aging DOE Matrix .....	43
Table 8. Full Aging Matrix with Quantity Tested .....	44
Table 9. Moisture Levels as weight % of Main Propellant.....	48
Table 10. Summary of Laboratory Testing.....	52
Table 11. Exemplary Sensitivity Studies Completed to Validate the Model and Understand the Inflators .....	72
Table 12. Correlation of Cities Selected for this Study and the NHTSA Zones .....	73

**GLOSSARY OF KEY TERMS AND ACRONYMS**

°C	degrees Celsius
ATLAS	Reference to the Atlas Material Testing Solutions “Vehicle Environmental Testing Project – Project Number C0010361, Rev1a” Report
Burning Rate Slope	a measure of the change in burn rate as a function of pressure
Burning Rate	a measure of the linear rate (in/sec) at which propellant combusts
CaSO <sub>4</sub>	calcium sulfate
CFD	Computational Fluid Dynamics
CT	Computed Tomography
Deliquescent	the term for a chemical that can absorb enough water from the air to become a liquid solution
Desiccant	the term for a chemical that can function as a drying agent
DOE	Design of Experiments
ED	Energetic Disassembly, also known as rupture
Fault Tree	a structured, deductive approach to failure analysis
Fishbone	a structured approach to determining cause and effect, also called Ishikawa Diagrams
g	gram
Gas pycnometer	a lab instrument that uses gas displacement to measure density
HAH	high absolute humidity
Haystack	a description of the general shape in a pressure-time trace with a gentle, rounded curve typical of a regressive burn
ICAM	International Center for Automotive Medicine
ITC	Independent Testing Coalition
LDF	Linear Driving Force
LSM	Laser Scanning Micrometer
MEAF	Master Engineering Analysis File
mm	millimeter
MPa	megapascal
ms	millisecond
NGIS	Northrop Grumman Innovation Systems
NHTSA	National Highway Traffic Safety Administration
NOAA	National Oceanographic and Atmospheric Administration
OD	outer diameter
OEM	Original Equipment Manufacturer, also known as “automaker”
POF	Probability of Failure
Progressive burning surface area	a geometry where the propellant surface area available to burn increases over time
PSAN	phase-stabilized ammonium nitrate
PSPI-L	Takata nomenclature for a type of air bag inflator
RTR	Real-time Radiography, effectively an x-ray movie that allows visualization of real time events using continuous high-speed x-rays
TGA	Thermogravimetric Analysis
UF	Usage Factor

## Executive Summary

Northrop Grumman Innovation Systems (NGIS) conducted an independent investigation of Takata Phase-Stabilized Ammonium Nitrate (PSAN)-based inflators for the Independent Testing Coalition (ITC) whose members include BMW, FCA, Ford, GM, Honda, Mazda, Mitsubishi, Nissan, Subaru and Toyota. Phase I investigated the failure root cause of the inflators subject to National Highway Traffic Safety Administration (NHTSA) recalls 15E-040 to 15E-043 as reported in the “Takata Inflator Rupture Root Cause Report” released in September 2016 and included as Appendix A to this report.

Phase II consisted of a scientific aging program and predictive Probability of Failure (POF) modeling for seven Takata inflator designs with five propellant systems. The 4-year investigation involved more than 65,000 hours of testing and analysis by experienced scientists, engineers and technicians. The methodology followed a disciplined approach to investigate every potential factor, contributor or cause.

Investigation goals for both phases were to:

1. Identify root cause of the field failures
2. Evaluate the failure potential for a range of Takata PSAN (PSAN)-based inflators, including:
  - 2004/3110 PSAN-based propellant and booster systems (older)
  - Modified 2004/3110 with calcium sulfate or 13X desiccants
  - 2004L/AIB PSAN-based propellant and booster systems with 13X desiccant (newer)
3. Report key findings to ITC members, NHTSA and Takata’s successor company
4. Maintain technical integrity by remaining independent of outside influences

In Phase I, Northrop Grumman found that the inflators manufactured by Takata and subject to NHTSA recalls 15E-040 to 15E-043 are adversely affected by three factors - all of which contribute, and are required to be present, in order to cause a rupture when the inflator is deployed.

These factors are:

- The presence of pressed PSAN propellant without moisture-absorbing desiccant
- Long-term exposure to repeated high-temperature cycling in the presence of moisture
- Inflator design and manufacture that does not adequately prevent moisture intrusion under conditions of high humidity

Two modifiers impact the POF due to their effect on the severity of temperature cycling, i.e., higher vehicle cabin temperatures:

- Vehicle model (some models get hotter than others)
- Vehicle usage (some vehicles are more often left exposed to the external environment)

The POF key factors match the items identified through the fault tree process in the root cause determination and are shown in Figure 1. Consistently, a tropical or near tropical environment, such as in South Florida, is the greatest challenge with sustained high-temperature cycling and high humidity. Generally, smaller vehicles exhibited higher temperatures. Vehicle usage reflects how a driver uses and, especially, parks their vehicle. Field data and experimental work were

used to calibrate the model and were successfully employed with good agreement between the existing experimental data and the results achieved by the model. The usage reflects the degree of exposure to the environment including how hot the vehicle gets in direct sunlight. Higher temperatures and higher humidity result in faster aging.

It is appropriate to note that both Phase I and Phase II were limited in scope to aging related phenomena. Other failures related to manufacturing or other process or handling issues, the so-called “alpha” failures, are not the subject of these studies and data from those failures would have been inappropriate to include in these studies.

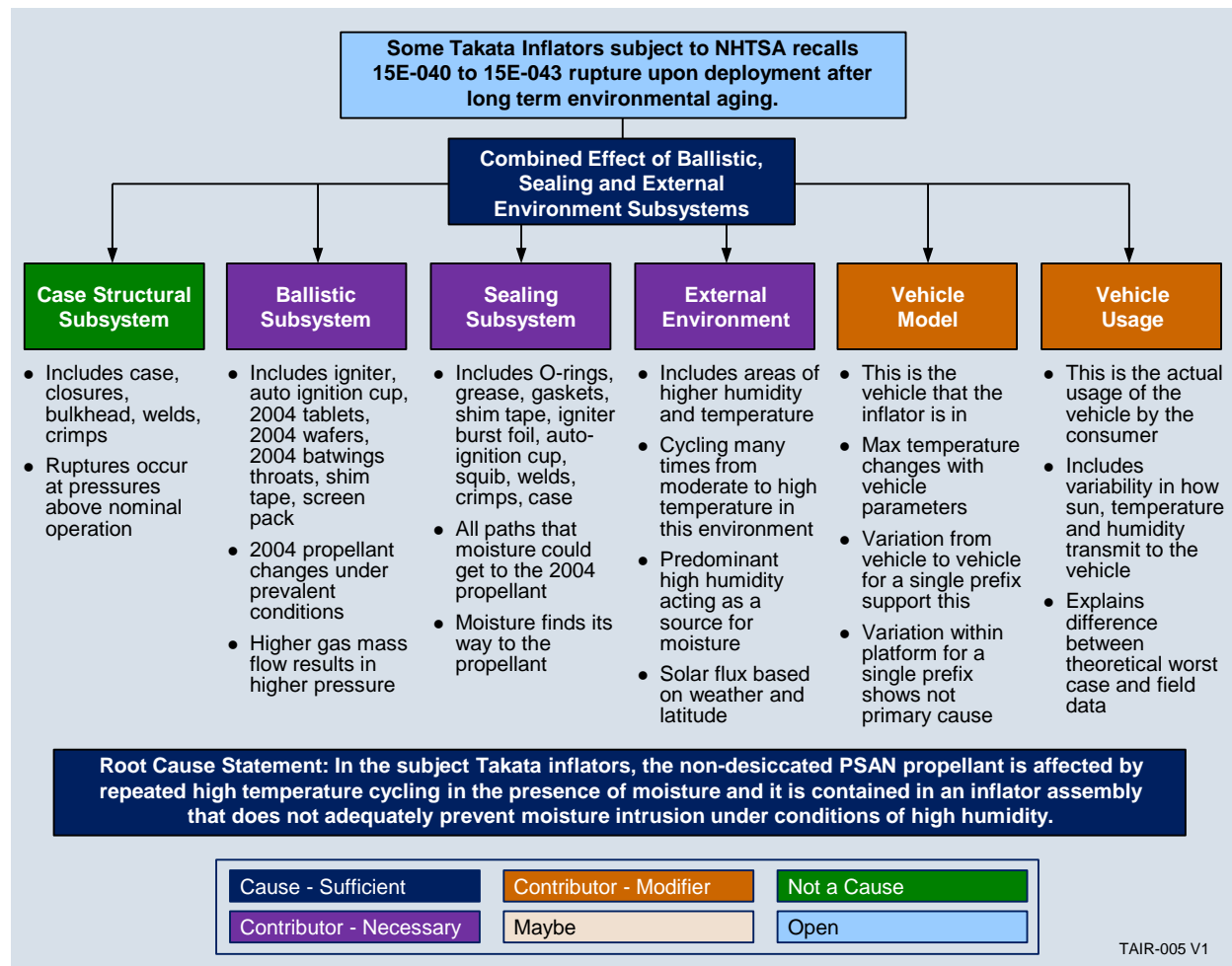


**Figure 1. Root Cause Fault Tree**

Significant questions answered in the Phase II scientific aging study and POF model development were:

1. Will desiccants provide protection to the inflator?
2. Will newer propellant combinations (including 2004L and AIB) provide improved response to the moisture and temperature cycling challenge?

Based on the scientific aging data, field return data and POF modeling, our answer to both of these questions is unequivocally, yes.

A critical follow-on question is more difficult to answer: how long until these inflators present a measurable risk to failure if deployed under the variations expected in the field. To look at the question, the POF model recognizes that the greatest risk is present for the most challenging combination of usage and vehicle maximum temperature in the most severe (e.g., tropical) environment. In all inflator designs and propellant combinations studied, the majority of combinations of these factors outside the most severe result in our model predicting no detrimental sign of aging for over 30 years.

With the wide range of inflator designs, severe aging conditions and uncertainty with the newer inflators for which there is limited field test data, we cannot say unequivocally that under severe conditions that at least some of the newer designs will not eventually degrade. A challenge with the newer, desiccated 2004L inflators is limited field aging data. The longest field exposure of these newer designs is roughly 10 years with some at only 6 years of age (defining age as years since manufacture). Clear trends would not have emerged within this timeframe.

With future data from these newer inflators after longer field exposure than the currently available 6-10 years, the Northrop Grumman POF models can be validated and the most conservative scenarios either verified or reduced in severity. This presents a potential, cautious approach going forward. This approach is shown graphically in Figure 2.

With newer inflators that have not yet shown signs of aging, there is a significant opportunity for improving the fidelity and accuracy of the model with enhanced anchoring data. Several approaches would be successful in this regard. Field monitoring, a targeted field return study or accelerated aging of selected field return samples would all provide added fidelity to the model. The additional test data could confirm if there is still no aging or if an aging model such as the notional aging **model 1** or **model 2** shown in Figure 2 are more correct. Action could be taken with a safety margin prior to the predicted onset of a POF if there is indication of aging or the validated model predicts aging is beginning.

In summary, our analysis confirms aging of non-desiccated older 2004/3110 inflators with significant differences in the rate of aging depending on inflator design variations, operating environment and vehicle temperature range. In the case of newer desiccated inflators, we see significant improvement in aging resistance. Desiccant provides protection at least until it becomes saturated and inflators with more desiccant exhibit longer protection in both 2004 and 2004L main propellants. However, the field age of 2004L-based inflators is just approaching the time in the field where potential indications of changes would potentially begin to emerge. We do not see an immediate threat but, out of an abundance of caution, recommend an ongoing, modest, well designed monitoring program focused on the desiccated 2004L propellant designs in the highest risk categories of climate and vehicle temperature.

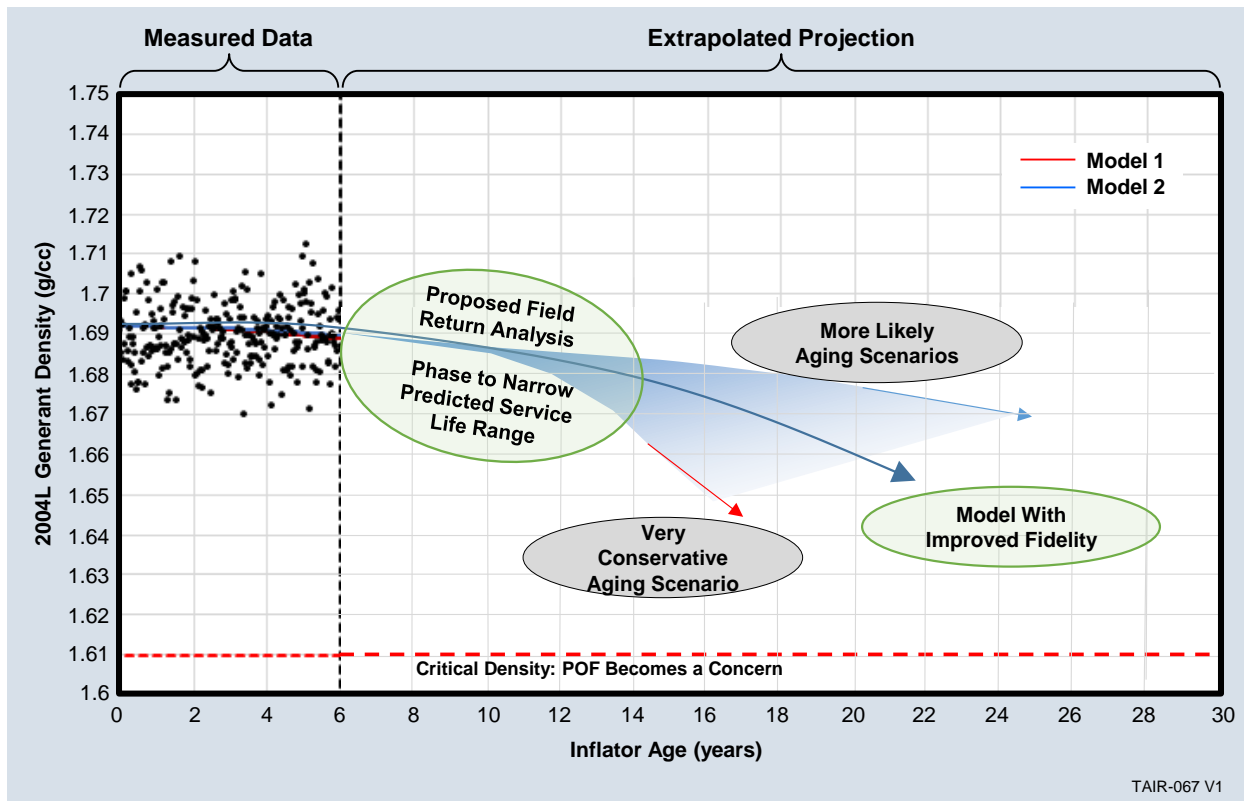


**Figure 2. Forward Looking Aging Showing Advantage of Future Testing or Surveillance Efforts in Determining the Future Aging of the 2004L Propellant-based Inflators.**

Field surveillance and return data on inflators that use 2004 propellant which have exhibited aging show a good correlation between density reduction and Probability of Failure (POF). For each inflator, a “critical density” is the density reduction at which the POF becomes significant. For the newer 2004L propellant-based inflators, sufficient time has not passed to allow definitive statements on whether eventual aging will occur. We do not expect it but the length of extrapolation means that the level of confidence to state unequivocally that there will not be issues is not possible today. Collecting data in one of several methods in the coming years will clarify the outcome.

### Investigation Scope

The investigation focused on determining the root cause of inflator failures covered by Takata recalls 15E-040 to 15E-043 and the POF of these and newer Takata PSAN inflators with desiccant. The specific inflators studied are listed in Table 1. These studies were directed towards POF based on the design of the inflators, rather than manufacturing problems. This does not mean that manufacturing problems do not play a role in certain failures, but these were not the emphasis of our investigation. Rather, our emphasis was on determining changes due to environmental aging, including changes influenced by inflator design differences and routine manufacturing variation.

The effort created a predictive aging model based on: 1) root cause analysis, 2) field return inflator testing, 3) scientific aging testing, and 4) laboratory testing. The investigation gathered inflator-specific model inputs and exercised the model to predict POF versus age for each inflator. Modeling utilized climate data from five U.S. cities and three vehicle cabin temperatures spanning from the highest cabin temperatures observed in field testing to the lower range observed. The predictions do not include a probability of injury if the inflator ruptures.

**Table 1. Propellant Systems Studied During Phase II**

Inflator	Type / Propellant Form	PSAN Formulation	Booster Formulation	Desiccant	Propellant System
PSDI-5 ZA	Driver / Tablet	2004	3110	None	1
PSDI-5D YT	Driver / Tablet	2004	3110	CaSO4	2
PSDI-5D GE	Driver / Tablet	2004	3110	13X	3
PSDI-X SV	Driver / Tablet	2004L	AIB	13X	5
PSPI-L FD	Passenger / Wafer	2004	3110	None	1
PSPI-LD DU	Passenger / Wafer	2004	AIB	13X	4
PSPI-X TX	Passenger / Wafer	2004L	AIB	13X	5

### Technical Approach

For the Takata airbag inflator investigation, we exploited the three-part approach to aging and surveillance that has been used in the rocket motor industry for decades. This approach is diagrammed in Figure 3. Part I of this approach is related to the identification and ranking of failure modes. Our Phase I investigation into the failure root cause of the inflators subject to NHTSA recalls 15E-040 to 15E-043 falls into this part. Phase I efforts included: 1) inflator design reviews, 2) identifying / verifying existing critical data, and 3) determining what was needed in Phase II.

Part II of our approach to aging and surveillance deals with identifying and developing the best analysis tools, determining appropriate tests and test specimens, acquiring aging data, quantifying aging mechanisms and verifying and validating prediction tools. Phase II of our Takata investigation belongs in Part II of the process shown in Figure 3. The predictive aging program in Phase II was comprehensive, covering the complete sequence of aging changes.

Phase II investigated three passenger inflators and four driver inflators as shown in Figure 4. All use either the 2004 or 2004L propellants, which combust PSAN propellant as the gas generant and have primary / secondary chambers, with the exception of the PSDI-X that has a shared chamber. Figure 5 shows key design highlights. This set of inflators was carefully selected to represent the widest range of inflator designs that are in the widest use in the field. This set, at the time selected, included the design of roughly 60% of the inflators in the field directly and designs that are closely related to over 90% of Takata manufactured inflators.

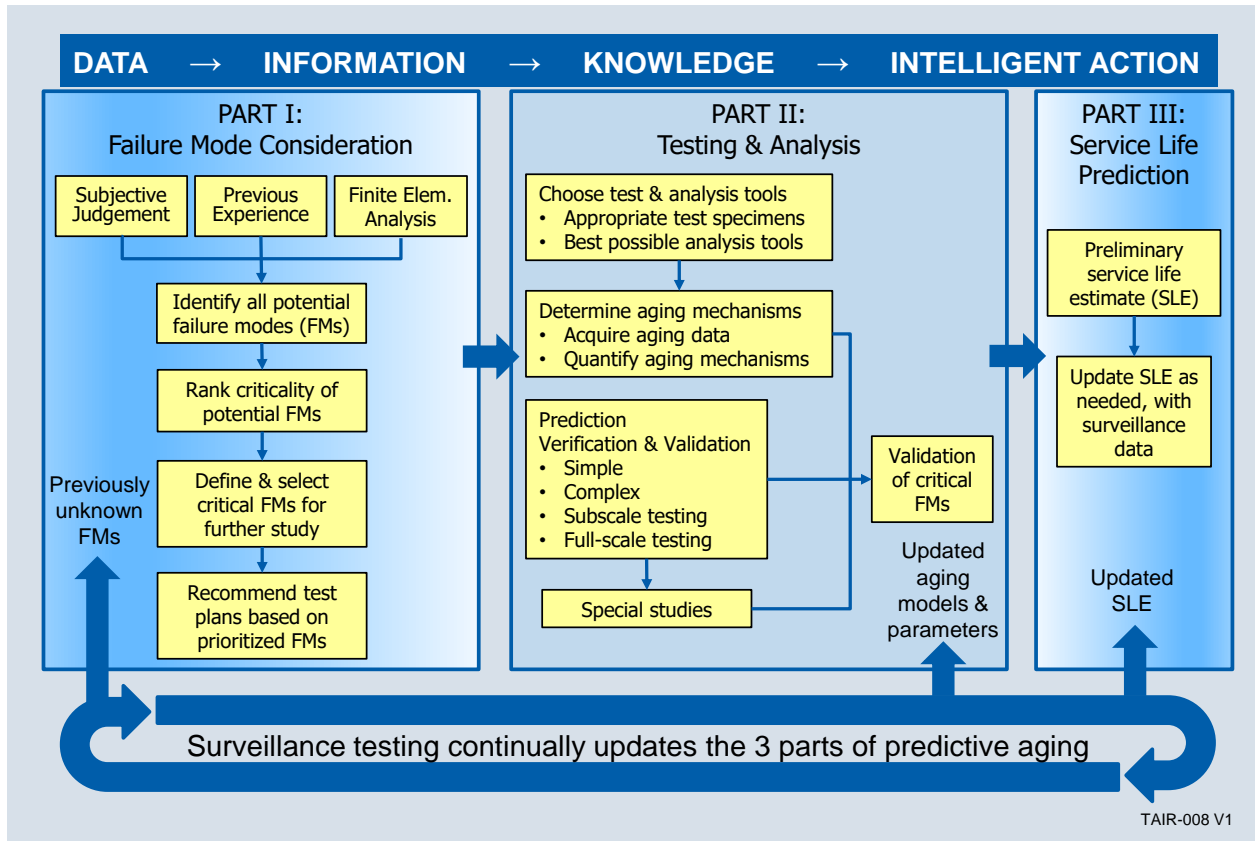


**Figure 3. Three-part Approach to Aging and Surveillance Used in the Rocket Motor Industry**

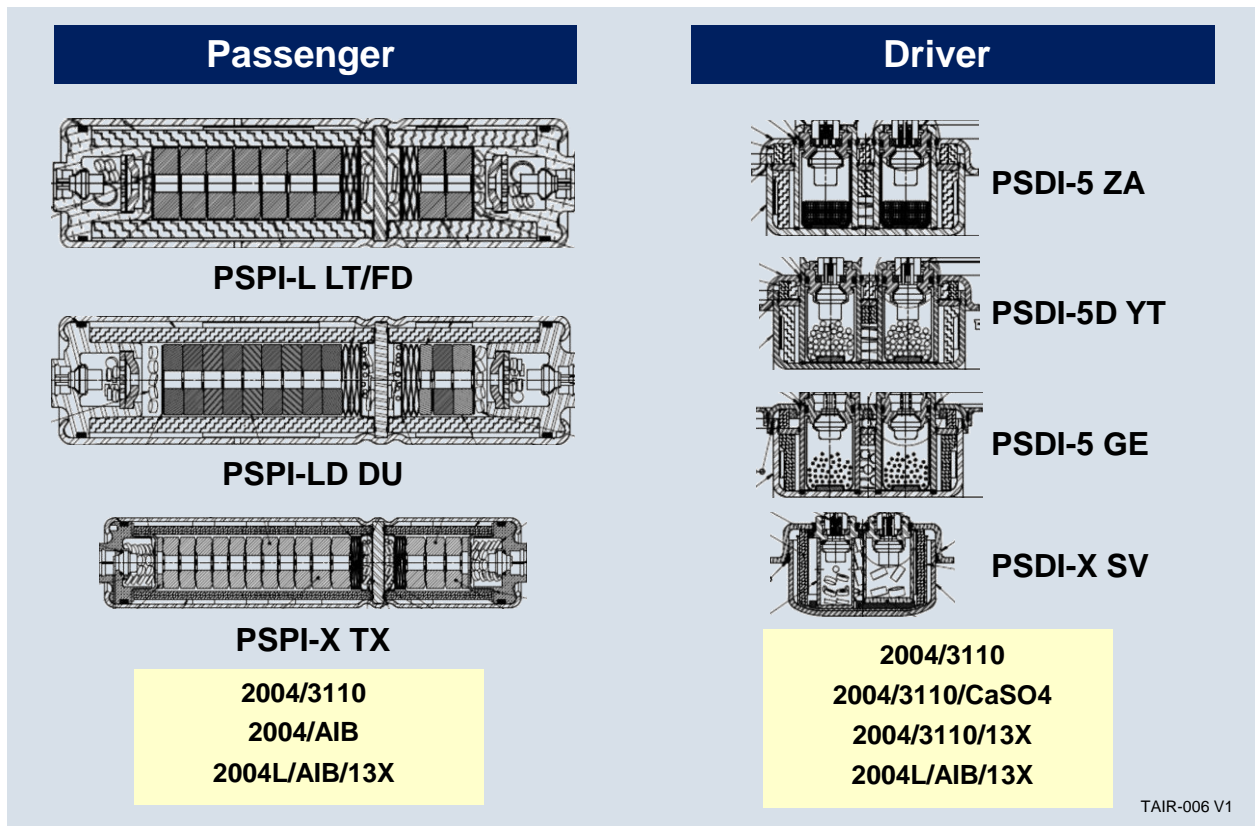


Figure 4. Inflators Investigated

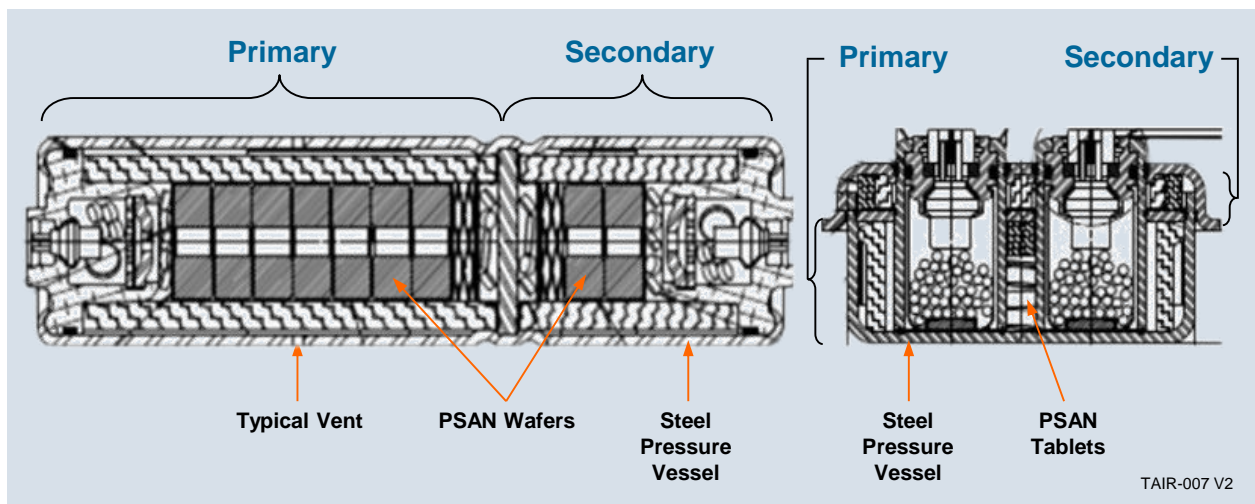


Figure 5. Design Highlights

These seven inflators cover the five propellant systems shown in Table 1. The systems include two primary PSAN propellants (2004 and 2004L), two booster propellants (3110 and AIB) and two desiccants (calcium sulfate [CaSO<sub>4</sub>] and 13X). Some heritage 2004/3110 systems without desiccant have a history of field ruptures and are subject to NHTSA recalls.

The 2004L/AIB/13X is the second generation Takata PSAN system. This newer system, with field data limited to 6 to 10 years, has no known field ruptures to date related to aging. There are examples of field events with ages inconsistent with aging phenomena. This set of inflators allows close tie to those older, baseline inflators with the most field data (PSDI-5 and PSPI-L).

This approach of using different propellant systems in different inflators allows the most direct comparisons and reduces the extrapolation needed to draw conclusions regarding newer systems that have limited field data. In each of these seven inflators, we selected a single specific model (or prefix) for detailed evaluation. There are typically several other prefixes with smaller design changes which, nonetheless, can be significant with regards to predicted POF versus time curves. More detailed examination of these inflators can yield these results.

Similarly, the five cities selected for use in executing the model were chosen because they span the range from very hot / very humid to hot / humid with seasons, to hot / dry, to wet / cool and finally to one with distinct seasons. This range spans climates seen in the United States and covers those expected to be most severe to those expected to be less severe. These data will provide insight into weather / geography dependent variation in POF. For complete references to the cities and terminologies used in multiple publications on climate zones, please refer to Appendix D.

Phase II covered three main efforts:

- Scientifically age inflators to obtain quantitative input for the predictive aging model under known conditions
- Develop a predictive-aging model based on the Phase I root cause investigation including factors identified in Figure 1
- Exercise the predictive-aging model to predict POF versus inflator age

While we utilized many of our standard “rocket motor analysis tools,” the unique characteristics of Takata inflators demanded the development of a unique predictive aging model. The model development consisted of iterations of the following:

1. Development of modular predictive model frameworks
2. Test data to verify / validate the performance of modules
3. Modification of the modules to better capture results of test data
4. Verify / validate performance of overall predictive aging model using field returned data from the Master Engineering Analysis File (MEAF)

After many iterations, the model was “finalized.” The output of the predictive aging model is the probability that an inflator will fail structurally (energetic disassembly or ED) if deployed. It is the output of this aging model that comprises Part III of our approach to aging and surveillance.

Details of this aging model are discussed below. The overall program flow of our Takata inflator investigation is shown in Figure 6.

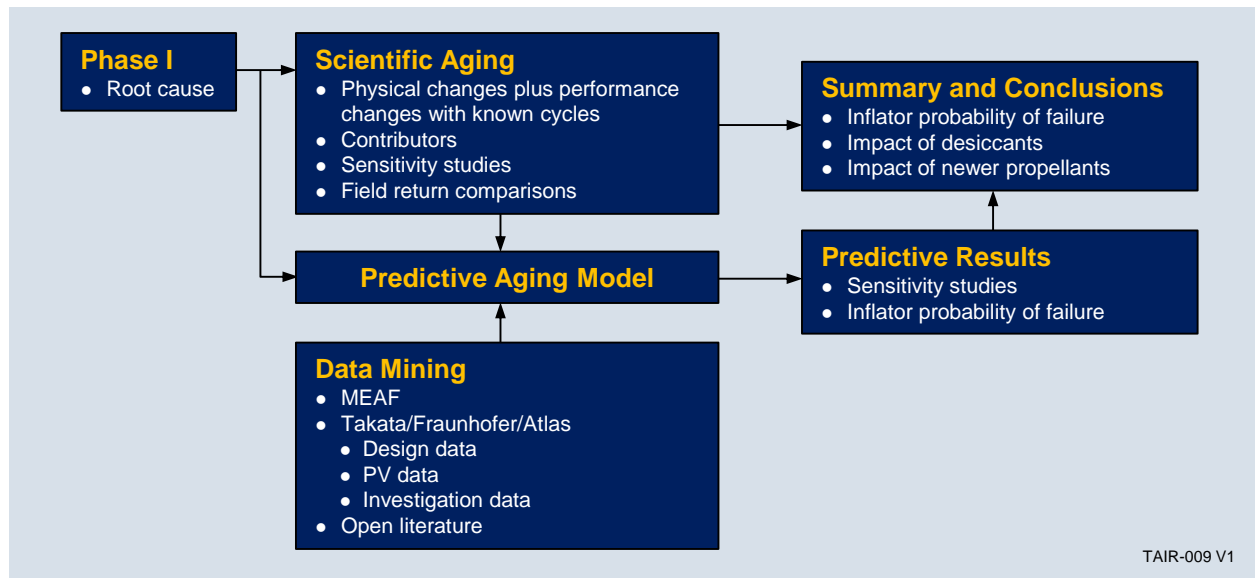


**Figure 6. Predictive Aging Program Flow**

Northrop Grumman assembled a multi-disciplined core team of senior investigators. Our team included experts in propellant chemistry, combustion, ballistics, design, manufacturing, predictive aging and failure analysis. Specialists in structures, heat transfer, Computational Fluid Dynamics (CFD) and testing were utilized from across the company.

### Summary Model Results and Conclusions

The model was exercised for each of the seven subject inflators. The results are presented here in a tabular format. The same data can be depicted other ways including POF curves, which are included in Appendix A. The table provides a compact yet complete picture of the response of each inflator design to the primary factors developed in the Phase I root cause investigation. Comparison of the various designs can be made by comparing results between the tables for the individual designs. After the table, several conclusions are drawn from the data.

This summary table contains a great deal of data and it is critical to read it correctly. It represents the model predictions for time to a 1 in 10,000 chance of an ED if the inflator listed in the left column is deployed. The next four columns identify the PSAN main grain propellant as the older 2004 or newer generation 2004L propellant, the booster formulation, whether there is a desiccant present and the amount of desiccant present relative to the propellant. The outputs are presented in years to a 0.01 POF (1% probability of failure) for the inflator in the climate (city), vehicle temperature band (T3 being the hottest vehicles and T1 being the coolest) and in the most severe vehicle usage scenario (first percentile vehicle). While a specific number is given for each number of years, typical ranges of +/- 5%-15% should be considered if evaluating a specific number of years but for comparison purposes, the numbers as presented should be utilized.

With the assumptions in this table for a 0.01 POF and the 1% vehicle, data should be interpreted as an estimate of the age of an inflator in that climate and vehicle temperature band crossing over the 1 in 10,000 chance of an ED threshold if the vehicle is involved in an accident such that the air bag deploys with a short delay between the primary and secondary chambers. Longer delays

between the primary and secondary chambers result in modest increases in the time to cross this threshold (see sensitivity studies in Appendix C).

As an example of interpretation, in Table 2 with PSPI-L FD/LT, if the question was when an inflator in a cooler, larger vehicle (T1) in an Atlanta-type climate will reach a 1 in 10,000 chance of ED, select the PSPI-L inflator rows, the T1 vehicle and come across to Atlanta and read >30 years as the predicted age for crossing this threshold.

In Table 2, the values for the inflators with 2004 as the main propellant are shown as single values. With the combination of work on the model and the abundant anchoring data on the key PSPI-L and PSDI-5 undesiccated inflators, the fidelity of the model is sufficient to show these distinct values as confident predictions including for the related desiccated 2004 propellant inflators. With the 2004L propellant-based inflators, PSPI-X and PSDI-X, sufficient data is not available to anchor these models. All of the preliminary studies, the scientific aging study and data from other investigators show that the 2004L propellant-based inflators are less susceptible to aging. The worst case conditions are reflected in Table 2 as the lower value in years until the 1 in 10,000 threshold is crossed. Sensitivity studies identified other conditions when greater than 30 years would be predicted. Further in this section, we discuss this range and later in the report paths to improved fidelity on this predictions. The results of the model run with our best parameters yields 25 years as the most likely number of years to 1 in 10,000 POF for the Miami T3 result for the PSPI-X. A similar value is predicted for the PSDI-X. The less severe conditions such as Atlanta or T2 vehicles for these inflators would not be expected to predict vulnerability using the baseline conditions.

**Table 2. Model Output as Years Until a Predicted Probability of 1 in 10,000 Chance of a Failure for an Inflator when Deployed**

Inflator Type	Main ID	Booster ID	Desiccant ID	Desiccant as % of Main in Primary	Platform Temp Band	Miami	Atlanta	Phoenix	Detroit	Seattle	Prefix
PSPI-L	2004	3110	NA	NA	T3	9	15	16	21	>30	LT
					T2	12	21	18	30		
					T1	21	>30	23			
PSDI-5	2004	3110	NA	NA	T3	9	17	>30	25	>30	ZA
					T2	14	26				
					T1	22					
PSDI-5D 13X	2004	3110	13X	4.4	T3	24	>30	>30	>30	>30	GE
					T2						
					T1						
PSDI-5D CaSO4	2004	3110	CaSO4	5.1	T3	24	>30	>30	>30	>30	YT
					T2						
					T1						
PSPI-LD	2004	AIB	13X	1.7	T3	23	>30	>30	>30	>30	DU
					T2						
					T1						
PSPI-X	2004L	AIB	13X	0.9	T3	16 to >30	27 to >30	>30	>30	>30	TX
					T2	23 to >30					
					T1						
PSDI-X	2004L	AIB	13X	1.3	T3	17 to >30	30 to >30	>30	>30	>30	SV
					T2	24 to >30					
					T1						

\*Note that the values in this table are shown as single value integers outside of the last two entries but should be considered to have +/- 5%-15% ranges. The values can be compared with each other directly. The values are for the specific prefixes shown in Table 1 and design differences may result in significantly different predictions. See Table 12 and Appendix D for a description of the cities used in this study.

There are four distinct, major conclusions that can be drawn from the modeling results.

1. These results are consistent with the root cause from Phase I of the investigation. Each of the five identified contributors (Figure 1) are reflected in these results.
2. The predicted time to 1 in 10,000 chance of failure is consistent with field return data for the systems with sufficient age in the field (PSPI-L and PSDI-5) and known POF from field returns (Figure 7 and Figure 8). These data were used to anchor and validate the model.
3. All of the desiccated systems showed significantly improved resistance to aging. With sufficient desiccant relative to propellant, this can protect the original 2004 propellant (see PSDI-5D and PSPI-LD inflators). If there is risk of greater than the reporting threshold in desiccated systems, it is localized to the most severe climate, hotter vehicles and the more or most challenging vehicle usage.
4. The newer propellant and booster formulations (2004L, AIB) provide distinct advantages over the baseline (2004, 3110) formulations in many lab experiments on moisture dynamics and nonconfined temperature / humidity cycling (not in an inflator). However, the model highlighted that a modest change in the equilibrium humidity in the confined space of an inflator results in significant variation in the predicted time to 0.01 POF for the 1% vehicle (1 in 10,000 aggregate). The data presently available are insufficient to predict that there will not be a time when the POF exceeds the threshold in the more severe combinations of conditions. The data shown here represent conservative estimates.

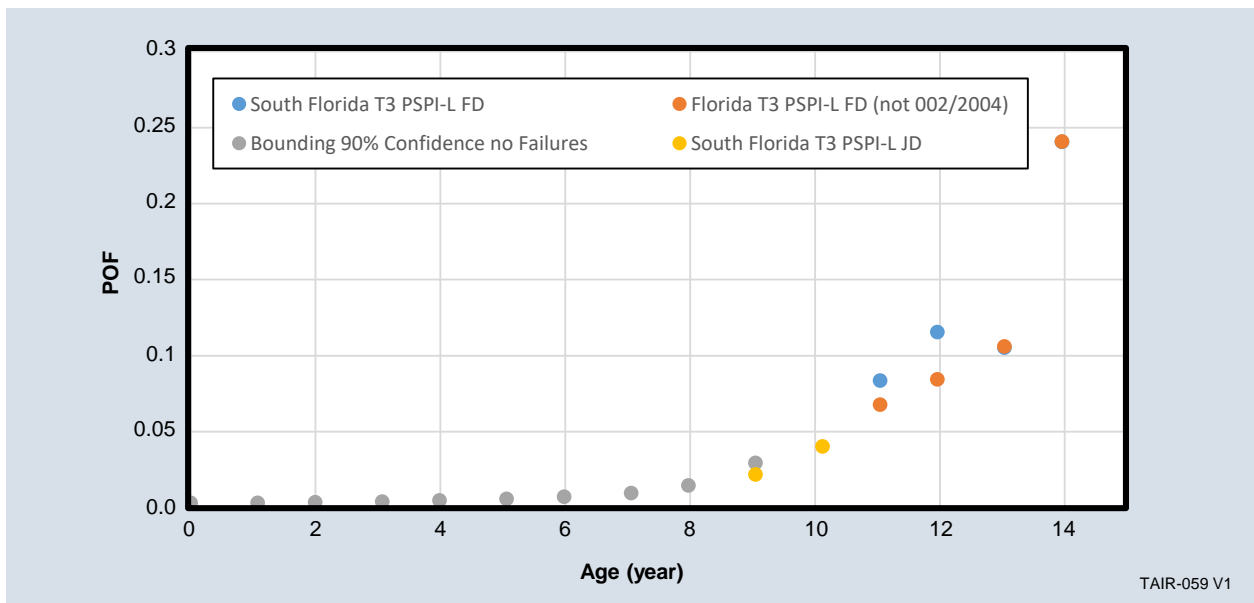


**Figure 7. Field Failure Rates for PSPI-L Inflators in T3 Highest Temperature Vehicles**  
 The field data validates the 0.01 POF for the highest usage vehicles showing the baseline departure for POF near 9 years. The grey data show the zero failure confidence limits calculated for ages with no failures. The three other data sets reflect field return failure rates for the inflators indicated.

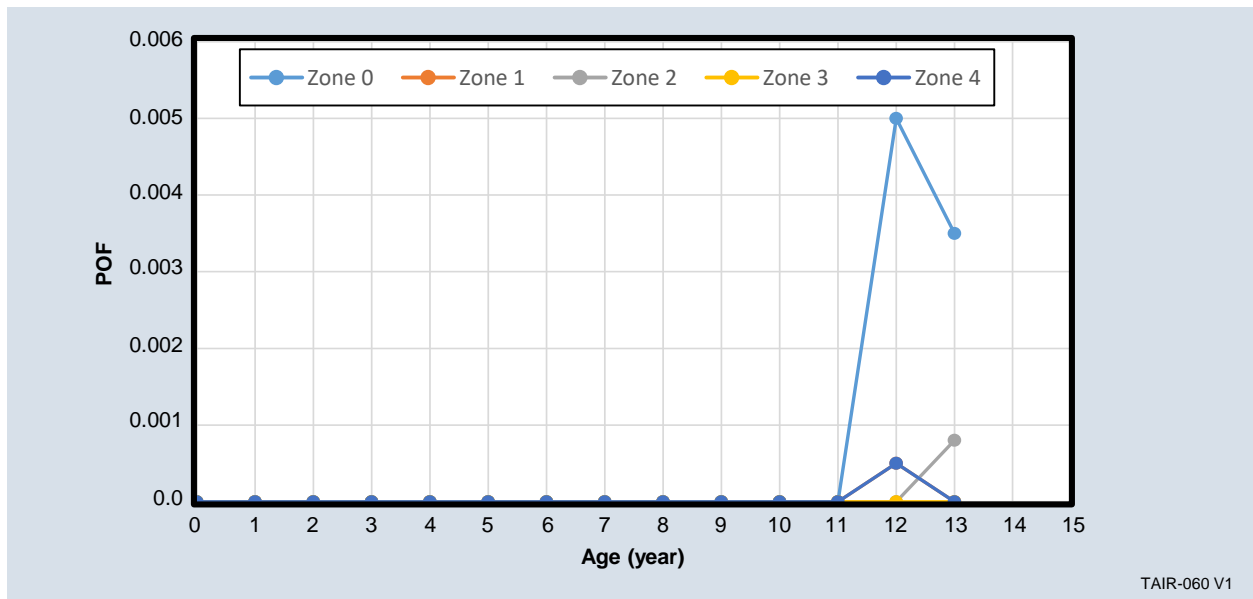


**Figure 8. Field Failure Rates for PSDI-5 Inflators in T2 Middle Temperature Vehicles**

The field data validates the 0.01 POF for the highest usage vehicles showing the baseline departure for POF near 14 years. Please note that the field inflators are just departing from the baseline at 12 to 13 years of age and exhibited failure probabilities below the 0.01 POF used as the calculated threshold in this study. These data validate that the model output is matching field data. It should be noted that no PSDI-5 data for a T3 vehicle in this time is available. See Table 12 and Appendix D for a description of the zones listed here.

Worth noting is that the amount of desiccant in the various desiccated inflator models is not consistent and may be a large factor in determining years to POF. We clearly determined that more desiccant is better. We found unrealistic the possibility that more desiccant would function as a mechanism to draw extra moisture into the inflator and become a source of moisture for more rapid aging after saturation. The same inflator listing with a column for desiccant as a percentage of main propellant weight (for the primary chamber) is shown in Table 2. The years to POF for the systems with higher relative amounts of desiccant would be expected to resist aging more effectively as is suggested by the data in Table 2. Unfortunately, these different ratios add a complication to the interpretation of the change from the legacy 2004 propellant to the newer 2004L propellant.

As mentioned in conclusion #4 above, the response of the 2004L propellant changes significantly with modest changes in the equilibrium humidity (moisture) level in an inflator. This would be expected to impact the model predictions for the PSPI-X and PSDI-X inflators. With the limited age of the 2004L propellant inflators, field data is not available to anchor the model. To examine the potential impact on the model predictions, two sensitivity studies were done with the PSPI-X inflators. It should first be noted that the newer propellant system inflator had a low amount of desiccant compared to other inflators. A 2004L propellant inflator with more than 2% desiccant to main propellant ratio would be predicted to exhibit little sensitivity to aging. Comparing the PSPI-L 2004 propellant baseline inflator to the most conservative output on the PSPI-X 2004L propellant inflator models shows significantly improved resistance to aging with no predicted aging in all but the most challenging climate. This system successfully protects in the Phoenix, Atlanta and Detroit climates. Only in the Miami climate and primarily with higher temperature vehicles do the trade studies suggest there is the possibility of aging.

In the first sensitivity study, the rate of 2004L growth when subjected to various equilibrium moisture conditions was examined. Three values were considered, extreme (above that expected to be seen in the field), a value within what is expected to be seen in the field, and a low moisture value. The results are shown in Table 3. In the most severe test, which we consider highly unlikely, the improvement of 7 years for the T3 vehicle from 9 years to 16 years and 1% usage to 0.01 POF (overall  $10^{-4}$  POF) is surprisingly low in light of preliminary lab data and TK Global collected Laser Scanning Micrometer (LSM) data.

Our analysis shows a significant inflection point near 45% relative humidity in the inflator headspace. Small changes in the input parameters result in significant changes in the prediction. A further predicted improvement of 2.5 to 5 years is seen in the change from the conservative moisture scenarios to more moderate ones as shown in Table 3. It takes a reduction of the growth rate of 2004L as represented by the third value in this table, but still higher than predicted by the LSM experiments, to achieve a prediction of the system being able to survive all environments. Inflators returned from the field exhibit either no sign of density reduction or, conservatively, perhaps the earliest beginning of aging. We consider this middle condition near the higher end of what would be experienced in the field and that value is represented in Table 2.

In the second trade study, the humidity achieved in the inflator at saturation was systematically varied around the critical 45% value. Values from 51% (the extreme condition in the first study) down to 40% final relative humidity were tested to determine the sensitivity to this parameter. The results are reported in Table 4. This study shows that modest changes in the final moisture equilibrium value as reflected in relative humidity inside the inflator in the field results alters the prediction of time to the  $10^{-4}$  overall POF for the 1% usage vehicle from 14 years to greater than 30. The small range of relative humidity is difficult to predict without anchoring data from field returns.

With the relative young age of the PSPI-X inflators in the field, the relevant anchoring data is not available. Our model suggests that the values from 40% to 44% relative humidity are most likely to be experienced in the Miami T3 (most severe) environment. The specific value that the model predicts is a 25 year time to the 1 in 10,000 overall POF corresponding to 42% peak relative humidity. We feel the 48% relative humidity is unlikely but out of an abundance of caution are leaving that as a potential, albeit low, probability outcome. This leads to the values of 16 to >30 years shown in Table 2.

With the age of these inflators in the field, at a minimum, even using the most conservative inputs considered possible in the field, we can say that any risk is several years in the future. However, due to the relatively young age of these inflators in the field (6 to 10 years), it is not possible to validate from field data which model most accurately reflects what will be the state of these most severely challenged inflators in the years to come. Hence, we recommend the consideration of acquiring further field data.

**Table 3. Probability of Failure for PSPI-X Inflators Showing the Impact on the Predicted Age Based on Adjustments in Model Parameters including an Extreme Level Not Predicted in the Field**

Vehicle	Miami	Atlanta	Phoenix	Detroit	Seattle
Including Extreme Humidity Possibility with 2004L Growth					
T3	14	22	>30	>30	>30
T2	19	>30	>30	>30	>30
T1	26	>30	>30	>30	>30
Including Mid-level Humidity with 2004L Growth					
T3	16	27	>30	>30	>30
T2	23	>30	>30	>30	>30
T1	>30	>30	>30	>30	>30
Lower Humidity with Reduced 2004L Growth Case					
T3	>30	>30	>30	>30	>30
T2	>30	>30	>30	>30	>30
T1	>30	>30	>30	>30	>30

**Table 4. Probability of Failure for PSPI-X Inflators Showing the Impact on the Predicted Age Based on Adjustments in Model Parameters in T3 Vehicles in Miami to 0.01 POF with 1% Usage. The values from 40% RH to 44% RH are considered most viable.**

Peak RH	Years
51	14
48	16
44	19
42	25
40	>30

The model output is for the specific scenario and not a predictor of risk of injury to a vehicle occupant. This 0.01 POF threshold in the first percentile vehicle usage represents the time to a 1 in 10,000 chance of rupture if that vehicle were involved in an accident that resulted in an inflator deployment with 5 ms delay between the primary and secondary chambers. These data are not a prediction of risk to the occupants, but provide a set of fundamental data that can be the initial input to an overall risk model. That prediction will also need to include probability of the vehicle being in an accident where the inflator will be deployed, passengers in the vehicle, number of vehicles in service, probability of accident with the 5 ms delay and other factors. This is not a prediction of a probability of an injury.

The rest of this report details the methodologies and results from the aging model and the scientific aging study. These data provide sufficient detail for one skilled in the art to fully understand, and, if desired, repeat the experiments and verify the results. Also included is a detailed description of inflator design and function as this plays heavily into the model development. At the end of the technical sections, a final summary of the technical data is presented.

## Predictive Aging Model

### Introduction

The predictive aging model begins with the environment from a given geographic location and finishes with a prediction of the probability that an inflator will ED if deployed. The model was developed using the foundation provided by our investigations performed in Phases I and II, including inflator design, propellant behavior in the presence of moisture and temperature cycling and ballistic performance of the inflator. The model employs a modular architecture so each module could be tested, parameterized and calibrated with test data (see: Key Inputs, Key Outputs, and Anchoring / Parameterization Data).

Modules were modified and improved until they were in agreement with test data. Most modules are science-based to improve predictive capability beyond where data is available. Empirical modules have been used when a science-based model is impractical and when a large amount of data is available so no, or minimal, extrapolation is necessary. The modules determine the state of the inflator (i.e., temperature, water content, propellant density, etc.) over time. MEAF data were used to anchor the model at both the module level, as well as the overall system level. This portion of the overall model is largely deterministic with empirical inputs.

The probability of ED or failure (POF) versus time is calculated using a Monte Carlo algorithm. Within each Monte Carlo iteration, random variates of model parameters are selected and used to calculate the peak inflator pressure and the inflator pressure capability. The ratio of the number of times the peak pressure exceeds the inflator pressure capability, to the number of Monte Carlo Iterations, is the calculated POF. This portion of the model is probabilistic based on the determined state of the overall system.

The inflator predictive aging model calculates the POF for various Takata inflators. Testing has demonstrated that temperature cycling, in the presence of moisture in the inflator, drives moisture transfer in and out of the PSAN propellant. Propellant moisture transfer is correlated to damage expressed as a reduction in propellant density. As density decreases, the probability that the inflator will experience a failure increases. Since the damage of the propellant depends on moisture and temperature, the POF depends on the inflator type, the climate where the vehicle resides, the type of vehicle and how that vehicle is used. The predictive aging model considers all of those variables in predicting a POF.

Figure 9 shows the general architecture of the predictive aging model. The model can be broken into three main parts: 1) the “environment module,” 2) the “inflator module” and 3) the “performance module.” The environment module uses weather data and calculates the humidity surrounding the inflator and the inflator temperature. The inflator module determines how much moisture enters or leaves the inflator, and the moisture moving between booster, propellant, desiccants and the inflator headspace. This moisture movement is used to calculate the cumulative damage integral (*Cintegral*) that is directly related to the moisture transfer into and out of the main propellant (2004 or 2004L). From the *Cintegral*, the density change of the propellant is calculated using inflator-specific data obtained from scientific aging built with known moisture levels. Finally, the performance module calculates the POF by calculating the peak pressure (with uncertainty) and comparing that to the inflator pressure capability (with uncertainty).

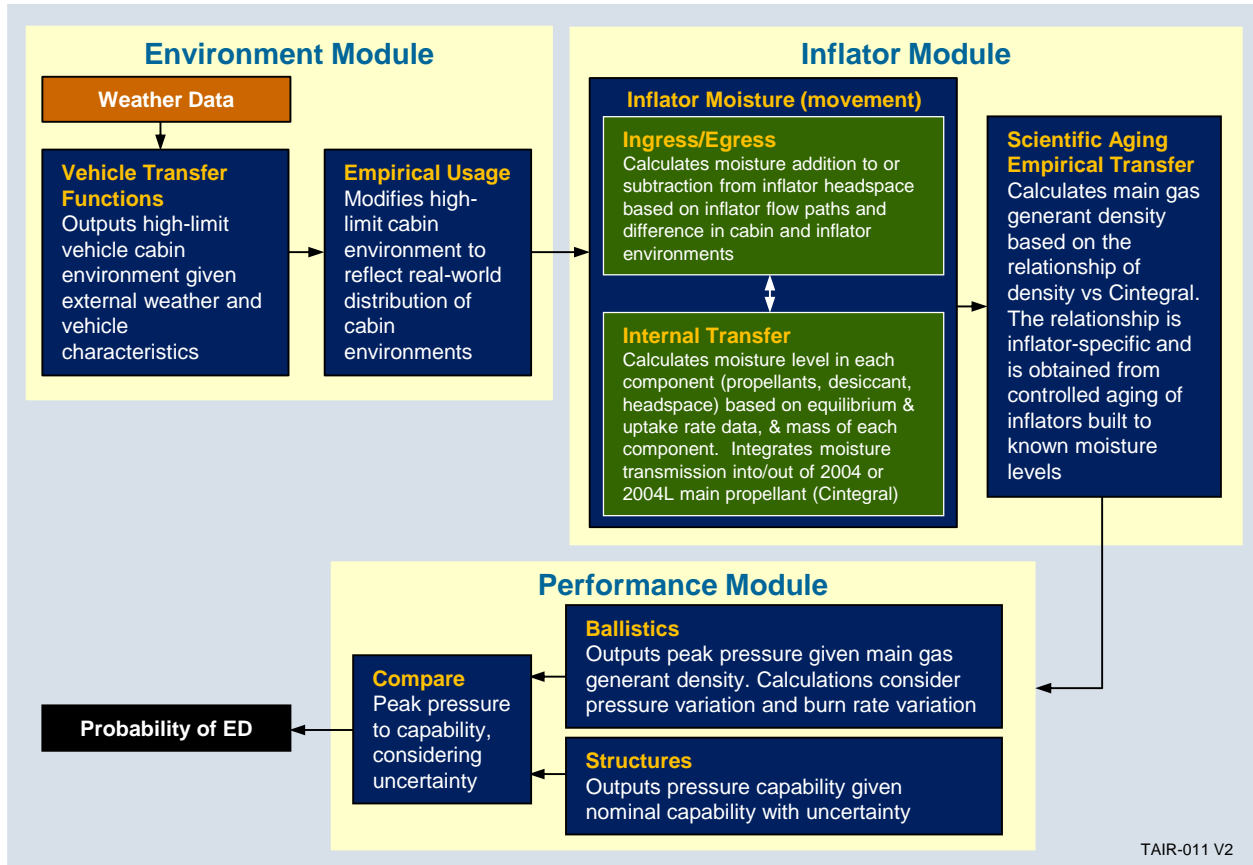


Figure 9. Architecture of the Takata Inflator Predictive Aging Model

### Environment Module

The first part of the environment module calculates the inflator temperature under the assumption that the vehicle is parked outside with the windows rolled up and is not in the shade. The following equation describes the vehicle cabin temperature  $T_c$

$$\frac{dT_c(t)}{dt} = \frac{A_w}{V_c \rho_{air} c_{p,air}} [C_1 h(T_{ambient}(t) - T_c(t)) + UF C_2 \tau G_{0,corrected}(t)] \quad 1$$

where  $A_w$  is the area of the windows,  $V_c$  is the volume of the vehicle cabin,  $\rho_{air}$  is the air density,  $c_{p,air}$  is the specific heat capacity of air,  $h$  is the convective heat transfer coefficient for air,  $T_{ambient}$  is the ambient temperature outside of the vehicle,  $\tau$  is the transmittance of solar radiation through the windows and  $G_{0,corrected}$  is the solar irradiance. An empirical usage factor ( $UF$ ) is included to account for variability in how a vehicle is used and is described in more detail. For a vehicle parked outside with the windows rolled up, the usage factor is set to  $UF = 1.0$ .

Equation 1 considers both convective and radiative heat transfer. The weighting of these two heat transfer terms ( $C_1$  and  $C_2$ ) are determined by fitting the model to measured inflator

temperature data for vehicles sitting in the sun. This module was validated using empirical data from field experiments on a range of vehicles (Atlas Material Testing Solutions “Vehicle Environmental Testing Project – Project Number C0010361, Rev1a” will refer to as “ATLAS” further in this report).

The model will work for any combination of inputs that match the characteristics of a given vehicle, geographic location (determines weather and incident angle for the sun), and usage factor. To provide data across the range of vehicles of interest, limit the number of vehicles cases that would need to be run and provide real-world calibration, we selected three specific vehicles from the ATLAS study. One was a vehicle that exhibited at or near the highest temperatures and was designated as T3. A mid-range vehicle was also selected and designated T2. Finally, a vehicle among those that exhibited the lowest peak temperatures was selected and designated as T1. These three vehicles and their associated models were used consistently through the model development and test runs.

The three temperature bands are shown graphically in Figure 10. They were selected and defined based on responses in a controlled environment of consistent testing in the Miami climate in August through September 2015. Roughly, T1 is vehicles that have maximum temperatures of the inflator below  $\sim 60^{\circ}\text{C}$ . The second band, T2 includes vehicles that exhibit maximum inflator temperatures up to  $\sim 65^{\circ}\text{C}$ . Finally, the highest temperature band, T3, represents those vehicles that have maximum inflator temperatures near or slightly above  $70^{\circ}\text{C}$ .

For exercising the model, a specific, representative vehicle was selected that fits the definition well. Certainly, the specific parameters for another vehicle would be slightly different. Care should be taken comparing the temperature data in this study with other efforts as many parameters would need to be controlled and validated to prove beyond reasonable doubt that the comparison between different data collection methods, times or locations can be made.

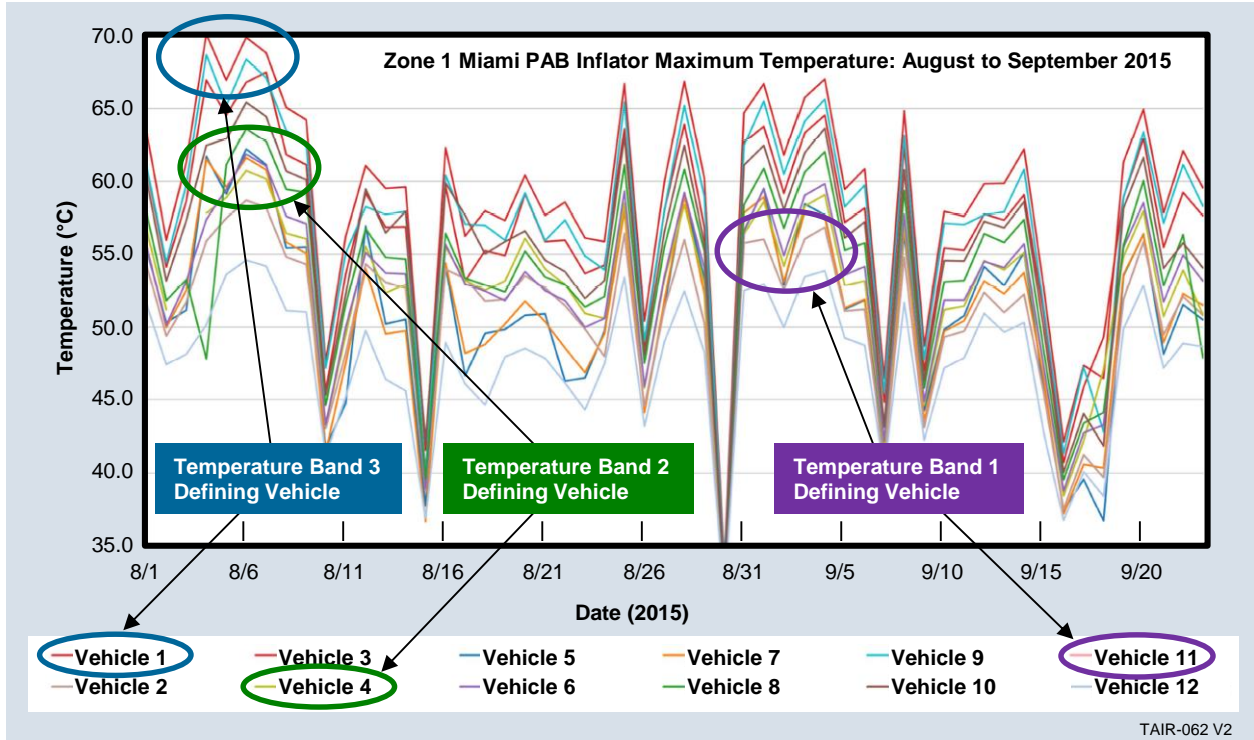


**Figure 10. Definition of Vehicle Temperature Bands Taken from Empirical Data.**

Data from the ATLAS testing showed that different vehicles exhibited different peak temperatures when exposed to identical conditions. Some exhibited higher maximum temperatures and others lower. This is characteristic of that vehicle. For our model development, we used three specific vehicles as archetypes of ranges of achieved temperatures. Our POF is reported by the vehicle temperature bands. Calculating the cabin humidity depends on the rate humidity can leak into or out of the vehicle, and depends on how the materials in the vehicle cabin hold and release moisture as a function of changing temperature. A schematic showing how moisture can leak into or out of the vehicle cabin and how a reservoir of moisture can be absorbed by materials in the car is shown in Figure 11. Because the vehicle is not sealed, moisture can enter or leave the vehicle cabin relatively easily. Furthermore, experiments showed that the reservoir releases moisture with increasing cabin temperature.



**Figure 11. Moisture Movement in a Vehicle Cabin**

The following three coupled equations describe the moisture leaking in and out of the cabin  $n_{H_2O}$  (Equation 2), the moisture absorbed by the cabin materials  $n_R$  (Equation 3) and the absolute humidity in the vehicle cabin  $AH_C$  (Equation 4):

$$\frac{dn_{H_2O}(t)}{dt} = k_1(AH_{ambient} - AH_C(t)), \quad 2$$

$$\frac{dn_R(t)}{dt} = k_2(n_R^*(VP_C(AH_C), T_C) - n_R(t)), \text{ and} \quad 3$$

$$\frac{dAH_C(t)}{dt} = \frac{0.001 \cdot mw_{Water}}{V_C} \left[ \frac{dn_{H_2O}(t)}{dt} - \frac{dn_R(t)}{dt} \right], \quad 4$$

where  $k_1$  and  $k_2$  are rate constants,  $AH_{ambient}$  is the ambient absolute humidity,  $V_C$  is the cabin volume and  $mw_{Water}$  is the molecular weight of water. The equilibrium number of moles of water absorbed in the cabin materials,  $n_R^*$ , is a function of cabin vapor pressure,  $VP_C$ , and temperature,  $T_C$ . The humidity vehicle transfer function has four parameters that are determined by fitting the model to measured vehicle humidity and temperature. The four fit parameters are the two rate constants  $k_1$  and  $k_2$ , as well as two parameters used to describe  $n_R^*$ .

The final part of the environment module deals with typical usage. The majority of vehicles are not parked outside in the sun for their entire lifetime, so an empirical usage factor ( $UF$ ) is used that captures the effects of parking the vehicle in the shade, “cracking” the windows, or parking in a garage. This factor has a value between 0 and 1 and scales the  $C_2$  weighting factor in Equation 1. The usage factor drops the maximum predicted temperature calculated with Equation 1. This approach to usage affects the predicted cabin temperature directly and the cabin humidity indirectly because of the dependence of the humidity transfer function on temperature. The usage factor is associated with the exposure of the car to the full effect of the ambient weather. For example, a lower  $UF$  would be expected for a car that spends much of the time in a climate controlled garage compared to one consistently parked outside in an area without shade. Interestingly, the most severe 1% of aging vehicles may not always be those with the highest temperature as this may lead to reduced moisture from drying and consequently slower aging. An obvious example of this phenomena is for vehicles in Phoenix where the vehicle temperature regularly exceeds that in Miami but inflators age much better. Further, the model predicts that even in the very humid Miami-like environment that the highest usage factor on the T3 vehicle is not the most rapidly aging but rather a 0.6-0.8 usage factor. At this lower usage factor, the model predicts higher moisture in the inflator and more moisture movement resulting in faster aging and greater density reduction.

There were two requirements needed to determine the empirical usage factor ( $UF$ ). First is a large dataset where the distribution of propellant density could be determined for a given platform, geographic location and inflator age. Second was an aging model that could predict the propellant density for a given platform, geographic location and inflator age. The  $UF$  was determined by running the Northrop Grumman aging model and comparing the predicted propellant density to the distribution of measured propellant densities for a given platform, geographic location and inflator age. By iteratively performing this procedure, the usage factors for different platforms and percentile vehicles were determined. MEAF data for the PSPI-L FD inflator was used to determine the usage factors since this was the largest dataset available and

provided the best distribution of measured densities. The usage factors for the different platforms and vehicle percentiles were determined from Zone 0 where most of the MEAF data was gathered. An empirical match was made to field return density reduction distributions. Usage factors were assumed to not be location dependent. A modest effort of monitoring vehicle typical usage in Zone 0 (West Palm Beach, FL) and Zone 4 (Northern Utah) was completed in 2018. These data supported the impact of usage on the environment actually experienced by an inflator. The data were indicative but not of sufficiently large number to be statistically useful in this study.

### Inflator Module

The inflator module takes the temperature and humidity calculated in the environment module and uses those as the inflator boundary conditions. The inflator module considers moisture leaking into and out of the inflator by considering both capillary-like leaks (i.e., leaks through small holes) as well as moisture permeability (i.e., moisture diffusing through O-rings or other polymeric materials). The inflator module also considers capillary-like leaks between the primary and secondary chambers. Inside the inflator, moisture transfer between booster, propellant and desiccant, via the inflator headspace, is calculated. An inflator module moisture movement diagram is shown in Figure 12.

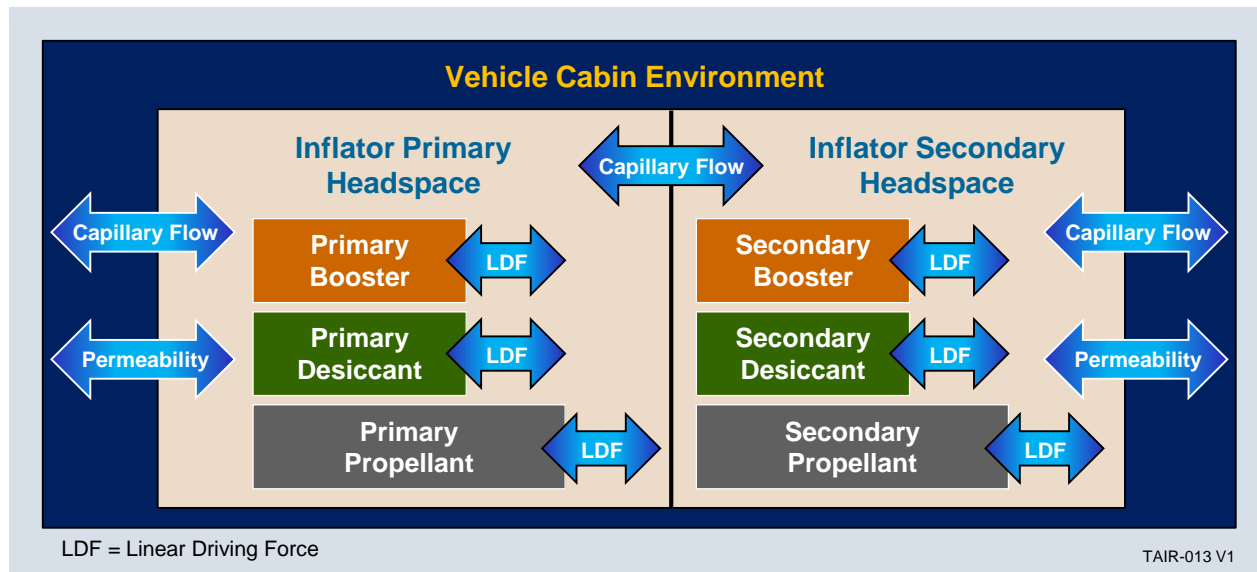


Figure 12. Inflator Moisture Movement Diagram

The equation describing capillary-like leak rate is described in Equation 5.

$$q_{air}(P_c, P_i, T) = \frac{1}{RT} \left\{ \frac{\pi r(t)^4}{16\eta l} (P_c^2 - P_i^2) + \frac{\sqrt{2\pi}}{6} \sqrt{\frac{RT}{0.001mw_{air}}} \frac{d(t)^3}{l} (P_c - P_i) \right\}. \quad 5$$

where  $R$  is the gas constant,  $r$  and  $d$  are the radius and diameter of the capillary,  $l$  is the capillary length,  $\eta$  is the viscosity of air and  $mw_{air}$  is the molecular weight of the air. The driving force depends on a difference in total pressure between the vehicle cabin ( $P_c$ ) and the interior of the

inflator ( $P_i$ ). For the case of a capillary-like leak between the primary and secondary chambers, the driving force depends on the pressure difference between the primary and secondary chambers. The capillary-like leak rate is tunable via leak radius and length.

The equation describing the moisture permeability leak rate is shown in Equation 6.

$$q_{H_2O}(\Delta VP, T) = \frac{1000 \cdot A_p \cdot \Pi(T) \cdot \Delta VP}{l_p \cdot mw_{Water}} \quad 6$$

where  $A_p$  is the area and  $l_p$  is the thickness of the material through which the moisture diffuses and  $\Pi$  is the permeability of the O-ring to moisture. The driving force for the permeability leak is a difference in vapor pressure  $\Delta VP$  between the vehicle cabin and the inflator interior.

The inflators typically contain two to three materials that can absorb water, namely the booster, propellant and desiccant. Since the moisture movement in and out of propellant is strongly correlated to material damage, and subsequently POF, the inflator module must track the movement of moisture in and out of these materials. The evolution of moisture concentration in each material is calculated using the linear driving force model shown in Equation 7.

$$\frac{dC_{H_2O}(t)}{dt} = k_{LDF}(T) \left( C_{H_2O}^*(T, VP) - C_{H_2O}(t) \right), \quad 7$$

where  $k_{LDF}$  describes the rate at which the system approaches equilibrium. Here the driving force is the difference between the current moisture concentration,  $C_{H_2O}$ , and  $C_{H_2O}^*$  (the equilibrium moisture concentration for a given  $T$  and  $VP$ ).

The linear driving force model requires moisture equilibrium models for each material, as well as equilibrium rate constants  $k_{LDF}$ . The moisture equilibrium models were either derived in house, or determined empirically, but all were anchored to measured data. The kinetics (i.e., moisture transfer rates) were also determined from analysis of moisture uptake data.

After calculating the moisture content history in the propellant, the damage can be estimated using the cumulative damage integral provided in Equation 8 .

$$C_{integral}(t) = \int_0^t \left| \frac{dC_{H_2O}(t')}{dt'} \right| dt' \quad 8$$

The *Cintegral* is directly related to the amount of moisture that enters and leaves the propellant and is driven by humidity cycling and / or temperature cycling in the presence of moisture. The *Cintegral* is strongly correlated with the change in propellant density and the density can be calculated using the inflator-specific master curve relating density to *Cintegral*. Master curves are generated for each inflator by using our scientific aging data where inflators, with known moisture levels, are aged in controlled conditions.

The critical output of the inflator module is the propellant density that is input into the performance module. Other intermediate calculations are also stored such as the moisture content

in the materials and the propellant diameter so they can be compared to measured values from field returned inflators.

### Performance Module

The heart of the inflator performance module is a Northrop Grumman, in-house, well-proven ballistics code that calculates inflator internal peak pressure. The code is based off of a mass flow rate balance as shown in Equation 9.

$$\dot{M}_{gen} = \dot{M}_{exit} + \dot{M}_{stored} \quad 9$$

where  $\dot{M}_{gen}$  is the mass flow rate generated by the combustion of the propellant,  $\dot{M}_{exit}$  is the mass flow rate exiting the inflator through the nozzles and  $\dot{M}_{stored}$  is the mass flow rate stored in the headspace of the inflator. The generated mass flow rate is provided in Equation 10.

$$\dot{M}_{gen} = \rho_{prop} A_{surface} r_b \quad 10$$

where  $\rho_{prop}$  is the propellant density,  $A_{surface}$  is the surface area of the propellant and  $r_b$  is the propellant burn rate. The mass flow rate exiting the inflator is shown in Equation 11.

$$\dot{M}_{exit} = \rho_{gas} A_{throat} v_{sonic} \quad 11$$

where  $\rho_{gas}$  is the density of the gas generated,  $A_{throat}$  is the cross-sectional area of the nozzle throat and  $v_{sonic}$  is the sonic speed of the gas. In steady-state conditions  $\dot{M}_{gen} = \dot{M}_{exit}$  and the inflator operates with a constant internal pressure (i.e., constant  $\rho_{gas}$ ). In general, the inflators are not in steady-state so the stored mass flow rate must also be considered as shown in Equation 12.

$$\dot{M}_{stored} = \frac{d}{dt} (\rho_{gas} V_{headspace}) \quad 12$$

where  $V_{headspace}$  is the inflator headspace volume. The operation of the inflator is very dynamic with many variables changing over time. For example,  $A_{surface}$  changes as the propellant breaks up and burns,  $r_b$  depends on  $\rho_{gas}$  (i.e., inflator pressure), and  $V_{headspace}$  changes as the propellant is burned.

To calculate the peak inflator pressure, the ballistics code considers a number of inflator-specific parameters including propellant mass, propellant geometry, density, inflator free volume, tape burst pressure, propellant burn rate versus pressure and density, igniter output, and combustion efficiency versus pressure. The density of the propellant is a critical value in the ballistics code because there can be a pronounced augmentation of the propellant burn rate as the density decreases. For anchoring, the pressure-time trace, and its variation, are matched to scientific aging tank testing.

The structural model outputs the inflator pressure capability, with uncertainty. The pressure capability and uncertainty were determined for each inflator using basic structural analysis techniques that consider inflator materials and design and are anchored to the results of pressure vessel testing.

The performance module uses a Monte Carlo approach to calculate the POF. Within each Monte Carlo iteration, the peak inflator pressure is determined considering the burn rate change (corresponding to the propellant density change) and other ballistics model input parameters, a subset of which are random variates. This peak inflator pressure is then compared to a random variate of inflator pressure capability obtained from the structural model. The ratio of the number of times the peak pressure exceeds the inflator pressure capability to the total number of Monte Carlo iterations is the POF. For the work presented here, 32,000 Monte Carlo iterations were performed at each time step.

It was impractical to run the complete ballistics code for each iteration of the Monte Carlo so a surrogate ballistics model was developed. This surrogate model is based on the results of running the ballistics model, in advance, to get the peak pressure for select model inputs. This Design of Experiments (DOE) results in a table of peak inflator pressures corresponding to the given model inputs. An example of a ballistics DOE table is shown in Table 5. The inherent variation referred to in Figure 13 is related to the variation in peak pressure in the pressure versus time traces for virgin inflators as highlighted in Figure 14. The augmented burning variation shown in Figure 13 refers to the variability in the burn rate curves for PSAN propellant with nominally the same density. This augmented burning variation is highlighted in Figure 14. The surrogate model is used each Monte Carlo iteration by using multivariable interpolation with the predicted propellant density, a random variate of augmented burning variation and a random variate of inherent variation as model inputs.

**Table 5. Example Ballistics DOE**  
**PEAK Pressure (MPa) Ballistic Simulation DOE**

Inherent Variation/Mass Balancing Factor, Mpa	Augmented Burning Variation	2004 Density, gm/cc				
		1.8	1.667	1.603	1.567	1.496
High	High			94.1	144	150
	Mean	44	44.0	76.2	140	147
	Low			43.1	134	143
Medium	High			75.5	138	148
	Mean	37.7	37.7	38.8	132	145
	Low			30.2	123	141
Low	High			34.0	112	146
	Mean	31.9	31.9	27.8	121	142
	Low			20.9	109	138

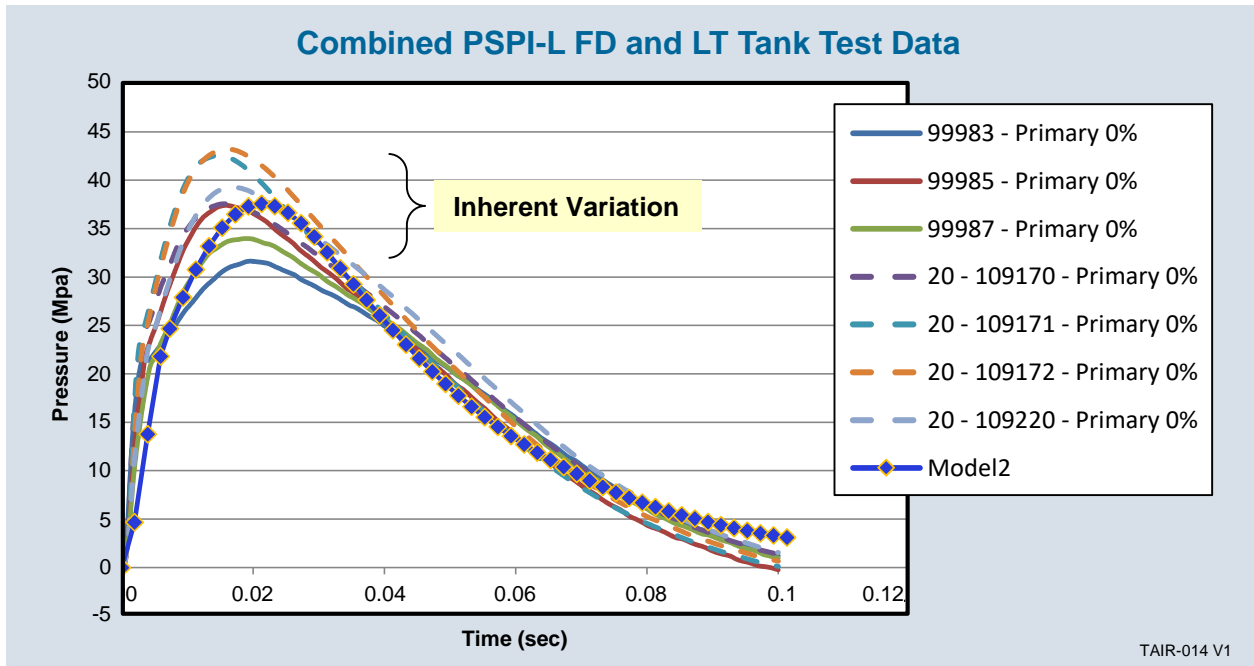


Figure 13. Pressure vs Time Traces for a Virgin Inflator Showing Inherent Variation

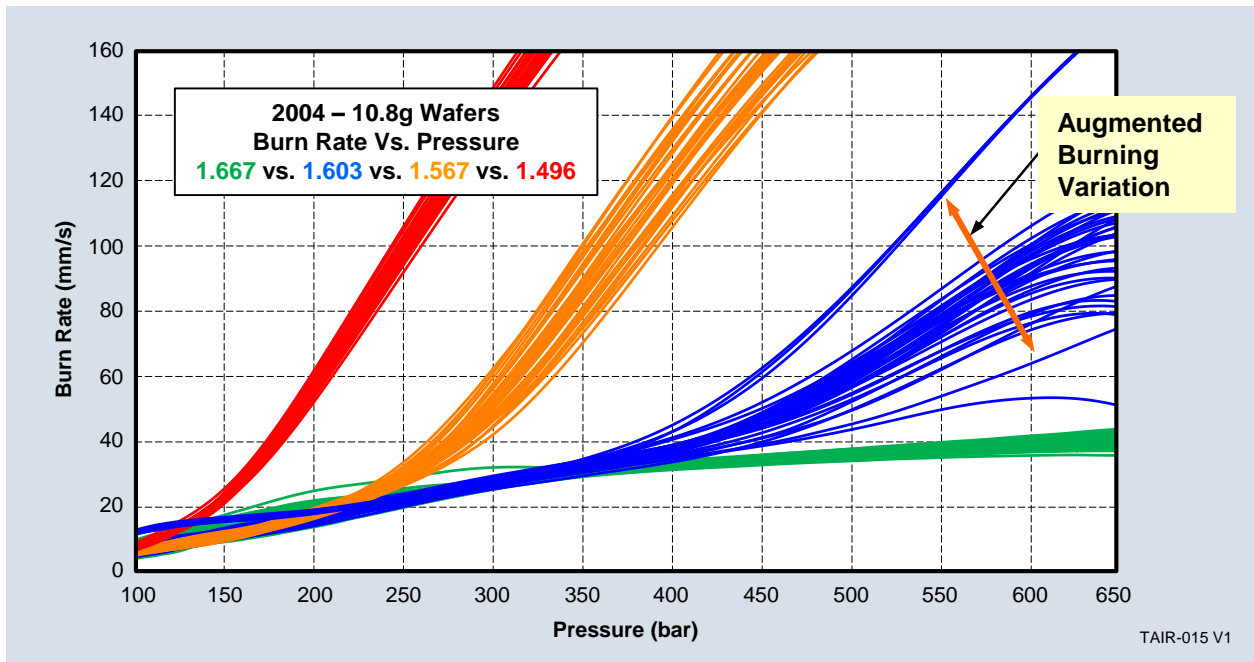


Figure 14. Apparent Burn Rate vs Pressure for Different Propellant Density with the Augmented Burning Variation Highlighted; Lower Density Results in Higher Pressure

**Key Inputs, Key Outputs, and Anchoring / Parameterization Data**

Model predictions are only as good as the data inputs. Quality data must define the boundary conditions and allow model parameters to be precisely determined. Anchoring data must be available to calibrate the model. Northrop Grumman utilized data from: 1) internal laboratory testing, 2) scientific aging, 3) weather data from the National Weather Service, 4) vehicle cabin environment (temperature and humidity) from ATLAS study and report, 5) vehicle and laboratory data from multiple Original Equipment Manufacturers (OEM), 6) a wide variety of laboratory data from Takata and 7) parameter values from the literature.

At multiple stages in the model, calibration and anchoring were done with the help of the MEAF. The MEAF is a large database, maintained by Takata, which contains results of testing performed on tens of thousands of field-returned inflators. Table 6 contains a relatively complete list of the key model inputs and outputs, describes the parameters of each subroutine, explains the data used to determine model parameters and lists the data to which the model was calibrated and / or anchored. Table 6 is not intended to be comprehensive, rather it illustrates the wide variety of data and data sources used by Northrop Grumman’s predictive aging model. Note the flow of data from one subroutine to the next and from the Environment Module, to the Inflator Module, and finally to the Performance Module.

**Table 6. Key Inputs, Model Parameters, Subroutines, Outputs and Parameterization / Anchoring Data for the Environment, Inflator and Performance Modules**

Inputs	Parameters	Subroutines	Outputs	Data for Parameterization and Anchoring
<b>Environment Module</b>				
<ul style="list-style-type: none"> <li>• National Weather Service (10-years of data for each location)</li> <li>• Geographic location</li> <li>• Vehicle Type</li> </ul>	<ul style="list-style-type: none"> <li>• Vehicle size</li> <li>• Glass geometry</li> <li>• Glass transmittance</li> <li>• Six fit parameters for vehicle transfer function model</li> </ul>	<b>Vehicle Transfer Function</b>	High-limit cabin temperature and humidity	<ul style="list-style-type: none"> <li>• ATLAS: vehicle response to external environment</li> <li>• OEM data</li> <li>• Literature values</li> <li>• Northrop Grumman-measured vehicle temperature and humidities</li> </ul>
<ul style="list-style-type: none"> <li>• High-limit cabin temperature and humidity</li> <li>• Vehicle usage level</li> </ul>	<ul style="list-style-type: none"> <li>• Usage Factor (UF)</li> </ul>	<b>Empirical Usage</b>	Modified cabin temperature and humidity	<ul style="list-style-type: none"> <li>• Statistical analysis of MEAF density to get percentiles by platform, zone and inflator</li> </ul>
<b>Inflator Module</b>				
<ul style="list-style-type: none"> <li>• Modified cabin temperature and humidity</li> </ul>	<ul style="list-style-type: none"> <li>• Capillary leak size</li> <li>• Permeability</li> </ul>	<b>Inflator Moisture Ingress / Egress</b>	How much moisture leaked into or out of inflator headspace	<ul style="list-style-type: none"> <li>• MEAF moisture vs age</li> <li>• OEM leak-rate data</li> <li>• Literature values for EPDM</li> </ul>

Inputs	Parameters	Subroutines	Outputs	Data for Parameterization and Anchoring
	<ul style="list-style-type: none"> <li>Permeability flow geometry</li> <li>Inflator headspace volume</li> </ul>			<ul style="list-style-type: none"> <li>permeability</li> <li>Inflator design information</li> </ul>
<ul style="list-style-type: none"> <li>How much moisture leaked into or out of inflator headspace</li> </ul>	<ul style="list-style-type: none"> <li>Gas generant and desiccant moisture equilibrium models</li> <li>Gas generant and desiccant moisture uptake rates</li> <li>Inflator headspace volume</li> <li>Gas generant and desiccant types and masses</li> </ul>	<b>Inflator Internal Moisture Transfer</b>	Moisture content in generants, desiccants and headspace. Cintegral for main generant.	<ul style="list-style-type: none"> <li>Moisture transfer experiments (T-Cell, Parr Bomb, etc.) by Takata and Northrop Grumman</li> <li>Moisture uptake experiments and vapor sorption analyzer (VSA experiments by Takata and Northrop Grumman)</li> <li>Moisture equilibrium experiments done in academia</li> <li>Inflator design</li> <li>MEAF moisture data</li> <li>Takata moisture specifications</li> </ul>
<ul style="list-style-type: none"> <li>Cintegral for main generant</li> </ul>	<ul style="list-style-type: none"> <li>Fit of density vs Cintegral data generated from analysis of scientific aging data</li> </ul>	<b>Scientific Aging (SA) Empirical Transfer Function</b>	Main propellant density	<ul style="list-style-type: none"> <li>Inflator-specific scientific aging data that includes temperature, number of cycles, total moisture and measured density</li> <li>MEAF data for starting propellant density</li> <li>MEAF data for evolution of density over time for a given platform and zone</li> </ul>
<b>Performance Module</b>				
<ul style="list-style-type: none"> <li>Main propellant density</li> </ul>	<ul style="list-style-type: none"> <li>Gas generant(s) mass</li> <li>Generants geometry</li> <li>Generant burn rate (pressure, density variation)</li> <li>Combustion</li> </ul>	<b>Ballistics</b>	Peak inflator pressure	<ul style="list-style-type: none"> <li>Scientific aging tank 0-time and 480 cycle nominal and mid-moisture tank pressures vs time traces</li> <li>Scientific aging heavyweight testing for igniter vs main grain</li> <li>Takata burn rate vs</li> </ul>

<b>Inputs</b>	<b>Parameters</b>	<b>Subroutines</b>	<b>Outputs</b>	<b>Data for Parameterization and Anchoring</b>
	efficiency (pressure) <ul style="list-style-type: none"> <li>• Throat area</li> <li>• Burst tape release pressure</li> <li>• Nominal inherent variation in peak pressure</li> <li>• Inflator headspace volume</li> </ul>			pressure, density and form factor <ul style="list-style-type: none"> <li>• Inflator design</li> <li>• Scientific aging dissection as-built parameters</li> <li>• Laboratory tests of field-return inflators</li> </ul>
<ul style="list-style-type: none"> <li>• Case Structural Capability</li> </ul>	<ul style="list-style-type: none"> <li>• Mean and standard deviation of pressure vessel capability</li> </ul>	<b>Structural</b>	Pressure capability	<ul style="list-style-type: none"> <li>• Takata pressure vessel test data</li> <li>• Inflator design and material specifications</li> <li>• Finite element analysis for failure modes and level</li> <li>• Closed form thin-wall pressure vessel calculations</li> <li>• Scientific aging ED vs no ED results</li> </ul>
<ul style="list-style-type: none"> <li>• Peak inflator pressure</li> <li>• Pressure capability</li> </ul>	<ul style="list-style-type: none"> <li>• Number of Monte Carlo (MC) runs. Each Monte Carlo iteration predicts ED, or no ED. Compares number of predicted EDs to total MC iterations</li> </ul>	<b>Compare Load to Capability</b>	<b>Probability of failure (POF)</b>	<ul style="list-style-type: none"> <li>• MEAF POF data by inflator, zone, platform and age</li> <li>• MEAF and field POF limit given no observed failures</li> <li>• MEAF POF vs propellant outer diameter (PSPI-L FD inflator only)</li> </ul>

Note: Overall predictive aging model inputs are bolded.

## Inflator Design

This section provides an understanding of the inflator designs by reviewing form and function at the part level. This section is organized by inflator subsystem. Passenger and driver inflators are discussed separately.

### Passenger Inflator

The three reviewed passenger inflators are similar in form and function. As such, they are discussed in general. A typical passenger inflator is shown in Figure 15 and Figure 16. These

inflators are packed with multiple parts, some of which have multiple functions. They have a larger primary chamber and a smaller secondary chamber. Primary and secondary combustion chambers are independent; they act as two separate inflators located next to each other. Each chamber is composed of seven subsystems:

- 1) PSAN wafers - Main propellant that generates most or all of the gas that fills the air bag
- 2) Igniter - An igniter assembly that lights the main propellant and helps fill the air bag
- 3) Filter - A combustion gas cooling system that cools high-temperature combustion products before they enter the air bag
- 4) Steel case - A pressure vessel to hold the pressure created from propellant combustion
- 5) O-ring and burst tape - A moisture protection system to protect the propellants from moisture
- 6) AI cup - An auto-ignition system to safely ignite the inflator in the event of a vehicle fire
- 7) Springs - A suspension system to control shock and vibration to the main propellant

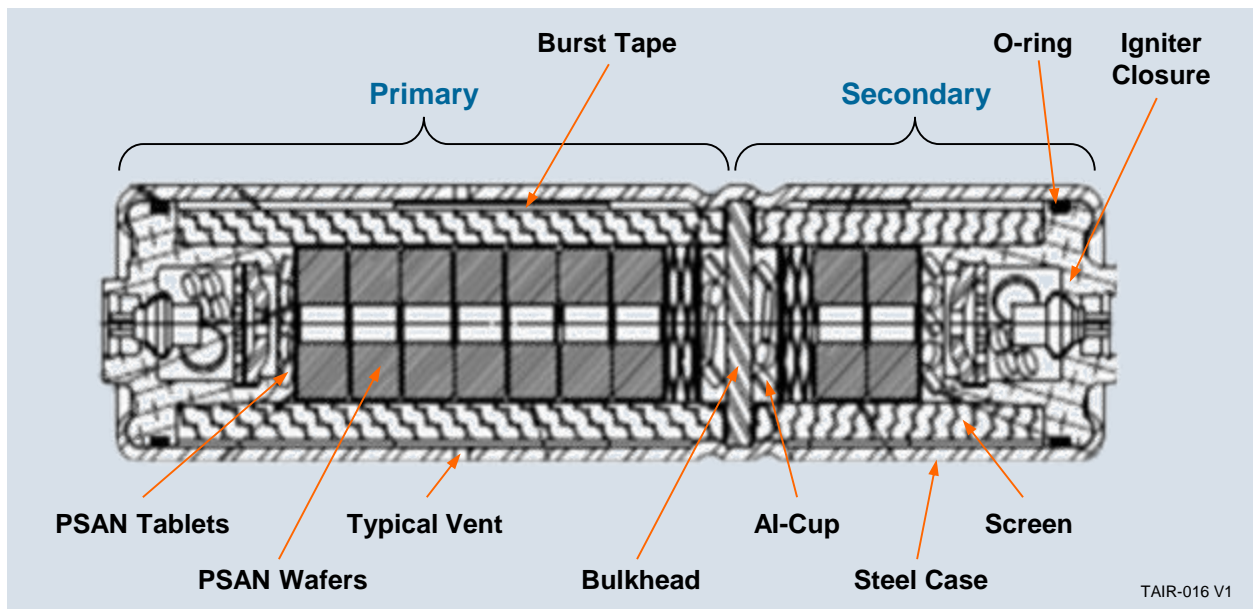
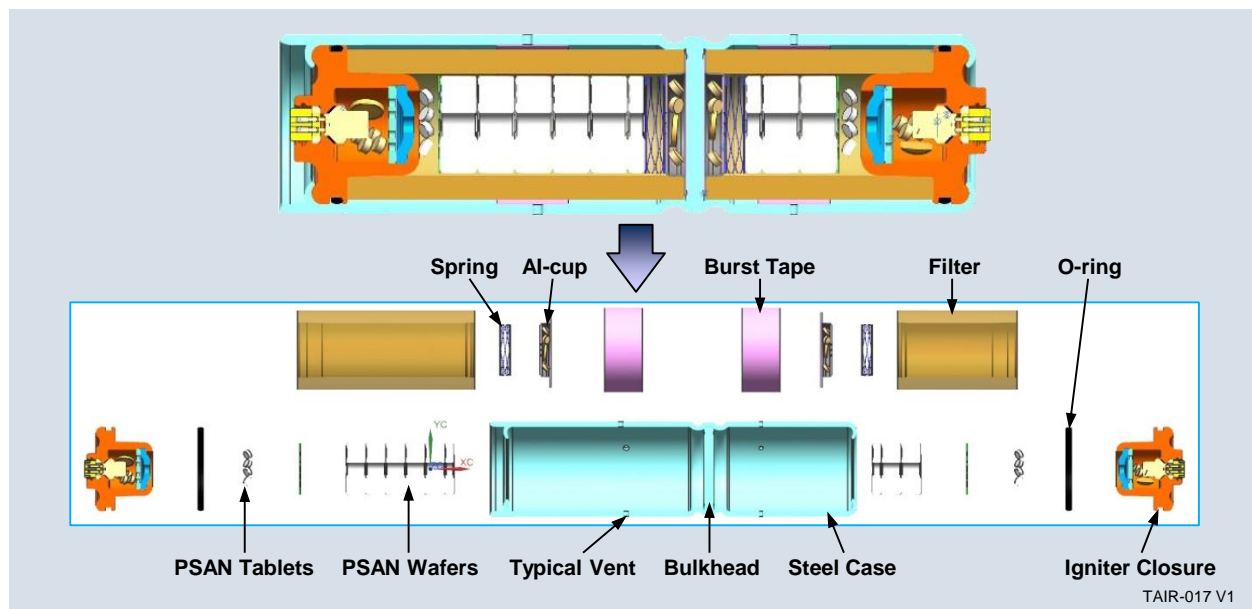


Figure 15. Typical Passenger Inflator Cross Section



**Figure 16. Typical Passenger Inflator Exploded View**

**Main Propellant**

The main propellant may be in wafer or tablet form (Figure 17). These inflators use 2004 or 2004L for the main propellant. Both 2004 and 2004L contain small amounts of materials with desiccating behavior (2004 contains 1.3% sodium bentonite, 2004L contains 0.25% fumed silica). The moisture capacity of 2004 is significantly greater than that of 2004L primarily due to five times higher level of the water absorbing sodium bentonite in 2004. Nominal initial density varies with propellant formulation and geometry. “Risers” on each wafer face help with flame spread during ignition.

Inflator	Sketch	Main Formulation	Wafer	Tablet	Initial Density
<b>PSPI-L LT/FD</b>		2004			1.675
<b>PSPI-LD DU</b>		2004			1.695
<b>PSPI-X TX</b>		2004L		None	1.664

**Figure 17. Main Propellant Geometries and Types**

Propellant gas generation rate depends on how fast the propellant burns and how much propellant surface area is available to burn. **Apparent burn rate of the main propellant increases with age.** Propellant wafers break on ignition (Figure 18) into many smaller pieces. These broken pieces affect the amount of available surface area. This break up is a design feature that is made to achieve desired gas generation rates. Wafer geometry is a design choice that affects the amount of burning surface area.

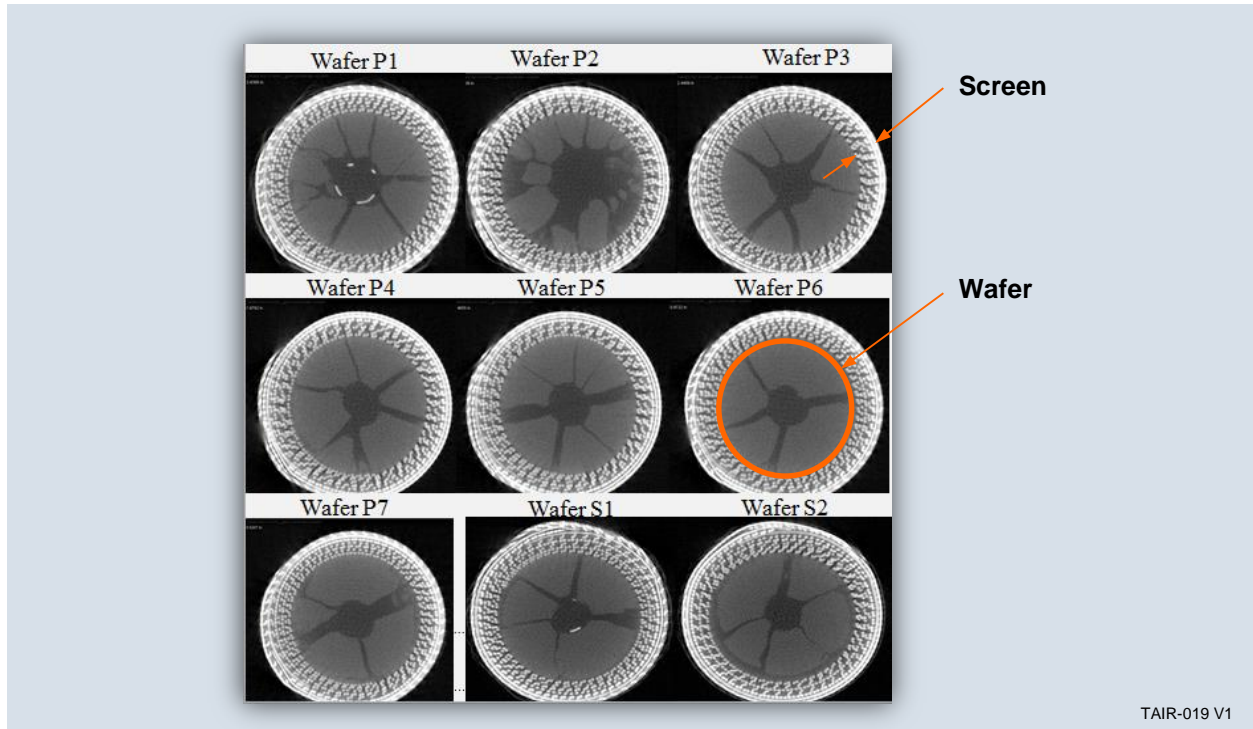


**Figure 18. Wafer Breakup on Ignition** CT images of quenched inflator tablets after ignition. These data show the typical increase in surface area from wafer break-up as a result of the ignition transient.

### Ignition System

A typical passenger igniter assembly is shown in Figure 19. The closure holds the igniter propellants and serves as an end closure for the pressure vessel. Using the campfire analogy, the initiator is the match and the boost propellant is the kindling. The boost propellant provides the heat needed to light the main propellant. **The boost propellant competes with the main propellant for moisture that is inside the inflator. This competition affects how the main propellant ages.**

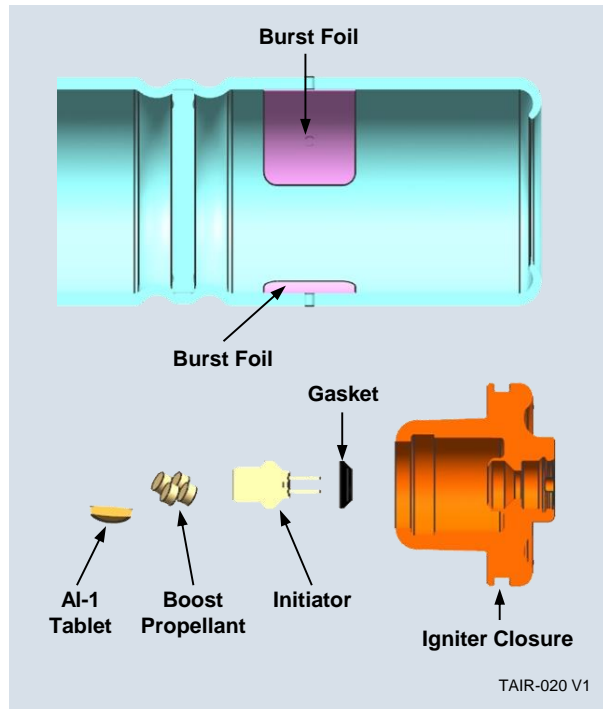


**Figure 19. Typical Passenger Ignition System**

*Moisture in the boost propellant may increase or decrease igniter output.* Igniter output affects wafer breakup on ignition. Higher output increases breakup and likelihood of ED; reduced output decreases breakup and the likelihood of ED.

The burst foil is not part of the igniter, but it is part of the ignition system. The main propellant does not burn well at low pressure. The burst foil keeps the vents closed, allowing pressure to build. Main design choices affecting burst pressure are foil thickness and vent diameter. Typical design burst pressure is 20 MPa.

The burst foil also serves as part of the moisture seal system, with the job of keeping moisture from entering the inflator through the vents.

### Gas Cooling System

A typical screen is shown in Figure 20. The screen is made of layered perforated steel and may also include a layer of ceramic paper. The screen protects the thin-wall airbag from rupture by absorbing heat from the combustion gases and trapping hot particles. The screen does not play a significant role in aging or rupture.



Figure 20. Typical Passenger Cooling Screen

### Pressure Vessel

The pressure vessel is shown in Figure 21. The cylinder is made of mild steel, which allows crimping the bulkhead and end closures in place. Closure O-rings block combustion gases from exiting during operation and serve as part of the moisture sealing system. The steel bulkhead is shared by the primary and secondary chambers. It is crimped on both sides and has no additional seal to stop gas or moisture flow between the primary and secondary chambers. If pressure gets high enough due to aging of the main propellant, the pressure vessel will rupture. However, the pressure vessel does not cause rupture.

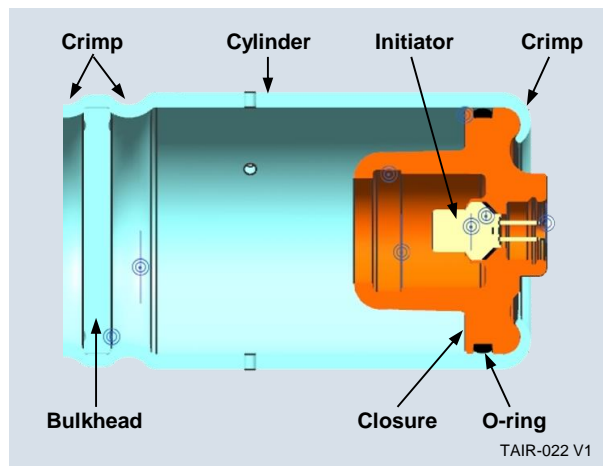


Figure 21. Typical Passenger Pressure Vessel

### Moisture Protection System

*The moisture protection system* (Figure 22) *affects when, and how fast, moisture ages the propellants.* Desiccant competes with the propellants for moisture inside the inflator. Multiple seals slow moisture transfer between the inflator interior and the environment outside the inflator. The closure-to-cylinder interface is addressed with an O-ring. The vents are covered with burst tape. The initiator-to-closure interface is sealed with a gasket or O-ring. Moisture can diffuse through the plastic initiator body, the O-rings and the adhesive on the foil seal. Moisture can travel between primary and secondary chambers through the bulkhead crimp.

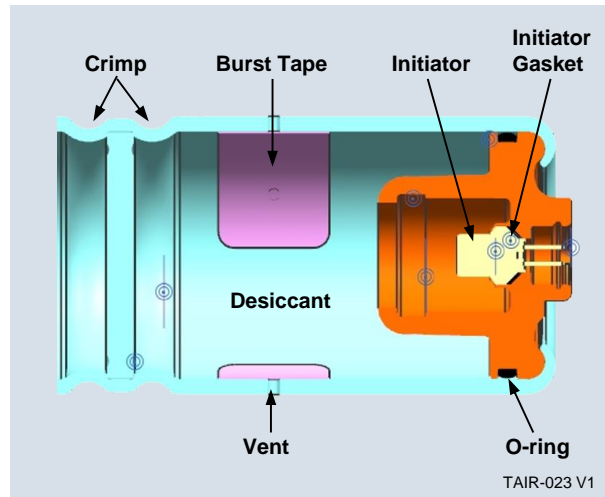


Figure 22. Typical Passenger Moisture Protection System

### Auto-ignition System

The main propellant burns faster when it is hotter. If it gets hot enough, the main propellant will light by itself. The steel pressure vessel gets weaker when it gets hotter. The job of the auto-ignition system is to prevent inflator rupture if exposed to fire, by having it deploy before it gets too hot. One AI-1 tablet is located in each AI-cup (Figure 23) and in each igniter (Figure 19). AI-1 auto-ignites at a relatively low temperature. In a fire, the intent is that the AI-1 tablets replace the initiator as the “match” in the ignition system. Inflators that use 3110 boost propellant use an AI-1 tablet. Inflators that use AIB boost propellant do not use AI-1, since AIB lights at a relatively low temperature. *AI-1 releases moisture as it degrades over time at higher temperatures. In turn, this limited amount of moisture will contribute to the overall moisture dynamic and may affect aging of the main propellant.*



Figure 23. Typical Passenger AI Cup

## Suspension System

Passenger inflators use one or more wave springs to control motion of the wafers and tablets (Figure 24). At ignition, output of the igniter pushes against the right face of the right wafer. This accelerates the wafer stack to the left, compressing the wave spring. When the spring reaches full compression, the wafers experience a sudden stop. This sudden stop becomes the part of the force that breaks the wafers into smaller pieces. Spring force varies depending on inflator design and manufacturing tolerances. Spring height and spring force are design choices that affect wafer breakup on ignition.

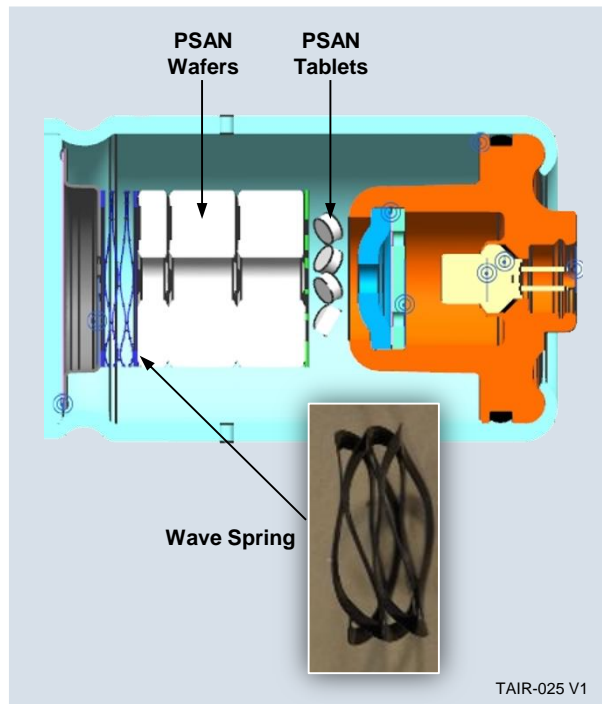
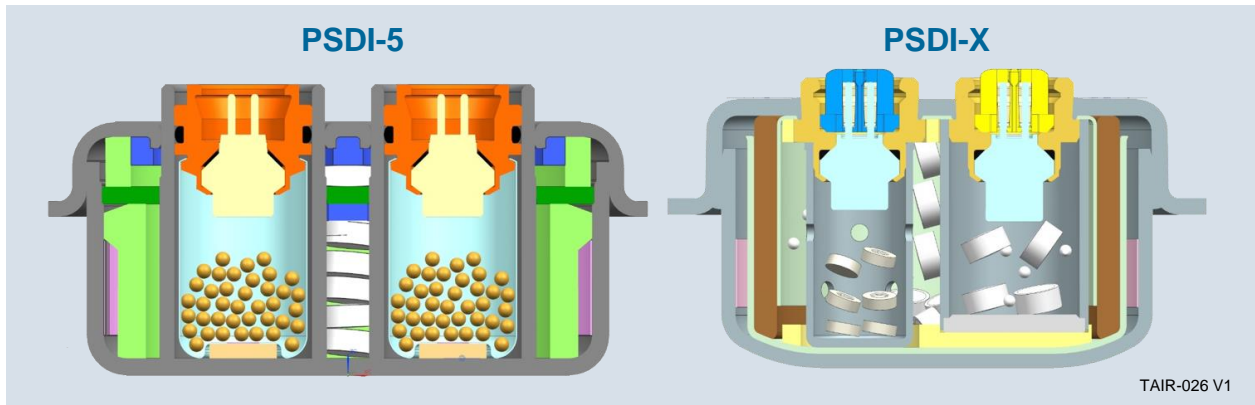


Figure 24. Typical Passenger Wafer Suppression System

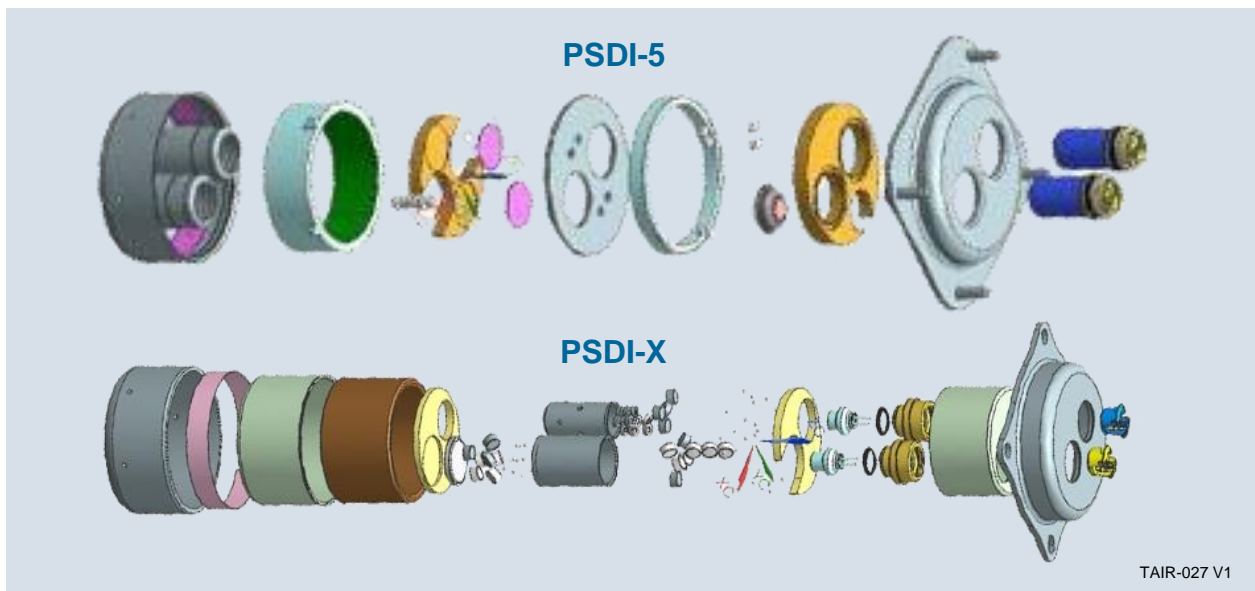
**Wave spring compression of the wafers can retard aging.** Long-term wafer compression in the presence of moisture causes the wafers to fuse together. Fusing may slow aging because less wafer surface is exposed. Fusing tends to reduce inflator pressure because the wafers break into fewer pieces during ignition.

## Driver Inflators

Three variants of the PSDI-5 inflator and one variant of the PSDI-X inflator were included in the study. PSDI-5 and PSDI-X section views are shown in Figure 25. Exploded views are shown in Figure 26. Driver inflators are “tuna can” shaped to fit in a steering wheel. Like passenger inflators, driver inflators are packed with multiple parts, some with multiple functions. They also have primary and secondary chambers. Unlike the passenger inflators, these driver inflators have dependent primary and secondary combustion; i.e. primary and secondary combustion gases share the same vents. Driver and passenger inflators have the same seven subsystems.



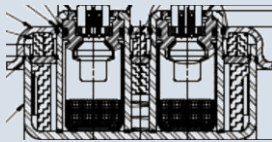
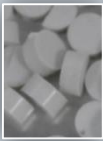
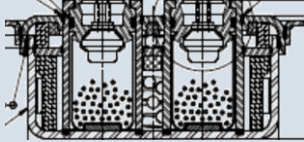
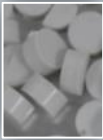
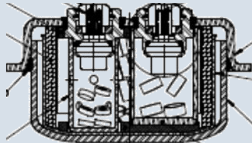
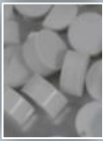
**Figure 25. Driver Inflators Section View**



**Figure 26. Driver Inflator Exploded View**

**Main Propellant**

The driver main propellant (2004 or 2004L) is in tablet form (Figure 27). Nominal initial density varies with formulation and geometry.

Inflator	Sketch	Main Formulation	Tablet	Initial Density
PSDI-5		2004		1.708
PSDI-5D		2004		1.708
PSDI-X		2004L		1.692

TAIR-028 V1

Figure 27. Driver Inflator Main Propellant Forms

Propellant gas generation rate depends on how fast the propellant burns and how much propellant surface area is available to burn. In general, tablets do not break on ignition. Design choices that affect the amount of burning surface area are the number of tablets and tablet size.

As with the passenger inflators, *density of the main propellant decreases with age. Apparent burn rate of the main propellant increases with age.*

### Ignition System

A typical PSDI-5 igniter assembly is shown in Figure 28. The closure holds the initiator and serves as an end closure for the pressure vessel. A can crimps to the closure and holds the boost propellant. As with the passenger ignition system, burst foil keeps the vents closed, allowing pressure to build. Typical design burst pressure is 20 MPa. The burst foil also serves as part of the moisture seal system, with the job of keeping moisture from entering the inflator through the vents.

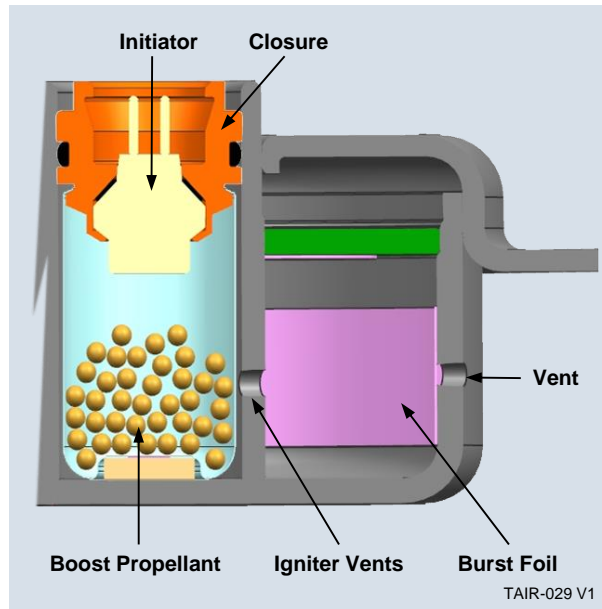


Figure 28. PSDI-5 Ignition System

Figure 29 shows the PSDI-X ignition system. This inflator has different igniters for the primary and secondary chambers. The primary uses a standard initiator and boost propellant to light the primary main propellant tablets. The secondary has no boost propellant. It uses a large initiator to push off the secondary barrier cap, which exposes the secondary propellant to the ongoing primary combustion.

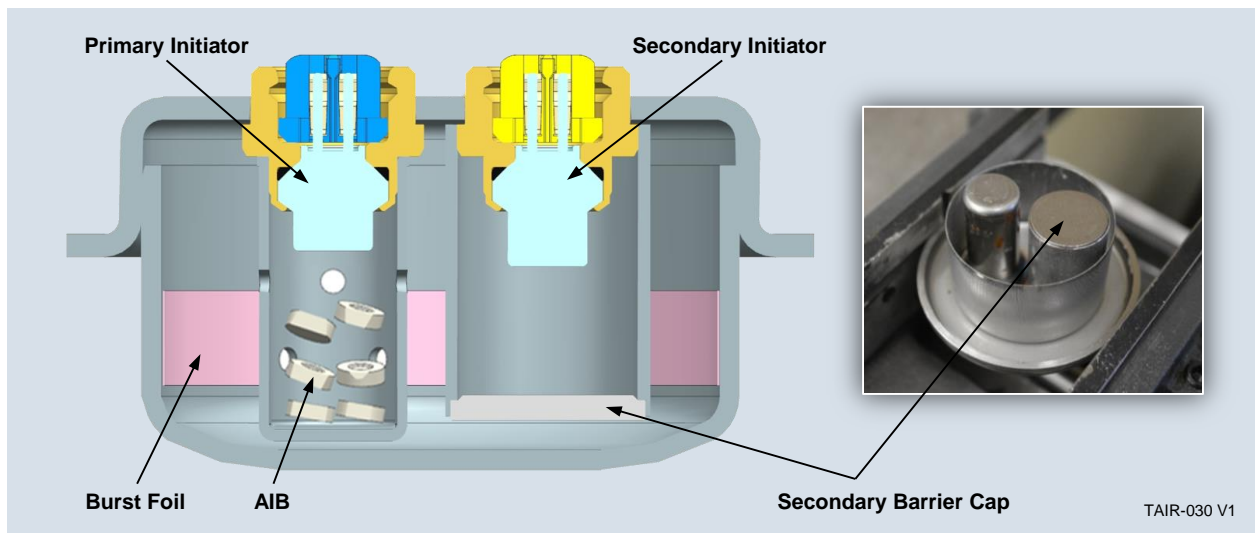


Figure 29. PSDI-X Ignition System

As with the passenger inflators, *the boost propellant competes with the main propellant for moisture that is inside the inflator. This competition affects how the main propellant ages.*

### Propellant Gas Cooling System

Figure 30 compares PSDI-5 and PSDI-X cooling systems. As with the passenger inflators, the screen is made of layered perforated steel or compressed mesh wire and may also include a layer of ceramic paper. PSDI-5 uses a radial flow screen. The PSDI-X adds inner and outer baffles to force axial flow through the screen. Neither screen type plays a notable role in aging or rupture.

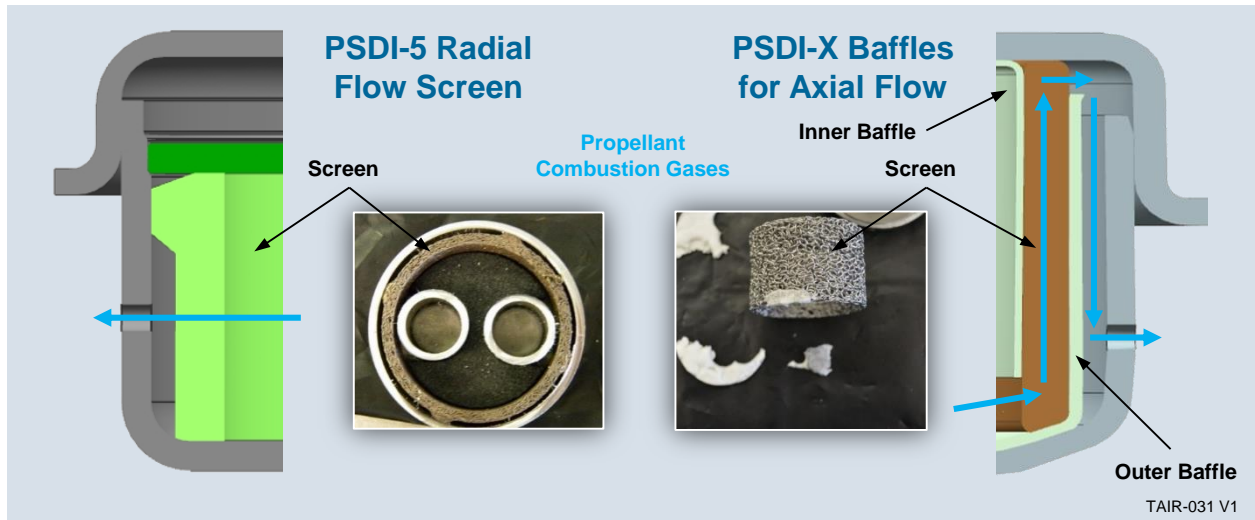


Figure 30. Propellant Gas Cooling System

### Pressure Vessel

The PSDI-5 pressure vessel is shown in Figure 31. The base, cap, bulkhead and igniter columns are a welded assembly. The initiator is crimped to the igniter closure and the igniter closures are crimped to the igniter columns. Closure O-rings and initiator gaskets block combustion gases from exiting during operation and serve as part of the moisture sealing system. The steel bulkhead separates the primary from the secondary. It has one-way ports, which hold primary-side pressure, but allow secondary propellant gas to flow to the primary side.

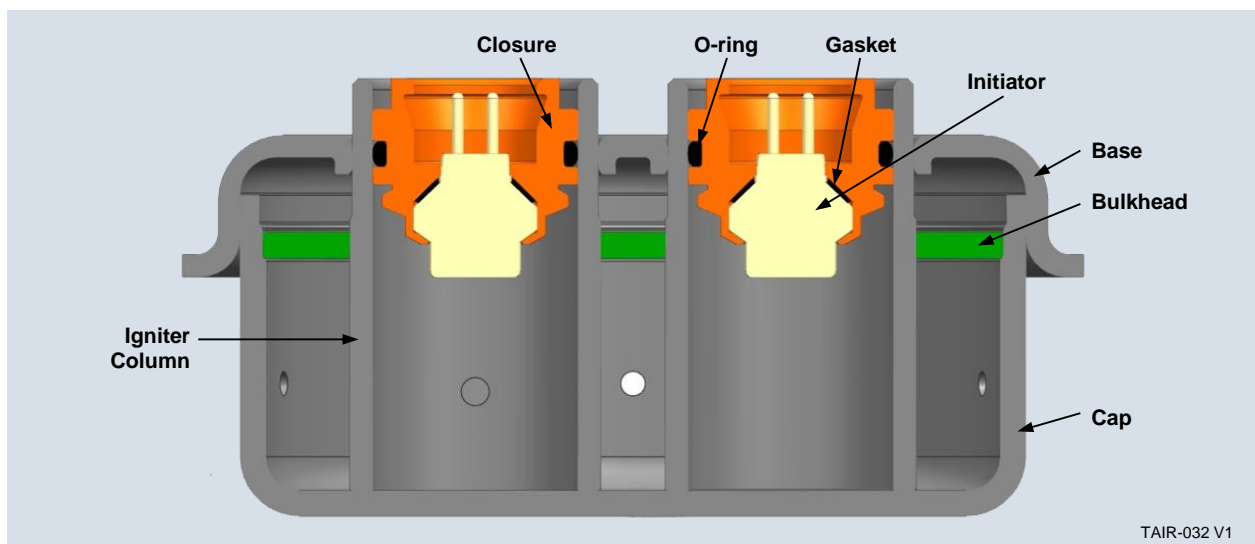
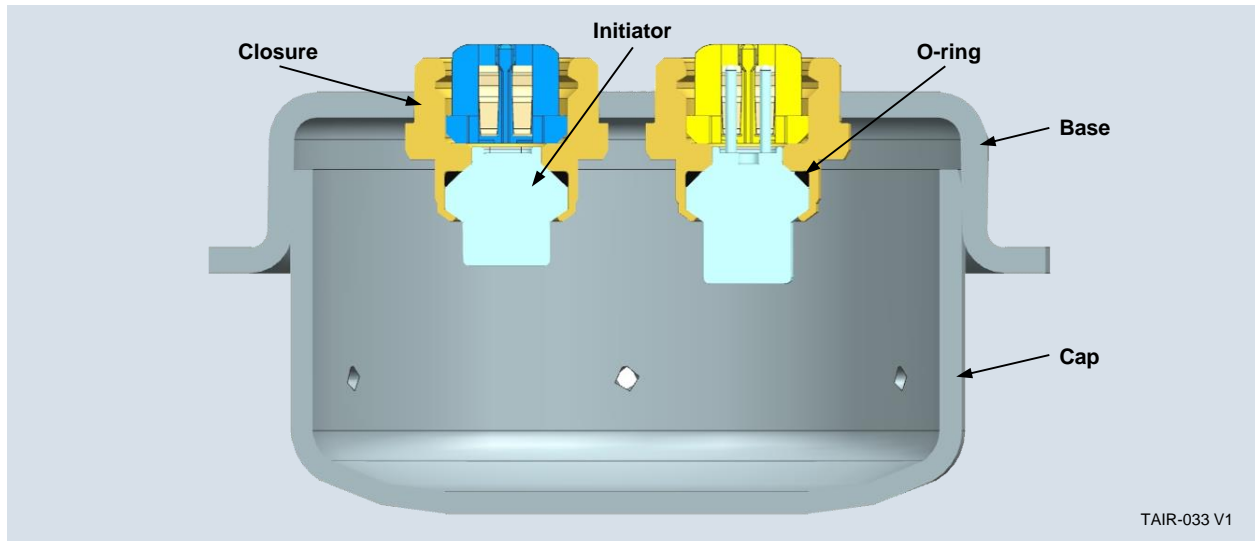


Figure 31. PSDI-5 Pressure Vessel

The PSDI-X pressure vessel is relatively simple (Figure 32). Base, cap, and igniter closures are welded into an assembly. No igniter columns join cap to base. There is no bulkhead to tie to cap or base. The initiators use an O-ring seal to block combustion gases from exiting.

As with the passenger inflators, the driver inflator pressure vessels will rupture if stressed beyond their design capability, but they do not cause rupture.



**Figure 32. PSDI-X Pressure Vessel**

**Moisture Protection System**

*As with the passenger inflators, the driver inflator moisture protection system affects when and how fast moisture ages the propellants.*

The PSDI-5 moisture protection system is shown in Figure 33. Desiccant (if used, see Table 2) competes with 2004 and 3110 propellants for moisture. Multiple seals slow moisture transfer between the inflator interior and the exterior environment. The closure-to-cylinder interface is addressed with an O-ring. The vents are covered with burst tape. The initiator-to-closure interface is sealed with a gasket. Moisture can diffuse through the plastic initiator body and gaskets. Moisture can travel between primary and secondary chambers through the port seal tape.

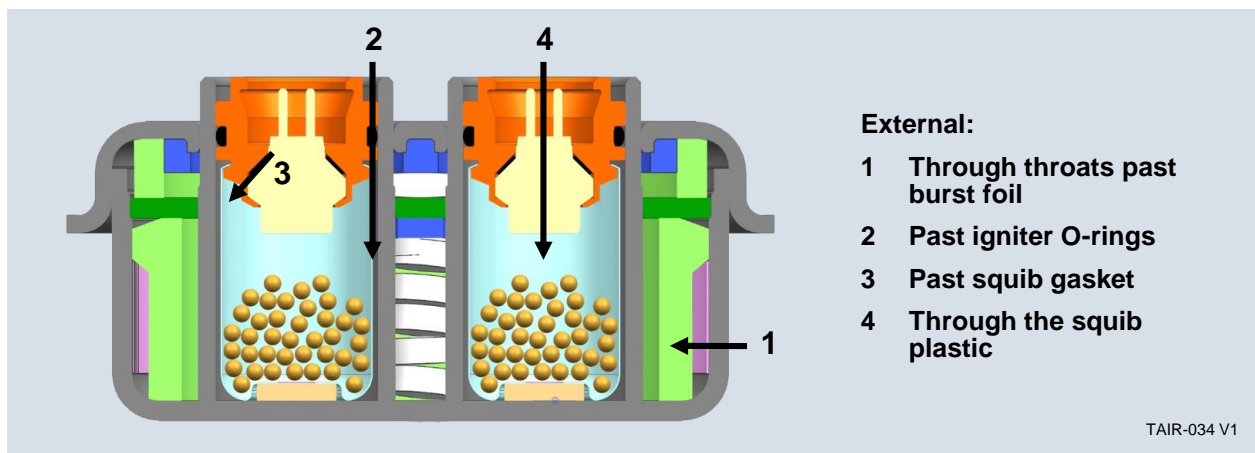


**Figure 33. PSDI-5 External Leak Paths**

The PSDI-X moisture protection system is shown in Figure 34. 13X desiccant competes with the 2004 and AIB propellants for moisture. The closure-to-cap interface is welded. The vents are covered with burst tape. The initiator-to-closure interface uses an O-ring. Moisture can diffuse through the plastic initiator body. Moisture travel between primary and secondary chambers must pass the secondary barrier cap press fit.

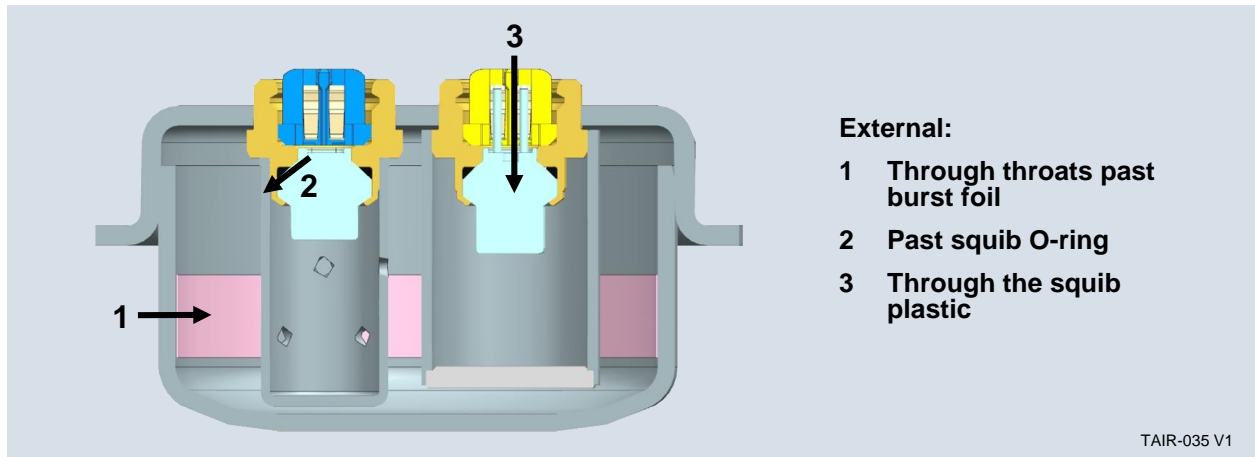


Figure 34. PSDI-X External Leak Paths

### Auto-ignition System

PSDI-5 uses AI-1 tablets at the base of each igniter and one in a cup at the top of the inflator (Figure 35) PSDI-X uses AIB primary boost propellant to handle auto ignition.

As with the passenger inflators, *AI-1 releases moisture as it degrades over time at higher temperatures. In turn, this limited amount of moisture will contribute to the overall moisture dynamic and may affect aging of the main propellant.*

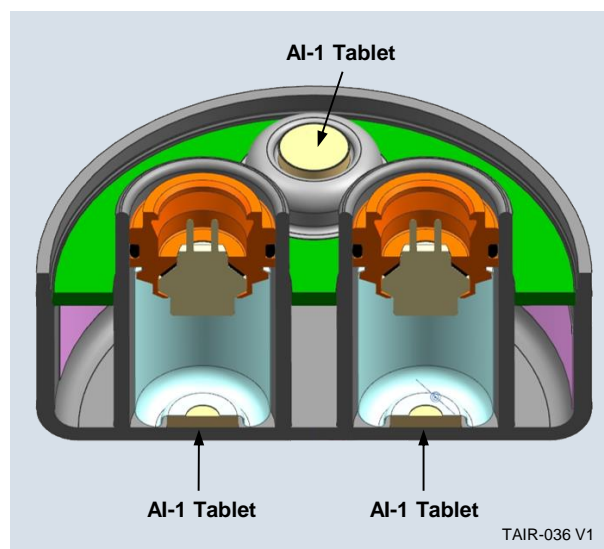
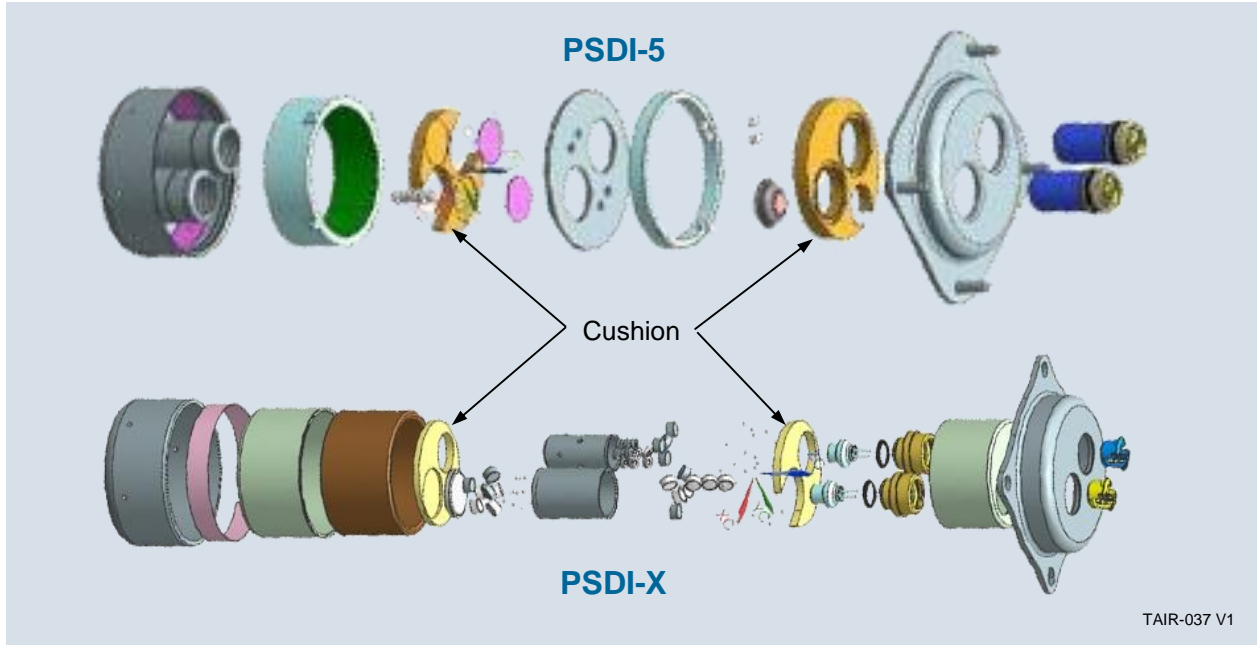


Figure 35. PSDI-5 Auto Ignition System

### Suspension System

Driver inflators use a wool or ceramic foam cushion to control rattle and protect the bulk-loaded tablets from shock and vibration (Figure 36). Driver inflator suspension does not play a significant role in aging-induced rupture.



**Figure 36. Driver Tablet Suspension System**

## Scientific Aging Test Program

The objective of the scientific aging program was to obtain quantitative statistically significant data under known conditions that could provide the needed rate inputs to the predictive aging model. Field aging provides real-world aging, but aging variables are unknown and time to get the data leaves little advance warning if a remedy is needed.

With scientific aging, the variables are controlled and variable combinations are defined. For accelerated aging, one of the controlled variables needs to be altered beyond that seen in the field. Options for inflators could include cycling to higher temperatures or shortening temperature cycle times. Northrop Grumman conducted studies to understand moisture dynamics of the propellants and selected shorter temperature cycles in lieu of higher temperatures to most closely reproduce the field aging mechanism.

Both pre-loaded and naturally-aspirated methods of adding moisture to the inflators were considered. Northrop Grumman chose the pre-loaded method to have known quantities of moisture in each inflator. The basic DOE used three moisture levels and three temperature cycles for nine moisture / temperature combinations as shown in Table 7.

**Table 7. Accelerated Aging DOE Matrix**

Moisture	Temp Cycle (°C)		
High	20-50	20-60	20-70
Medium	20-50	20-60	20-70
Low	20-50	20-60	20-70

The seven inflators identified previously that each have a primary and secondary chamber were tested at each condition. In total, the DOE had 14 different high, medium, and low moisture levels. We tested the inflators at 0, 240, 480, 960, 1440, and 1960 cycles. In addition, a set of inflators were held at a constant temperature of 20°C for the entire duration of cycling. The full aging matrix, showing number of inflators tested at each condition, is shown in Table 8. In total, we tested over 3,740 scientifically aged inflators, and 188 field-return inflators.

Target moisture levels were selected using available field-return data (non-desiccated 2004 systems). As desiccated 2004L systems became available, Northrop Grumman added an additional moisture level to the PSDI-X SV system to better represent moisture levels reached in the field. Moisture levels identified as extreme are considered to be values above what we predict for the field. Those tested have shown that the 2004L propellant will show aging but only under these severe conditions.

We do not believe these conditions will be duplicated in the field but do not have field data to anchor and prove that position due to the relatively young field age of the 2004L based inflators.

Hardware flow is shown in Figure 37. Inflators were built at Takata to Northrop Grumman specifications. After receipt at Northrop Grumman, each inflator was individually sealed in moisture-resistant bags. Inflators then proceeded to the accelerated aging program.

Table 8. Full Aging Matrix with Quantity Tested

Inflator		Cycles	0,Constant 20	240			480			960			1440			1920			Field Returns
		Moisture	Temp Cycle																
			NA	20-50	20-60	20-70	20-50	20-60	20-70	20-50	20-60	20-70	20-50	20-60	20-70	20-50	20-60	20-70	
PSPI-L FD/LT	Primary	High	14	2	1	2	12	6	12	7	6	12	2	2	2	5	4	9	
		Med	14	2	1	2	12	6	12	7	6	12	2	2	2	5	4	8	
		Low	14	2	1	2	12	6	12	7	6	12	2	2	2	5	4	9	
	Secondary	High	14	2	1	2	12	6	12	7	6	12	2	2	2	5	4	9	
		Med	14	2	1	2	12	6	12	7	6	12	2	2	2	5	4	8	
		Low	14	2	1	2	12	6	12	7	6	12	2	2	2	5	4	9	
PSPI-LD DU	Primary	High	14	2	1	2	7	6	7	7	6	7	2	2	2	5	3	4	
		Med	14	2	1	2	7	6	7	7	6	7	2	2	2	5	3	5	
		Low	14	2	1	2	7	6	7	7	6	7	2	2	2	5	3	4	
	Secondary	High	14	2	1	2	7	6	7	7	6	7	2	2	2	5	3	4	
		Med	14	2	1	2	7	6	7	7	6	7	2	2	2	5	3	5	
		Low	14	2	1	2	7	6	7	7	6	7	2	2	2	5	3	4	
PSPI-X TX	Primary	Extreme	14	2	1	2	7	6	7	7	6	7	2	2	2	5	4	5	60
		Med	14	2	1	2	7	6	7	7	6	7	2	2	2	5	4	5	
		Low	14	2	1	2	7	6	7	7	6	7	2	2	2	5	4	5	
	Secondary	Extreme	14	2	1	2	7	6	7	7	6	7	2	2	2	5	4	5	
		Med	14	2	1	2	7	6	7	7	6	7	2	2	2	5	4	5	
		Low	14	2	1	2	7	6	7	7	6	7	2	2	2	5	4	5	
PSDI-5 ZA	Primary	High	14	2	1	2	6	6	6	6	6	6	2	2	2	5	4	4	17
		Med	14	2	1	2	6	6	6	6	6	6	2	2	2	5	3	4	
		Low	14	2	1	2	6	6	6	6	6	6	2	2	2	5	4	4	
	Secondary	High	14	2	1	2	6	6	6	6	6	6	2	2	2	5	4	4	
		Med	14	2	1	2	6	6	6	6	6	6	2	2	2	5	3	4	
		Low	14	2	1	2	6	6	6	6	6	6	2	2	2	5	4	4	
PSDI-5D YT	Primary	High	14	2	1	2	6	6	6	6	6	6	2	2	2	5	4	5	39
		Med	14	2	1	2	6	6	6	6	6	6	2	2	2	5	4	5	
		Low	14	2	1	2	6	6	6	6	6	6	2	2	2	4	4	5	
	Secondary	High	14	2	1	2	6	6	6	6	6	6	2	2	2	5	4	5	
		Med	14	2	1	2	6	6	6	6	6	6	2	2	2	5	4	5	
		Low	14	2	1	2	6	6	6	6	6	6	2	2	2	4	4	5	
PSDI-5D GE	Primary	High	14	-	-	-	8	7	8	8	7	8	8	7	8	8	7	8	
		Med	14	2	1	2	6	6	6	6	6	6	2	2	2	5	5	5	
		Low	14	2	1	2	6	6	6	6	6	6	2	2	2	5	5	5	
	Secondary	High	14	-	-	-	8	7	8	8	7	8	8	7	8	8	7	8	
		Med	14	2	1	2	6	6	6	6	6	6	2	2	2	5	5	5	

Inflator		Cycles	0,Constant 20	240			480			960			1440			1920			Field Returns
		Moisture	Temp Cycle																
			NA	20-50	20-60	20-70	20-50	20-60	20-70	20-50	20-60	20-70	20-50	20-60	20-70	20-50	20-60	20-70	
		Low	14	2	1	2	6	6	6	6	6	6	2	2	2	5	5	5	
PSDI-X SV	Primary	Extreme	14	2	1	2	6	6	6	6	6	6	2	2	2	5	4	5	
		High	14	-	-	-	8	7	8	8	7	8	8	7	8	8	7	8	
		Med	14	2	1	2	6	6	6	6	6	6	2	2	2	5	4	5	
		Low	14	2	1	2	6	6	6	6	6	6	2	2	2	5	4	5	
	Secondary	Extreme	14	2	1	2	6	6	6	6	6	6	2	2	2	5	4	5	
		High	14	-	-	-	8	7	8	8	7	8	8	7	8	8	7	8	
		Med	14	2	1	2	6	6	6	6	6	6	2	2	2	5	4	5	
		Low	14	2	1	2	6	6	6	6	6	6	2	2	2	5	4	5	

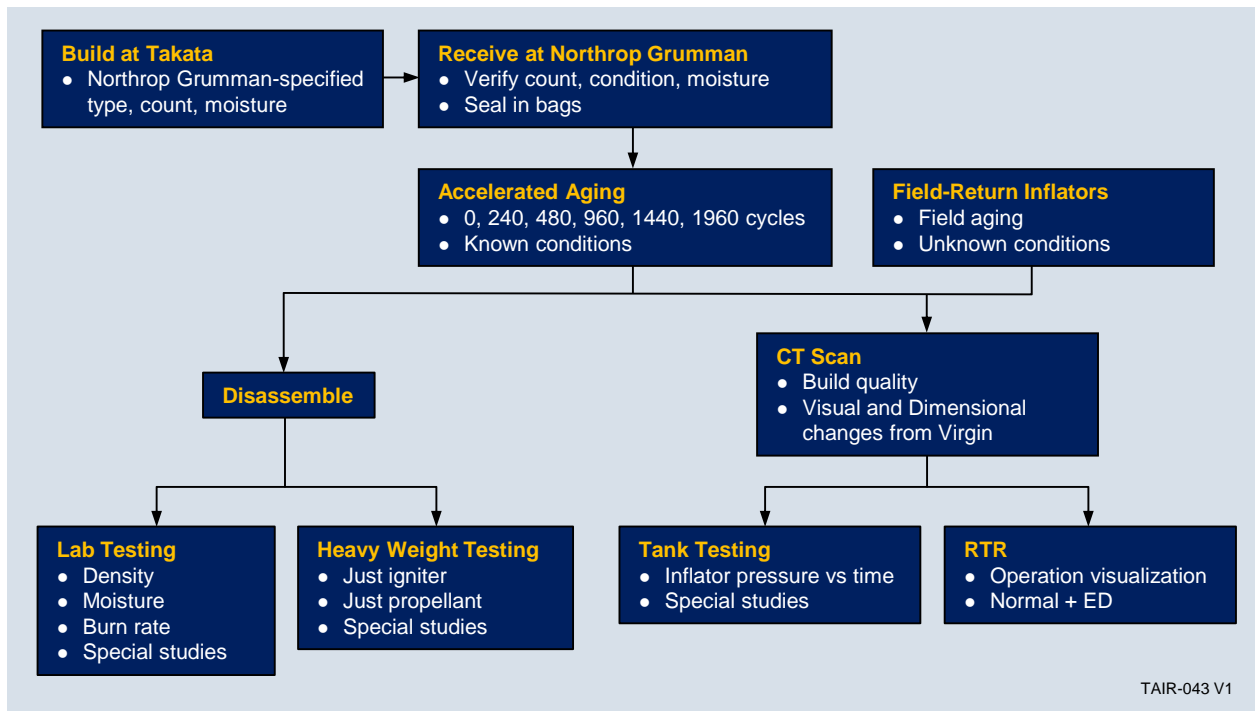


**Figure 37. Hardware Flow**

**Moisture Levels**

Our goal was to test moisture levels spanning the useful life of a fielded inflator. Low moisture was to represent newly-built inflators. Mid moisture was an in-between level typical of inflators in the middle of their useful life. High moisture was to represent inflator moistures near the end of their useful life.

The Takata MEAF data for PSPI-L inflators offered quantitative field data for the moisture targets (Figure 38 and Figure 39). The high level was determined using data from Takata report “SPI, PSPI-L Field Analysis Moisture” based on dissection results of more than 7000 PSPI-L inflators from Zone 1. The 99th percentile value for the secondary chamber was ~0.70% at 18 years and ~0.30% at 18 years for the primary chamber. Our goal was to bracket realistic high moisture levels.

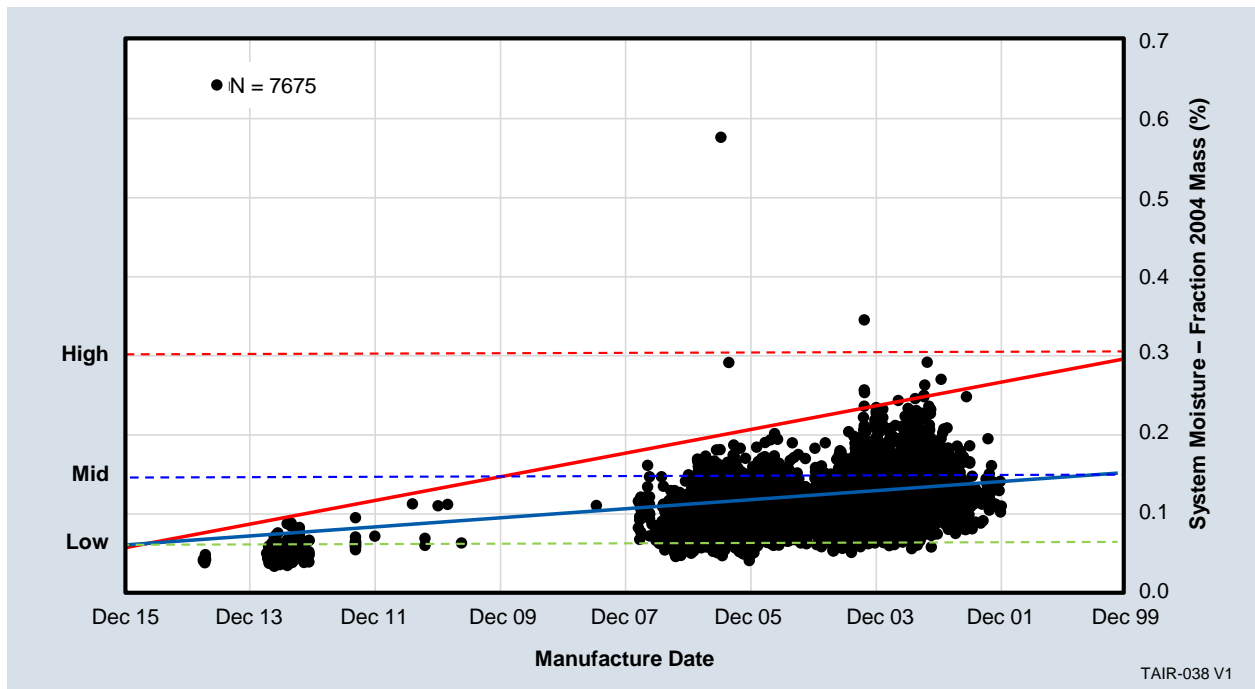


Figure 38. MEAF PSPI-L Primary Chamber Moisture Levels in Zone 1

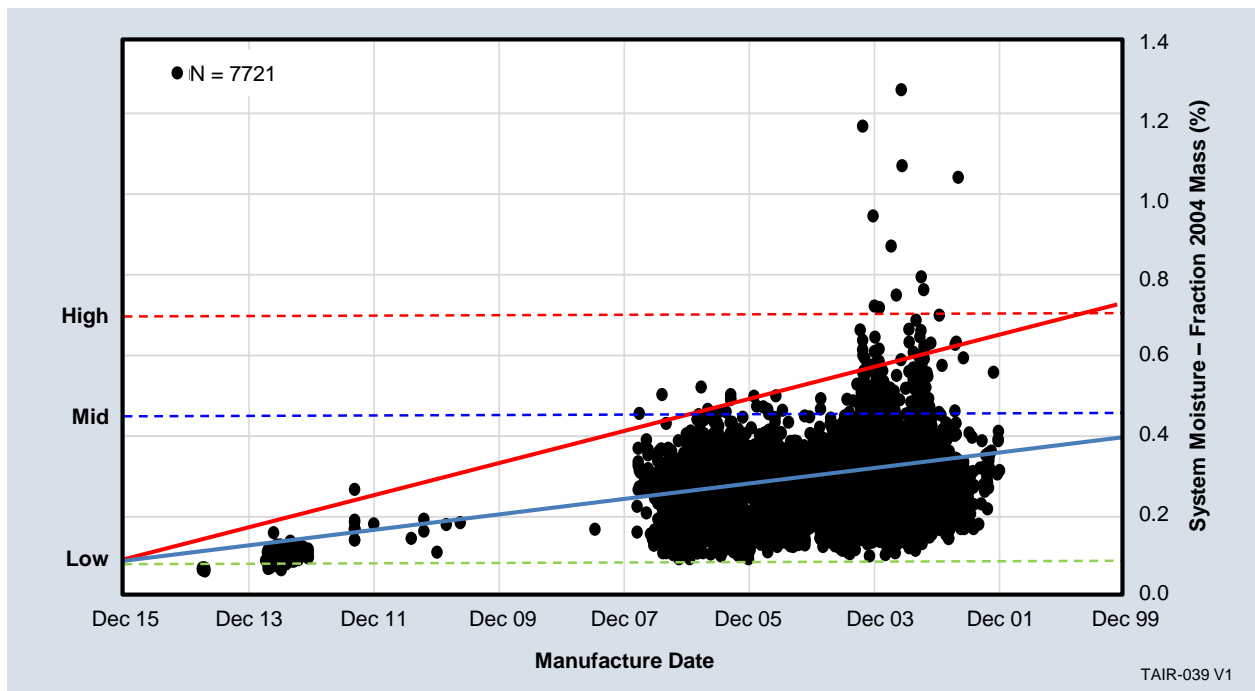


Figure 39. MEAF PSPI-L Secondary Chamber Moisture Levels in Zone 1

We used these same target moisture levels for all the inflator types independent of propellant system when we established target moisture levels for the DOE. For desiccated inflators, we modified the moisture levels as follows:

- **Mid-level primary:** 0.15 % based on weight of main propellant, before addition of desiccant having typical factory moisture
- **Mid-level secondary:** 0.45 % based on weight of main propellant, before addition of desiccant having typical factory moisture
- **High-level primary:** 0.15 % based on weight of main propellant, before addition of saturated desiccant
- **High-level secondary:** 0.45 % based on weight of main propellant, before addition of saturated desiccant

At the time moisture levels were set, there was no field-returned data containing 2004L propellant with saturated desiccant. Moisture levels were selected based on available 2004 MEAF data. Testing later indicated 2004L moisture capacity was significantly less than that of 2004 and the moisture levels of 2004L inflators were higher than what was found in the MEAF. The highest 2004L levels were subsequently relabeled extreme for the PSPI-X and PSDI-X inflators. An additional build of PSDI-X was fabricated at a moisture content that was considered high but achievable for Zone 0. Table 9 summarizes the target and as-built moisture levels.

**Table 9. Moisture Levels as weight % of Main Propellant**

Inflator	Chamber	Target Moisture			
		Low	Mid	High	Extreme
PSPI-L FD/LT	Primary	New Factory Nominal	0.15	0.3	NA
	Secondary		0.45	0.7	
PSPI-LD DU	Primary		0.15	0.15*	NA
	Secondary		0.45	0.45*	
PSPI-X TX	Primary		0.15	NA	0.15*
	Secondary		0.45		0.45*
PSDI- 5 ZA	Primary		0.15	0.3	NA
	Secondary		0.45	0.7	
PSDI-5D YT	Primary		0.15	0.15*	NA
	Secondary		0.45	0.45*	
PSDI-5D GE	Primary		0.15	0.15**	NA
	Secondary		0.45	0.45**	
PSDI-X SV	Primary		0.15	0.15**	0.15*
	Secondary		0.45	0.45**	0.45*

Moisture level = (weight of moisture in boost propellant + main propellant)/weight of main propellant

\* Used saturated desiccant. Mid and low moisture inflators had desiccant with typical starting moisture.

\*\* Used saturated desiccant dried at 70°C for 16 hrs.

These levels of moisture were selected to provide data regarding the rate of propellant density reduction under different conditions that an inflator may experience over the life of the vehicle. The as-built moisture reflects what all inflators experience during the first years in the field. The mid-moisture reflects the condition in inflators that achieve this level of moisture after several years of exposure to a higher humidity environment and temperature cycling. The high moisture

level reflects the low percentage of inflators that have this level of moisture after >10 years of exposure to the most challenging of humidity and temperature cycling environments such as would be experienced in south Florida for a T3 vehicle (highest temperature) which a high usage. This range provides data that fed the scientific aging study and spans the potential life of inflators under conditions up to the most challenging experienced in the field.

**Temperature Levels**

Temperature levels were set to bracket high vehicle cabin temperatures in Miami Florida. High and low temperatures were based on ATLAS testing. ATLAS obtained vehicle internal environments for a range of vehicles and external environments (see discussion on Atlas report in Environment Module section).

Figure 40 shows a range of peak cabin temperatures for summer in Miami. Figure 41 shows that 24-hour summer cycle in Miami. Based on this data, Northrop Grumman chose a common “night” temperature of 20°C and the three peak temperatures of 50, 60, and 70°C.

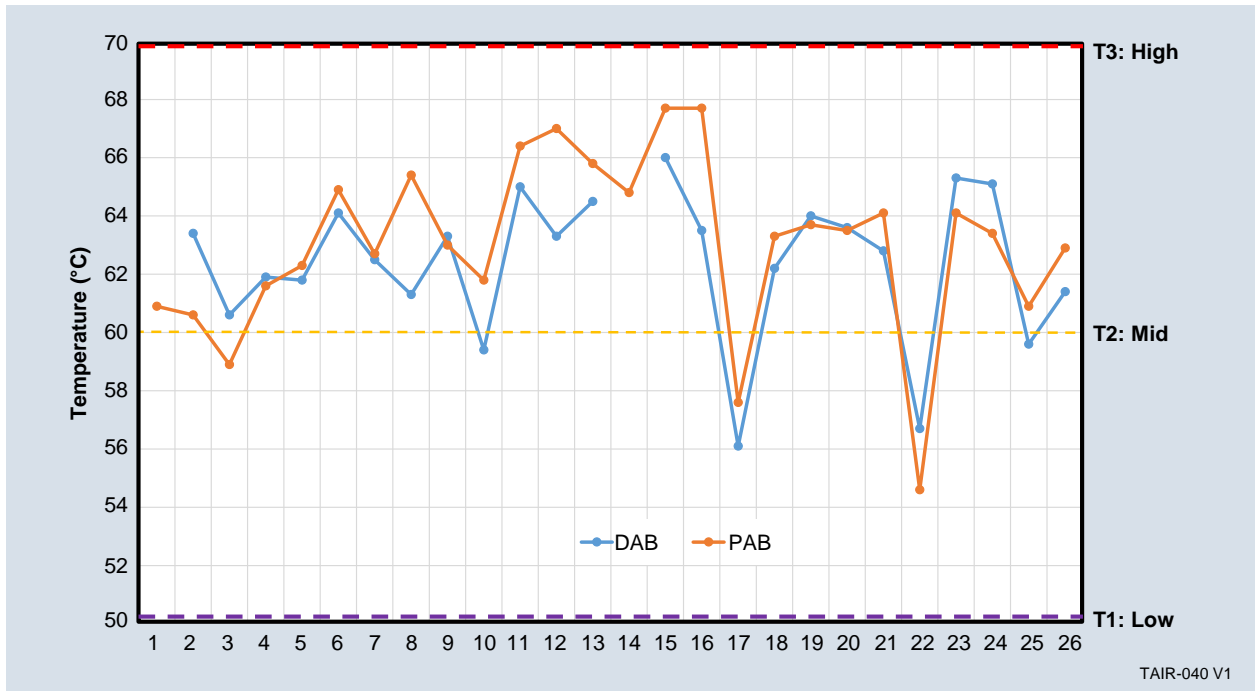


**Figure 40. Vehicle Peak Temperatures from ATLAS Testing**

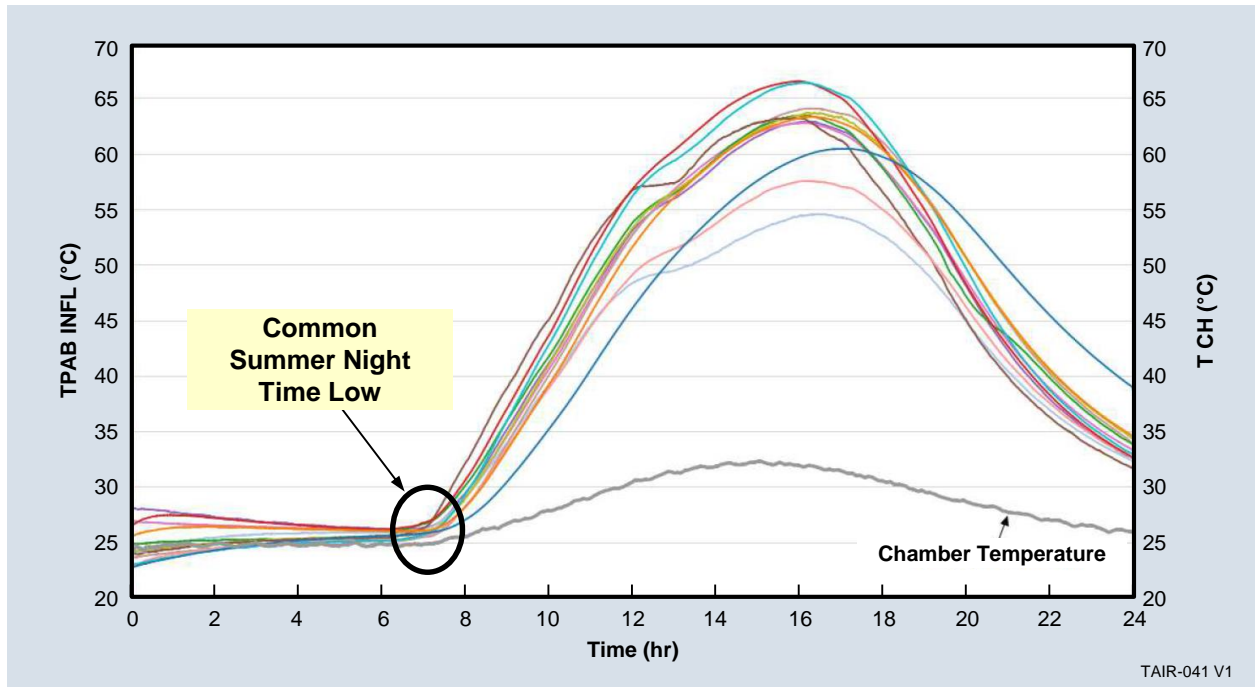


**Figure 41. PAB Inflator Temperature – Chamber Soak ATLAS Zone 1**

### Temperature Cycle

The typical daily cycle has approximately 16 hours at cooler temperatures and 8 hours at hotter temperatures. Moisture equilibrium studies were conducted by monitoring the internal humidity and temperature of an inflator during thermal cycling. The study showed how moisture moves between propellants and the time required for moisture levels to reach equilibrium as shown in Figure 42. Based on these studies, a 4-hour cycle was selected (2 hours hot and 2 hours cold) as achieving best balance between the opposing needs of achieving full equilibrium and adequate speed.

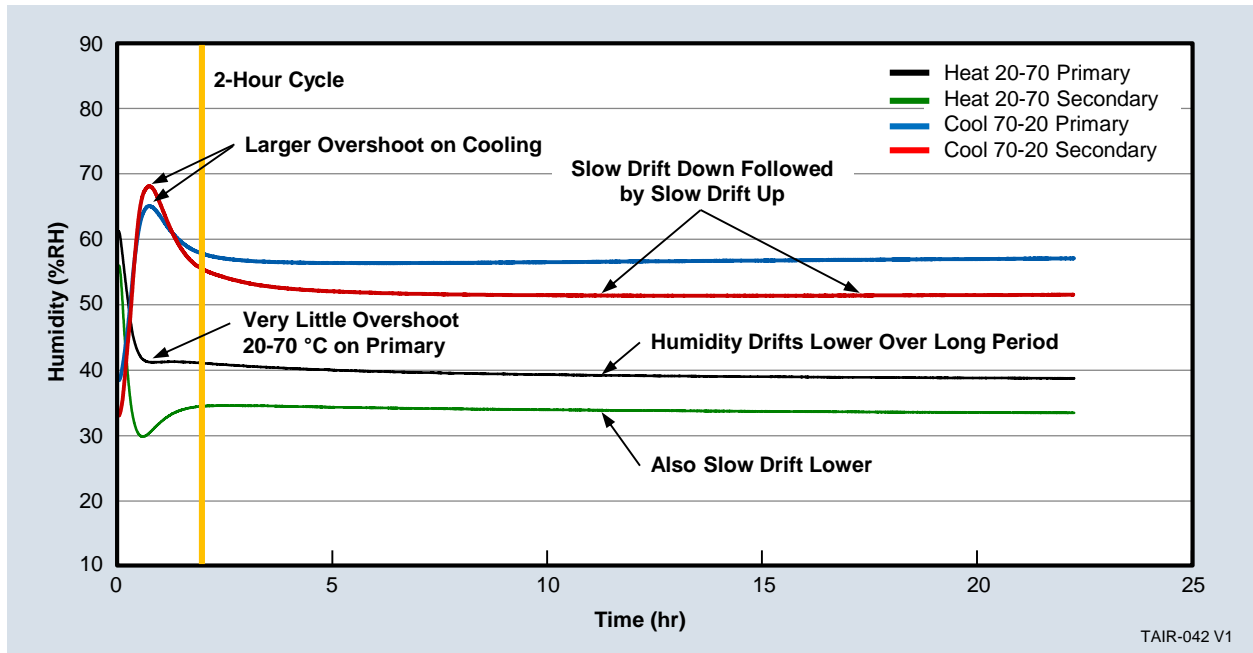


**Figure 42. Humidity Equilibrium Study**

Figure 37 shows the hardware flow. Inflators were newly built for this study by Takata to Northrop Grumman specifications. Inflators were individually sealed in moisture-resistant bags after acceptance. At pre-determined cycling intervals, inflators were pulled for testing.

Inflators were either disassembled or CT-scanned and deployed in tank testing or Real Time Radiography (RTR) testing. The individual parts of the disassembled inflators were used for laboratory testing or went on to deployment testing in our heavyweight hardware which facilitated collection of pressure data above normal inflator failure values. This test flow allowed us to obtain data on how the inflator parts aged, and then relate this to how the inflator system performed.

**Laboratory Testing Overview**

A wide range of laboratory testing was performed on inflators from the scientific aging program and on field-returned inflators. Testing was conducted to monitor changes as inflators age and to provide inputs to the aging model. By testing both scientific-aged and field-returned inflators, Northrop Grumman was able to determine how well the scientific aging mimics aging in the field. Table 10 lists some of the laboratory tests performed to track inflator aging and provide data for aging model inputs.

**Table 10. Summary of Laboratory Testing**

Inflators for Propellant Testing	Inflators for Tank Testing
Driver / Passenger	Driver / Passenger
Moisture levels in booster, propellant and desiccant	CT scanning
Weight of booster and propellant	ICAM analysis
Caliper dimensions of booster and propellant	Outer diameter of propellant from CT scan
Calculated propellant density	Wafer stack height (passenger only)
Closed bomb burn rate of propellant	
Scanning electron microscopy <ul style="list-style-type: none"> <li>• Propellant surface-roughness</li> <li>• Propellant morphology</li> </ul>	
AI-1 <ul style="list-style-type: none"> <li>• Color</li> <li>• Weight</li> <li>• Thermogravimetric analysis</li> </ul>	
Propellant crush strength	

Critical data to understanding inflator aging and parameterizing the aging model are highlighted in the following sections: Moisture Testing section documents the change in moisture levels for inflators in scientific aging. Moisture levels are critical to our aging model because they strongly effect the rate at which inflators age. This rate of aging, as determined from our scientific aging experiments and from aging in the field, is used directly in the aging model to predict the POF.

The Propellant Density section discusses the density changes as inflators are scientifically aged. The density was chosen because a reduction in propellant density can strongly augment the propellant apparent burning rate and actual gas generation rate and is one of the best predictors of POF. Where possible, comparisons are made between the results of scientific aging and aging in the field.

**Moisture Testing**

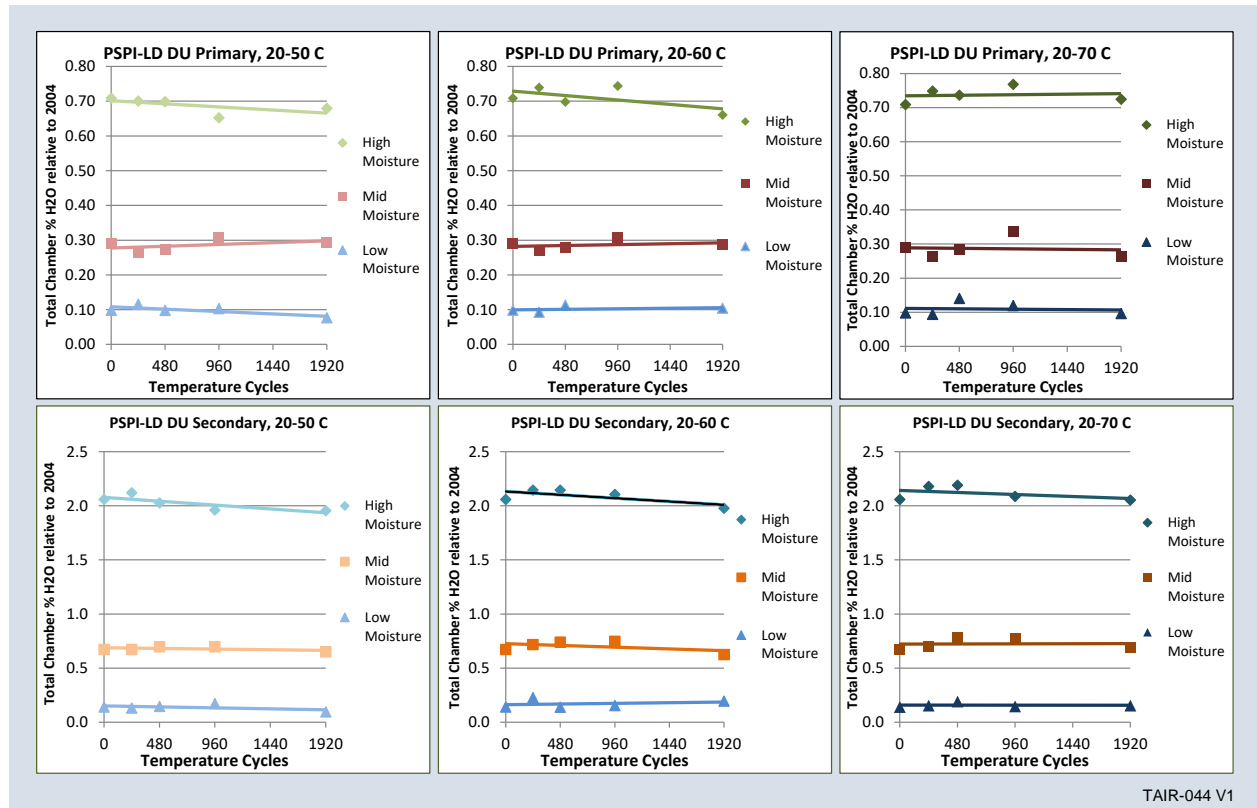
Different levels of moisture were added to virgin inflators that entered into scientific aging. How moisture levels change during scientific aging can reveal important information about the behavior of the inflators and the propellants. In this section, the total inflator moisture level evolution is shown for exemplary inflator types studied as part of the scientific aging test matrix. While not shown here, similar data are available for all of the seven inflators we investigated.

Conscious efforts were taken to minimize adsorption or desorption of moisture from the propellants and desiccants during assembly, inflator machining, disassembly and laboratory preparation for moisture analysis. The inflators were sealed in moisture barrier bags during scientific aging. Over the course of aging, moisture from the inflator may exit the inflator and remain within the moisture barrier bag. Conversely, whatever moisture may have been sealed within those bags may enter the inflator during aging. Care was taken to avoid unintended sources or transfer of moisture and the experimental data showed very little actual variation. Slow diffusion of moisture may also occur in and / or out of the moisture barrier bags due to the

possibly large water vapor pressure gradients and the stress induced by the extreme aging conditions.

*PSPI-LD DU*

An exemplary passenger inflator is the PSPI-LD DU. The moisture levels in the DU inflators are remarkably constant throughout temperature cycling, as seen in Figure 43. The three moisture levels are well-separated and one would expect noticeably different aging corresponding to those levels.



TAIR-044 V1

**Figure 43. Total Moisture in 3110, AIB and 13X as a Function of Temperature Cycles for PSPI-LD DU Inflators**

*PSDI-5 ZA*

As seen in Figure 44, the moisture levels of the PSDI-5 ZA inflators are not as constant as they were for the PSPI-LD DU. One likely difference is the different sealing systems for driver and passenger inflators. Inadvertent moisture loss or gain may be more likely for PSDI-5 inflators since they use granular 3110 booster instead of tableted AIB and 2004 in the form of high surface area 0.16 gram tablets instead of 8.1 gram wafers. The larger surface-to-volume ratios of the propellants in PSDI-5 inflators more readily adsorb and desorb moisture than in their passenger inflator counterparts. However, the moisture levels are reasonably constant in the sense that throughout the 1,920 cycles, the three moisture levels are distinctly separate. These three distinct levels are expected to promote noticeably different aging rates.

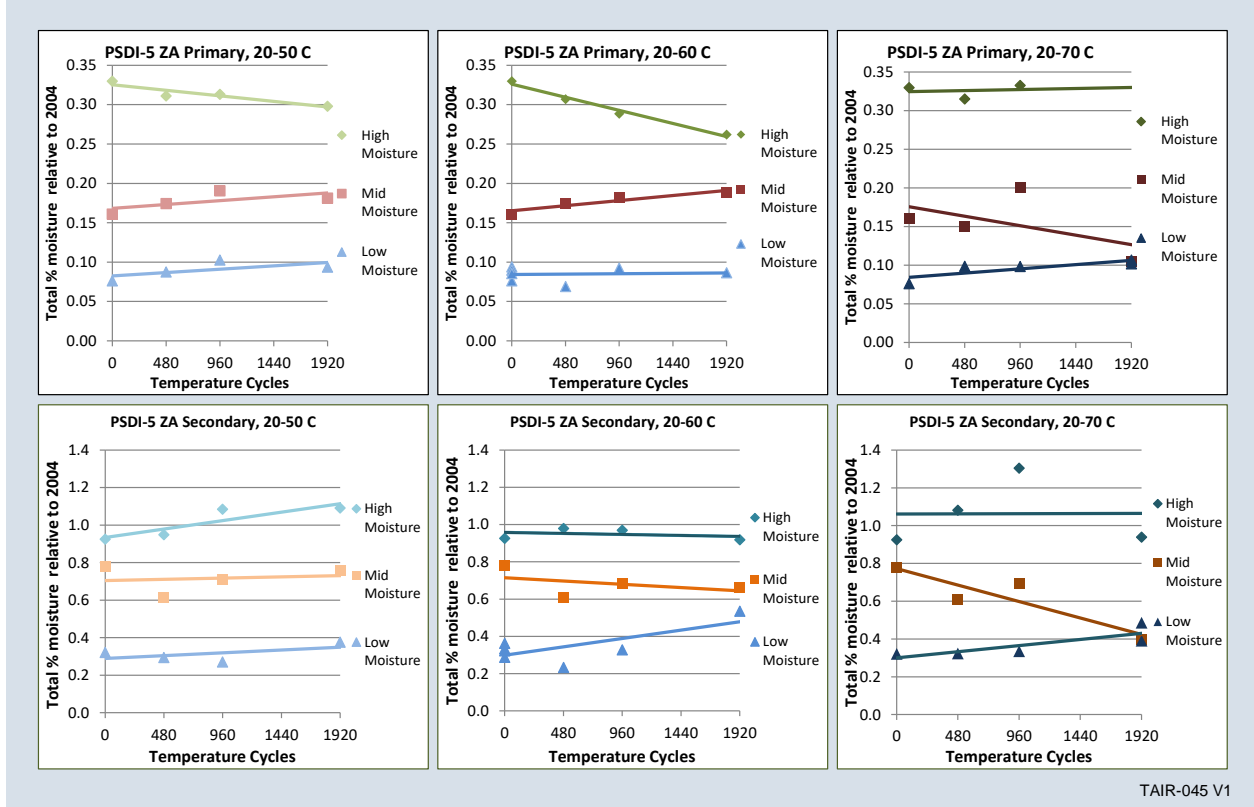
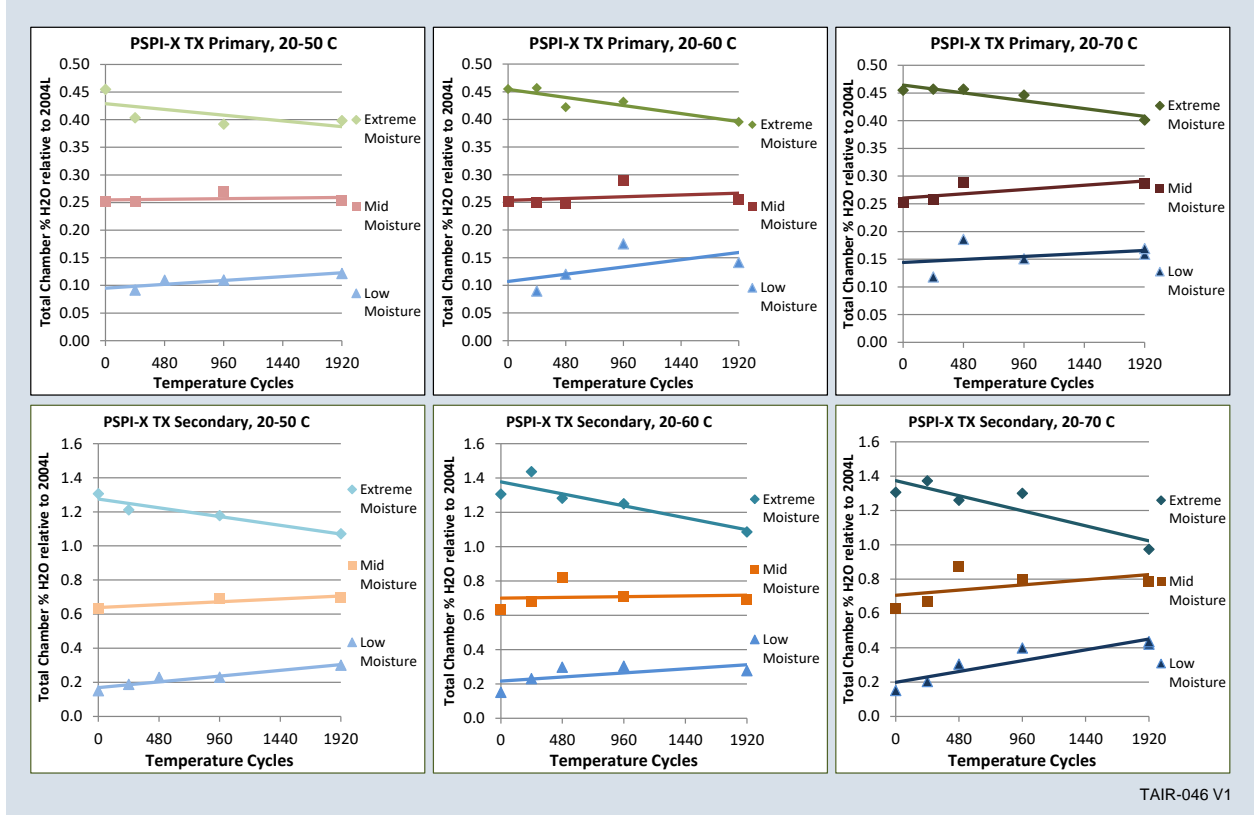


Figure 44. Total Moisture in 3110 and 2004 as a Function of Temperature Cycles for PSDI-5 ZA Inflators

PSPI-X TX

As seen in Figure 45, the total moisture levels in the PSPI-X TX inflator remained roughly constant over 1,920 temperature cycles. In all cases, for the extreme moisture level, the inflators experienced loss of moisture over the course of temperature cycling. This moisture loss could indicate that the extreme moisture level is too high due to the much lower moisture capacity of 2004L and AIB relative to inflators with 2004 and/or 3110 and the inflator is losing water in an attempt to reach an equilibrium with its surroundings. For all cases where the desiccant is not fully saturated (low- and mid-moisture levels), there is an increase in total moisture over the course of temperature cycling. This is an indication that the inflators are either pulling in moisture or extracting the very small amounts available from other parts of the inflator in an attempt to reach an equilibrium state with the surrounding conditions.



TAIR-046 V1

Figure 45. Total Moisture in AIB, 2004L and 13X as a Function of Temperature Cycles for PSPI-X TX Inflators

*PSDI-X SV*

The total moisture in PSDI-X SV inflators is not as clear as for all of the other inflators studied. As seen in Figure 46, the ordering of what we call the low-, mid- and high-moisture levels in the primary chambers is not well separated. The primary chambers of the extreme-moisture inflators have higher outset moisture and tablets therein degrade more quickly than the other moisture levels. Although, the secondary mid-, high- and extreme-moisture measurements are grouped closely together, the extreme tablets degraded the most. This suggests that our method of measuring total moisture for SV secondary chambers may not be adequate to distinguish between moisture levels. The SV secondary chamber does not contain AIB, which has a higher moisture capacity than 2004L. The high surface area 2004L tablets may readily lose / gain moisture during inflator disassembly and preparation for moisture analysis.

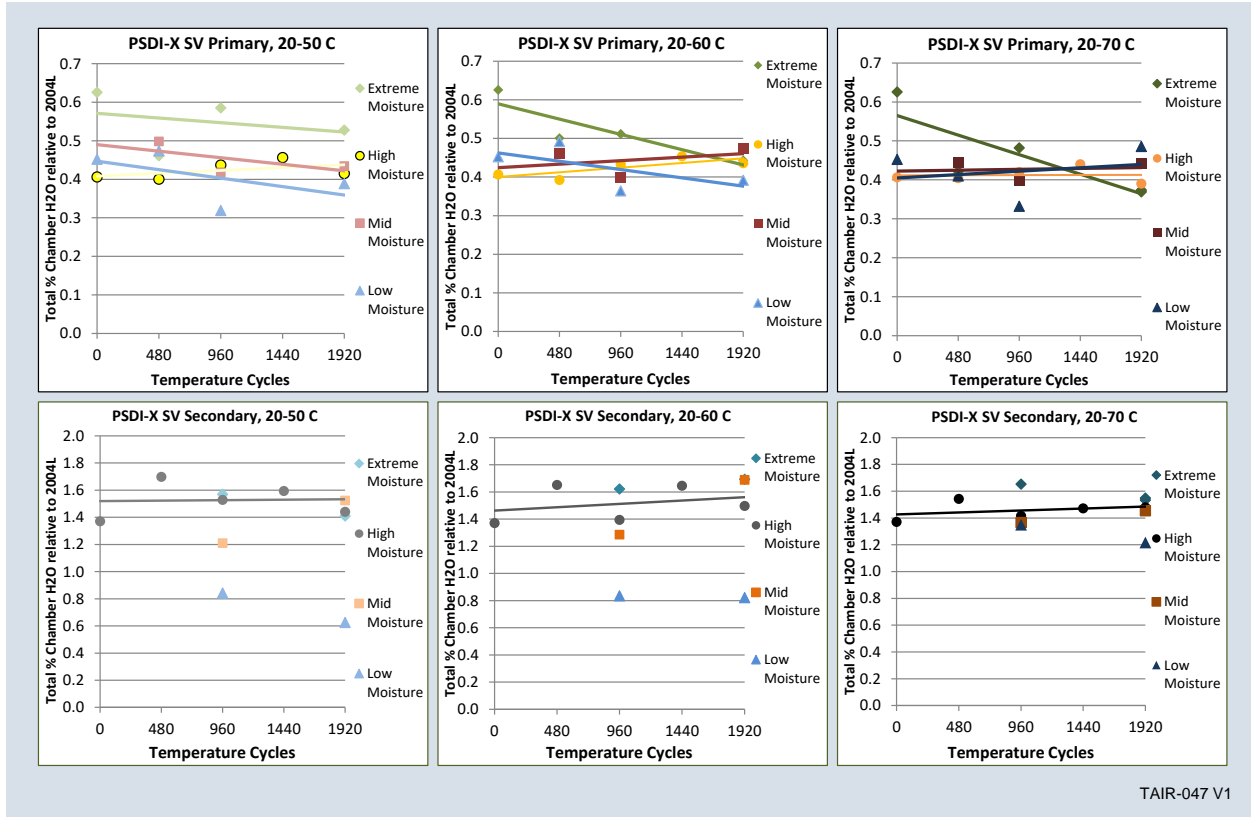


Figure 46. Total Moisture in AIB, 2004L and 13X as a Function of Temperature Cycles for PSDI-X SV Inflators

### Moisture Summary

The actual moisture levels of inflators with the 2004 / 3110 propellant system (PSPI-L LT, PSDI-5 ZA, PSDI-5D YT and PSDI-5D GE) did a reasonable job of spanning moisture levels seen in field-returned inflators. Because the moisture capacity of 2004L and AIB are lower than 2004 and 3110, under the same moisture conditions, inflators with 2004L and / or AIB (PSPI-X TX, PSDI-X SV and PSPI-LD DU) had been built with moisture levels that are higher than predicted to be observed in the field. For inflators with these higher moisture levels, temperature cycling promoted loss of tablet and / or wafer integrity, eventually causing some of these to turn to powder. High moisture levels in the desiccants (13X and CaSO<sub>4</sub>) for inflators built with high- or extreme-moisture levels are in excellent agreement with the desiccant moisture levels of field-returned inflators where the desiccant has time to reach saturation. For both field-returned inflators and inflators in scientific aging, when the desiccant is below the saturation level, the moisture content in the booster and propellant remains low.

### Propellant Density

Propellant aging damage can be measured in various ways including: 1) propellant outer diameter, 2) density, 3) porosity, 4) surface roughness, etc. The best metric related to probability of Takata airbag inflator ED is density. A relatively small drop in propellant density can augment the apparent propellant burn rate, sufficient augmentation can result in an ED as has been discussed in the Performance Module section of this report.

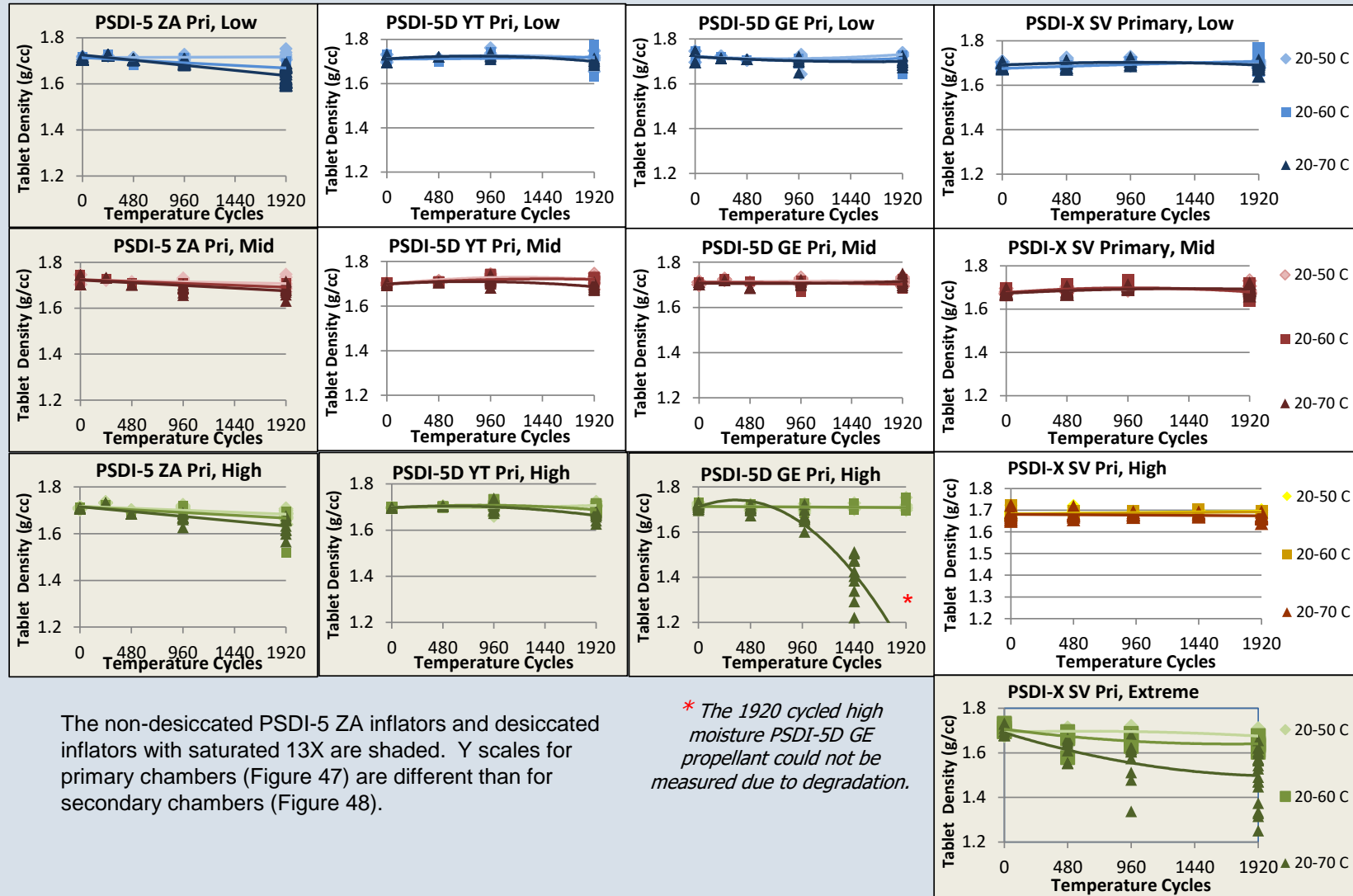
Propellant density was measured in one of two ways. Dissected samples were weighed and divided by the calculated volumes from caliper measurements. Tank-tested inflator propellant densities were determined using outer diameter measurements of tablets or wafers from inflator Computed Tomography (CT) scans using a MATLAB program developed by the International Center for Automotive Medicine (ICAM). The CT-based approach must be calibrated to actual caliper measurements performed on dissected inflators. Furthermore, without dissecting the inflators, it is not possible to get the weight of the propellant so an average propellant weight is used that was determined from inflator dissections. Extensive experimental work measuring diameter and density establish a relationship between diameter and density for different propellant configurations. For this section the discussion is limited to the “caliper density”.

### *Propellant Tablet Density*

The scientific aging caliper density results versus temperature cycles for tablets in driver inflators are shown in Figure 47 and Figure 48. For undesiccated inflators, temperature cycling causes a reduction in propellant density. For desiccated inflators, as long as the moisture level in the desiccant is below the moisture saturation limit of the desiccant, there is little decrease in tablet density through 1,920 temperature cycles. Generally speaking, the 20 to 70°C temperature cycle induces more propellant damage than the 20 to 60°C cycle, which in turn is worse than the 20 to 50°C cycle. Isothermal aging of select inflators indicates that moisture alone is not sufficient to cause propellant aging. This shows that desiccant is highly effective at mitigating propellant damage as long as the desiccant moisture level is below the saturation point of the desiccant.

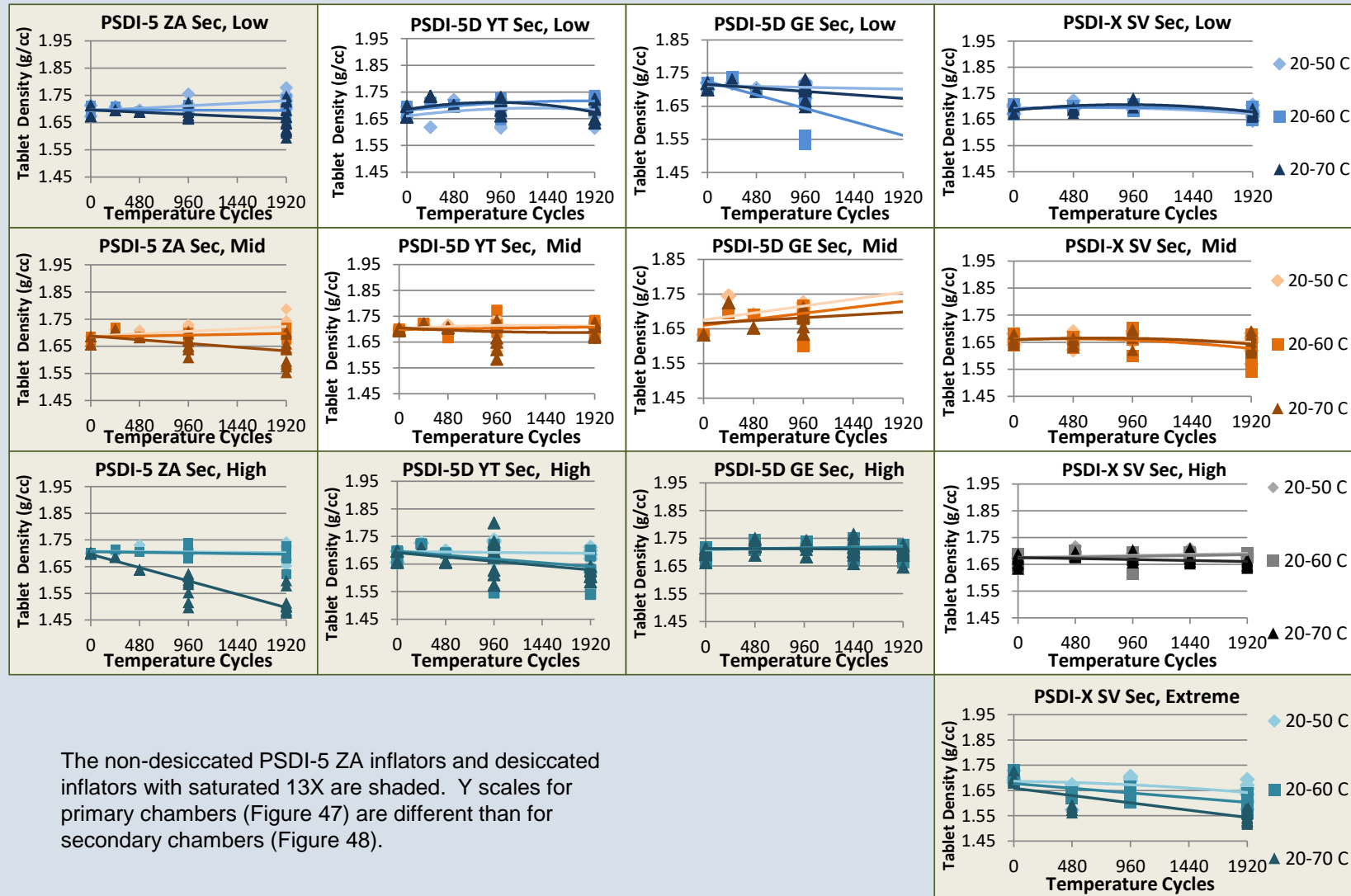
Inflators with higher moisture levels tend to age faster than the same inflator with less moisture. Since the secondary chambers were built with a higher moisture level than the primary chambers, the propellant in the inflator primary chamber ages slower than the propellant in the secondary chamber.

The tablet outer diameters measured from field-returned inflators are in the range observed for tablets originating from corresponding inflators in the scientific aging. Since there is a direct relationship between tablet outer diameter and density, the densities achieved in the scientific aging likely bracket what is currently observed in the field.



TAIR-048 V2

Figure 47. Driver Inflator 2004/2004L Primary Tablet Caliper Density Measurements



The non-desiccated PSDI-5 ZA inflators and desiccated inflators with saturated 13X are shaded. Y scales for primary chambers (Figure 47) are different than for secondary chambers (Figure 48).

TAIR-049 V2

Figure 48. Driver Inflator 2004/2004L Secondary Tablet Caliper Density Measurements

For the PSDI-X SV inflator primary chamber, it is interesting to note the dramatic difference in aging between the mid-moisture and extreme-moisture inflators. For the mid-moisture level, temperature cycling induces virtually no change in tablet density. For the extreme-moisture inflators, temperature cycling induces a decrease in tablet density.

There is very little detectable difference in total moisture between the mid- and extreme-moisture levels of the PSDI-X SV. This may be due to the 2004L testing technique or there may be a moisture-level “cliff” where the propellant is relatively immune to aging, but ages very rapidly if on the other side.

Figure 47 and Figure 48 indicate lower tablet densities than those currently measured in field returns for some inflators. There are two primary possible reasons for this difference: 1) the inflator was built with a moisture level that is higher than that predicted to occur in the field and labeled as “extreme” (PSDI-X SV for example) or 2) the inflator is relatively new and therefore field aging time has not yet reached the lower densities seen in the artificial aging program (PSDI-5 GE for example).

### *Propellant Wafer Density*

The scientific aging caliper density results versus temperature cycles for wafers in passenger inflators is shown in Figure 49 and Figure 50. Many of the same things can be said for wafer aging as for tablet aging. Temperature cycling of un-desiccated inflators causes wafer density to drop. For desiccated inflators, unsaturated desiccant effectively prevents the wafer density from changing. The 20 to 70°C temperature cycle is worse than the 20 to 60°C cycle, which in turn is worse than the 20 to 50°C cycle. Isothermal aging of select inflators indicates that moisture alone is not sufficient to cause wafer propellant from aging. Finally, the aging of wafers in the secondary chambers is generally faster than in the primary chamber due to the higher moisture content in the secondary.

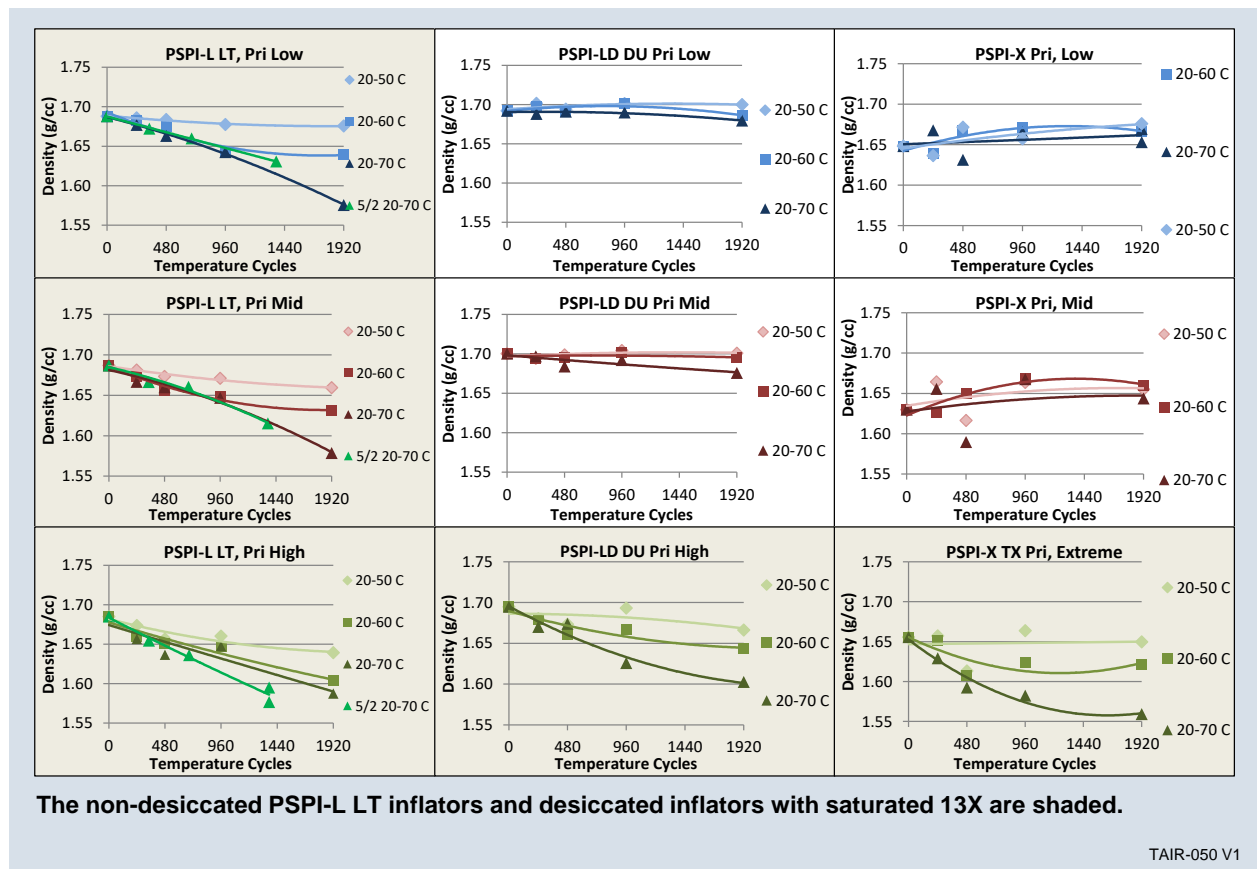
While it can be generally stated that higher moisture levels age wafers more quickly, the effect that different moisture levels have on inflator aging is not as straight forward for wafers as it is with tablets. Each passenger inflator is fitted with a spring to keep tension on the wafer stack. This spring force compresses the wafers over time and reduces the wafer stack height. Wafers with higher moisture are softer and more susceptible to this compression resulting in larger-than-expected wafer outer diameters and lower-than-expected wafer heights. The wafer design includes ridges to maintain an air gap between wafers in the stack. These ridges are the first to be flattened when the moisture content is high. Once the ridges are flattened, the air gap between wafers is eliminated and the surface-to-volume ratio of the propellant in the stack is decreased. This slows the rate at which moisture can go in and out of the propellant during temperature cycling, which could slow wafer aging.

The effect flattening has on aging is likely exaggerated for short temperature cycles such as those used in the scientific aging. Data indicates that for mid- and high-moisture inflators, it takes about 480 4-hour cycles for these ridges to be flattened, at which point the rate of propellant aging is reduced. For nominal moisture levels, the propellant is not soft enough for these ridges to be eliminated and there is not an associated slowing of wafer aging. These conclusions are also supported by the 5-days on, 2-days off aging (labeled 5/2) of high-moisture PSPI-L LT inflators. For these 5/2 experiments the high-moisture inflators appear to age more quickly than their counterparts undergoing continuous aging since the moisture has sufficient time to penetrate the propellant during the two off-days. Note that for tablets, this pronounced change in

the rate of propellant aging is not observed since the tablets are not stacked and do not experience this change in surface-to-volume ratio.

As with tablets, Figure 49 and Figure 50 indicate lower wafer densities than those currently measured in field returns for some inflators. The same two potential primary reasons for this difference are valid: 1) the inflator was built with a moisture level that is higher than that predicted to occur in the field and labeled as “extreme” (PSPI-X TX for example) or 2) the inflator is relatively new and therefore field aging time has not yet reached the lower densities seen in the artificial aging program.

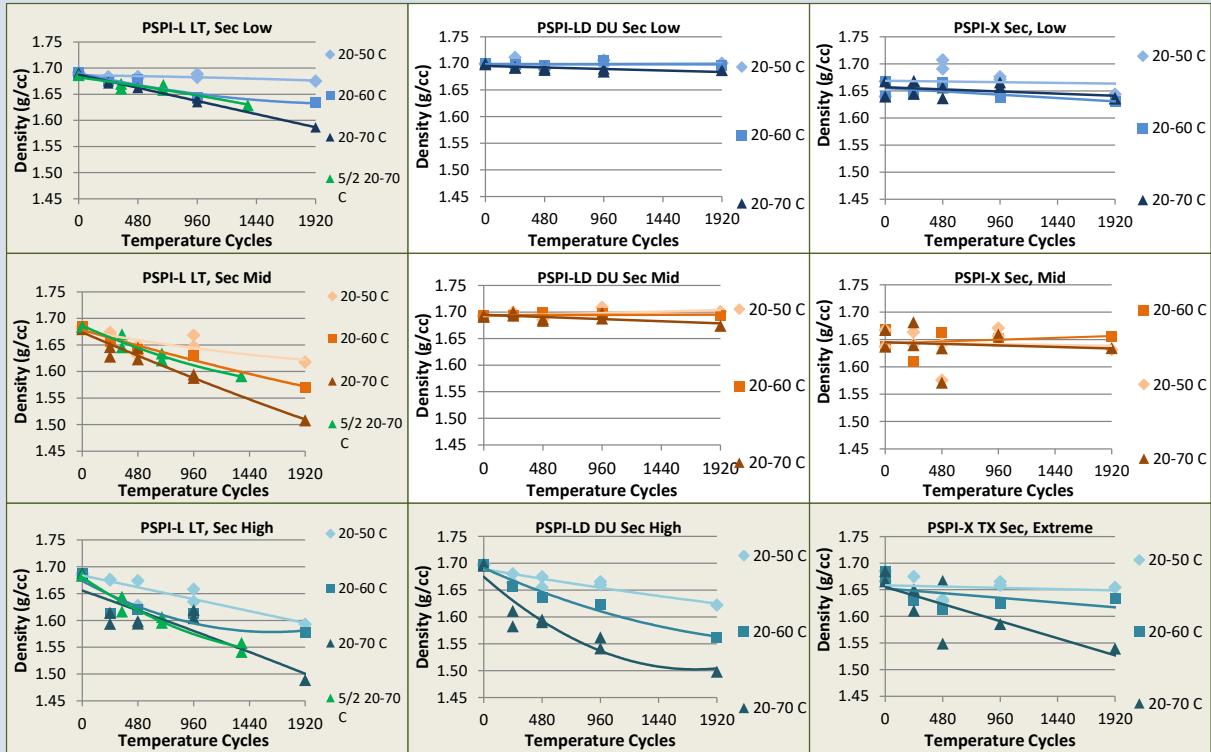
For both tablet and wafer systems, desiccated inflators with the highest moisture levels experience similar amounts of aging over 1,920 cycles as their un-desiccated counterparts. This may appear to contradict the modeling results that suggest these desiccated inflators have a much longer service life. The reason the desiccated inflators have a longer service life is because the desiccant protects the propellant from aging until the desiccant is saturated, whereas aging of propellant in un-desiccated inflators begins when those inflators enter the field.



The non-desiccated PSPI-L LT inflators and desiccated inflators with saturated 13X are shaded.

TAIR-050 V1

**Figure 49. Passenger Inflator 2004/2004L Primary Caliper Density Measurements**  
 The non-desiccated PSDI-5 ZA inflators and desiccated inflators with saturated 13X are shaded. Y scales for primary chambers (Figure 49) are different than for secondary chambers (Figure 50).



The non-desiccated PSPI-L LT inflators and desiccated inflators with saturated 13X are shaded.

TAIR-051 V1

Figure 50. Passenger Inflator 2004/2004L Secondary Caliper Density Measurements

Propellant Density Summary

The general scientific aging trends are summarized below:

- The propellants lost density when temperature cycled in the presence of moisture
  - Propellants exposed to moisture without temperature cycling did not result in density loss
  - Temperature cycling without moisture did not result in density loss. This was noted in inflators with unsaturated desiccant, which protected the propellants from density loss
- Higher temperature cycling causes more propellant damage (20 to 70°C > 20 to 60°C > 20 to 50°C)
- In general, higher moisture levels age propellant faster
- Flattening of the propellant wafer stack may cause wafers to age somewhat differently than tablets
- PSAN in desiccated inflators suffers more damage if the desiccant is over-saturated

Propellant Burn Rate

Burn rate is a critical propellant characteristic and input for inflator system performance modeling. Typical Takata press density versus burn rate characterization is shown in Figure 51. This figure shows 10.8-gram wafers pressed to four different densities. Each of the four burn rate

versus density curves show an increase in burn rate with pressure. At very low pressure, all the density curves show the same burn rate. As pressure increases, the reduced-density curves diverge. For a density of 1.603, the burn rate is 2.5 times the nominal burn rate at 65 MPa. All of Takata's PSAN propellants show these same general trends, but the quantitative burn rate values change with propellant type and propellant geometry.

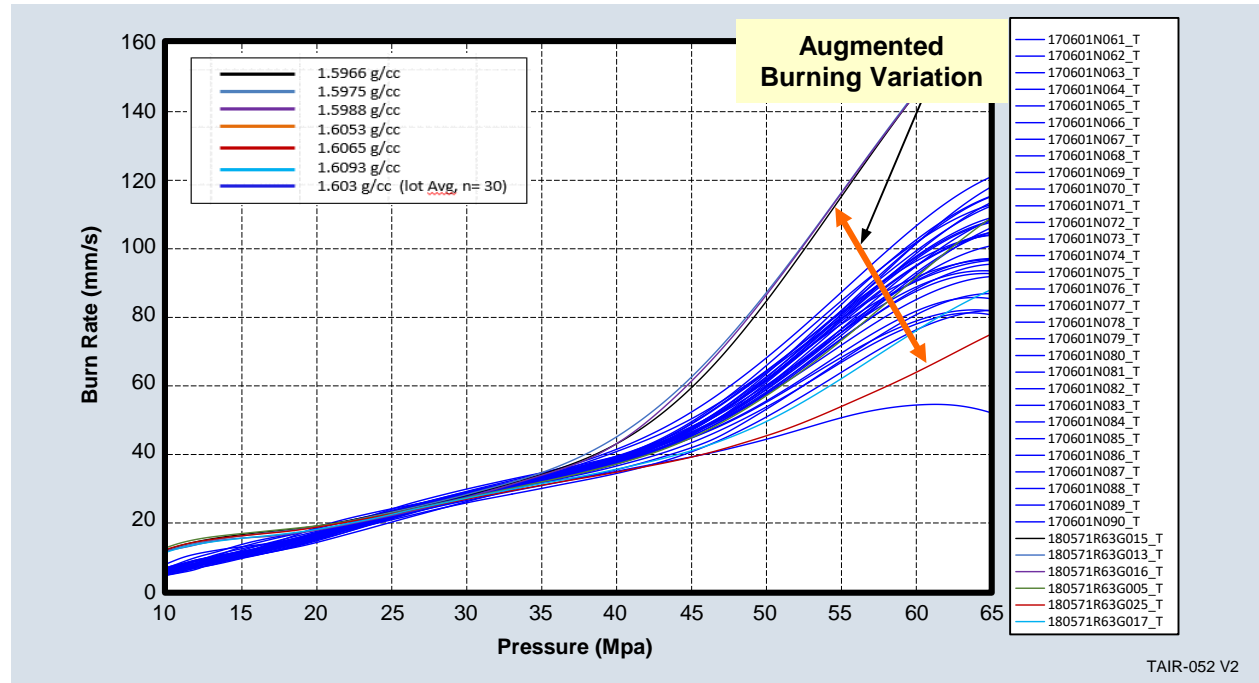
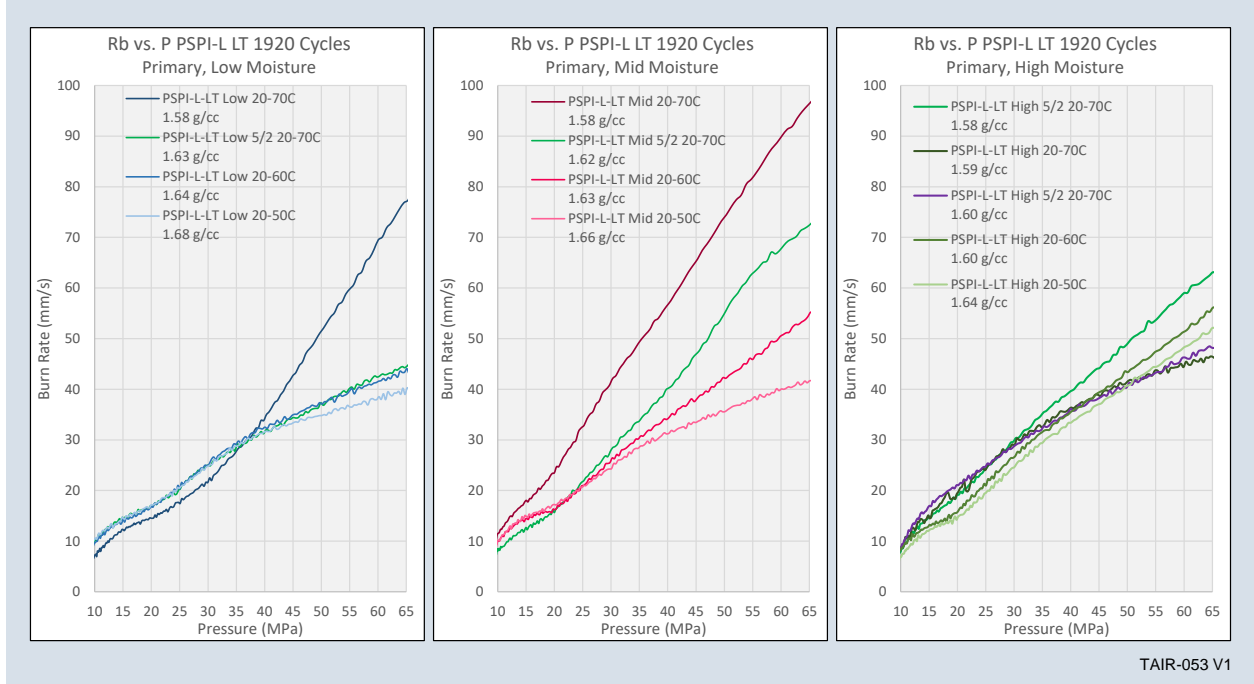


Figure 51. Propellant Density Decrease Can Yield Augmented Burning. Data courtesy of Takata

Wafers from PSPI-L FD/LT inflators that experienced 1,920 temperature cycles showed signs of augmented burning as shown in Figure 52. While not shown, indication of augmented burning was noticed for 2004 wafers from PSPI-L FD/LT inflators cycled for 960 four-hour cycles.



TAIR-053 V1

**Figure 52. Burn Rate vs Pressure Plots for 2004 Wafers from PSPI-L FD/LT Inflators Cycled 1,920 4-Hour Cycles.** *The deviation to higher slope indicates the undesired increase in apparent burn rate.*

Results from artificially aged PSPI-LD DU inflators are shown in Figure 53. Signs of augmented burning are less for the thinner DU wafers than for the thicker LT/FD wafers. The wafer from the low moisture inflator cycled to a maximum temperature of 70°C exhibits the lowest burn rate in high pressure regimes.

Results from extreme moisture PSPI-X TX wafers are shown in Figure 54. The wafer from the 20 to 70°C extreme moisture inflator exhibited augmented burning characteristics.

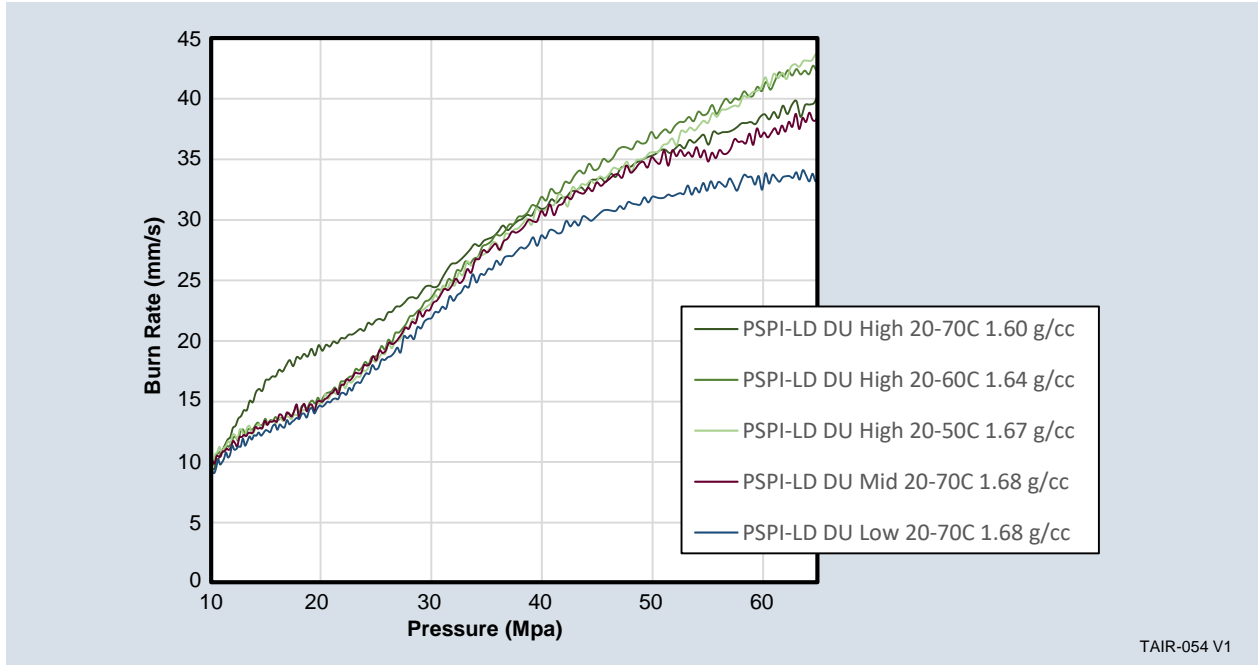


Figure 53. Burn Rate vs Pressure Plots for 2004 Wafers from PSPI-LD DU Inflators Cycled 1,920 4-Hour Cycles

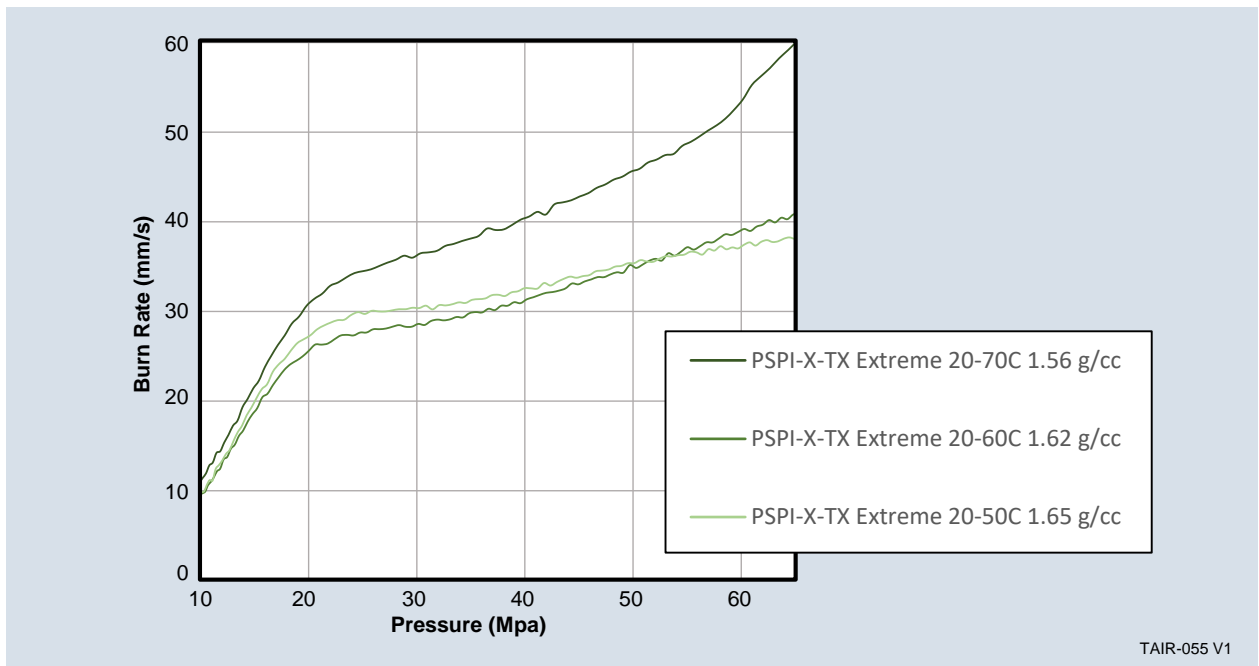
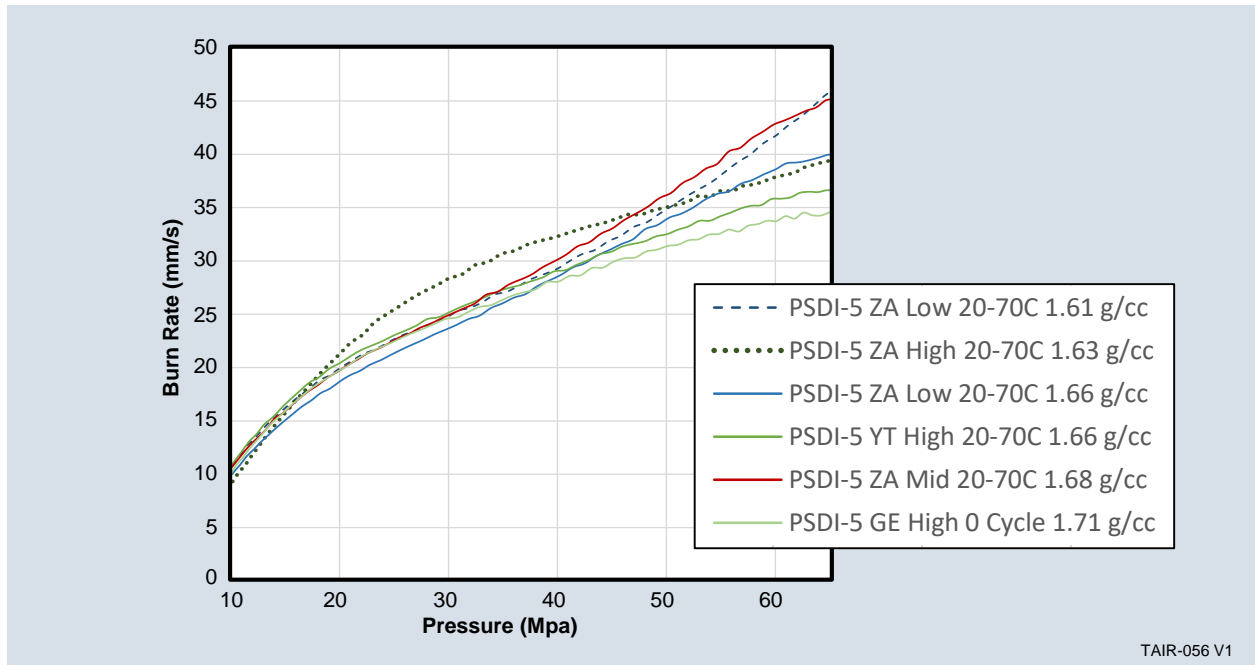


Figure 54. Burn Rate vs Pressure Plots for 2004 Wafers from PSPI-LD DU Inflators Cycled 1,920 4-Hour Cycles. The increase in slope behavior is not the same in this extreme moisture as in the PSPI-LT inflators suggesting a different phenomenon.

Results from tablets with higher moisture contents and / or temperatures are shown in Figure 55. The PSDI-5 ZA low moisture, 20 to 70°C inflator had the lowest density and greatest signs of augmented burning at the full 1,920 cycles. The low moisture inflators developed augmenting burning more slowly than those with higher moisture. The trace shape for tablets from the high-moisture PSDI-5 ZA cycled to a maximum temperature of 70°C has a different trace shape in the burn rate versus pressure plots than the others. Tablets from 20 to 70°C inflators show the greatest burn augmentation followed by those from 20 to 60°C inflators. While not shown, no signs of augmented burning were observed in tablets from the PSDI-5 ZA and YT field returns and 1,920 cycle, artificially aged PSDI-5D YT inflators.



**Figure 55. Burn Rate vs Pressure Plots for 2004 Tablets from PSDI-5/5D Inflators Cycled 1,920 4-Hour Cycles**

Tablets of 2004L in PSDI-X SV inflators show augmented burning at densities of 1.51 g/cc and 1.48 g/cc. Tablets may be showing initial signs of augmented burning at a density of 1.64 g/cc (Figure 56).

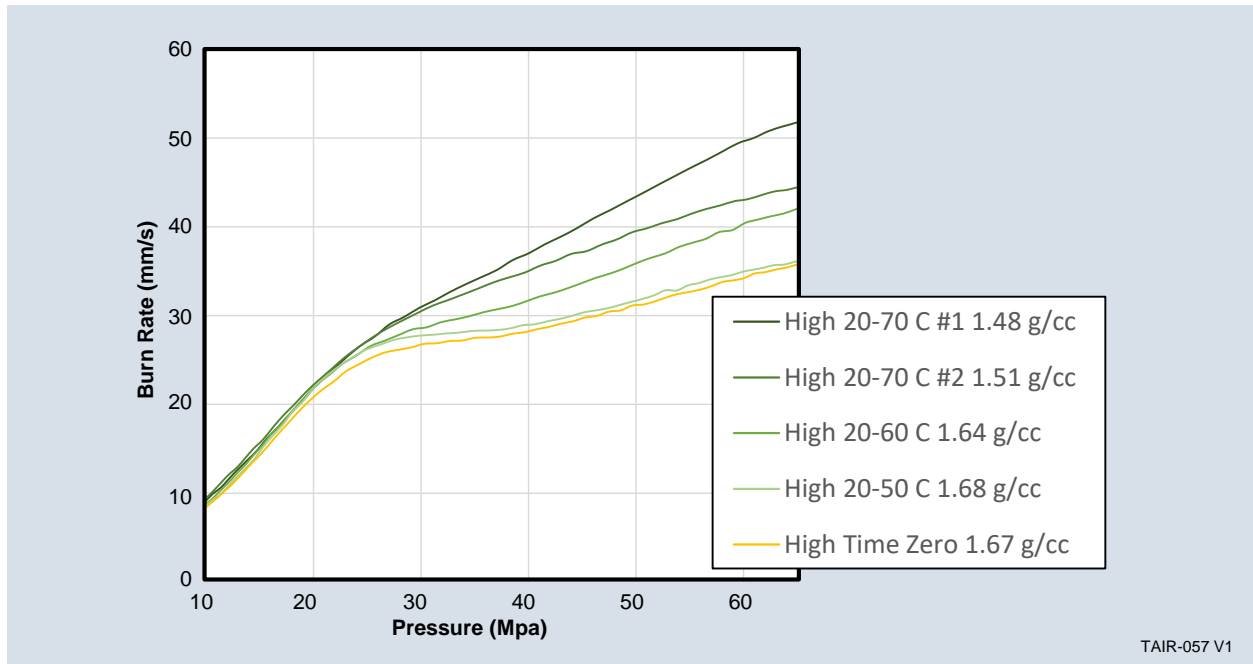


**Figure 56. Burn Rate vs Pressure Plots for 2004L Tablets from PSDI-X SV Inflators Cycled 1,920 4-Hour Cycles**

The key finding related to burn rate is:

- Northrop Grumman data and Takata data show an apparent burn rate increase with density decrease termed “augmented burning” for both the 2004 and 2004L propellants

### Tank Testing

Density versus peak combustion pressure plots are presented of all inflators that were tank tested during the aging study portion of this program (Figure 57 through Figure 63). Approximately 1,600 inflators tests were conducted in the 60L tank, 250 were tested in go no-go test fixture and 450 were tested in heavyweight fixtures.

The densities in the figures were calculated based on dimensional analysis from CT scans performed on every inflator. Driver inflators were more challenging in obtaining clear CT images. The figures shown for driver inflators include the density points for inflators where accurate dimensional data could not be obtained due to either poor image quality or degraded propellant tablets. These points were artificially set to a density of 1.45 and plotted in orange.

### Observations

**Overall:** It appears that most inflators in this group began to produce higher than nominal pressures when propellant densities reached 1.56 to 1.59 g/cc. Exceptions to this were the extreme-moisture level conditions, where pressures began to deviate almost immediately.

**PSDI-5D YT Secondary:** Several of the high-moisture samples show very low density values. The secondary chambers of PSDI-5D YT and PSDI-5D GE contain a ceramic paper cushion that can cause distortion of the secondary tablets that may result in measured densities that are artificially low. This is especially true of the YT version that contains 3.5 grams of 2004 tablets in the secondary chamber. The GE version contains only 2.0 grams of the 2004 tablets.

**PSDI-5D GE Secondary:** This is the only inflator chamber where high densities were seen (>1.68 g/cc). Although the reason for this is unclear, the data was corroborated through physical caliper measured dimensional analysis.

**PSDI-5D GE High Moisture:** In the case of 1,440 and 1,920 inflators cycled between 20 and 70 °C, several, if not all, of the 2004 tablets were distorted beyond recognition or had turned to powder (Figure 64).

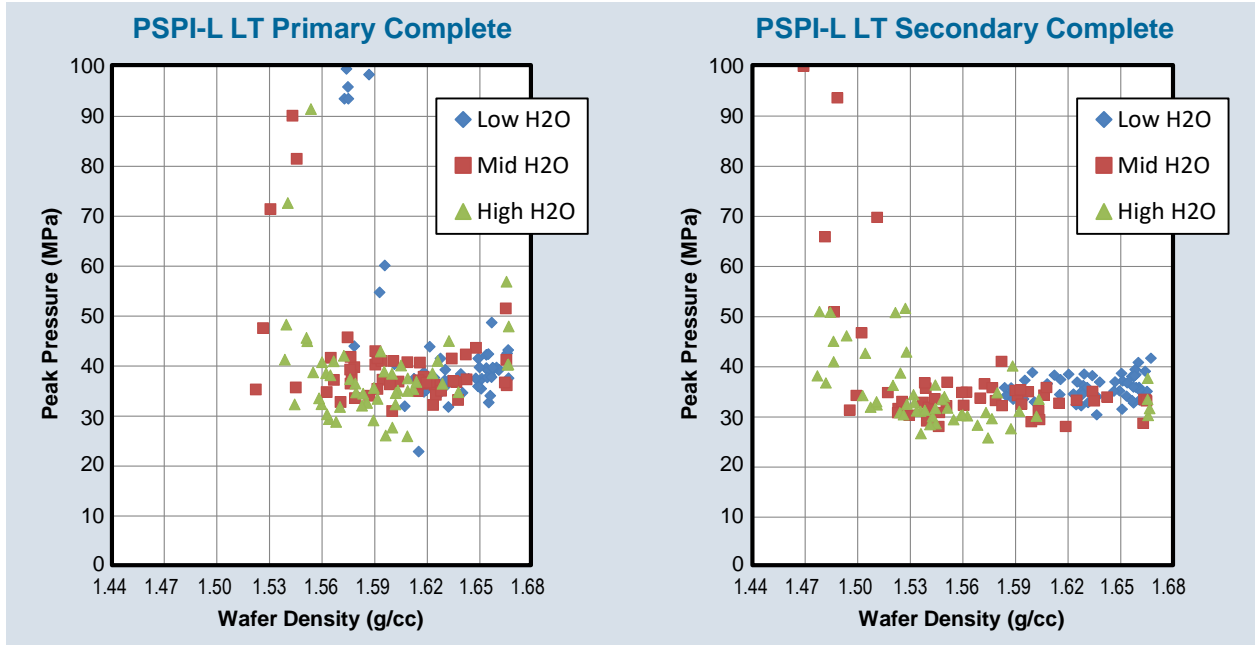


Figure 57. PSPI-LT Density vs. Peak Combustion Pressure

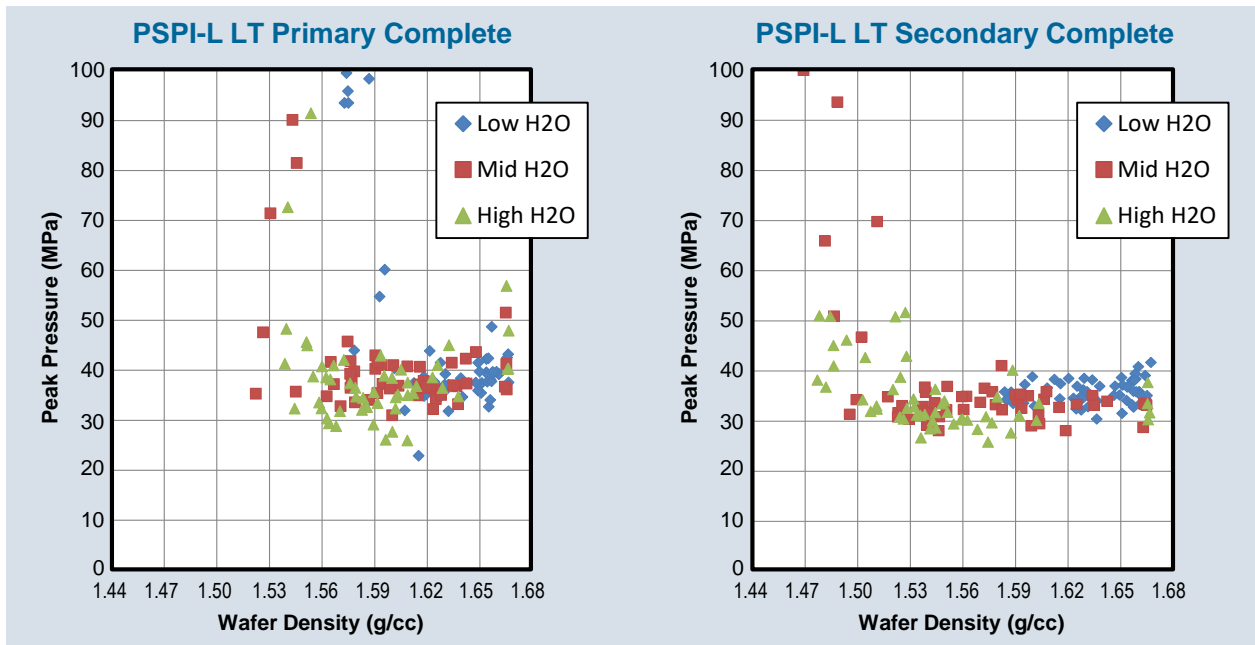


Figure 58. PSPI-LD DU Density vs. Peak Combustion Pressure

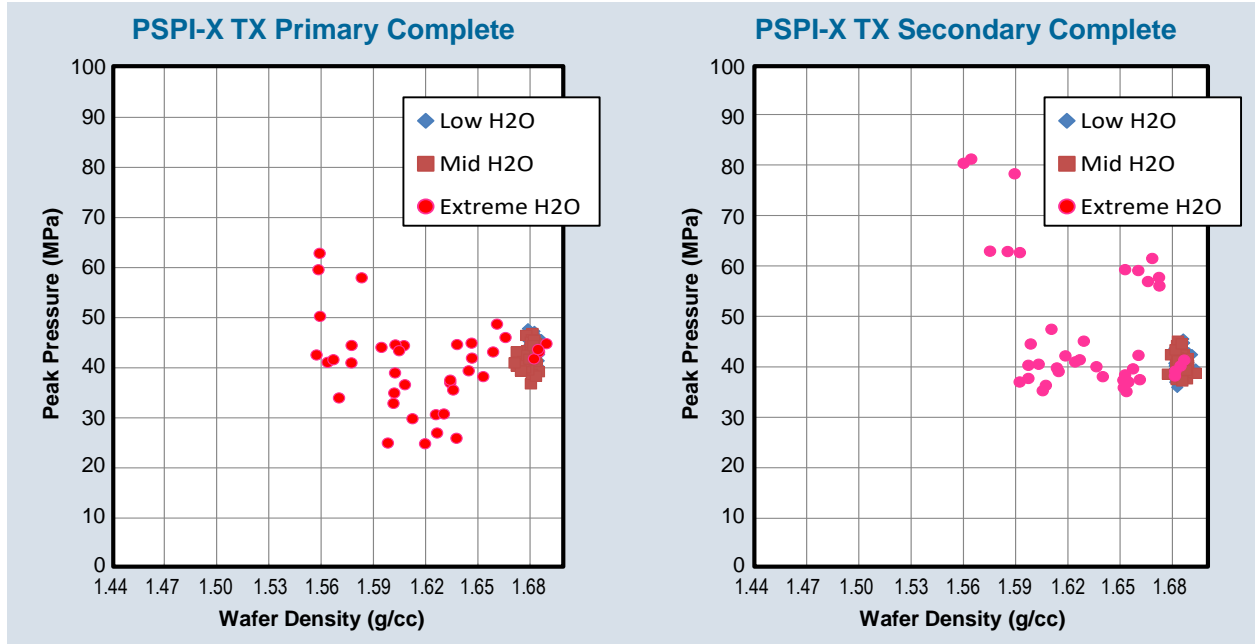


Figure 59. PSPI-X TX Density vs. Peak Combustion Pressure

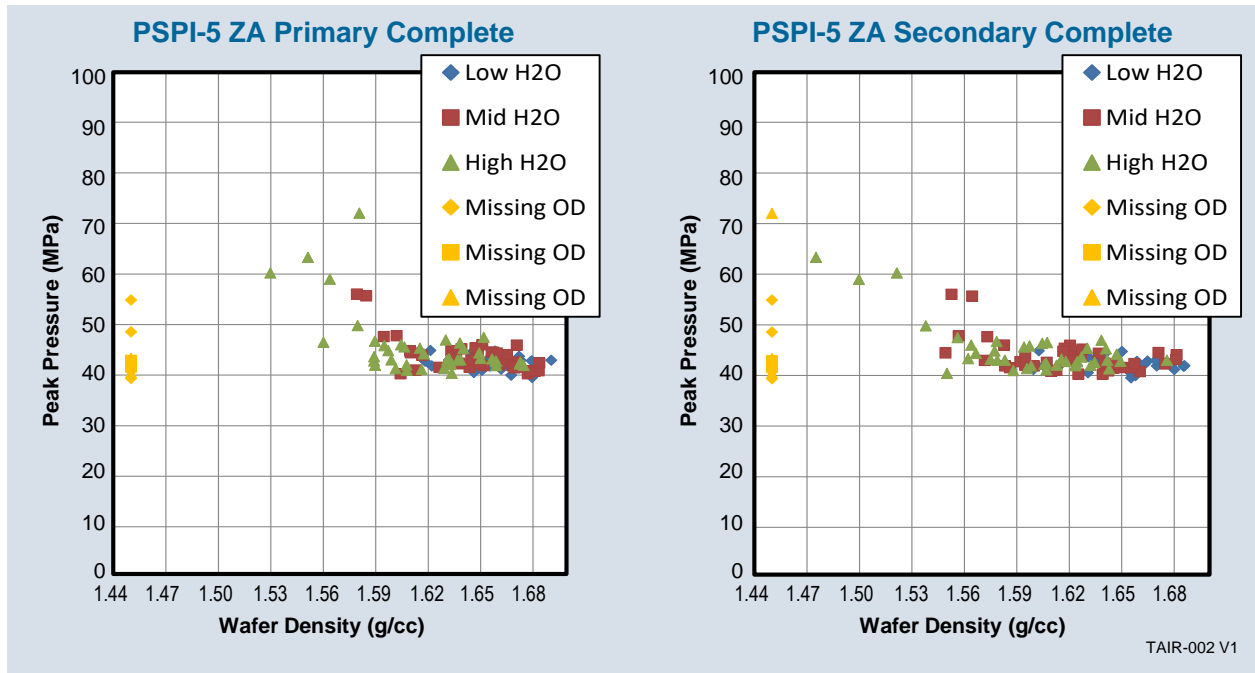


Figure 60. PSDI-5 ZA Density vs. Peak Combustion Pressure

TAIR-002 V1

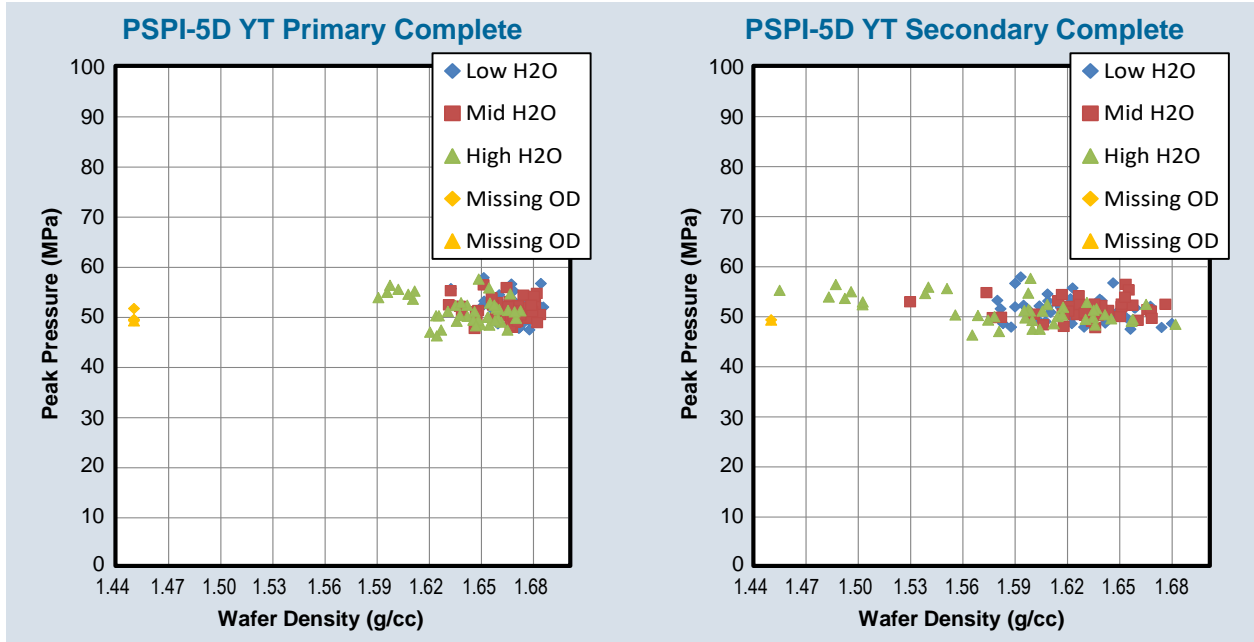


Figure 61. PSDI-5D GE Density vs. Peak Combustion Pressure

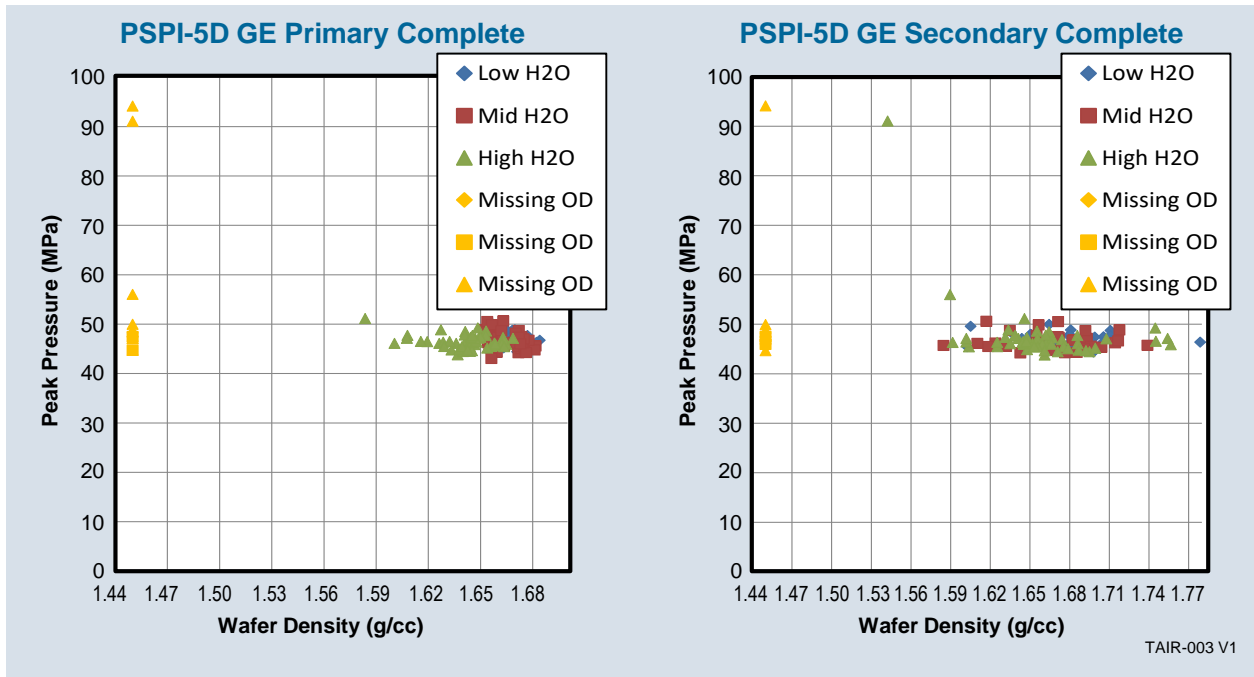
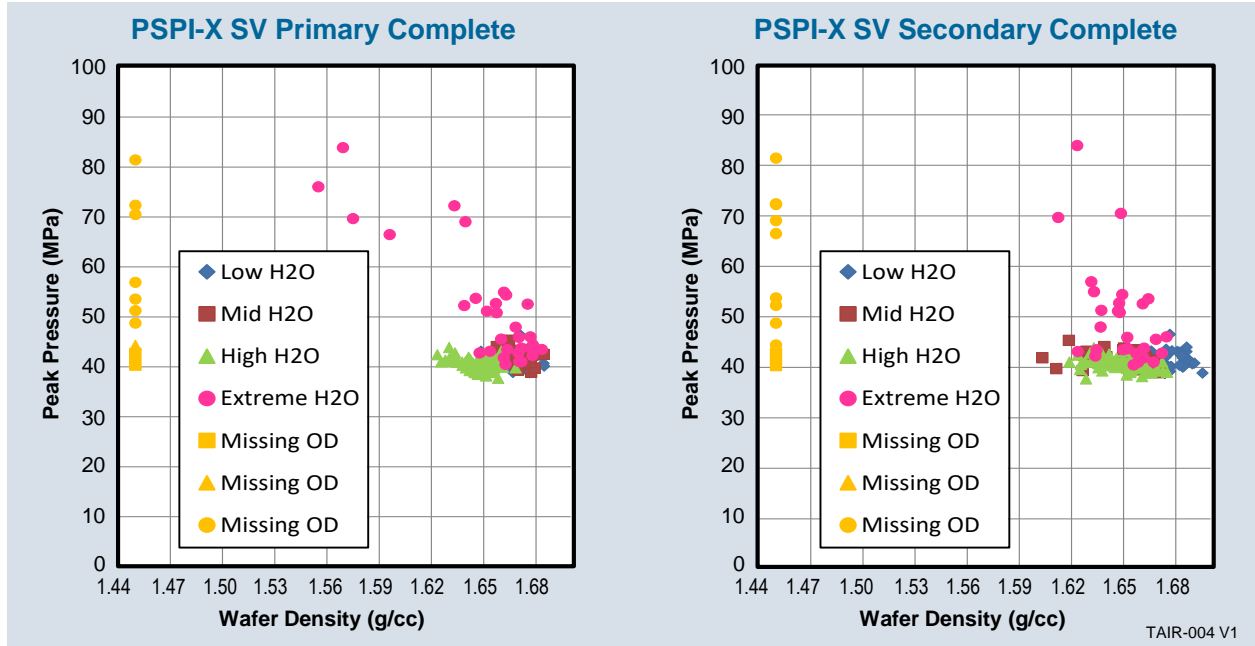
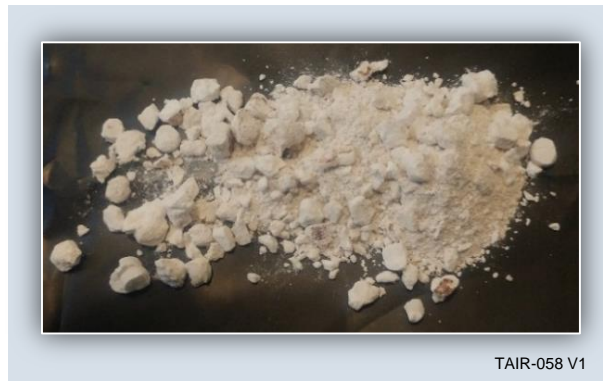


Figure 62. PSDI-5D GE Density vs. Peak Combustion Pressure

TAIR-003 V1



**Figure 63. PSPI-X SV Density vs. Peak Combustion Pressure**



**Figure 64. Tablets Removed From the Primary Chamber of a High Moisture PSDI-5D GE Inflator Cycled 1920 Times from 20 to 70 C**

## Sensitivity Studies and Key Assumptions

### Sensitivity Studies

Sensitivity studies, the way that the output of the model responds to changes in inputs, were used extensively to validate and understand the model and to deepen our insight into the inflators, their design and engineering characteristics and how they age. Sensitivity studies were done on three different levels. There were global studies or full end-to-end experiments that ran the entire inflator aging model for the full determination of impact on the POF for an inflator. We executed more than thirty of these end-to-end sensitivity studies. The second level was those done for individual modules in the model. These were primarily to validate the modules and to compare

against and calibrate with field-return data as available. The third and lowest level was in the individual, physics-based equations and these were used to fix the constants and calibrate to field data. A large number of iterations were done at these lower two levels to construct, test and validate the individual parts of the model. Several were discussed in the previous sections describing the individual modules and equations. A listing of the global sensitivity studies are given in Appendix B. Five notable examples are described in Table 11 in tabular form and are representative of the approach taken and utility of the studies. It is worth calling specific attention to the first line for equilibrium moisture values in the 2004L propellant based inflators.

**Table 11. Exemplary Sensitivity Studies Completed to Validate the Model and Understand the Inflators**

Subject of Study	Purpose(s) of Study	Key Outcome
Moisture in Inflators (cited earlier)	With limited field age for inflators containing 2004L as the propellant, the equilibrium moisture levels at ages critical to the overall study of $\geq 10$ years are not available from the field. This study modeled how small changes in those values impact the aging of the inflators.	A modest shift in the equilibrium relative humidity from 40% to 50% results in a shift of over 2X in the calculated time to age. This reinforced the value of further data to improve the fidelity of the model. See Table 4 earlier in this report.
Hydroburst Input Data	Compare various data sources for hydroburst data and impact of POF prediction	Use of Takata acceptance data, though static, and variation provided most accurate input to the model; this was not a source of the initial manufacturing variation observed
Starting Density and Moisture	Determine the impact of small variation in the initial pressed density of tablets or wafers on the aging of the inflators. Similarly, determine the impact of modest changes in the amount of moisture in the propellants at the time of manufacture.	Small variation, within what is difficult to establish from the measured data (<0.02 g/cc) can have an impact of the time to a given POF. In contrast, unless a very low inflator leak rate is assumed, the initial moisture level has a relatively minor impact on the inflator aging since the moisture dynamics in and out of the inflator dominate.
Inflator Leak Rate	Validation and calibration of module, prediction of impact manufacturing fault (leakers)	Model calibrated with primary diffusion leak with rate sufficient to match field return data; higher leak rates result in much shorter times to 0.01 POF
Impact of Augmented Burning Variability	A module-level study to determine impact of the variation of observed burning rate augmentation at a specific density from aging or low pressed density lab studies.	The magnitude of the range of variability was a factor but not large because once density low enough for significant augmented burning was achieved, typically, the variation was all above the capability of the pressure vessel.

The sensitivity studies filled a critical role in establishing confidence in the validity and high-fidelity of the model for all 2004 propellant-based inflators, desiccated or not. It also highlighted the utility of the model for 2004L propellant-based inflators with the identification of the value of obtaining further data to improve the fidelity of the model for these 2004L propellant inflators.

**Key Assumptions**

In developing an aging model and utilizing data, there are necessary estimations, extrapolations, interpolations, simplifications and assumptions. In aggregate, we refer to all of these as assumptions. They range from global in level to very small items. These are necessary to develop and execute the model. For example, the National Oceanographic and Atmospheric Administration (NOAA) weather data used was based on detailed data available for each of the five climatic conditions (zones represented by the five cities).

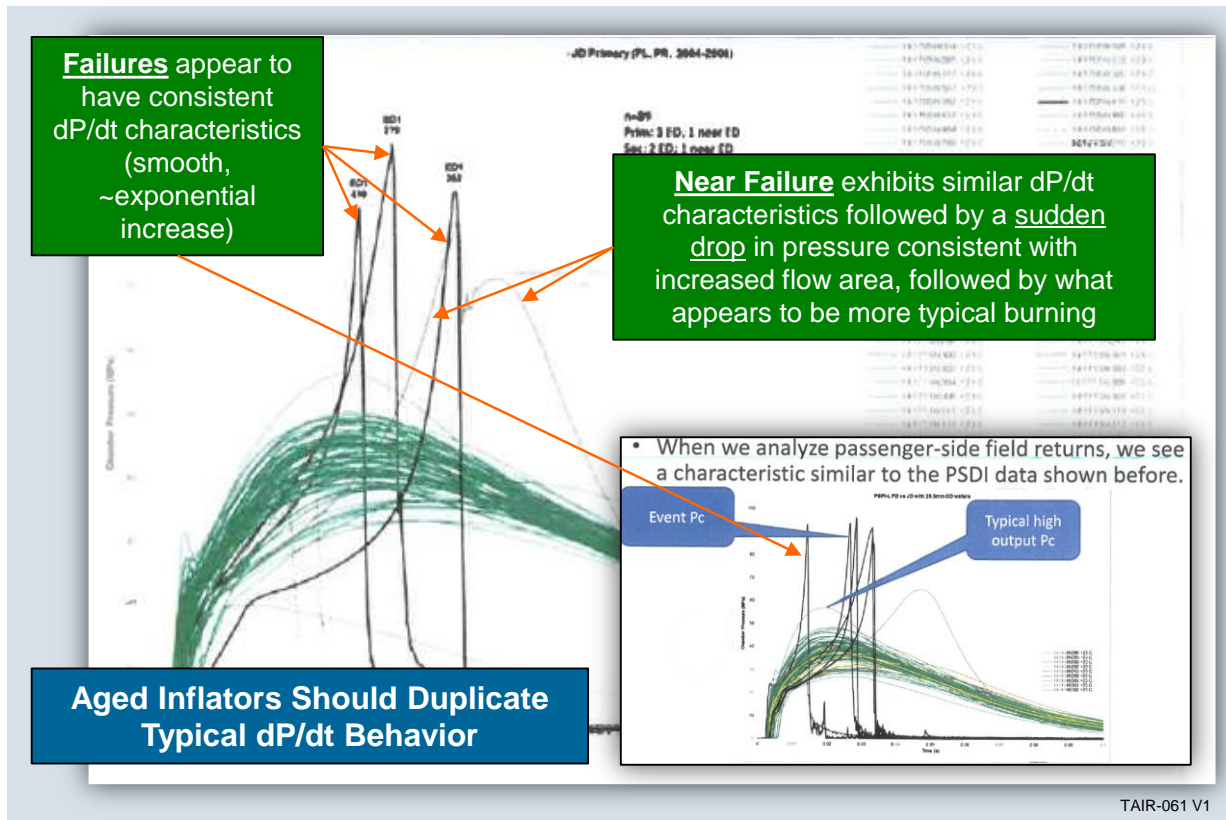
There are two assumptions in the use of this data. First, that the data for the city is reasonably representative of the broad climate class of interest. The second is that with ten years of detailed data in hand, we repeated that data three times to get to the desired thirty years. The assumption there is that the newer weather data used is not significantly different than what was experienced in the preceding twenty years. For reference, a correlation between the five cities chosen for this study and the NHTSA zone designation is given here in Table 12. For a more complete discussion of the climate zones, please refer to Appendix D.

**Table 12. Correlation of Cities Selected for this Study and the NHTSA Zones**

City	NHTSA Recall Zone	Takata Updated Zone
Miami	<b>A</b> - Hot and Humid	<b>1</b> - High AH (>15 g/m <sup>3</sup> )
Atlanta	<b>A</b> - Hot and Humid	<b>2</b> - Coastal Moderate-High AH (~13 g/m <sup>3</sup> )
Phoenix	<b>B</b> - Less Hot and Humid	<b>5</b> - High Temperature Low AH (~7 g/m <sup>3</sup> )
Detroit	<b>C</b> - Least Hot and Humid	<b>3</b> - Central Temperate Moderate AH (~10 g/m <sup>3</sup> )
Seattle	<b>C</b> - Least Hot and Humid	<b>4</b> - Coastal Cool Low-Moderate AH (~8 g/m <sup>3</sup> )

The key assumption in the study relates to the 2004L-based inflators. In the case of the inflators using 2004 propellant, there is excellent data that the scientific aging reproduced that aging in the field to a remarkable degree. The density reductions, ballistic performance and failures of these scientifically aged inflators were superimposable on the field returns. This is most clearly observed in the ballistic data. The characteristic “shelf” behavior of these inflators as shown in Figure 65 is undeniably similar in the two systems. This provides a high level of confidence that the scientific aging data can be reliably used in estimating and projecting on future behavior in these systems. It overall validates the model developed in this study in that the field data was faithfully reproduced. In the case of the 2004L propellant-based inflators, there are no examples of field-aged inflators that have shown aging. Based on the relatively young age of these inflators, we would not predict to observe anything but, perhaps, the earliest signs of changes. Hence, we do not have concrete proof that the scientific aging of the 2004L propellant will be the same as in the field. This is a significant assumption (Figure 66).

A listing of these estimations is included in Appendix B along with the table of Sensitivity Studies.



TAIR-061 V1

Figure 65. PSPI and PSDI Pressure vs Time Ballistic Testing Exhibits a characteristic Ballistic Response to Lower Density due to Field Aging

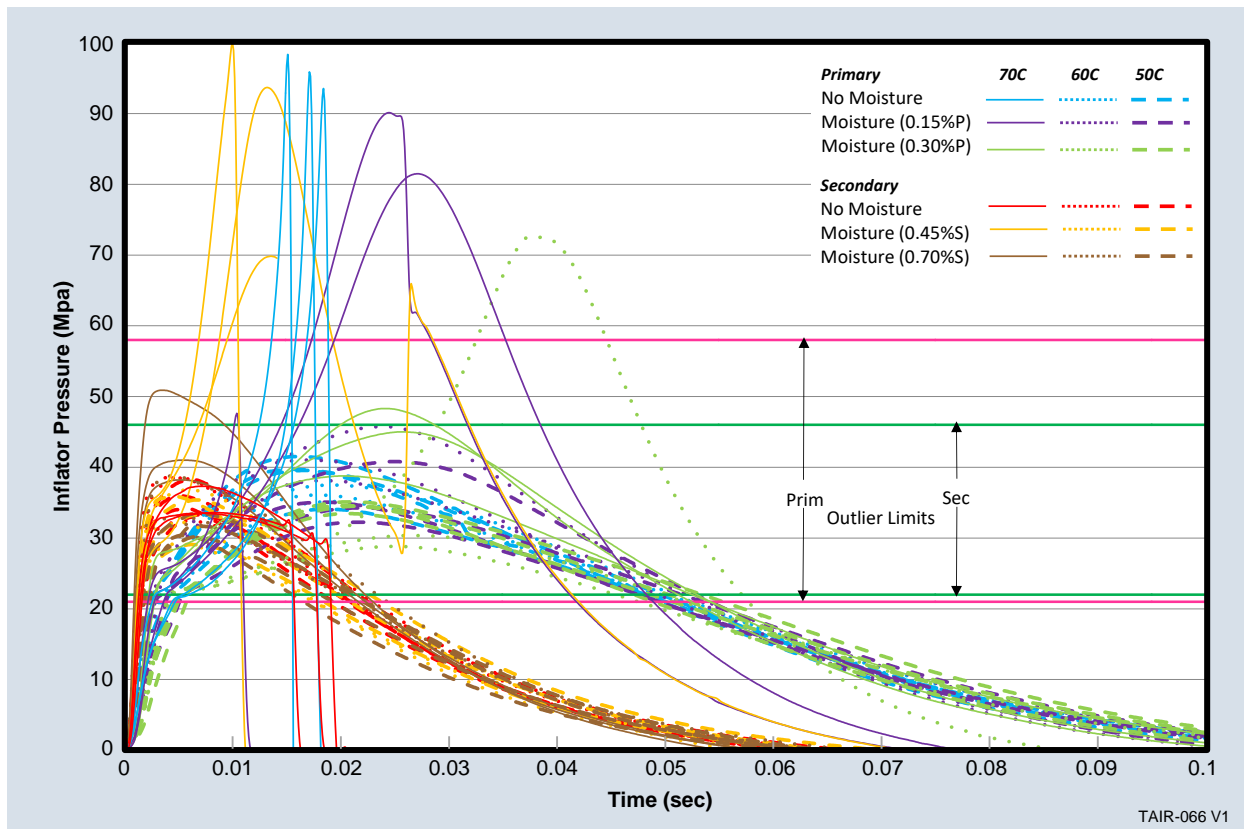


**Figure 66. PSPI Inflators from the Scientific Aging Study Exhibit the same characteristic Ballistic Response to aging as the Field-aged Inflators.** This validates many aspects of the Scientific Aging study including moisture levels selected, temperatures selected, cycle times selected and number of cycles in the study.

## Summary and Conclusions

This section provides a brief summary, in bullet form, of the overall effort as completed by NGIS.

- We built a comprehensive Predictive Aging model based on Phase I failure mode:
  - Change in ballistic response (maximum pressure during deployment) due to temperature cycling in presence of moisture
  - Model is semi-empirical with portions that are deterministic and the final POF probabilistic. Most sub-routines are physics-based and have good input data and sufficient anchoring data.
    - Good weather input data from existing database (NOAA)
    - Good vehicle temperature and humidity data and translation to inflator (from ATLAS work, OEMs and NGIS)
    - Good equilibrium and rate data for moisture movement (Phase I and II data, OEM data and Takata data)
  - Density change with moisture / temperature cycling is the only subroutine that is primarily empirical. We do not have a physics-based model of the mechanisms that drive density change. Therefore, the scientific aging data is critical.

- C-integral versus density is the empirical data that ties model predictions of aging time and exposure to the scientific aging data of how the propellants in the inflator responded
- Inflator dimensional model for ballistic model is built using engineering drawings provided by Takata and is precise
- Burn rate as a function of propellant density (burning rate augmentation at lower densities) is empirically derived through low pressed density wafer and tablet studies
- Capability of inflator body for pressure is well characterized and does not degrade over time; ED is a result of high-pressure event on deployment
- Ballistic models uses point value for density and known variabilities to create a probability of failure for that condition
- The baseline, undesiccated 2004/3110 inflators (PSPI-L and PSDI-5), had sufficient field data of relevant age to firmly anchor and validate the model
- All other inflators are of later manufacture with 2004L propellant. The field data is not a sufficient number of years to anchor the model fully; the purpose of the model was to predict what will happen as these later (largely desiccated) inflators experience longer times in the field.
- We conducted a scientific aging program on seven inflators to obtain critical inputs for predictive aging model; measured change under known moisture content, temperature range and number of cycles.
  - Useful information was obtained from the scientific aging study
    - Density change at known moisture levels for every inflator
    - Provided a range of response with significant sensitivity of the outcome based on the input and curve fit
  - These data created the C-integral curves used to predict propellant density under the cumulative effects over time of humidity and temperature exposure and cycling.
- Both 2004 and 2004L PSAN propellants lose density when cycled in presence of moisture
  - 2004 propellant shows response at lower humidity level than 2004L
  - Lab experiments show that 2004L has a significantly lower propensity to absorb moisture at moderate humidity levels (<40%) than does 2004 propellant
  - Moisture level necessary for 2004L to be effected is in the range of the maximum predicted to be achieved in the field in the most severe environment. With limited field data, it is not known if this moisture level will be seen in the field. Determining this is a significant opportunity to increase the accuracy and fidelity of the model.
- Both 2004 and 2004L have burn rate increase with loss of density
  - Similar rate of burning rate augmentation for similar density reductions
  - The data supporting this is laboratory low-pressed density studies completed by Takata and field return data for older, 2004 propellant based inflators
  - It is a yet to be proven assumption that 2004L propellant will age similarly in the field as those inflators are not of sufficient age to have exhibited this behavior.
- Desiccant is an effective preventer of aging
  - Stops PSAN aging so long as the desiccant is not saturated
  - Every desiccated inflator is predicted to be significantly more resistant to density reduction over time compared to undesiccated inflators
  - Higher ratio of desiccant to propellant results in longer protection
  - Sufficient desiccant can protect an inflator even in severe environments

## Paths to Increased Model Fidelity

NGIS is not intending to propose further scope to the ITC. This is not to say that NGIS would not be willing to support future efforts and maintain the products developed. It is our contention that the purpose of the project requested by the ITC has been completed. Our opinion is that the newer generation inflators have shown significant improvement in aging. With all predictive aging models, there is uncertainty that increases the farther into the future and away from validating data the prediction is called to look. The anchoring data for the older PSAN propellants, designated 2004, is sufficient for confidence in the overall fidelity of the model and its predictions. With the newer PSAN propellants, designated 2004L, the fidelity of the models will benefit from further data to anchor. There are three specific approaches to increase the fidelity of the model with age that we would state are technically supported broadly.

- Surveillance in the field (ongoing)
  - X-series inflators as they continue to age in the field
    - Primarily PSPI-X and PSDI-X with 2004L/AIB/13X but consider all 2004L inflators
    - Monitor for available data for any field events with these inflators
    - Take advantage of any parts that become available for secondary reasons to test for signs of aging
- Field return testing (ongoing)
  - X-series inflators with limited data due to age of inflators in the field
    - Specifically PSPI-X and PSDI-X with 2004L/AIB/13X
    - Only for inflators with lower ratio of 13X to 2004L propellant (<1.5%)
    - Focused, small surveillance in Zone 0, Temperature band 3 vehicles
    - One time testing in 3 to 5 years to validate trend of zero aging or identify direction and rate
- Field return aging study (near term, one time)
  - X-series inflators with limited data due to age of inflators in the field
    - Specifically PSPI-X and PSDI-X with 2004L/AIB/13X
    - Gather maximum age inflators from most severe aging for climate (Miami) and vehicle temperature (Temperature Band 3)
    - Suggests sufficient number for statistical viability
    - Test 100 to 200 in current state to see moisture, propellant density reduction
    - Accelerate rest (300 to 600) under temperature cycles as in scientific aging but with no further internal moisture addition but in the presence of external humidity such as in the Miami climate
    - Measure for any changes in density over 960 cycles (half of scientific aging) and determine trends to close effort

## Addenda

### A. Sources of Information and Acknowledgements

The scope of the project as presented to Northrop Grumman (then Orbital ATK) by The Independent Testing Coalition (ITC) was to pursue root cause and ramifications using all available information. The investigation was not limited in focus or breadth or depth of investigation. There was not any direction given by the ITC. No limitations were imposed on avenues of the investigation or range of questions asked. We received consistently strong support from each member of the ITC. Each ITC member willingly shared relevant data they had.

We received critical support from Takata and TK Global. They supplied proprietary engineering drawings to support our modeling. Takata provided aged and new inflators as well as inflator hardware, raw materials and access to their engineering and manufacturing facilities. Takata met with us on several occasions to respond to our questions. Takata also provided access to their Master Engineering Analysis File (MEAF).

We also met with individuals from Fraunhofer ICT as arranged by Takata and with faculty from Penn State to discuss their studies. National Highway Traffic Safety Administration (NHTSA) personnel provided relevant information regarding their in-house investigations and from their review of efforts by all other parties.

We considered all the data we gathered as relevant to the investigation and sought to include every possible source in our work. We independently verified data from all sources to ensure that we could stand by all the critical data we cite as relevant to our investigation.

### B. ITC Membership and Purpose

Formed in December 2014, the ITC has as its sole purpose to conduct an independent and comprehensive investigation of the technical issues associated with Takata airbag inflators. The ITC comprises ten automakers that have Takata airbags subject to the noted recalls in their passenger and light truck vehicles: BMW, Fiat Chrysler Automotive, Honda, Ford, GM, Mitsubishi, Mazda, Nissan, Subaru and Toyota.

### C. Northrop Grumman Relevant Qualifications and Background

The Northrop Grumman team was primarily located within our Propulsion Systems business unit in Utah. We called on expertise relevant to the project from across the company and outside of our company for specific technical capabilities and for real-time radiography and computed tomography image analysis. The core team has extensive experience in the design, research and development, testing and manufacture of propellants, explosives and pyrotechnics including many years of experience with automotive inflators. Northrop Grumman is not involved in the inflator business today and, as such, is well positioned to serve as an objective investigator on this project. We provided the best technical personnel and used the best of the tools at our disposal to provide an accurate and objective assessment.

## Appendix A. Probability of Failure Curves and Full Tables for the Seven Inflators

The full tables for all of the inflators in this study and corresponding representations of the same data in a graph format are presented here. Please refer to the rest of the report for a description of the tables and how to read and interpret them.

For each of the inflators, with the exception of the PSPI-TX inflator, one master table is shown and the associated curve representation of the data. For the PSPI-X TX, the three tables referred to in the main body of the report are all shown here. In the graph format, only the Mid-Nom moisture master curve assumption is included. For a discussion of those three PSPI-X TX scenarios, please refer to the main body of the report.

### Passenger 2004-based Inflators

PSPI-L LT/FD Years to 0.01 POF						
Percentile	Vehicle	Miami	Atlanta	Phoenix	Detroit	Seattle
1st Percentile	T3	8	15	16	20	>30
	T2	12	21	17	29	>30
	T1	20	>30	22	>30	>30
5th Percentile	T3	9	16	16	23	>30
	T2	14	22	18	>30	>30
	T1	26	>30	28	>30	>30
25th Percentile	T3	11	20	17	27	>30
	T2	25	>30	28	>30	>30
	T1	>30	>30	>30	>30	>30

PSPI-LD DU Years to 0.01 POF						
Percentile	Vehicle	Miami	Atlanta	Phoenix	Detroit	Seattle
1st Percentile	T3	22	>30	>30	>30	>30
	T2	>30	>30	>30	>30	>30
	T1	>30	>30	>30	>30	>30
5th Percentile	T3	24	>30	>30	>30	>30
	T2	>30	>30	>30	>30	>30
	T1	>30	>30	>30	>30	>30
25th Percentile	T3	28	>30	>30	>30	>30
	T2	>30	>30	>30	>30	>30
	T1	>30	>30	>30	>30	>30

**Passenger 2004L-based Inflators**

PSPI-X TX Years to 0.01 POF (All data master curve)						
Percentile	Vehicle	Miami	Atlanta	Phoenix	Detroit	Seattle
1st Percentile	T3	13	21	>30	>30	>30
	T2	18	>30	>30	>30	>30
	T1	25	>30	>30	>30	>30
5th Percentile	T3	15	25	>30	>30	>30
	T2	19	>30	>30	>30	>30
	T1	>30	>30	>30	>30	>30
25th Percentile	T3	17	>30	>30	>30	>30
	T2	>30	>30	>30	>30	>30
	T1	>30	>30	>30	>30	>30

PSPI-X TX Years to 0.01 POF (Mid-Nom moisture master curve)						
Percentile	Vehicle	Miami	Atlanta	Phoenix	Detroit	Seattle
1st Percentile	T3	16	26	>30	>30	>30
	T2	22	>30	>30	>30	>30
	T1	>30	>30	>30	>30	>30
5th Percentile	T3	18	>30	>30	>30	>30
	T2	23	>30	>30	>30	>30
	T1	>30	>30	>30	>30	>30
25th Percentile	T3	21	>30	>30	>30	>30
	T2	>30	>30	>30	>30	>30
	T1	>30	>30	>30	>30	>30

PSPI-X TX Years to 0.01 POF (Hypothetical curve)						
Percentile	Vehicle	Miami	Atlanta	Phoenix	Detroit	Seattle
1st Percentile	T3	30	>30	>30	>30	>30
	T2	>30	>30	>30	>30	>30
	T1	>30	>30	>30	>30	>30
5th Percentile	T3	>30	>30	>30	>30	>30
	T2	>30	>30	>30	>30	>30
	T1	>30	>30	>30	>30	>30
25th Percentile	T3	>30	>30	>30	>30	>30
	T2	>30	>30	>30	>30	>30
	T1	>30	>30	>30	>30	>30

**Driver 2004-based Inflators**

PSDI-5 ZA Years to 0.01 POF						
Percentile	Vehicle	Miami	Atlanta	Phoenix	Detroit	Seattle
1st Percentile	T3	9	16	>30	24	>30
	T2	14	25	>30	>30	>30
	T1	22	>30	>30	>30	>30
5th Percentile	T3	10	19	>30	27	>30
	T2	15	27	>30	>30	>30
	T1	28	>30	>30	>30	>30
25th Percentile	T3	12	22	>30	>30	>30
	T2	27	>30	>30	>30	>30
	T1	>30	>30	>30	>30	>30

PSDI-5D GE Years to 0.01 POF						
Percentile	Vehicle	Miami	Atlanta	Phoenix	Detroit	Seattle
1st Percentile	T3	23	>30	>30	>30	>30
	T2	>30	>30	>30	>30	>30
	T1	>30	>30	>30	>30	>30
5th Percentile	T3	25	>30	>30	>30	>30
	T2	>30	>30	>30	>30	>30
	T1	>30	>30	>30	>30	>30
25th Percentile	T3	>30	>30	>30	>30	>30
	T2	>30	>30	>30	>30	>30
	T1	>30	>30	>30	>30	>30

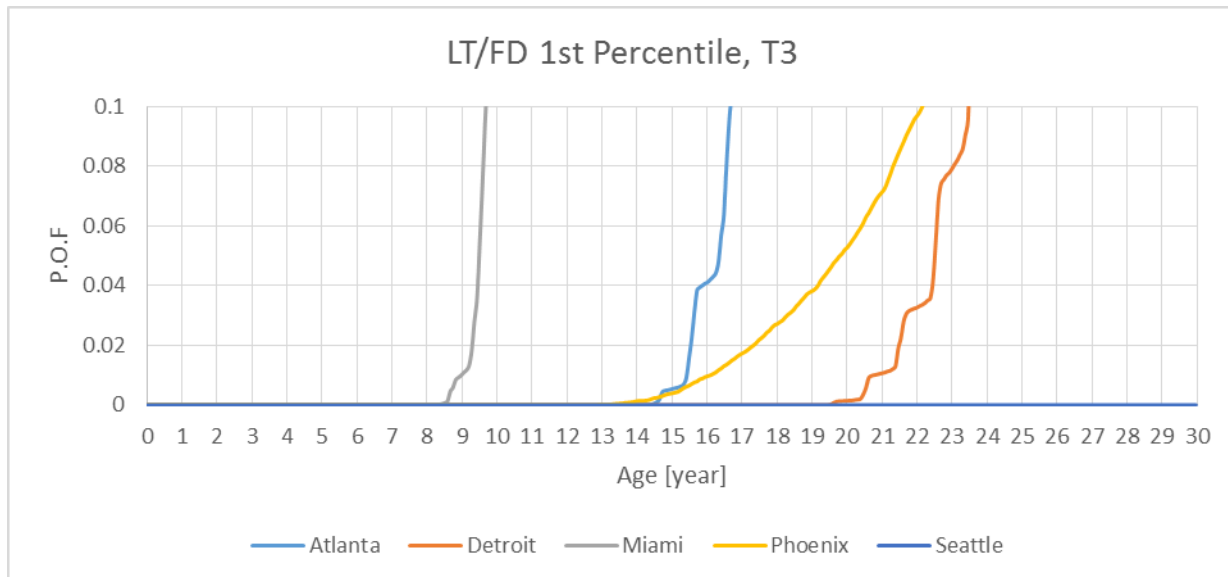
PSDI-5D YT Years to 0.01 POF						
Percentile	Vehicle	Miami	Atlanta	Phoenix	Detroit	Seattle
1st Percentile	T3	23	>30	>30	>30	>30
	T2	>30	>30	>30	>30	>30
	T1	>30	>30	>30	>30	>30
5th Percentile	T3	26	>30	>30	>30	>30
	T2	>30	>30	>30	>30	>30
	T1	>30	>30	>30	>30	>30
25th Percentile	T3	>30	>30	>30	>30	>30
	T2	>30	>30	>30	>30	>30
	T1	>30	>30	>30	>30	>30

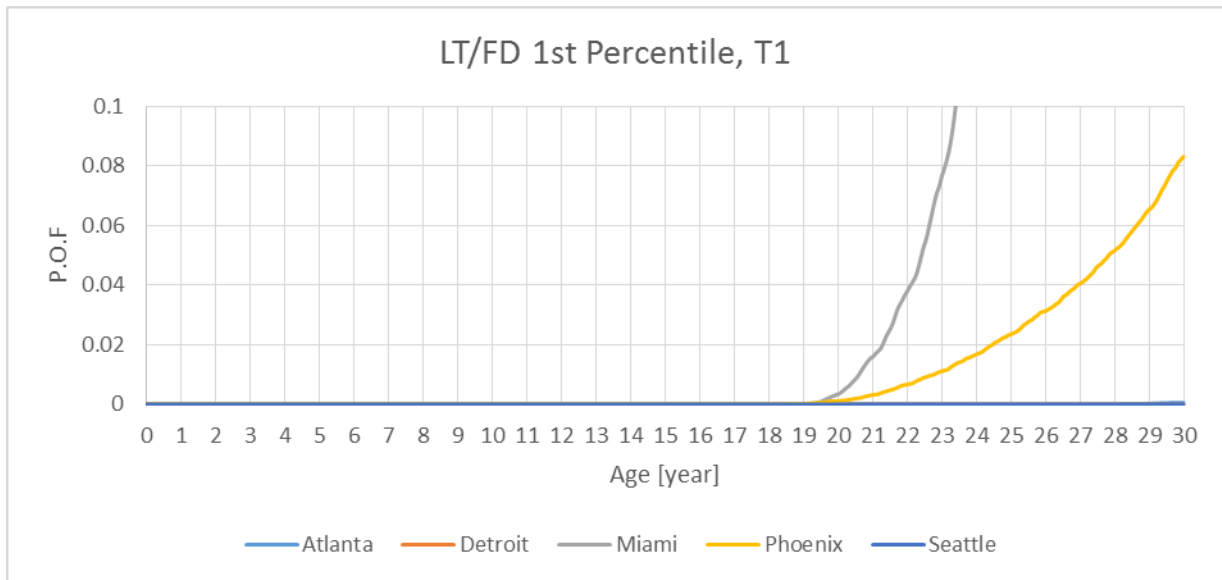
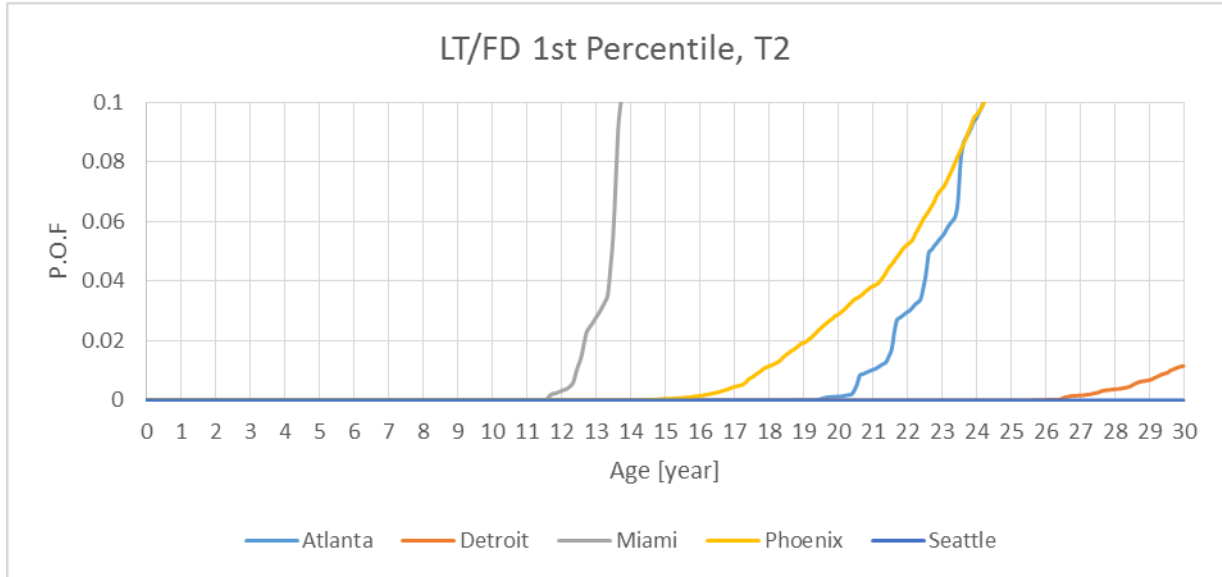
**Driver 2004L-based Inflators**

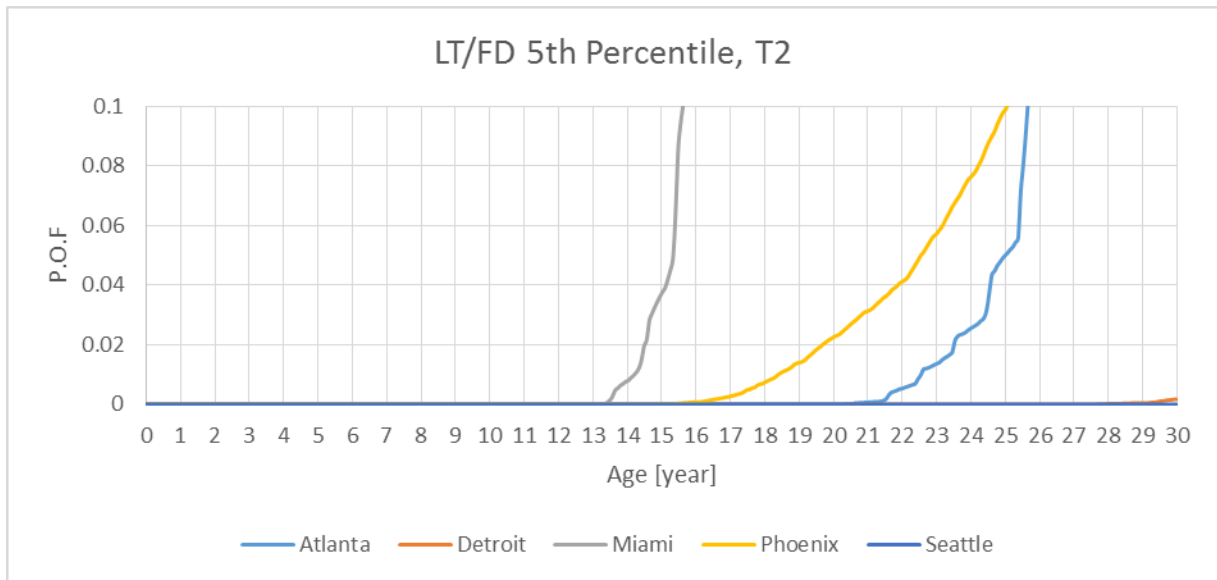
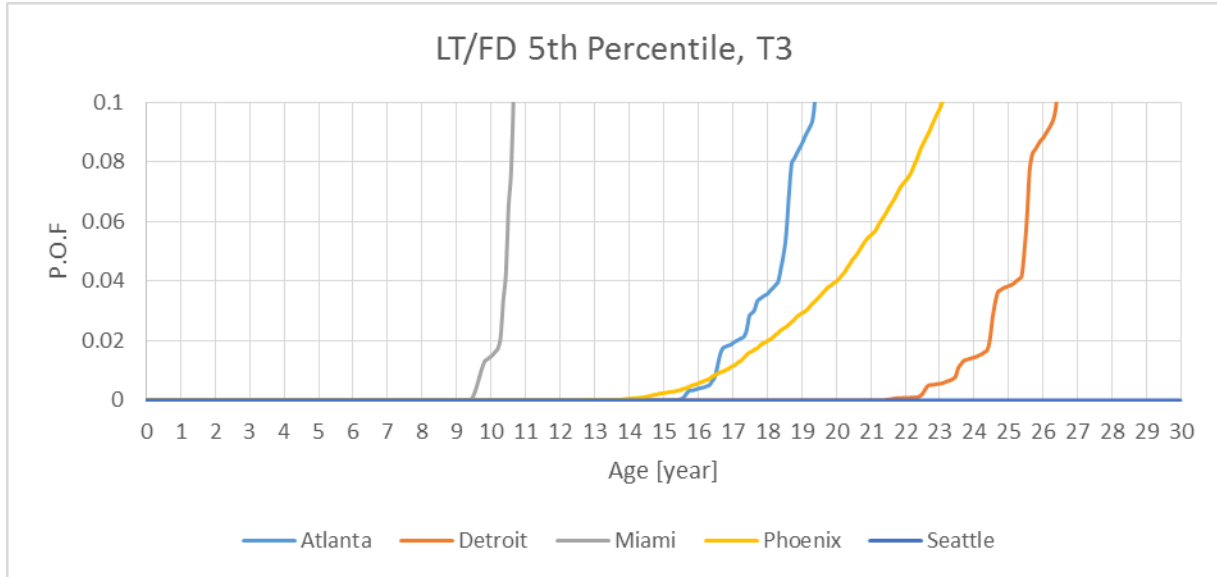
PSDI-X SV Years to 0.01 POF (No Extreme Moisture Linear Fit)(Extrapolating)						
Percentile	Vehicle	Miami	Atlanta	Phoenix	Detroit	Seattle
1st Percentile	T3	16	29	>30	>30	>30
	T2	23	>30	>30	>30	>30
	T1	>30	>30	>30	>30	>30
5th Percentile	T3	19	>30	>30	>30	>30
	T2	24	>30	>30	>30	>30
	T1	>30	>30	>30	>30	>30
25th Percentile	T3	22	>30	>30	>30	>30
	T2	>30	>30	>30	>30	>30
	T1	>30	>30	>30	>30	>30

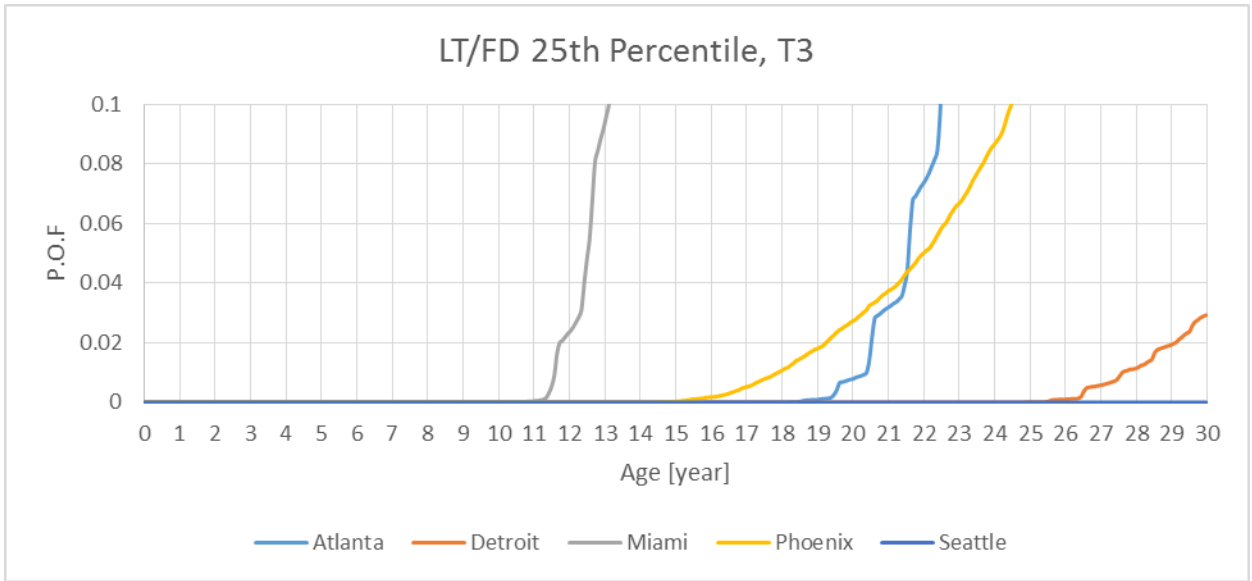
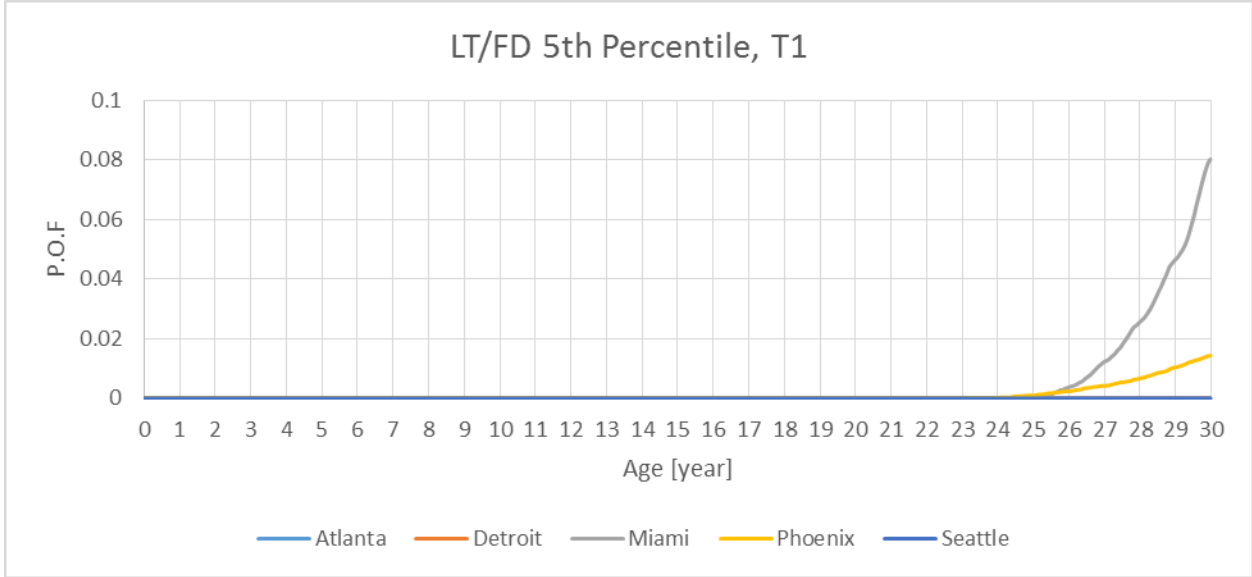
The curves as presented below are focused on the probability of failure from 0 to 0.1 POF to allow easier reading of this most critical data. The data can be represented with other ranges. Only those with nonzero POFs are shown.

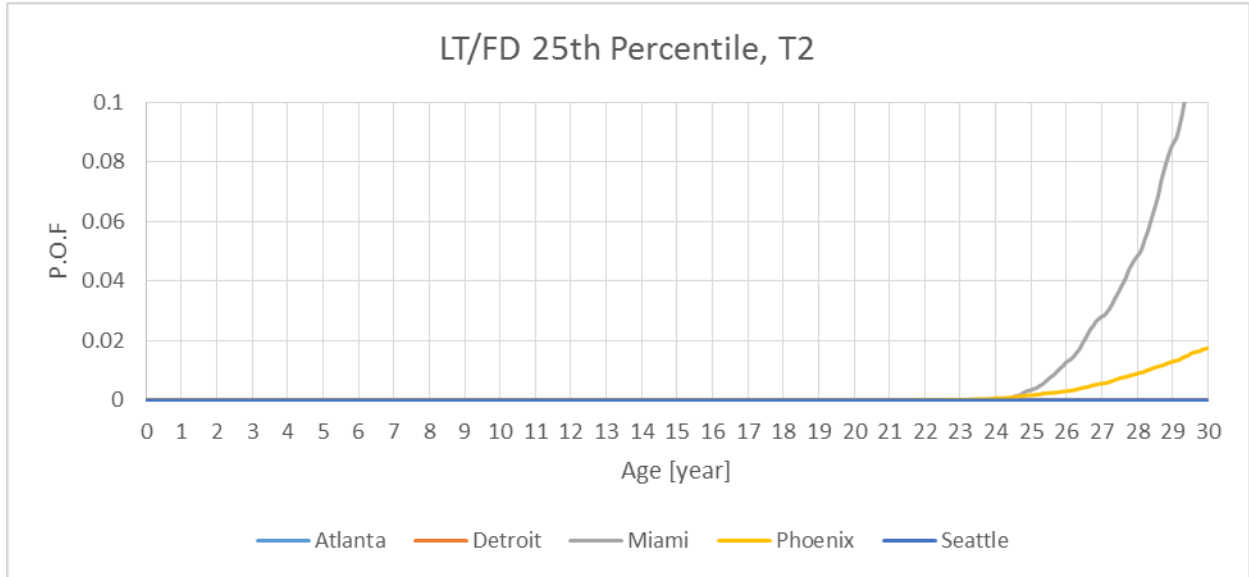
**POF Curves for PSPI-L FD**



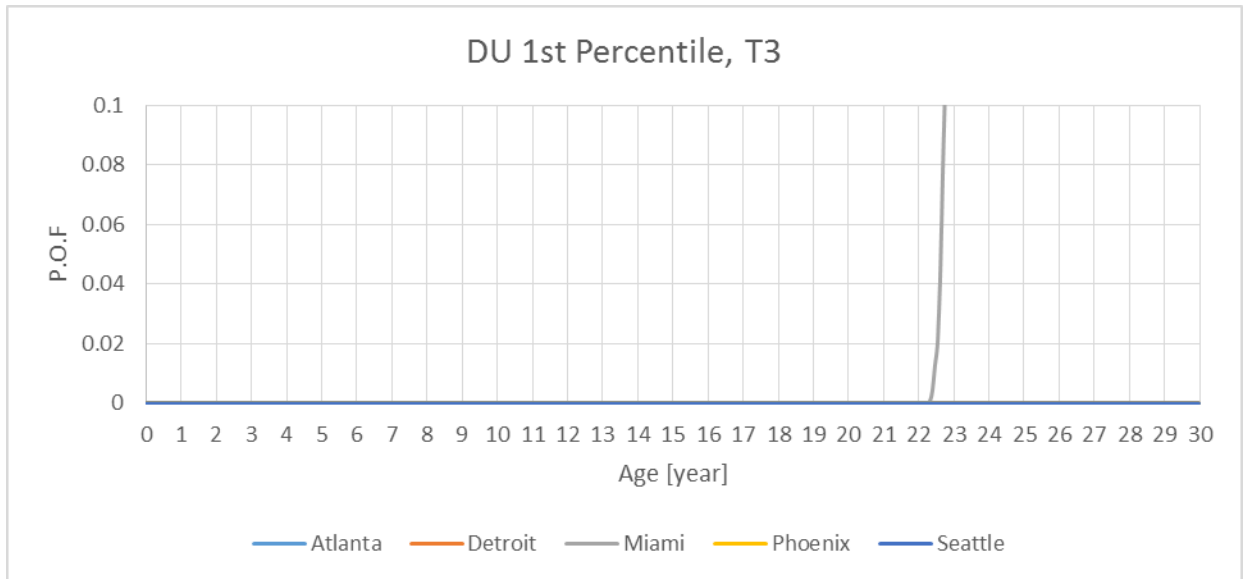


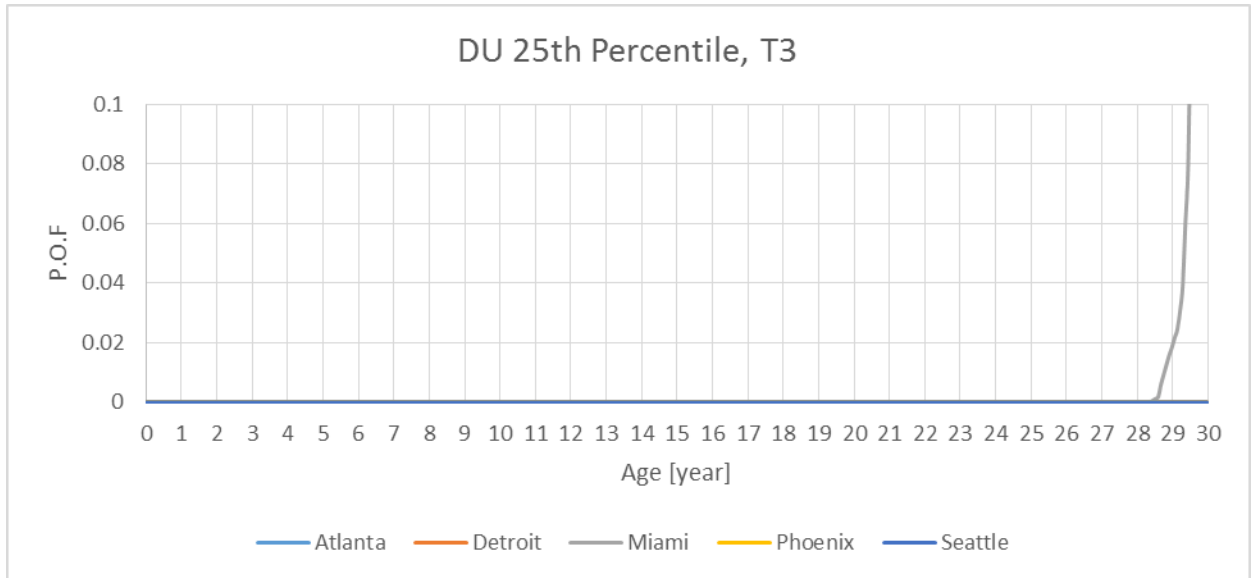
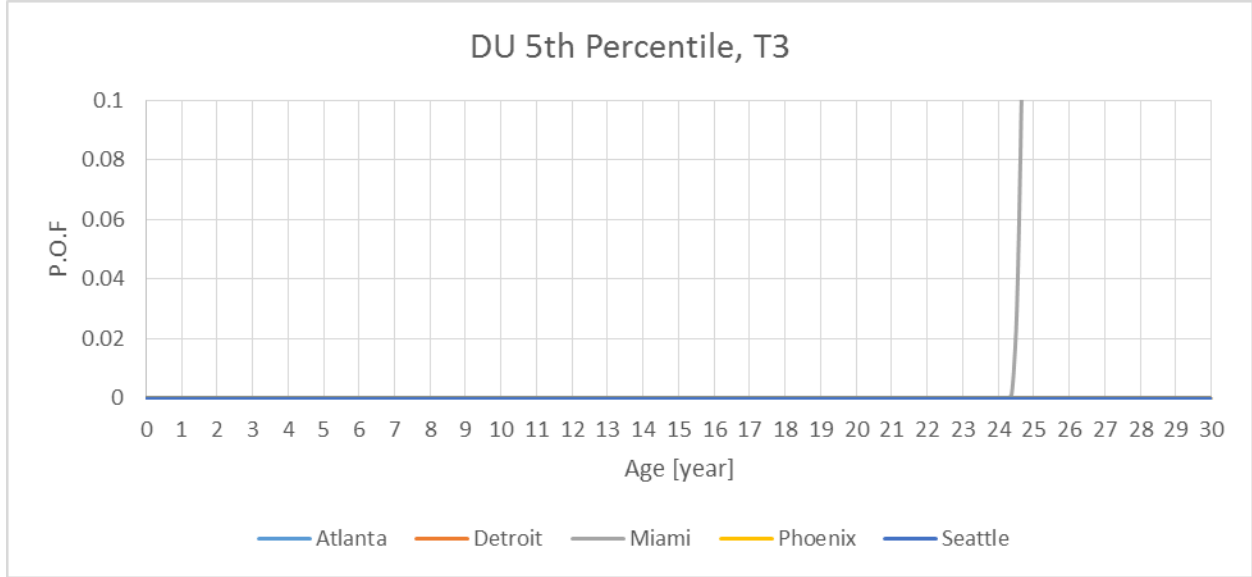






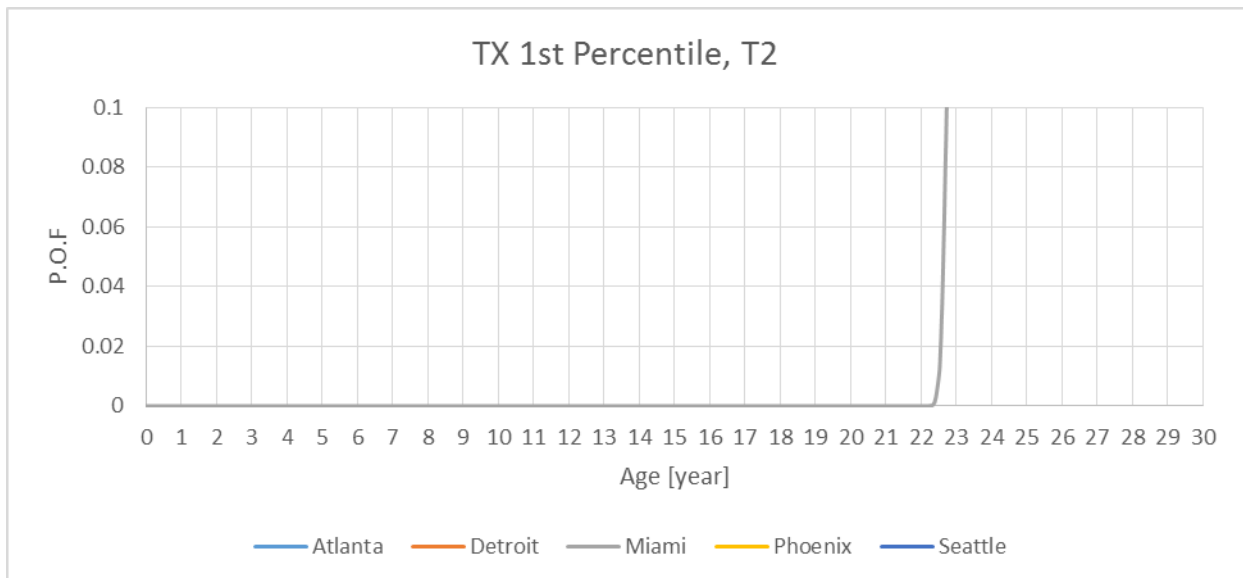
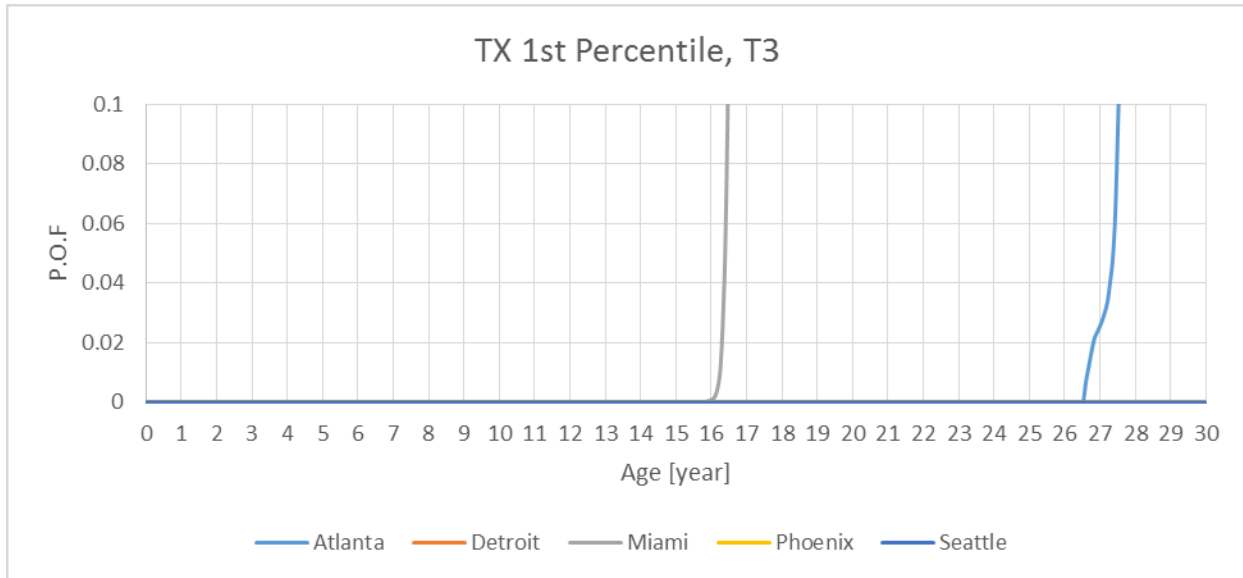
### POF Curves for PSPI-LD DU

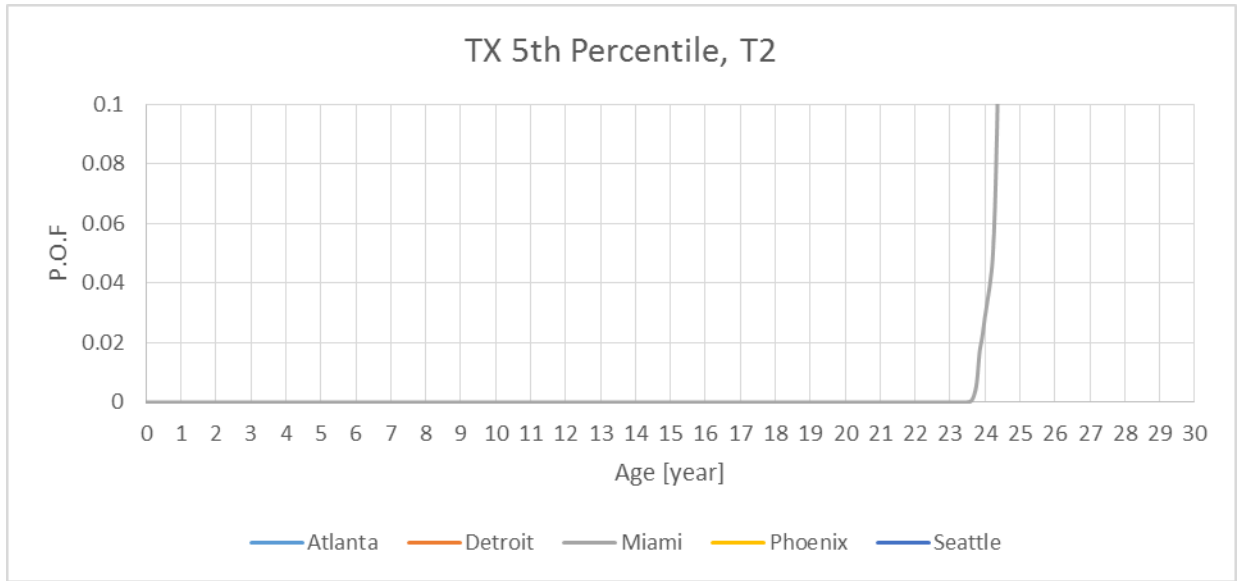
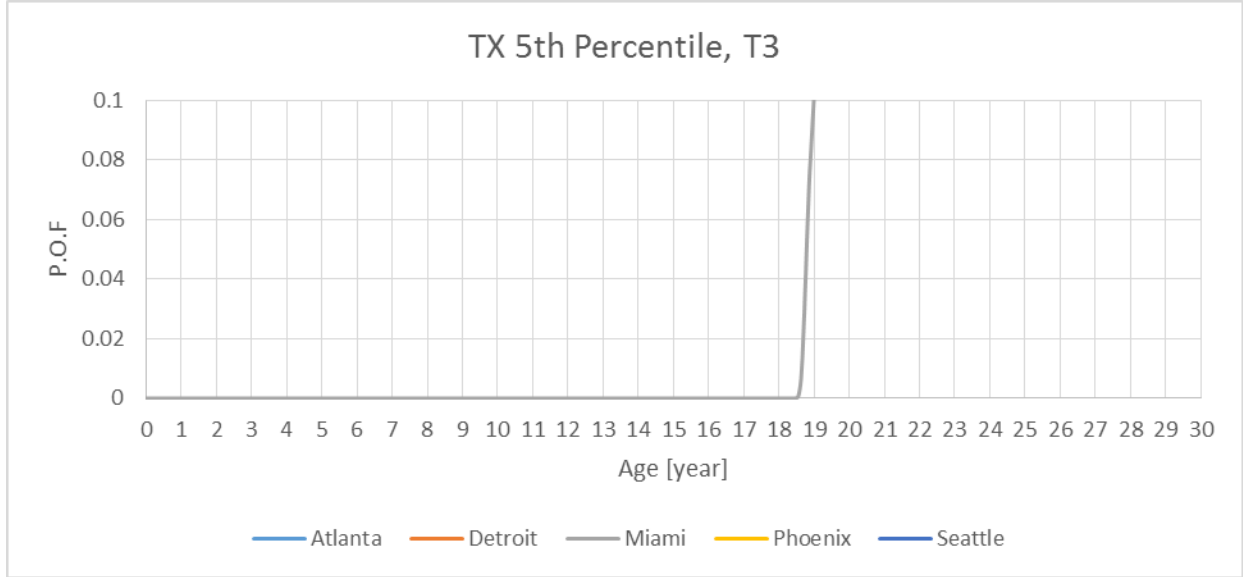


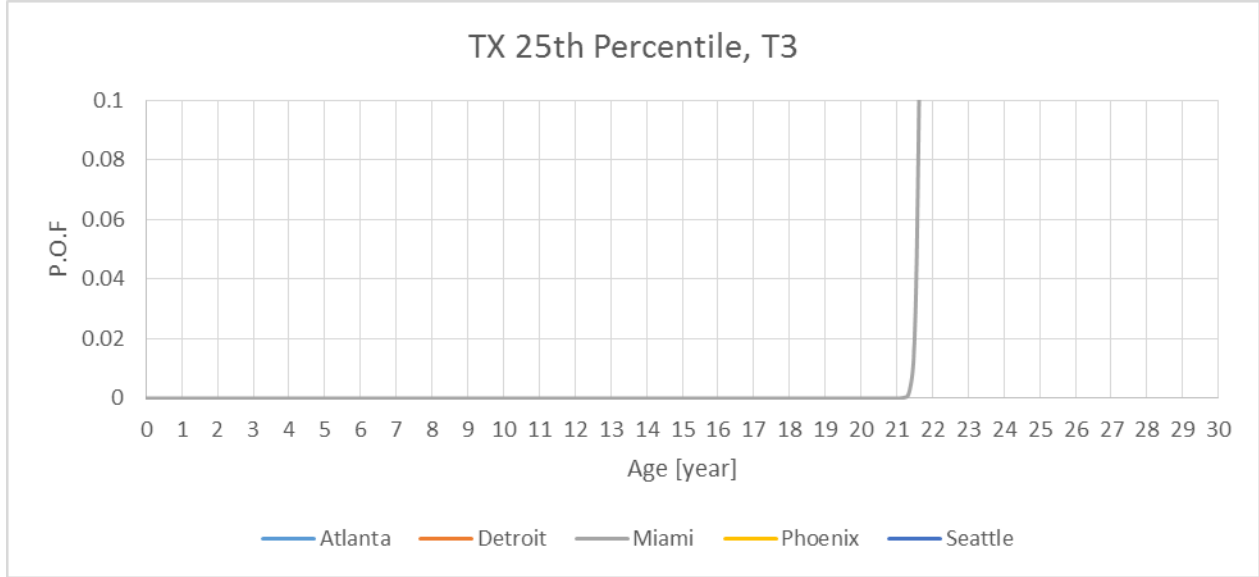


**POF Curves for PSPI-X TX**

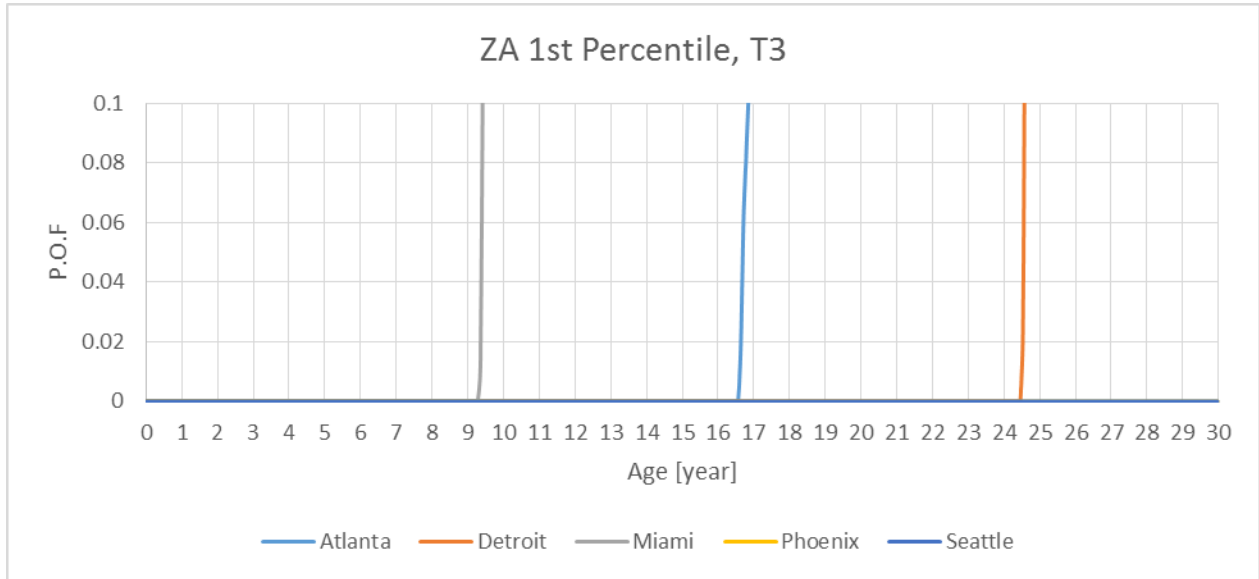
The graphs for the Mid-Nom Moisture Master Curve Assumption are shown. These are among the most conservative scenarios for the PSPI-X TX inflator. As was discussed in the main text, it has been shown that small changes in equilibrium relative humidity result in significant changes in predicted aging for the 2004L propellant based inflators. While we believe the most like scenario shows a 25 year time to the 0.01 POF in the Miami environment and T3 vehicle (see Table 4) and related discussion. These figures can be used for comparison of these various scenarios, vehicle percentiles and climates.

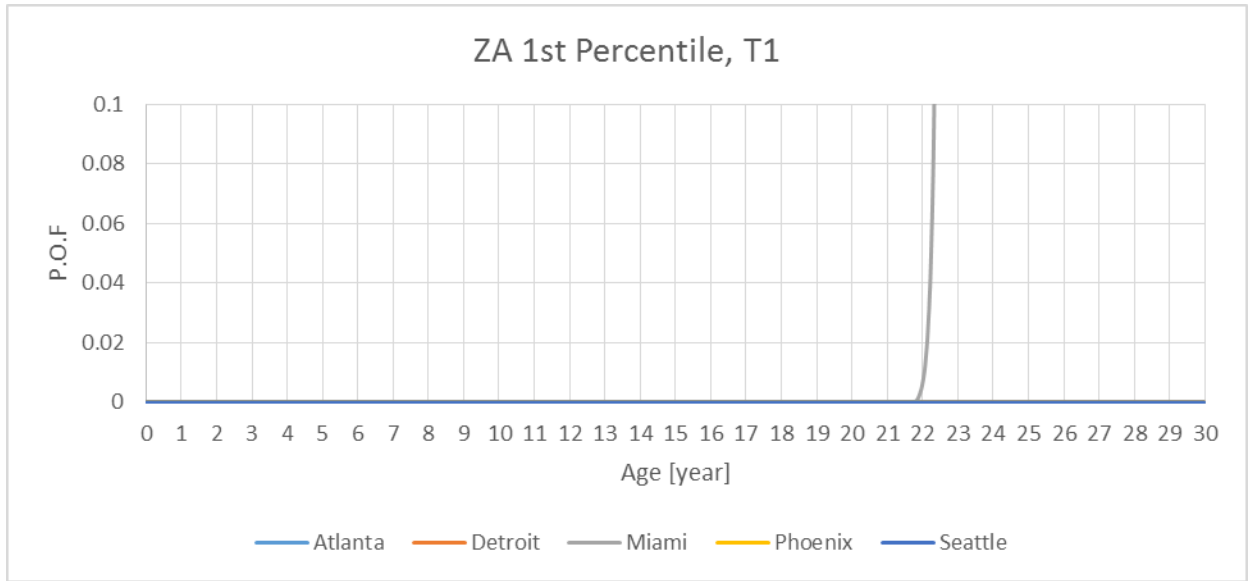
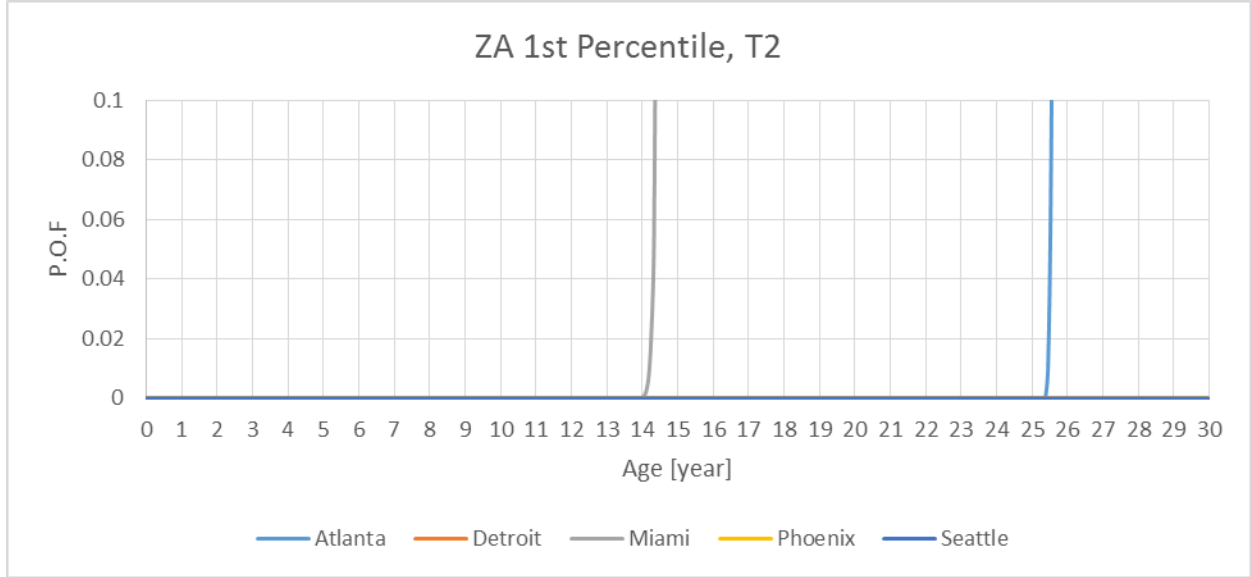


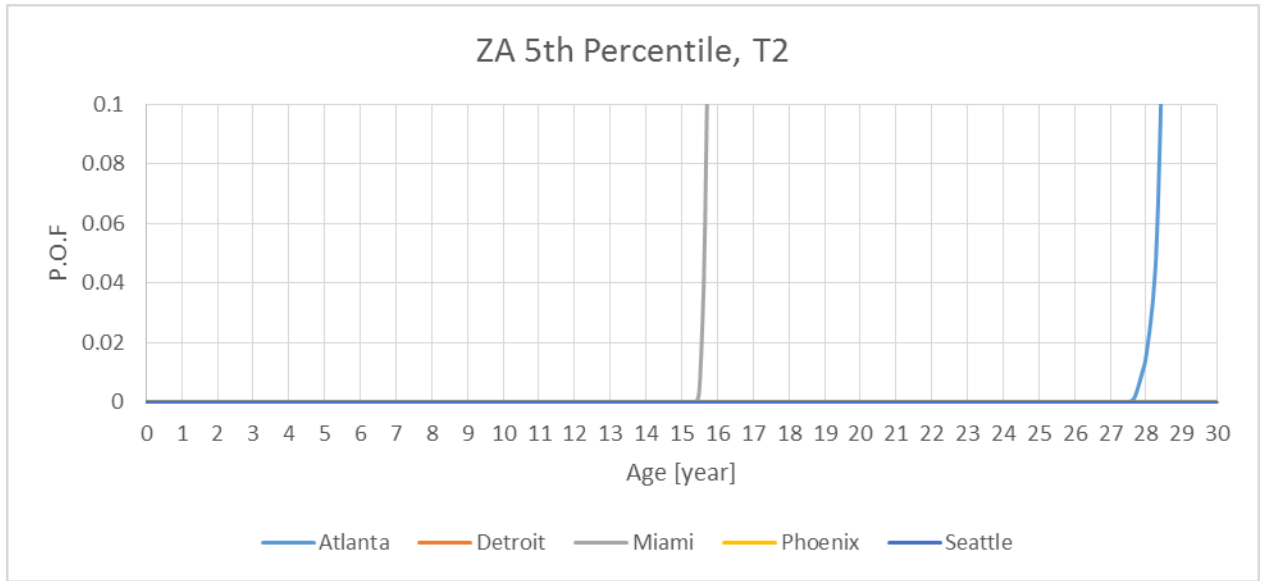
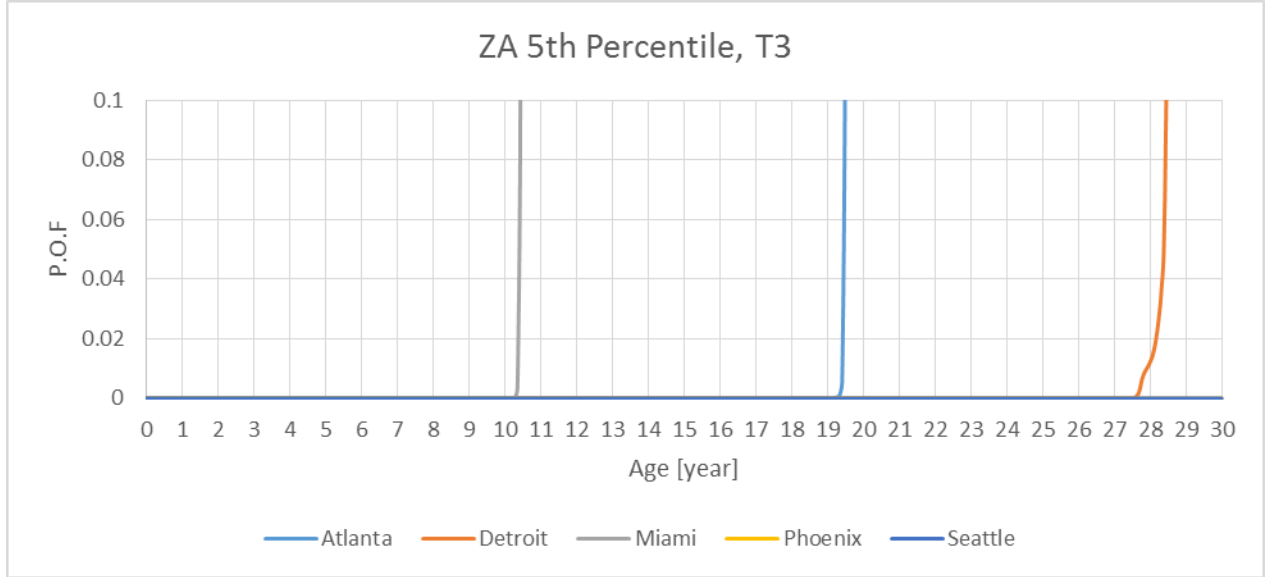


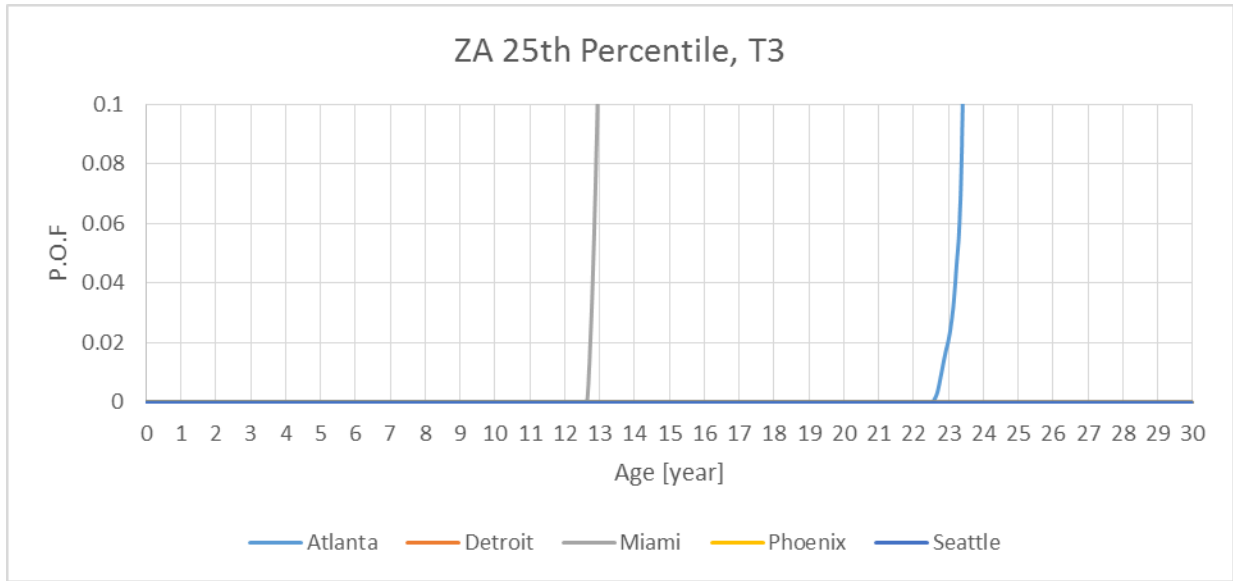
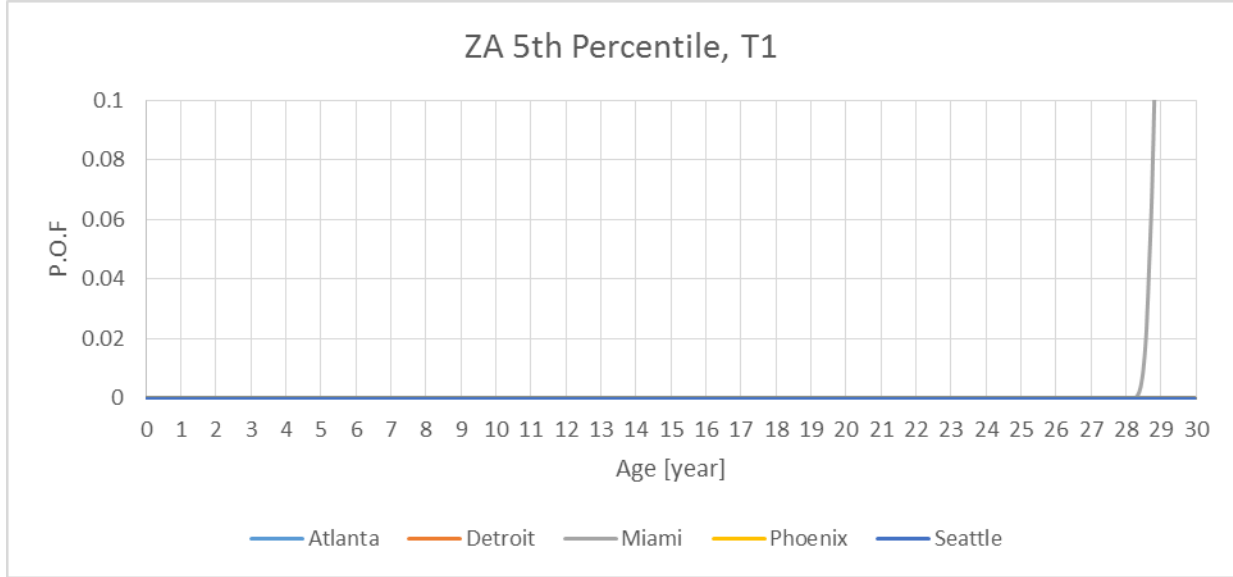


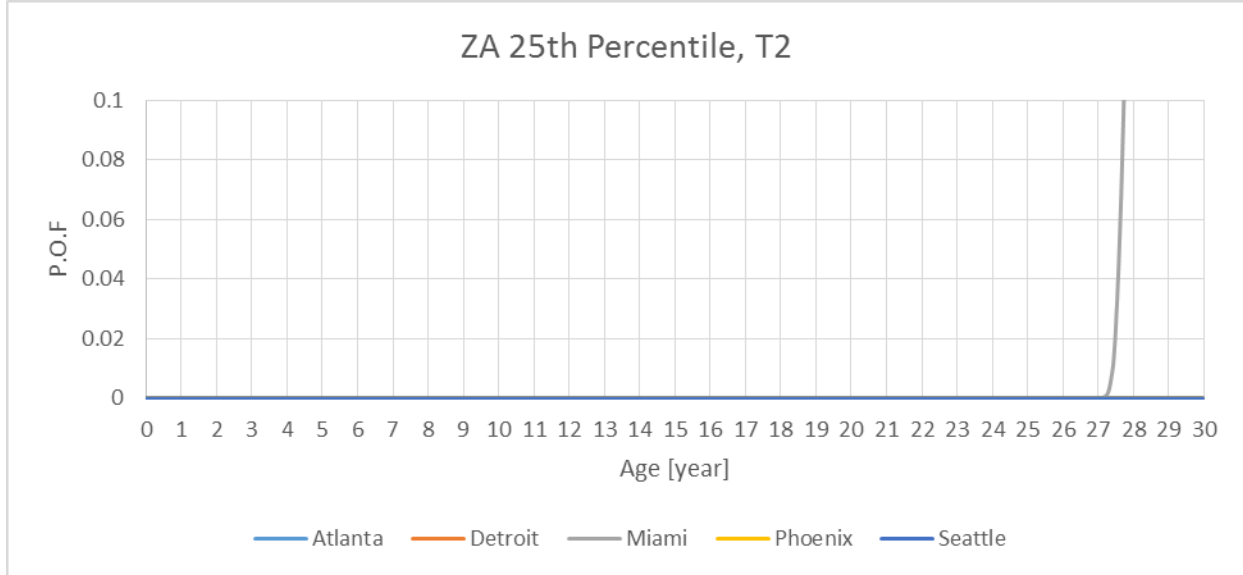
### POF Curves for PSDI-5 ZA



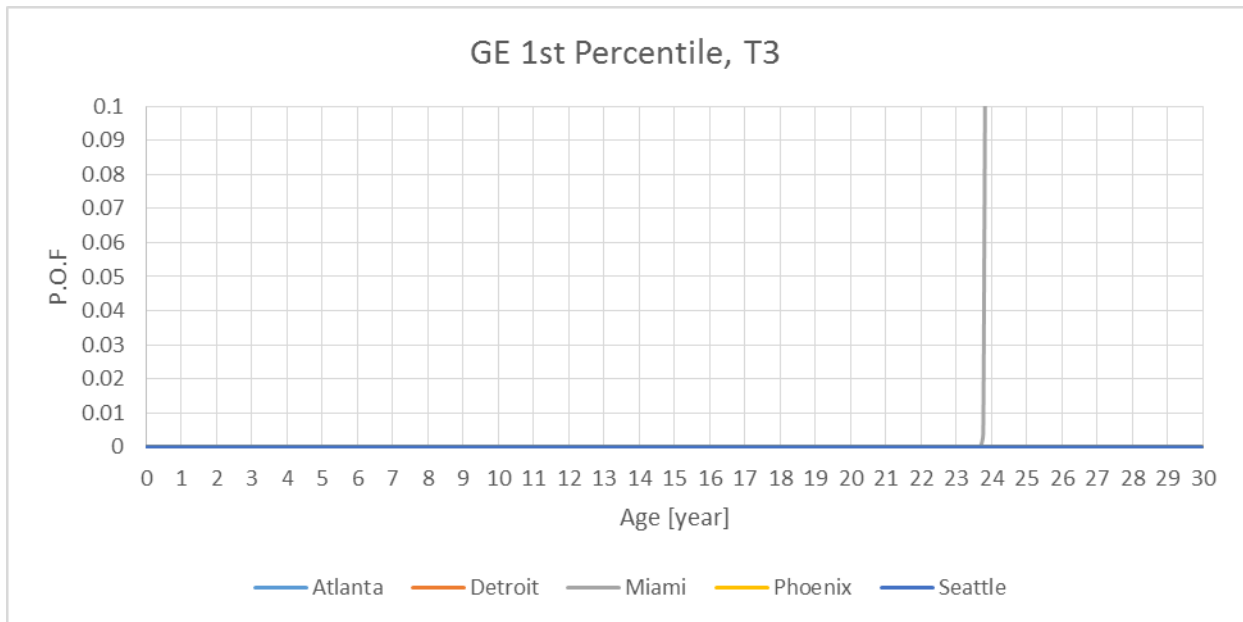


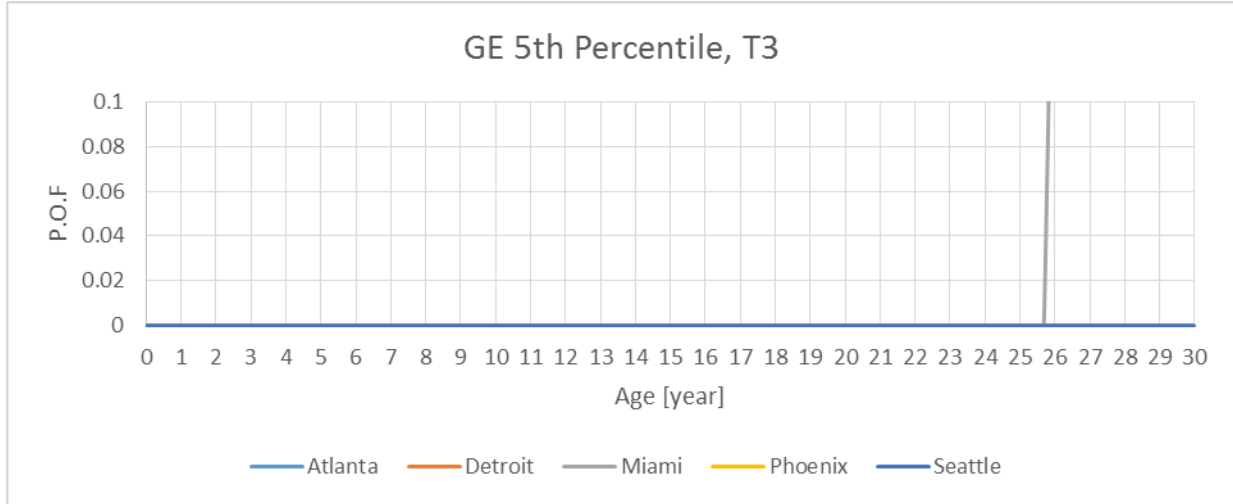




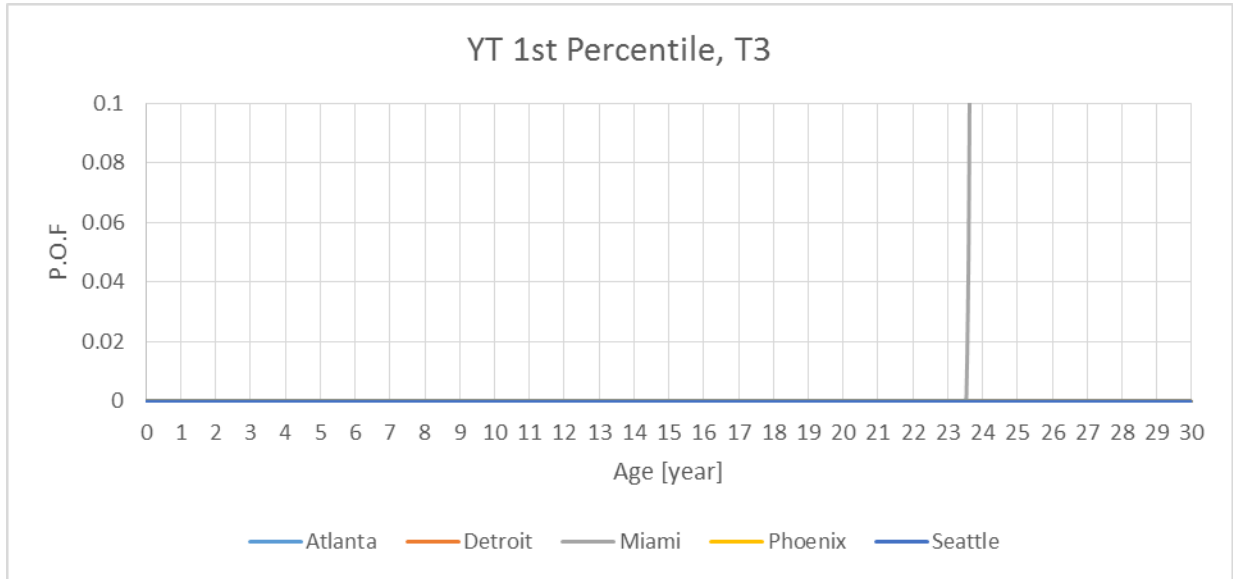


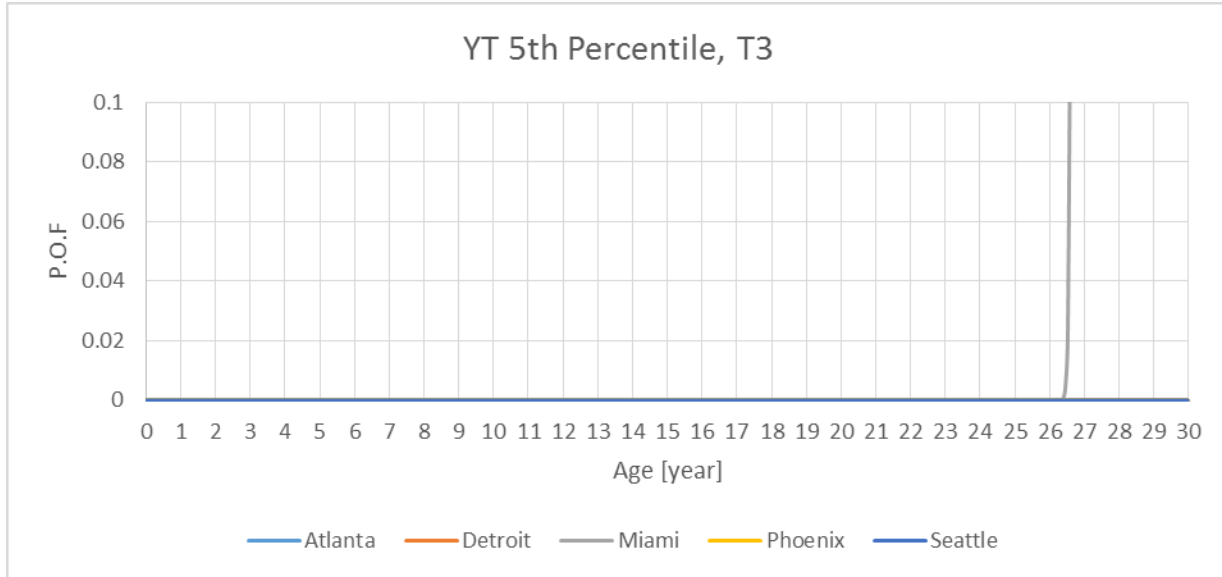
**POF Curves for PSDI-5D GE**





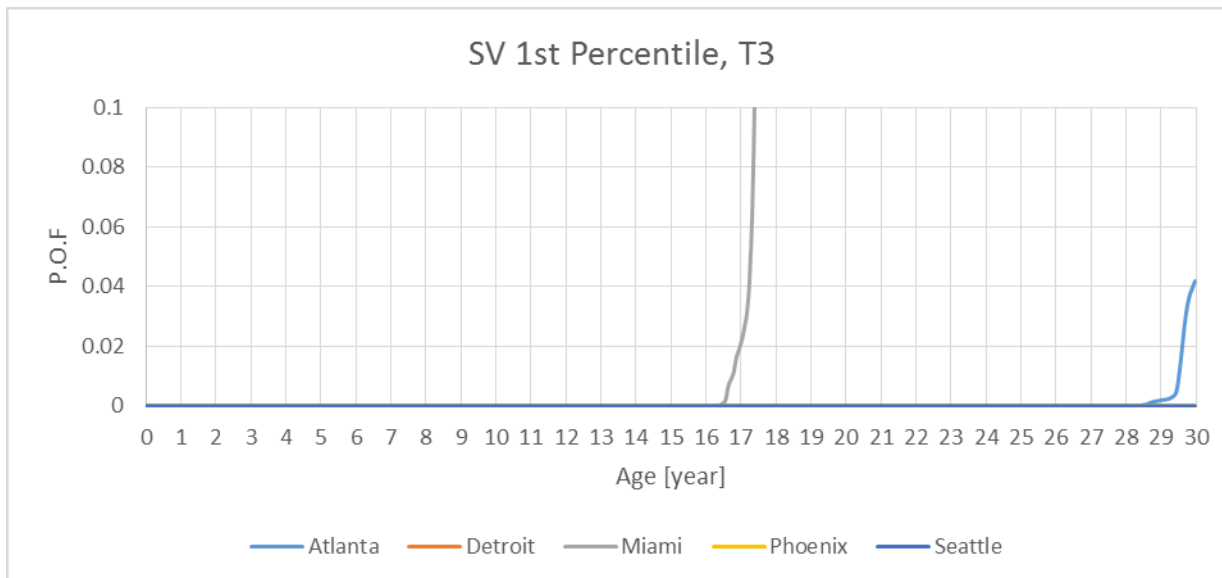
**POF Curves for PSDI-5D YT**

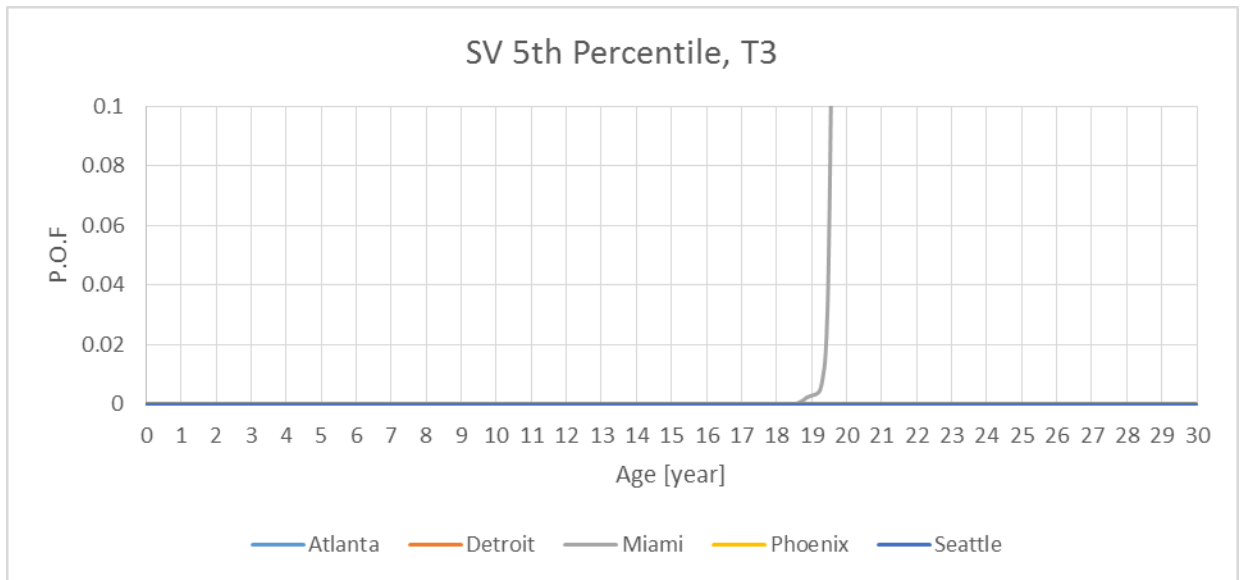
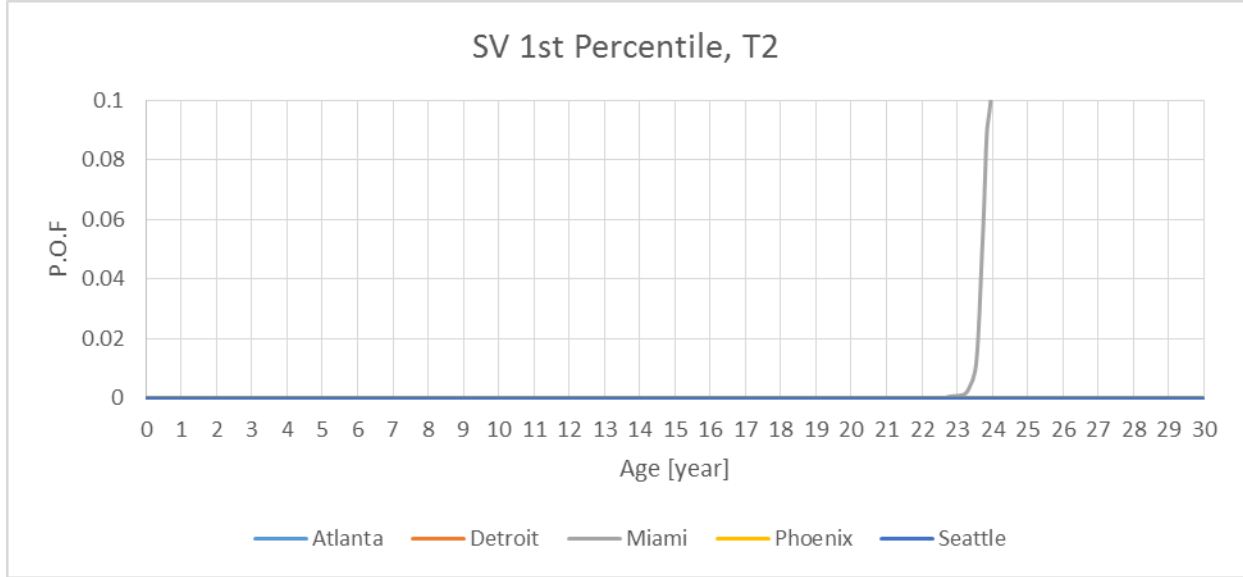


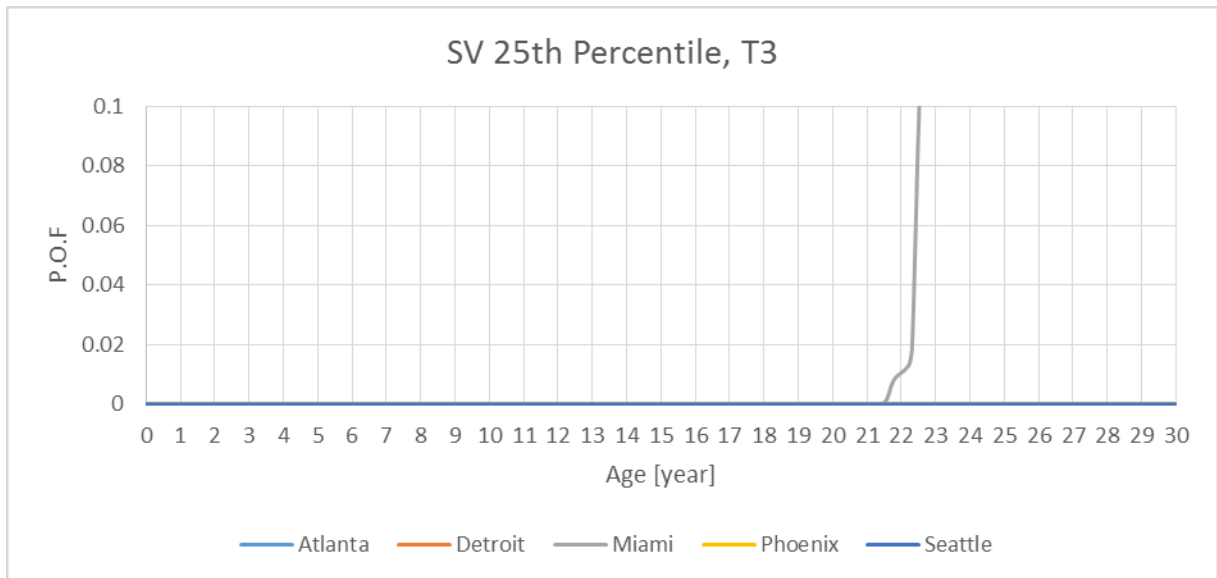
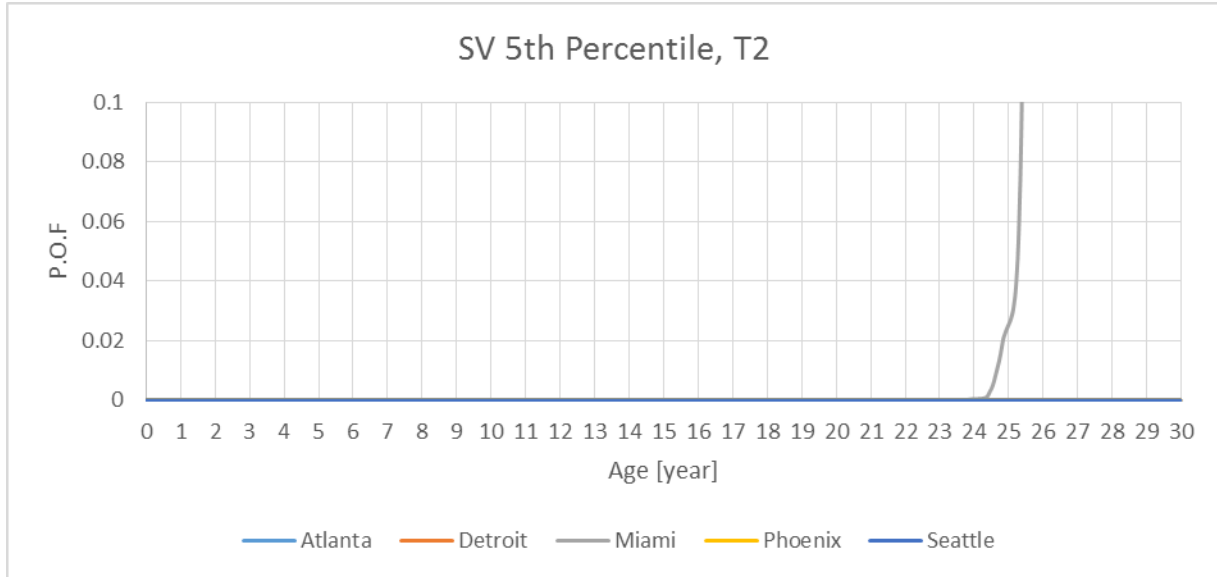


**POF Curves for PSDI-X SV**

Similar to the PSPI-X TX, these graphs are among the most conservative scenarios for the PSDI-X SV inflator. As was discussed in the main text, it has been shown that small changes in equilibrium relative humidity result in significant changes in predicted aging for the 2004L propellant based inflators. Analogous to the PSDI-X TX, we believe the most like scenario shows a 25 year time to the 0.01 POF in the Miami environment and T3 vehicle (see Table 4) and related discussion. These figures can be used for comparison of these various scenarios, vehicle percentiles and climates.







## **Appendix B. Detailed Trade Study Table of Results**

A large number of specific trade studies were done using the completed predictive model. These were done for final calibration and validation of the model and to test hypotheses regarding the impact of various changes in the input files, conditions or aging parameters.

Inflator	Sensitivity Study	Purpose of Study	Key Learning	Unit	From	To	Miami weather, 1st Percent usage, T3 vehicle, 1% POF [Years to reach this POF]		
							From	To	% Difference
PSPI-L FD/LT	Capillary Leak Radius	Determine impact of different leak and diffusion rates on model age. Used to calibrate and validate the baseline model against field data.	Calibrated leak and diffusion rates for the model. Excessive leak rate or artificially low leak rate results in underestimation or over estimation of years to 0.01 POF compared to field data.	m	0.000003	0.000005	9	10.4	15.56
	Capillary Leak Radius			m	0.000003	0.00001	9	5.4	-40.00
	Permeability A/L			m	nominal	1.2*nominal	9	7.8	-13.33
	Permeability A/L			m	nominal	1.3*nominal	9	7.3	-18.89
	Starting Density	Impact of manufacturing variation or data input.	Starting density is relatively important.	kg/m <sup>3</sup>	1673.43	1653.43	9	7.8	-13.33
	Critical Density	Impact of variation in ballistic model output as a function of density.	Lower critical density results in prediction of longer time to 0.01 POF with relatively high sensitivity to this number. Variability in augmented burning data suggests this is one of the larger uncertainties in the study.	kg/m <sup>3</sup>	1613.41779	1593.41779	9	9.66	7.33
	Hydroburst Critical Pressure	Impact of variation in inflator body strength.	Modest change at most.	MPa	99	90	9	8.6	-4.44
Hydroburst Critical Pressure Sigma	MPa			3	6	9	8.8	-2.22	
PSDI-5D YT	Primary Chamber Initial Total Moisture	Does variation in initial moisture impact aging.	Moderate change has moderate impact at most.	g	0.05617	0.03617	23.5	25.5	8.51
	Not Firing Secondary Ballistics Model (Crit. Density)	Determine impact of firing only the primary chamber without subsequent firing of the secondary chamber	Firing only the primary chamber slightly reduces the critical density and results in a modest change at most.	kg/m <sup>3</sup>	1622	1616	23.5	24	2.13
	Starting Density	see above under PSPI-L FD/LT	see above under PSPI-L FD/LT; this design is less sensitive than PSPI-L	kg/m <sup>3</sup>	1701.631	1681.631	23.5	22.5	-4.26
	Critical Density	see above under PSPI-L FD/LT	see above under PSPI-L FD/LT; this design is less sensitive than PSPI-L	kg/m <sup>3</sup>	1622.939262	1602.939262	23.5	24.5	4.26
PSDI-5D GE	Primary Chamber Initial Total Moisture	Does variation in initial moisture impact aging. In this case, nearly saturating the 13X desiccant during manufacture.	Nearly saturating the 13X desiccant at time zero results in shorter time to 0.01 POF	g	0.108426	0.21681	24	13.5	-43.75
	Starting Density	see above under PSPI-L FD/LT	see above under PSPI-L FD/LT; this design is much less sensitive than PSPI-L	kg/m <sup>3</sup>	1710	1690	24	23.5	-2.08
	Critical Density	see above under PSPI-L FD/LT	see above under PSPI-L FD/LT; this design is much less sensitive than PSPI-L	kg/m <sup>3</sup>	1622.49701	1602.49701	24	24.5	2.08
PSPI-X SV	Primary Permeability A/L	see above under PSPI-L FD/LT	see above under PSPI-L FD/LT	m	nominal	0.8333*nominal	17	19.39	14.06
	Capillary Leak Radius	see above under PSPI-L FD/LT	see above under PSPI-L FD/LT	m	0.0000025	0.000003	17	17.33	1.94
	Master Curve Options	Impact of including or not including data from "extreme" moisture levels in the master curve for aging	Inclusion of extreme moisture data in master curve has a dramatic impact. Condition is not expected in the field and was not included in final conclusions.	N/A	No Extreme Moisture Pri & Sec Linear Fit	All Moistures Primary Chamber Master Curve	17	12	-29.41
	Starting Density	see above under PSPI-L FD/LT	see above under PSPI-L FD/LT; this design is similar sensitivity to PSPI-L	kg/m <sup>3</sup>	1692.031	1672.031	17	15.4	-9.41
	Critical Density	see above under PSPI-L FD/LT	see above under PSPI-L FD/LT; this design is similar sensitivity to PSPI-L	kg/m <sup>3</sup>	1610.183284	1590.183284	17	18.5	8.82
PSPI-X TX	Permeability A/L	see above under PSPI-L FD/LT	see above under PSPI-L FD/LT	m	nominal	1.2*nominal	13.5	11.6	-14.07
	Master Curve Options	Impact of including or not including data from "extreme" moisture levels in the master curve for aging	Inclusion of extreme moisture data in master curve has a dramatic impact. Condition is not expected in the field and was not included in final conclusions.	N/A	All data	Mid-Nom moisture only	13.5	16	18.52
	Starting Density	see above under PSPI-L FD/LT	see above under PSPI-L FD/LT; this design is more sensitive than PSPI-L	kg/m <sup>3</sup>	1664	1644	13.5	10.6	-21.48
	Critical Density	see above under PSPI-L FD/LT	see above under PSPI-L FD/LT; this design is more sensitive than PSPI-L	kg/m <sup>3</sup>	1625.736853	1605.736853	13.5	15.5	14.81

Inflator	Sensitivity Study	Purpose of Study	Key Learning	Unit	From	To	Miami weather, 1st Percent usage, T3 vehicle, 1% POF [Years to reach this POF]		
							From	To	% Difference
	Relative Humidity	Test for various levels of relative humidity inside the inflator. See discussion in main body of this report.	Internal inflator RH is a critical parameter and predicted time to 0.01 POF is impacted significantly.	Frac.	1	0.7,0.8,0.9	13.5	24.5,18.5,15.5	81,37,15
PSPI-LD DU	Primary Chamber Initial Total Moisture	Does variation in initial moisture impact aging.	Moderate change has moderate impact at most.	g	0.173233	0.153733	22.5	22.35	-0.67
	Starting Density	see above under PSPI-L FD/LT	see above under PSPI-L FD/LT; this design is less sensitive than PSPI-L	kg/m <sup>3</sup>	1693.308	1673.38	22.5	21.2	-5.78
	Critical Density	see above under PSPI-L FD/LT	see above under PSPI-L FD/LT; this design is less sensitive than PSPI-L	kg/m <sup>3</sup>	1621.552009	1601.552009	22.5	23.61	4.94
PSDI-5 ZA	Capillary Leak Radius	see above under PSPI-L FD/LT	see above under PSPI-L FD/LT	m	0.000003	0.000002	9.5	8.6	-9.47
	Capillary Leak Radius	see above under PSPI-L FD/LT	see above under PSPI-L FD/LT	m	0.000003	0.00001	9.5	4.5	-52.63
	Permeability A/L	see above under PSPI-L FD/LT	see above under PSPI-L FD/LT	m	nominal	0.6667*nominal	9.5	12.5	31.58
	Starting Density	see above under PSPI-L FD/LT	see above under PSPI-L FD/LT; this design is less sensitive than PSPI-L	kg/m <sup>3</sup>	1706.642	1686.642	9.5	8.5	-10.53
	Critical Density	see above under PSPI-L FD/LT	see above under PSPI-L FD/LT; this design is less sensitive than PSPI-L	kg/m <sup>3</sup>	1617.348711	1597.348711	9.5	9.81	3.26

## **Appendix C. Interim Report by NGIS**

*This page intentionally left blank*



# Takata Inflator Rupture Root Cause Summary Report

Submitted by:  
**Orbital ATK for the Independent Testing Coalition**

Submitted to:  
**National Highway Traffic Safety Administration**

**September 2016**





**TABLE OF CONTENTS**

	<u>Page</u>
Executive Summary .....	1
Investigation Scope .....	1
Technical Approach Overview.....	1
Statistical Analysis .....	4
Modeling and Simulation.....	7
Laboratory Experiments .....	18
Root Cause .....	21
Continuing Efforts.....	23
Addenda .....	24
A. Sources of Information and Acknowledgements.....	24
B. ITC Membership and Purpose .....	24
C. Orbital ATK Relevant Qualifications and Background.....	24



**LIST OF FIGURES**

	<u>Page</u>
Figure 1. Overarching Project Process.....	4
Figure 2. Failure Rates in PSPI-L for a Single Vehicle Model in Florida.....	5
Figure 3. Wafer Outer Diameter, Crimp (case) Outer Diameter and Failure Probability for PSPI-L for a Single Vehicle Model.....	6
Figure 4. Summary of Similarities and Differences for Passenger Inflators.....	8
Figure 5. Comparison and Contrast of Major Design Differences in Takata Driver and Passenger Dual Chamber Inflators.....	9
Figure 6. Typical Ballistic Traces.....	10
Figure 7. Similarities in Operating Features of Takata Driver and Passenger Inflators.....	11
Figure 8. Schematic Representation of Burn Rate and Pressure Plot.....	12
Figure 9. Potential of Ignition and Auto Ignition Propellants to Cause an ED.....	13
Figure 10. Closed Pore Impact on Burning Surface.....	14
Figure 11. Change in High Pressure Regime Slope.....	16
Figure 12. Impact of Porosity and Permeability.....	17
Figure 13. Potential Leak Paths in Takata Inflators.....	18
Figure 14. Passenger Inflator Primary Crimp Data.....	18
Figure 15. Headspace Moisture Above 2004 and 3110 Propellants with Moisture Added as a Function of Temperature.....	19
Figure 16. Examples of Fused Wafers and Tablets.....	20
Figure 17. Density Measurements for 2004 Propellant Wafers.....	21
Figure 18. Real Time Radiography Still Images.....	22
Figure 19. Summary Fault Tree.....	23

**LIST OF TABLES**

	<u>Page</u>
Table 1. Summary of the Five Major Fault Tree Branches Developed and Investigated on This Study.....	3
Table 2. Field Return Failure Rates in PSPI-L.....	7
Table 3. Moisture Competition Experiment for 2004 and 3110 Propellants in a Closed System.....	20



## GLOSSARY OF KEY TERMS AND ACRONYMS

Burning Rate	.....	a measure of the rate at which propellant is combusts
Burning Rate Slope	.....	a measure of the change in burn rate as a function of pressure
Deliquescent	.....	the term for a chemical that can absorb enough water from the air to become a liquid solution
Desiccant	.....	the term for a chemical that can function as a drying agent
°C	.....	degrees Celsius
ED	.....	energetic disassembly
Fault Tree	.....	a structured, deductive approach to failure analysis
Fishbone	.....	a structured approach to determining cause and effect, also called Ishikawa Diagrams
g	.....	gram
Gas pycnometer	.....	a lab instrument that uses gas displacement to measure density
HAH	.....	high absolute humidity
Haystack	.....	a description of the general shape in a pressure-time trace with a gentle, rounded curve typical of a regressive burn
ITC	.....	Independent Testing Coalition
Mdot	.....	mass (gas) generation rate
MEAF	.....	Master Engineering Analysis File
Mm	.....	millimeter
NHTSA	.....	National Highway Traffic Safety Administration
OD	.....	outer diameter
OEM	.....	original equipment manufacturer
Progressive burning surface area	.....	a geometry where the surface area available to burn increases over time
Regressive burning surface area	.....	a geometry where the surface area available to burn decreases over time
PSAN	.....	phase-stabilized ammonium nitrate
PSPI-L	.....	Takata nomenclature for a type of air bag inflator
RTR	.....	real time radiography, effectively an x-ray movie that allows visualization of real time events using x-rays



## **Executive Summary**

Orbital ATK has conducted an independent investigation on behalf of the Independent Testing Coalition (ITC) and found that certain inflators made by Takata are adversely affected by three factors - all of which contribute, and are required to be present, in order to cause rupture when initiated.

These factors are:

- The presence of pressed phase-stabilized ammonium nitrate (PSAN) propellant without moisture-absorbing desiccant
- Long-term exposure to repeated high-temperature cycling in the presence of moisture, and
- An inflator assembly that does not adequately prevent moisture intrusion under conditions of high humidity

This investigation applies solely to inflators subject to National Highway Traffic Safety Administration (NHTSA) recalls 15E-040 to 15E-043. These recalls account for approximately 23 million inflators installed in vehicles in the U.S. from ten auto manufacturers.

The thirteen-month investigation involved more than 20,000 hours of testing and analysis by experienced scientists, engineers and technicians. The methodology followed a disciplined approach to investigate every potential factor, contributor or cause. It began with a detailed fishbone analysis and included detailed documentation on the adjudication of over fifty unique fault tree blocks.

It was deemed critical to thoroughly understand root cause prior to commencing aging and surveillance studies. To begin such a study without an understanding of the critical factors, and their approximate contribution to the failure, runs the risk of a result that may empirically match a limited data set or reproduce a few field results but be inaccurate for the broader application to the universe of relevant inflators and conditions. A carefully designed accelerated aging test program, based on understanding of the root cause and contributing factors, is the focus of the next phase of the Orbital ATK investigation.

## **Investigation Scope**

The investigation focused on determining the root cause of inflator failures covered by Takata recalls 15E-040 to 15E-043. These studies were directed towards identifying long-term changes that could give a higher probability of failure based on the design of the inflators, rather than manufacturing problems. This does not mean that manufacturing problems do not play a role in failures, but these were not the emphasis of our investigation. Rather, our emphasis was on determining changes due to environmental aging, including changes influenced by inflator design differences and routine manufacturing variation. Ongoing work will examine newer inflators that contain PSAN produced by Takata, including those not under recall by NHTSA which contain desiccant.

## **Technical Approach Overview**

Based on the complexity of this problem, we felt that a disciplined, patient and well-designed approach that would provide archival documentation of each conclusion was required. A fishbone analysis was completed to ensure complete coverage of all possible factors. The items



from the fishbone then were used to generate the top-level fault tree and serve as a check for completeness (Figure 1). Next, the overall fault tree architecture was developed. In all, over 50 unique fault tree elements that went as deep as six levels on some branches were investigated and adjudicated through a formal process. Each block was assigned to one of five categories:

- A. Cause – Sufficient
- B. Contributor – Necessary
- C. Contributor – Modifier
- D. May Be a Contributor
- E. Not a Contributor

No items were left simply as open at the end of the root cause analysis. One fault tree block on the driver inflator fault tree was designated as “may be a contributor” due to insufficient test data on the driver inflator failures. All other blocks were closed with detailed documentation in one of the other four categories. The fault tree was used to define technical scope of detailed investigations and reduced the amount of nonproductive or duplicative experimentation and investigation. A summary of the five top-level fault tree branches along with supporting and refuting evidence is given in Table 1.

The technical scope of the effort was designed to use three complementary technical approaches to serve as checks on each other, increasing the probability of an accurate result. This three-legged stool of statistical analysis, engineering analysis and laboratory experiments involved over 2,000 different materials, inflator parts and inflators (see summary in Figure 1).



Inflator Rupture Root Cause Summary Report

**Table 1. Summary of the Five Major Fault Tree Branches Developed and Investigated on This Study.**

*This disciplined approach includes documenting key supporting and refuting data for each fault tree block. This report provides interim and summary data. This table provides a brief overview of the key arguments for and against each fault tree block being a cause or contributor to the rupture event. Compare to final fault tree in Figure 19 at the end of this report.*

	Case Structural Subsystem	Ballistic Subsystem	Seal Subsystem	External Environment	Vehicle Model
<b>Description</b>	Ruptures occur below design pressure	Higher gas flow results in higher pressure	Seal system allows moisture to find its way to the main propellant where grain growth occurs	High ambient humidity and temperature cycling from moderate to high temperature	Differences in vehicles change the environmental conditions experienced by the inflator
<b>Key Supporting Evidence</b>	Pressure data from Takata reports some ruptures below max operating pressure for both primary and secondary	Normal pressure traces show a rounded, "haystack" profile. We know of no ruptures with a haystack profile, even if the haystack profile exceeds maximum expected operating pressure. All rupture profiles show a steep pressure increase prior to rupture, indicating a change in ballistics. Testing in heavyweight hardware has validated higher pressures.	Passenger and driver inflators have multiple leak paths. Takata data shows inflators take on moisture over time. Original equipment manufacturer (OEM) testing showed every possible leak path did leak for aged inflators. Tolerance stack up for older passenger closure seal allows for below design O-ring compression.	Overwhelming percentages of failures both in field ED events and in field returns are from areas of high absolute humidity and high temperature. Mechanisms for wafer growth, which also correlates with ED events, require moisture and temperature cycling such as in High Absolute Humidity (HAH) areas.	Examples of the same prefix inflator show significantly different ED rates from field returns. PSPI AB shows a higher rate in one vehicle model, lower rates in three others, and a zero rate in two more models. Different vehicles reach different maximum temperatures under same test conditions.
<b>Key Refuting Evidence</b>	Detailed structural analysis of inflators and materials of construction showed full capability. Examination of test equipment shows possibility for low measurement. Every failure shows a distinctive "runaway" pressure trace regardless of reported pressure.	Not aware of refuting evidence. Have not reviewed every single ED pressure trace measured.	Inflators pass helium leak check. Simple ingress of moisture and moisture level necessary to cause ED are not clearly known.	There are a few specific examples of ED events that were not from vehicles in the HAH areas. Environment is within what would be predicted for these areas and system should have met expected conditions.	Failures cluster in prefixes whether there are multiple platforms or not. Even in exception examples, wafer OD correlates with ED rate suggesting another mechanism. PSPL-L FD for a sedan model shows a significant variability in ED rate by month of manufacture while still correlating with higher crimp and wafer OD.
<b>Conclusion</b>	<b>Not a contributor</b>	<b>Necessary Contributor</b>	<b>Necessary Contributor</b>	<b>Necessary Contributor</b>	<b>Contributor - Modifier</b>



Inflator Rupture Root Cause Summary Report

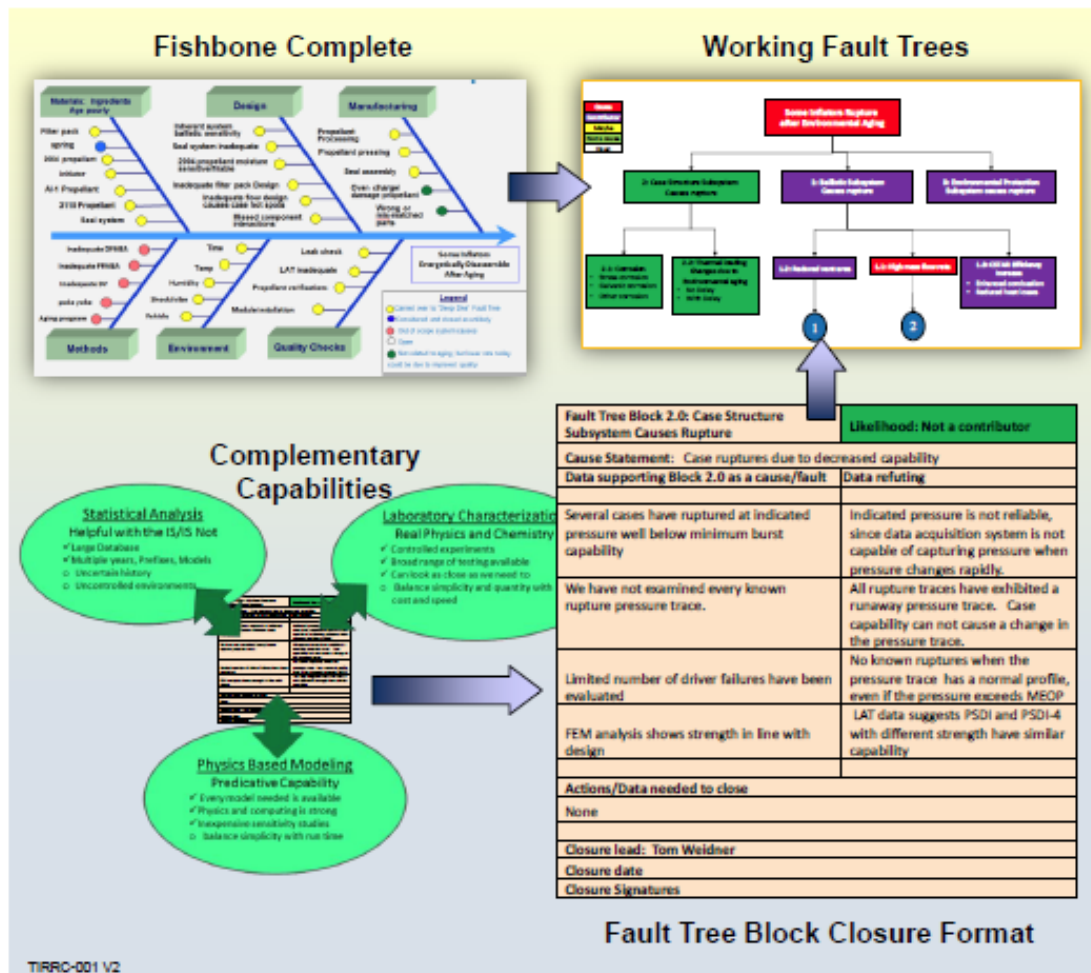


Figure 1. Overarching Project Process.

The disciplined process for root cause started with an industry-standard fishbone which was used to populate an extensive fault tree. A multi-disciplinary approach serves as checks on each other to reduce probability of errors. Full documentation of the fault tree including a formal closure process will provide a complete record for future reference.

Statistical Analysis

Statistical analysis primarily focused on the Master Engineering Analysis File (MEAF) which is the definitive set of Takata test information related to the investigation. We also reviewed databases of field failures and further information gathered by several automakers. We searched extensively for any significant correlations in the databases using standard statistical tools and techniques. As expected, the statistical conclusion reached by others regarding geographical distribution was confirmed. At a higher granularity, some of the geographical differentiations are striking, including failure rate differences between generally similar environments such as north and south Florida (Figure 2). Other items of significant interest included correlations with probability of failure based on wafer diameter and outer crimp diameter (Figure 3). Statistical analysis also shows failure rate differences across multiple vehicle platforms for the same





interactions. The statistical analysis was vital to 1) frame the problem, 2) define areas to explore in a controlled laboratory or modeling environment, and 3) provide anchoring points for investigation results. The interaction of external environment (weather and geography) with the internal vehicle environment (platform and what the actual inflator experiences) is an area where further investigation will be done in the next phase of the effort to develop aging models for non-recalled inflators.

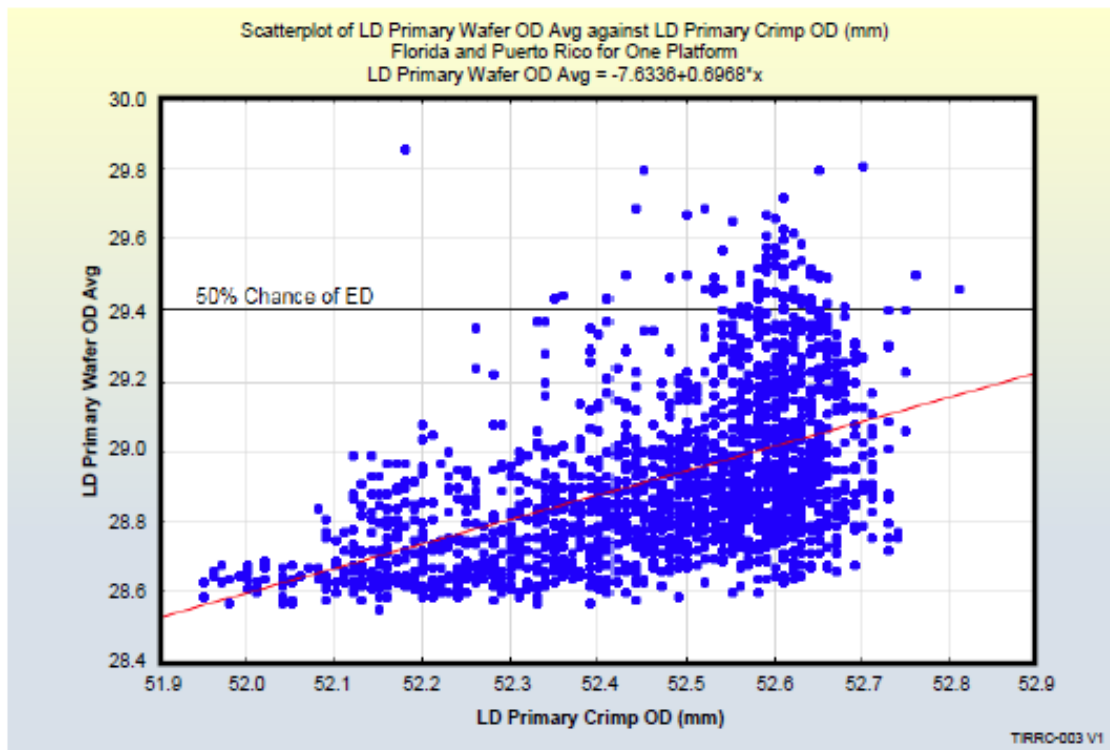


**Figure 3. Wafer Outer Diameter, Crimp (case) Outer Diameter and Failure Probability for PSPI-L for a Single Vehicle Model.**

*The amount of data scatter seen here is typical of many of the statistical relationships but shows a trend.*



**Table 2. Field Return Failure Rates in PSPI-L.**

Data replicated show the range of failure rates for similar or the same inflator design in different vehicles (platforms). These data are an argument for vehicle model as a contributor. It also highlights the challenge as there are convoluting and complicating factors including age of inflators.

Prefix	Platform	Number Tested That Failed	Total Tested	Failure Percentage
FD	A	188	6452	2.91%
	B	12	1698	0.71%
	C	0	9264	0.00%
	D	0	1787	0.00%
	TBD/Other	0	159	0.00%
JD	A	151	13862	1.09%
	E	2	398	0.50%
	B	10	3303	0.30%
	D	2	1611	0.12%
	F	1	1889	0.05%
	TBD	2	4125	0.05%
	G	14	30190	0.05%
	H	0	3230	0.00%
	I	0	244	0.00%
	J	0	116	0.00%
	Other	0	187	0.00%
WQ	TBD/Other	0	87	0.00%

### Modeling and Simulation

Physics-based modeling and simulation is one of the three main legs of the investigation; complementing the statistical analysis and laboratory testing (Figure 1). The Takata family of inflators is complex in design, manufacture and operation. Orbital ATK employed a broad range of design and analysis capabilities to help understand normal operation and causes for abnormal operation. Our modeling and simulation efforts employed the best available ballistic, metal structures, propellant structures, seals and computational fluid dynamics/heat transfer codes and analyses to help understand these inflators.

In order to find design similarities and differences that could correlate with failure rate differences, Orbital ATK developed a family tree based on type and prefix and a part-by-part inflator comparison. Because of the large number of family members, we also looked for designs that are functionally similar and different (Figure 4).



Inflator Rupture Root Cause Summary Report

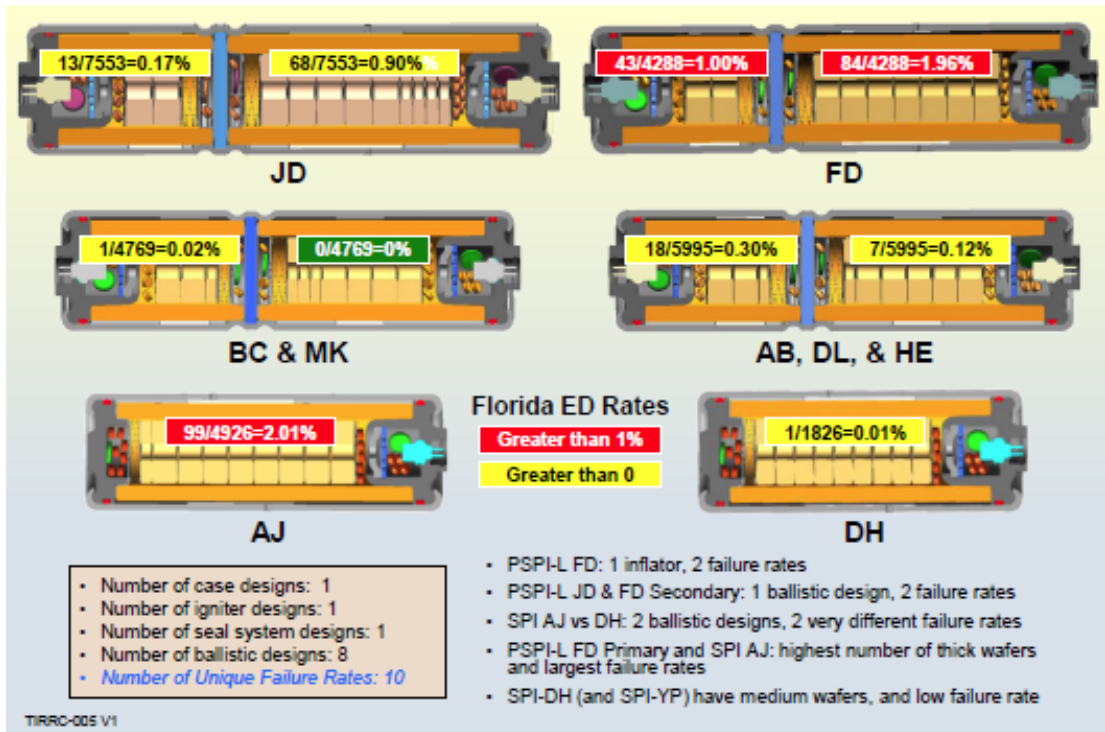


**Figure 4. Summary of Similarities and Differences for Passenger Inflators.**

*These summaries guide where more detailed engineering analysis and testing will be most likely to identify root causes and contributors. The rupture rate on field return tests is shown for each inflator chamber superimposed on that chamber.*

Analysis of the passenger branch showed a common case design, seal system design and igniter design with eight unique ballistic designs. Since the main hardware designs are the same but ballistic designs are different, this suggests a focus on ballistic differences will help to understand differences in energetic disassembly (ED), or rupture rate. This analysis shows that designs that superficially appear similar can be quite different in the ED rate. Detailed analysis is yielding insights on these differences. Each of these points is a clue in understanding the root cause.

Detailed design analysis and comparison was also done for the driver branch of inflators. This allowed us to examine the driver and passenger designs for similarities and differences (Figure 5) that could account for the order of magnitude higher passenger-branch failure rate. Key differences include: 2004 propellant geometry, igniter closure seal design, igniter design and screen pack design.



## Inflator Rupture Root Cause Summary Report

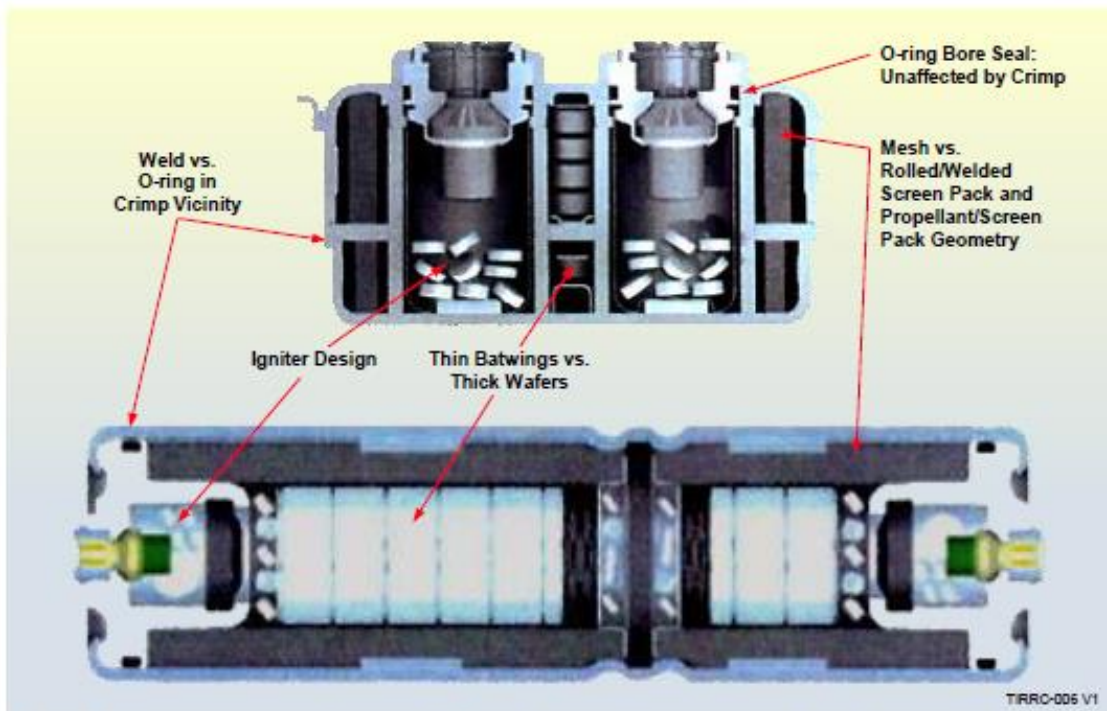


Figure 5. Comparison and Contrast of Major Design Differences in Takata Driver and Passenger Dual Chamber Inflators.

*While functionally similar (see Figure 7), understanding these differences is relevant to understanding differences in ED rates.*

Detailed structural analysis was done for both driver and passenger inflators. In general, we found the design minimum capability to be in line with reported values from Takata lot acceptance testing. In the driver design, we searched for stress concentrations, particularly those that align with bends and joint welds. We examined the possibility of locations where ingested water could collect and cause corrosion, especially when coupled with propellant dust. We performed thermal analysis looking for the potential for strength reduction of the secondary chamber due to heat soak. In no case were the contributions deemed large enough to reduce the pressure capability sufficiently to be a contributor to increased ED probability.

Although we have no evidence of structural failure at normal pressure, there is data showing ED events are associated with runaway ballistics (Figure 6). While some of the failure traces indicate failure below design capability, a separate analysis showed this is likely due to the capability of the data acquisition system.

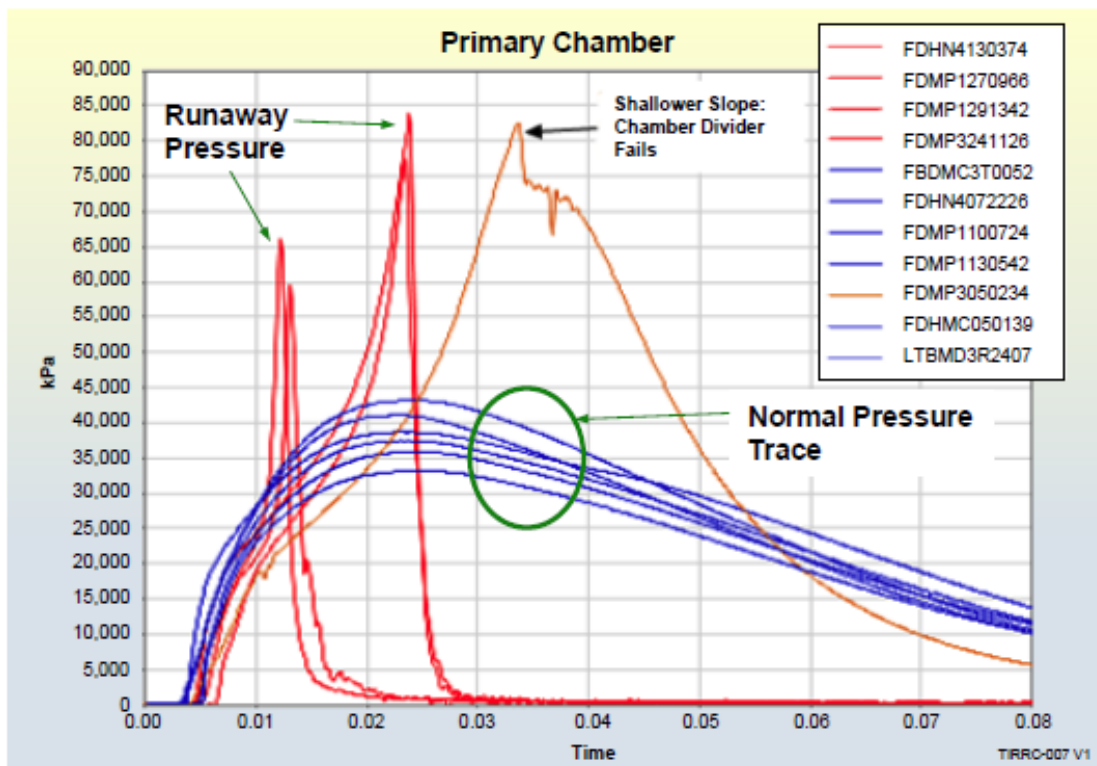


Figure 6. Typical Ballistic Traces.

Shown here are typical pressure-time traces for nominal operation and runaway pressure of an ED. The rounded, "haystack" of the nominal operation is indicative of regression normal to the propellant surfaces. The unique shape of the ED trace provides information regarding what ballistic effects could lead to this shape of trace.

We conducted a wide range of ballistic modeling to help understand potential causes for ED. We modeled both driver and passenger inflators, but studied the passenger inflators in greatest depth. We chose this approach because 1) driver and passenger inflators are functionally similar (Figure 7), and 2) the PSPI-L primary chamber has a wealth of ED data. First, we conducted ballistic analysis to gain an understanding of normal operation for these complex inflators. We then looked at deviations from normal operation that could result in the pressure trace associated with ED. This pressure trace typically shows an initial pressure rise followed by a short "pause" where the pressure rise rate slows followed by a rapidly increasing rate of pressure rise to a pressure that causes a rupture of the inflator housing. This sort of rapid pressure increase is often associated with a progressive burning surface or one that is increasing in the amount of available surface area to burn. This is consistently and strikingly different from the rounded or "haystack" pressure trace associated with normal operation (Figure 6). This kind of "haystack" trace is typical of what would be expected in a normal burn of wafers or tablets of the kind in these inflators. This "haystack" is referred to as a regressive surface area trace due to the wafers or tablets having the highest surface area at the time of ignition followed by a consistent reduction of the available burning surface area as they get smaller burning from the outside in.



Inflator Rupture Root Cause Summary Report

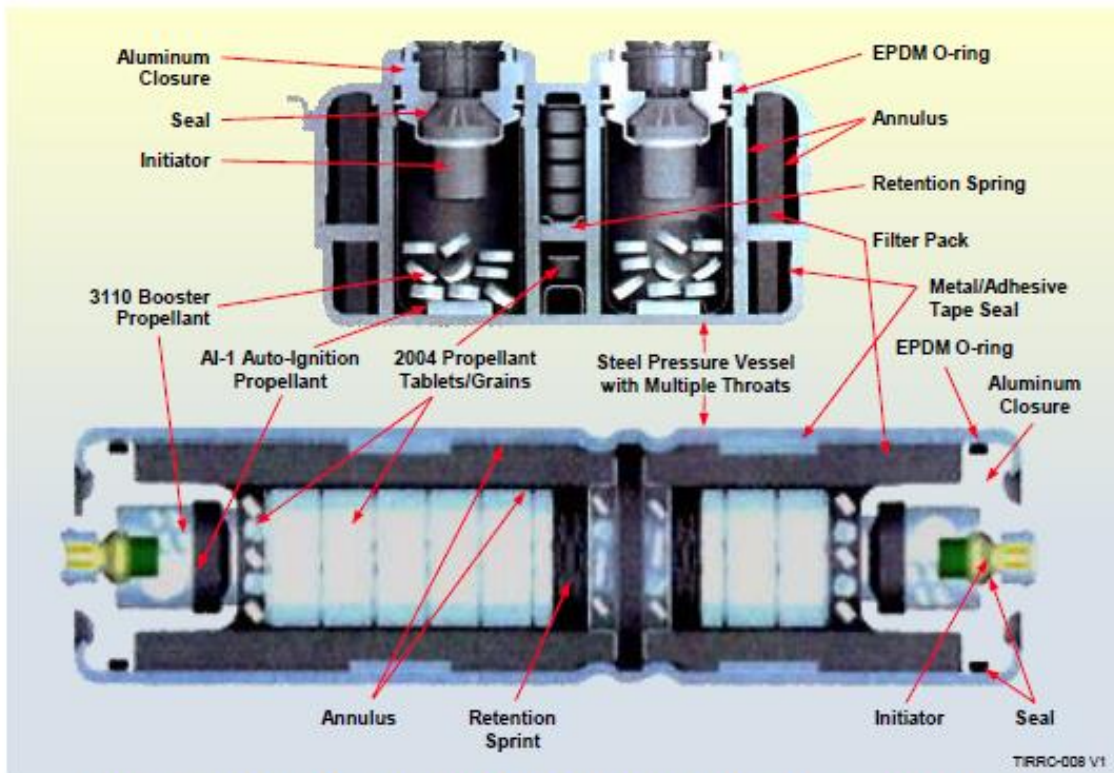


Figure 7. Similarities in Operating Features of Takata Driver and Passenger Inflators.

While there are certain differences (Figure 5), there are many similarities in propellants, materials and designs for the inflators under recall. These similarities allow conclusions regarding both designs to be reached on several key parameters.

We performed significant ballistic modeling to understand normal operation to develop a foundation for understanding higher pressure and ED events. We started with the basics: burn rate and surface area of the main 2004 propellant. Burning rate in propellants is described by the equation here, referred to as St. Robert's Law:

$$r = aP^n$$

In this equation,  $r$  is the burn rate,  $a$  is a constant,  $P$  is the pressure and  $n$  is the pressure exponent often referred to as the burn rate slope. Since it is an exponential equation, typical plots are done as log of the burn rate versus log of the pressure which results in a straight line (Figure 8) for a typical combustion process. Changes in the exponent, or slope, have a profound effect on the burn rate. Burn rate combined with available surface area determines the rate that gas is produced. An ED occurs when gas is generated faster than it can move through the screens and out the vents built in the inflator.



Burn rate data for virgin wafers showed a high burn rate slope ( $\sim 0.8$ ) at low pressure. In the pressure range near the maximum achieved in normal operation, a lower slope ( $\sim 0.5$ ) is observed. This is discussed in further detail below. These properties are critical to normal operation of these inflators and relevant to understanding the reasons for ruptures. At low pressures, this propellant burns very slowly and can extinguish. At a higher pressure, the burning rate is sufficient to generate gas at the right rate to inflate the air bag. If the pressure increases significantly beyond design, the burning rate also increases resulting in more gas, more pressure and an eventual ED. This iterative pressure/burn rate building results in the typical shape of the pressure-time curve for an ED (Figure 6). These measured burn rate and slope data are the input used for modeling the behavior of this system. We used the lower slope in our baseline modeling because it is the pressure exponent near the maximum pressure.

Wafers break into smaller pieces on ignition. We conducted multiple studies on this breakup. All breakup models resulted in regressive surface area versus distance burned. Variation in breakup strongly influenced peak pressure, but did not change the basic haystack profile. More breakup resulted in higher peak pressure and lower tail-off pressure. Sufficiently high break-up (essentially pulverizing wafers at the extreme) results in an overpressure event.

We examined the potential of the ignition propellants to cause ED. Specifically, we looked at the PSPI-L secondary chamber because of the relatively high ratio of ignition propellant weight to 2004 wafer weight (Figure 9a). We found that 1) we could double the ignition propellant mass flow rate without a significant change in peak pressure, and 2) if we added all the auto ignition propellant at peak pressure we could not increase pressure enough to cause ED (Figure 9b). This important finding helped focus our propellant investigation on the 2004 main propellant.

We examined four theoretical potential causes for ED: 1) increasing burning surface area, 2) increasing burn rate, 3) throat blockage, and 4) increasing combustion efficiency. Mechanisms for increasing burning surface are: a) continued breakup after ignition, and b) burning of interior fractures, cracks and pores. Continued breakup remains a possible cause, but we were able to rule out interior (closed) pore burning (Figure 10) as a primary contributor.

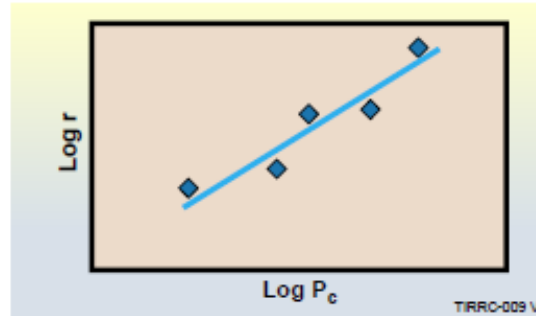
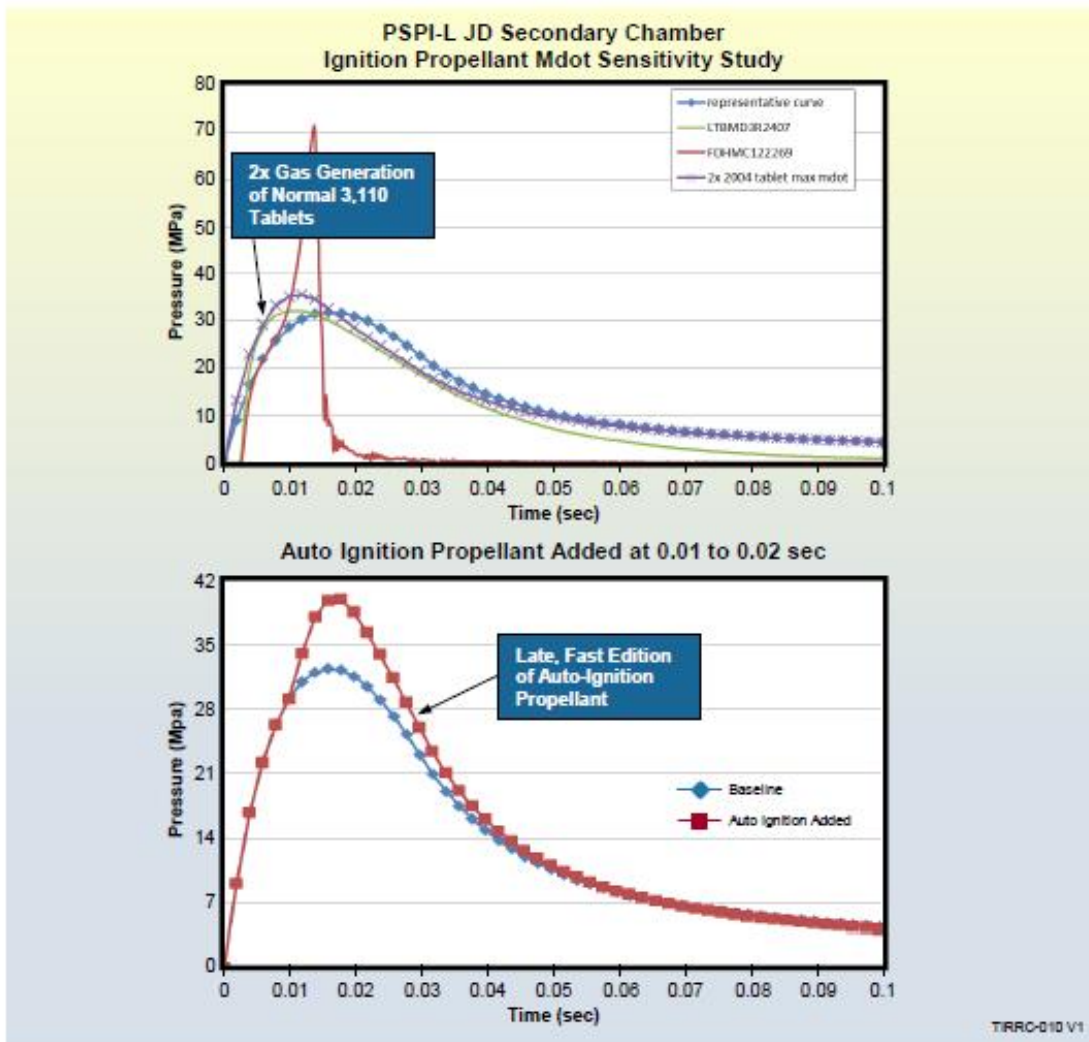


Figure 8. Schematic Representation of Burn Rate and Pressure Plot.

*Propellants combust following an exponential relationship of pressure and burn rate. With a high slope of the line, burn rate rises rapidly with increasing pressure. Such propellants exhibit larger changes in burn rate and gas production than those with lower slopes.*



**Figure 9. Potential of Ignition and Auto Ignition Propellants to Cause an ED.**

*These two figures show data from gas or pressure generation studies (Mdot, gas generation rate) on the potential of the igniter closure 3110 propellant (top) or the auto ignition propellant (bottom) to cause an ED. Even under extreme cases, these propellants cannot of themselves cause an ED. This focused our studies on the main 2004 propellant.*

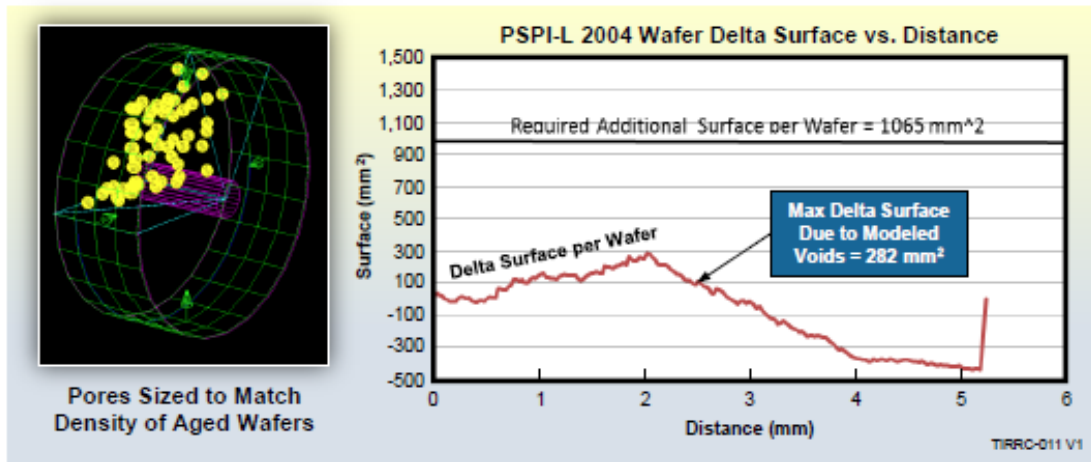


Figure 10. Closed Pore Impact on Burning Surface.

*Calculations were done matching the lowest wafer density from field returns by adding closed pores to otherwise nominal wafers. With this matched density, closed pores are insufficient to explain the surface area increase needed to result in an ED event. It may contribute, however. This analysis does not apply to connected pores where there are potential gas paths as discussed below.*

Our investigation identified throat blockage as a potential contributor, but not a cause. Several inflators showed abnormal flame plumes at the throats prior to ED and several filter packs showed bucking under the throats in post-test inspection; these observations are consistent with the thermal-structural analysis that showed concentrated heating under the throats. However, the filter packs show little pressure drop even when pressed against the case inner wall. In order to block a throat, the filter pack would have to get hot enough and weak enough to compress into a throat, without being weak enough to blow through the throat under the high pressure associated with ED.

Combustion efficiency is associated with the actual pressure level achieved compared to the theoretical pressure level reached from burning the propellant completely in the absence of heat losses. Heat losses to the filter pack are significant and result in lower combustion efficiency. Closed bomb testing indicates combustion efficiency may increase with pressure. If the inflator is on the way to ED, then increasing combustion efficiency will aggravate the pressure increase by producing more gas for a given amount of 2004 propellant burned. Going forward, we intend to examine combustion efficiency changes with pressure using our heavyweight test hardware.

We examined multiple potential causes for the apparent increase in 2004 burn rate. We looked at a number of phenomena known to the ballistics technical community including: oscillatory burning, high base burn rate, erosive burning, burning due to preheating the propellant and permeable burning. Of these causes examined, permeable burning showed potential to contribute to ED.



Orbital ATK and Penn State data<sup>2</sup> showed the potential for low-density 2004 propellant to have a slope increase at high pressure compared to the normal slope at high pressure (Figure 11). Modeling the effect of slope change shows that increasing slope from the baseline value of 0.5 to 0.8 is enough to reach ED pressure levels. This ballistic change most likely is caused by the permeable and porous burning noted below.

Permeable burning is a mechanism that can increase burn rate by preheating the propellant. 2004 propellant burn rate increases with temperature until the auto-ignition temperature is reached. If the propellant is porous (volume is available for hot gas to fill) and permeable (hot gases can flow to the free volume), then hot gas has the potential to preheat the propellant to the depth the permeability extends (Figure 12). This can express itself in what appears to be “in-depth” burning as the hot gases ignite more surface area of the propellant below the normal advancing surface. In a parametric studies completed to test this phenomenon, 2% porosity is typical of virgin propellant, and 10% porosity is similar to aged propellant. For the study, three values for the permeability constant, Gamma, were chosen that span the range likely for this material and to model the potential impact from a change in permeability. This example showed the potential for a 50% burn rate increase due to changes in porosity and permeability. This theoretical underpinning may serve to explain the empirically measured “Integrated Burning Rate” data reported by Takata. Understanding the mechanism will allow validation of appropriate aging models.

---

<sup>2</sup> Essel, J.T., Boyer, E., Kuo, K.K., and Zhang, B., “Transient Burning Behavior of Phase-stabilized Ammonium Nitrate Based Airbag Propellant”, *Int. J. of Energetic Materials and Chem. Propellants*, Vol. 11, pp. 473-486, 2012

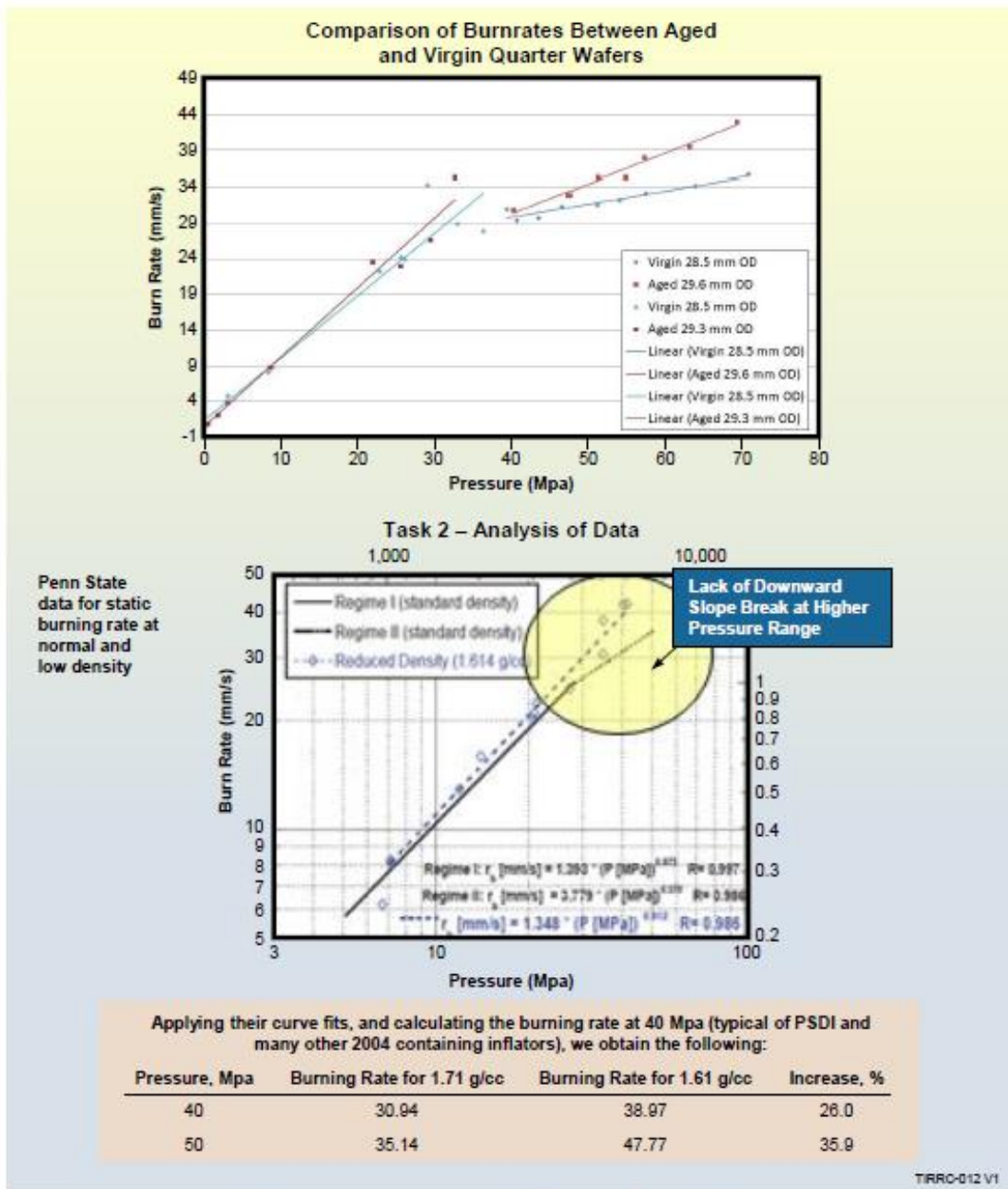
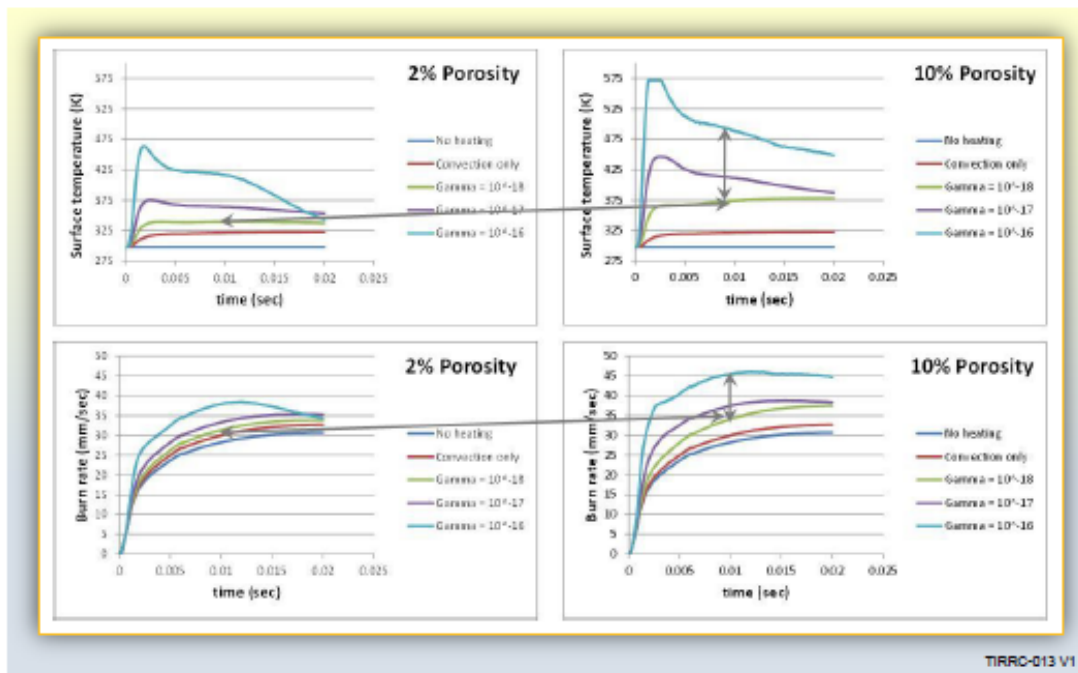


Figure 11. Change in High Pressure Regime Slope.

Data at several locations have shown similar data as depicted here from Orbital ATK (top) and Penn State (bottom). This change in apparent slope at higher pressure is consistent although graphically represented several different ways. Several phenomena can result in this apparent slope change as noted below.



**Figure 12. Impact of Porosity and Permeability.**

*These four figures graphically depict the dramatic effect on in-depth heating and burning rate with increasing porosity and permeability to hot gases. Each graph shows data for no heating and for increasing levels of permeability (gamma). This in-depth heating along gas paths is consistent with the real time radiography, pycnometry data and ED event ballistic traces.*

Analysis of the seal systems showed that each driver and passenger inflator has multiple potential leak paths (Figure 13). The leak path of greatest concern is the passenger closure O-ring seal (Figure 14). Based on nominal dimensions for the closure, O-ring and case (away from the crimp zone), O-ring squeeze is excellent. Unfortunately, the closure crimp footprint overlays the O-ring sealing footprint. This design/manufacturing feature allows the possibility of no O-ring squeeze at the maximum engineering-allowed crimp outer diameter (OD) of 52.65 mm. In addition, many inflators were built with crimp ODs that exceed the allowed value. These paths result in greater moisture movement in and out of inflators than what would be calculated based on diffusion through a rubber O-ring and is consistent with reports from Takata, Fraunhofer ICT and original equipment manufacturers (OEM) of higher moisture levels in field return inflators. This moisture movement is critical to generate the observed growth in wafer diameter.



Inflator Rupture Root Cause Summary Report

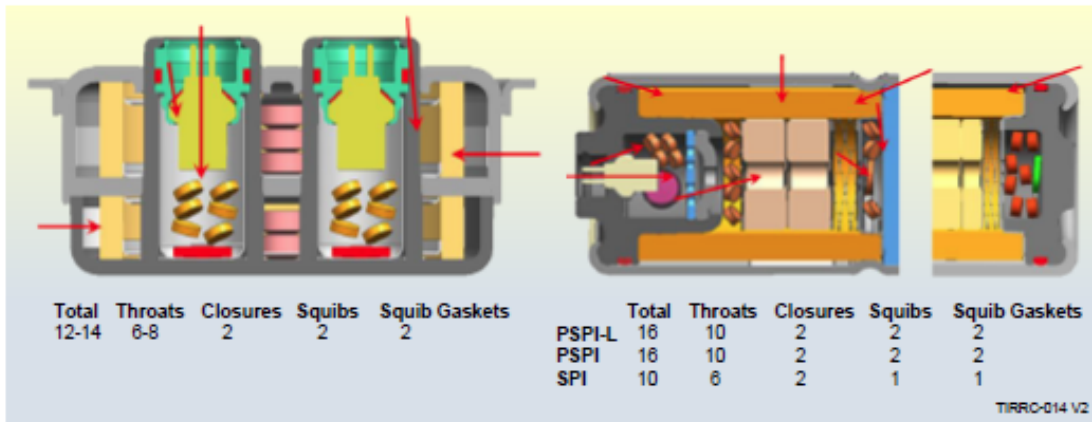


Figure 13. Potential Leak Paths in Takata Inflators.

Several different seals are present in both passenger and driver inflators (marked by red arrows). While a great deal of emphasis has been placed on the passenger crimp and O-ring, every seal is a potential path for moisture to enter the inflator and must be considered in any valid moisture transport model.

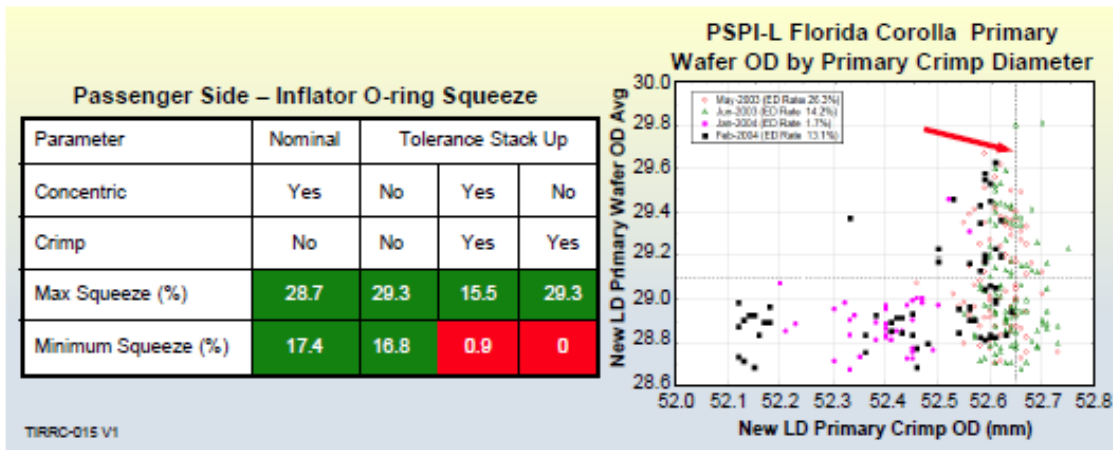


Figure 14. Passenger Inflator Primary Crimp Data.

The table on the left presents results from analysis using a proprietary tool developed by Orbital ATK to be a more accurate measure of O-ring squeeze. The tool was developed due to the criticality of O-ring seals in rocket motors. The data on the right show that manufacturing in the time frame of interest for these recalls (2003 and 2004 shown here), that a measurable percentage of all primary crimp diameters exceeded the engineering allowed maximum of 52.65 mm (marked by the red arrow).

### Laboratory Experiments

There was a wide range of activities that we broadly grouped under laboratory experiments. The range is from detailed chemical analysis of raw materials to metallurgical investigations of inflator hardware to heavyweight ballistic analysis to static and dynamic x-ray analyses. The specific work performed was driven by the needs derived from the fault tree closure efforts.

Several noteworthy conclusions can be drawn from our laboratory experiments:



1. There is no significant chemical degradation or chemical composition change occurring to a sufficient degree in the 2004 propellant or in the 3110 propellant after field exposure which could contribute significantly to the failure rate. That is, PSAN is still the same chemical when aged under the conditions typical in the subject inflators. While the chemical constituents do not change, in contrast, changes in the shape and size and growth in pores, cracks or fissures in pressed wafers, tablets or batwings are observed.
2. Moisture transport inside an inflator follows expected behavior of the hygroscopic, desiccating and deliquescing behaviors that would be expected for these materials based on general principles of chemistry. That is, sodium bentonite, which is a component of both the 2004 and 3110 propellants, can function as a drying agent and PSAN can absorb significant amounts of moisture if available. There are not dramatic cliffs but rather gradual changes as a function of temperature, as shown in the experiments conducted by Fraunhofer ITC and confirmed by our efforts. However, these cumulative changes over the temperature range to which the inflator is exposed appear to be significant. Figure 15 and Table 3 report critical lab data describing moisture transport.
3. The 2004 propellant wafers in passenger inflators grow after repeated temperature cycling with moisture present (transitioning in and out of propellant grains). This effect was observed in both wafers and tablets in primary and secondary chambers of passenger inflators (Figure 16). The growth results in reduced envelope density but very little change in pycnometry density, suggesting that the increased volume is void spaces that are connected (Figure 17). These connected pores, flaws or fissures allow hot gas penetration resulting in increased mass flow when ignited (porous and permeable burning).

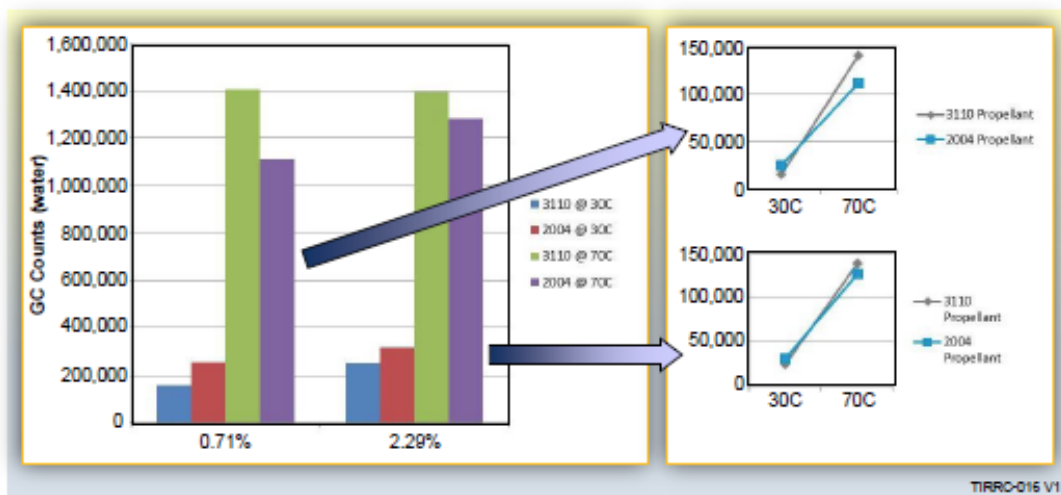


Figure 15. Headspace Moisture Above 2004 and 3110 Propellants with Moisture Added as a Function of Temperature.

*In each case, the change in the amount of water that is available is dramatic when transitioning from 30°C to 70°C. This suggests transport is much more likely at the higher end of the range. The 3110 propellant shows a modest increase in propensity to give up moisture compared to 2004. This variability gives rise to the "x-graph" when suitably drawn although the effect is not as dramatic as suggested in some depictions.*



Inflator Rupture Root Cause Summary Report

**Table 3. Moisture Competition Experiment for 2004 and 3110 Propellants in a Closed System.**

Data reported here are percent moisture in the propellant. The initial conditions were six open vials containing dried 3110 propellant and 2004 with a known percentage (2%) of moisture. They were first allowed to equilibrate for 5 days at ambient. A significant amount of moisture moved from the moist 2004 propellant to the dry 3110. Cycles at higher temperature with two additions of small amounts of water mimicking HAH conditions followed by simple heating showed slow movement back towards the 2004 from the 3110. This matches the data in Figure 15 and quantifies the mobility under these relevant conditions. Further experiments at 50°C and 60°C along with smaller amounts of water are planned.

Mass Propellant	1.14 g 2004	1.90 g 2004	3.08 g 2004	0.18 g 3110	0.32 g 3110	0.2 g 3110
Start	2.0	2.0	2.0	0.0	0.0	0.0
5 days ambient	1.4	1.7	1.6	3.1	2.4	2.6
Add 0.1 g water, heat to 70°C and let cool over night	3.6	2.7	2.3	8.5	6.2	5.2
Add 0.07 g water, heat to 70°C and let cool over night	5.6	3.7	2.6	12.1	8.5	6.7
Heat to 70°C and let cool over night	6.2	4.0	2.5	9.5	7.6	6.5
Heat to 70°C and let cool for 6 hours	6.3	4.1	2.5	8.8	5.9	5.9



**Figure 16. Examples of Fused Wafers and Tablets.**

Both tablets and wafers are often fused in inflators where there has been significant diameter growth in the wafer consistent with a process similar to Ostwald ripening. The kinetics of such processes are relevant to any aging models.



Inflator Rupture Root Cause Summary Report

Real time radiography (RTR) provided remarkable insight into the processes involved in both a nominal burn and during over-pressure events. This technique showed the typical fracture of wafers during ignition. In a nominal deployment, the regular burning normal to all surfaces is apparent. However, in an ED, the initial state shows less distinct wafers, consistent with wafers expanding into direct contact with each other. Fracture occurs on ignition, although perhaps less pronounced than in a nominal deployment. Initial burning is followed by a transition to a much higher mass consumption, consistent with ballistic traces and penetration of combustion gases through void spaces resulting in increased surface area (Figure 18).

**Root Cause**

The root cause statement is summarized in Figure 19. When all three necessary, mutually synergistic conditions are present, they combine to result in a single sufficient failure condition. The case, or enclosure, structural integrity was not found to be a contributor. The particular vehicle model or platform was found to be a contributing modifier. The magnitude of that effect will be examined in the next phase of the program as part of the aging and surveillance testing effort.

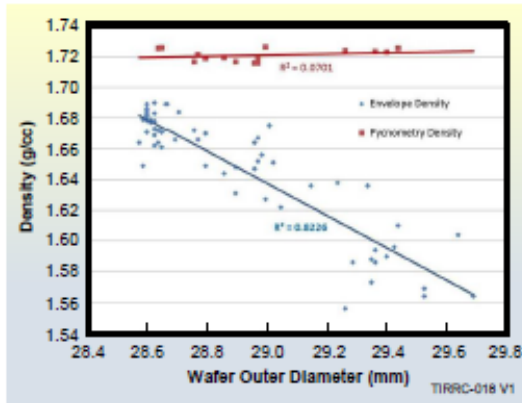


Figure 17. Density Measurements for 2004 Propellant Wafers.

Shown here are measurements of a large number of propellant wafers with increasing OD. Outer diameter has been correlated with likelihood of an overpressure event. These data show two different density measurement techniques. The envelope density method gives an overall geometrical density while the pycnometry density method allows gas penetration, yielding a result that remains constant due to accessibility to gas to the majority of low-density spaces or voids in the propellant. These data show that the low-density voids generally allow gas to pass from one to the next, suggesting connected or communicating voids.

program as part of the aging and surveillance testing effort.



Inflator Rupture Root Cause Summary Report



**Figure 18. Real Time Radiography Still Images.**

Shown above are individual frames from two RTR experiments with PSPI-L FD inflators showing the primary chamber. Stills 1-3 are from test #96553, which was a nominal firing. Stills 4-6 are from test #95179, which was an ED. The time sequence is from left to right. In the first pictures (1 and 4), differences can be seen with the distinct individual wafers with space between wafers in #1 and less distinct boundaries in #4 reflecting the wafer growth in #4. In pictures 2 and 5, the ignition has occurred and flame spread has begun. The typical fracturing of wafers is visible. Space between wafers from flame intrusion is now clear, which is not seen in the baseline (picture 4) for test #95179. In #3 and #6, radical differences are clear. In #3, regression of the surfaces, reducing wafer size but maintaining integrity, is observed. In #6, combustion at a much higher rate and in depth in the wafers is visible although some integrity remains as would be expected. Rupture occurred shortly thereafter attributed to excessive chamber pressure.

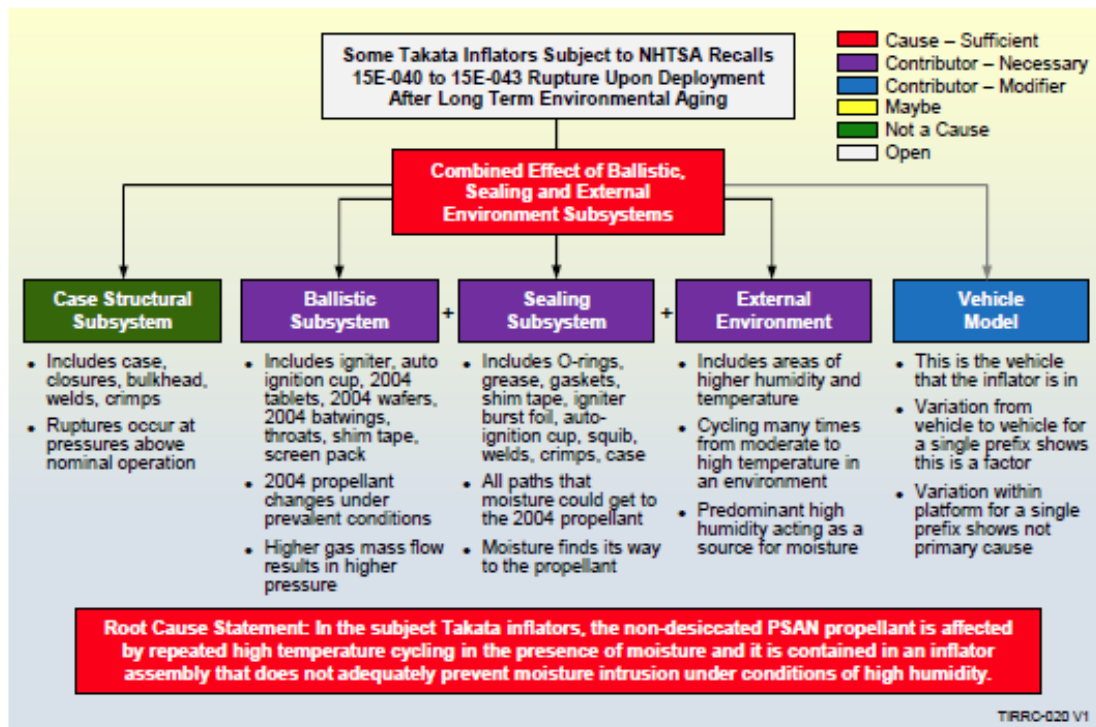


Figure 19. Summary Fault Tree.

The first level fault tree with the summary of the root cause is shown here. Please note the color key in the upper left. Compare to the summary of the supporting and refuting evidence shown in Table 1.

### Continuing Efforts

Our activities are moving into the next phase of the investigation, namely to focus on the performance of all inflators that are being used as replacement parts for current recalls, as well as desiccated inflators being used in existing vehicles. A primary question is whether the newer inflator designs are susceptible to failure under conditions that have resulted in ED events with inflators currently under recall.



## Addenda

### A. Sources of Information and Acknowledgements

The scope of the project as presented to Orbital ATK by The Independent Testing Coalition (ITC) was to pursue root cause and ramifications using all available information. The investigation was not limited in focus or scope. There was not any direction given by the ITC. No limitations were imposed on avenues of the investigation or scope of questions asked. We received consistently strong support from each member of the ITC. Each ITC member willingly shared relevant data they had.

We received critical support from Takata. They supplied proprietary engineering drawings to support our modeling. Takata provided aged and new inflators as well as inflator hardware, raw materials and access to their engineering and manufacturing facilities. Takata met with us on several occasions to respond to our questions. Takata also provided access to their Master Engineering Analysis File (MEAF).

We also met with individuals from Fraunhofer ICT as arranged by Takata and with faculty from Penn State to discuss their studies. National Highway Traffic Safety Administration (NHTSA) personnel provided relevant information regarding their in-house investigations and from their review of efforts by all other parties.

We considered all the data we gathered as relevant to the investigation and sought to include every possible source in our work. We independently verified data from all sources to ensure that we could stand by all the critical data we cite as relevant to our investigation.

### B. ITC Membership and Purpose

Formed in December 2014, the ITC has as its sole purpose to conduct an independent and comprehensive investigation of the technical issues associated with Takata airbag inflators. The ITC comprises ten automakers that have Takata airbags subject to the noted recalls in their passenger and light truck vehicles: BMW, Fiat Chrysler Automotive, Honda, Ford, GM, Mitsubishi, Mazda, Nissan, Subaru and Toyota.

### C. Orbital ATK Relevant Qualifications and Background

The Orbital ATK team was primarily located within our Propulsion Systems Group in Utah. We called on expertise relevant to the project from across the company and outside of our company for specific technical capabilities and for real time radiography and computed tomography image analysis. The core team has extensive experience in the design, research and development, testing and manufacture of propellants, explosives and pyrotechnics including many years of experience with automotive inflators. Orbital ATK is not involved in the inflator business today and, as such, is well positioned to serve as an objective investigator on this project. We were and are fully committed to providing the best technical personnel and using the best of the tools at our disposal to provide an accurate and objective assessment.

### **Appendix D. Correlation of Various Climate Zones and Cities**

Several reports, documents and websites have described various climate zones within the United States. In this appendix, references and links to several of these documents and the cities whose weather data was utilized in this study are collected for reference. This is simply for reference with no judgement on relative merit of the various approaches. The cities selected for this study to be representative of all the zones across the various methodologies.

<b>City</b>	<b>NHTSA Recall Zone</b>	<b>Takata Updated Zone</b>
Miami	<b>A - Hot and Humid</b>	<b>1 - High AH (&gt;15 g/m<sup>3</sup>)</b>
Atlanta	<b>A - Hot and Humid</b>	<b>2 - Coastal Moderate-High AH (~13 g/m<sup>3</sup>)</b>
Phoenix	<b>B - Less Hot and Humid</b>	<b>5 - High Temperature Low AH (~7 g/m<sup>3</sup>)</b>
Detroit	<b>C - Least Hot and Humid</b>	<b>3 - Central Temperate Moderate AH (~10 g/m<sup>3</sup>)</b>
Seattle	<b>C - Least Hot and Humid</b>	<b>4 - Coastal Cool Low-Moderate AH (~8 g/m<sup>3</sup>)</b>

Original Takata Zone (from Page 9 of Attached Report)

Or find on the web at:

[https://www.nhtsa.gov/sites/nhtsa.dot.gov/files/documents/takata-fraunhoferict-research\\_summary.pdf](https://www.nhtsa.gov/sites/nhtsa.dot.gov/files/documents/takata-fraunhoferict-research_summary.pdf)

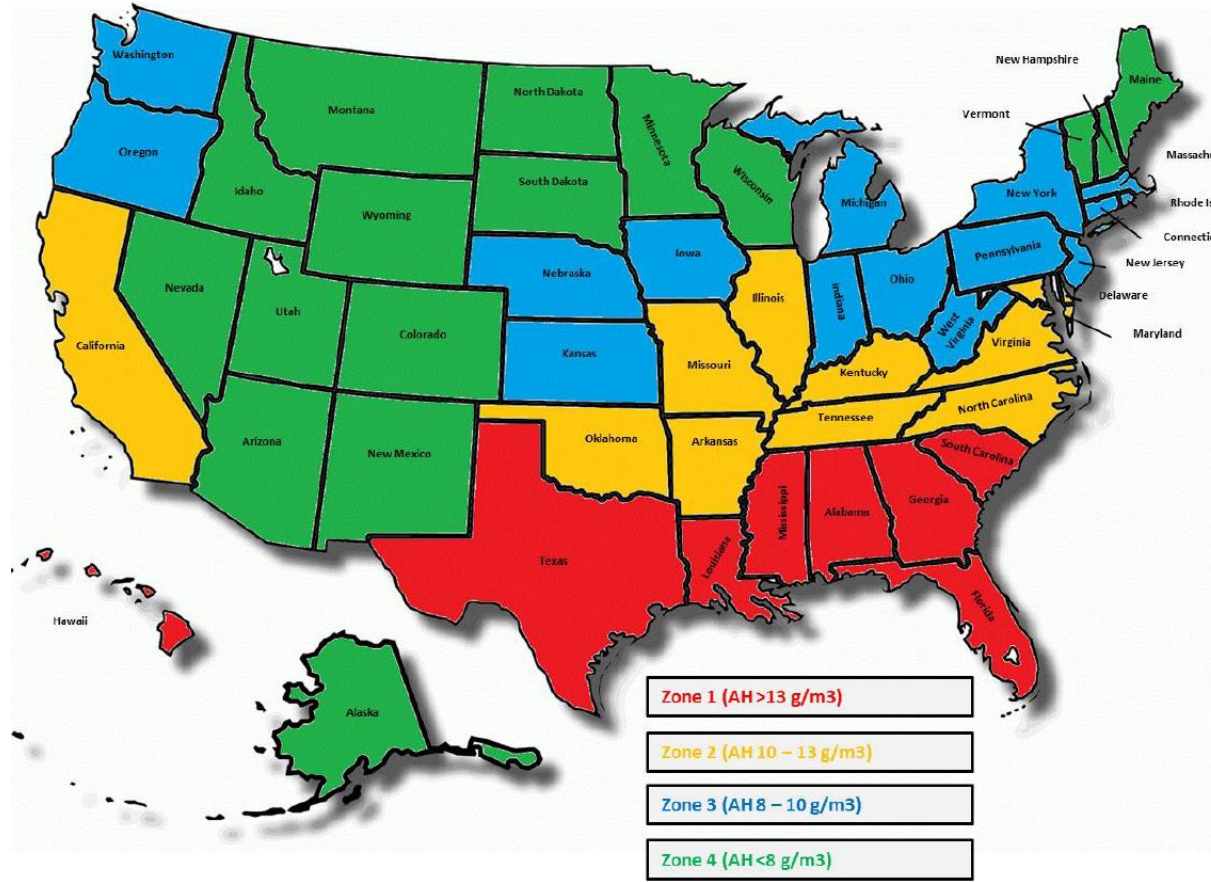
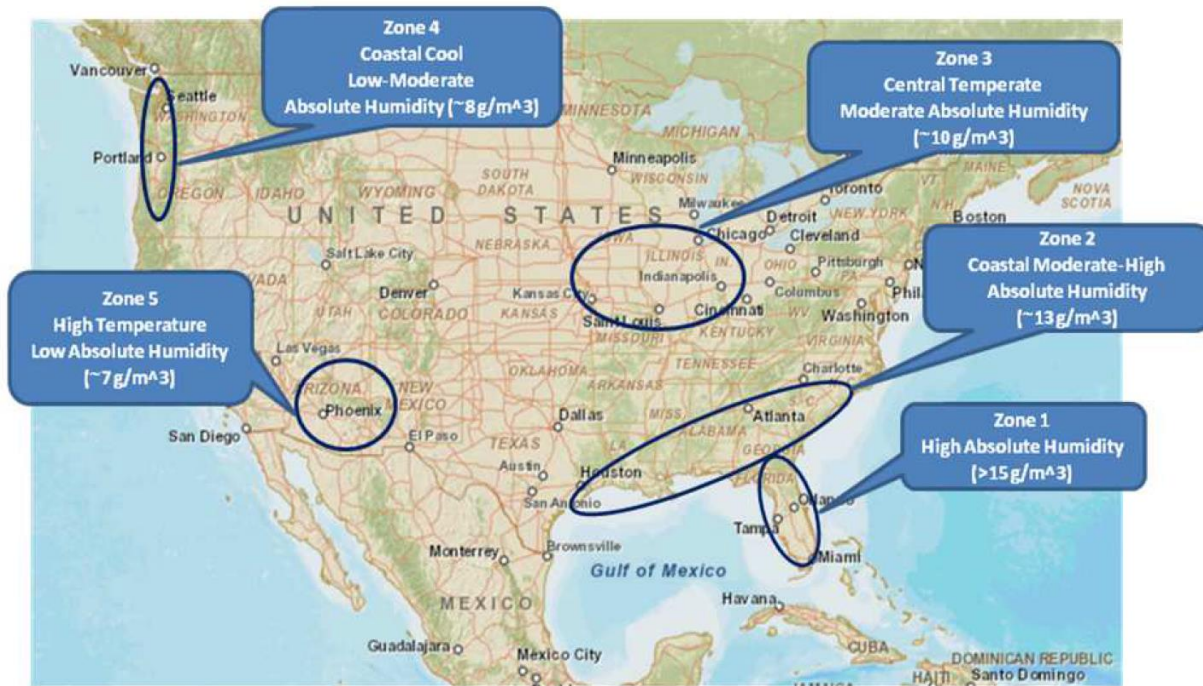


Figure 10: Original Four Climate Zones  
*Takata Updated Climate Zones (from Page 8 of ATLAS Report)*



### Climature Test Zones

- Zone 1 – High AH  
– >15 g/m<sup>3</sup>
- Zone 2 – Coastal Moderate-High AH  
– ~13 g/m<sup>3</sup>
- Zone 3 – Central Temperate – Moderate AH  
– ~10 g/m<sup>3</sup>
- Zone 4 – Coastal Cool – Low-Moderate AH  
– ~8 g/m<sup>3</sup>
- Zone 5 – High Temperature –Low AH  
– ~7 g/m<sup>3</sup>

Figure 2.2.a. Vehicle testing defined climate zones of interest for testing based on absolute humidity.

### *NHTSA Recall Zones Based on Temperature & Humidity*

See online:

<https://www.nhtsa.gov/equipment/takata-recall-spotlight>

Scroll down till you find the following

#### **Zone A: Hot and Humid**

Alabama, California, Florida, Georgia, Hawaii, Louisiana, Mississippi, South Carolina, Texas, Puerto Rico, American Samoa, Guam, the Northern Mariana Islands (Saipan), and the U.S. Virgin Islands

**Zone B: Less Hot and Humid**

Arizona, Arkansas, Delaware, District of Columbia, Illinois, Indiana, Kansas, Kentucky, Maryland, Missouri, Nebraska, Nevada, New Jersey, New Mexico, North Carolina, Ohio, Oklahoma, Pennsylvania, Tennessee, Virginia, and West Virginia

**Zone C: Least Hot and Humid**

Alaska, Colorado, Connecticut, Idaho, Iowa, Maine, Massachusetts, Michigan, Minnesota, Montana, New Hampshire, New York, North Dakota, Oregon, Rhode Island, South Dakota, Utah, Vermont, Washington, Wisconsin, and Wyoming

Searching online for NHTSA Takata Zone you can find several versions of this:

